# TOWARDS A GLOBAL AND HARMONIZED DATABASE FOR IN-DEPTH ACCIDENT INVESTIGATION IN EUROPE: THE DaCoTA PROJECT

**Eduardo del Pozo de Dios, Adrià Ferrer**
IDIADA Automotive Technology, Spain
**Julian Hill**
Transport Safety Research Centre, Loughborough University, United Kingdom
**Helen Fagerlind**
Vehicle and Traffic Safety Centre (SAFER), Chalmers University of Technology, Sweden
**Gabriele Giustiniani, Luca Persia**
Centre for Transport and Logistic (CTL), "Sapienza" University of Rome, Italy
Paper number 13-0489

## ABSTRACT

The aim with this paper is to describe the procedure for the development of a common methodology for research accident investigation and identifying and training new research teams across Europe. In-depth accident investigation has a great potential to provide researchers, car manufacturers and road administrations with valuable information on how and why accidents and injuries occur. The data can be used to determine the issues where efforts must be focused when research studies are conducted, crash protection countermeasures are designed and policy decisions are taken. Existing European databases are mainly focused on regional or specific stakeholder interests due to the lack of an international network, and there are significant differences in the information collected and how the database variables are coded. This lack of harmonisation precludes any detailed global analysis on the whole EU accident situation.

The EU co-funded the DaCoTA project - inspired by previous projects like SafetyNet and TRACE – intended to establish a Pan-European In-depth Accident Investigation Network and to create a European database that could include in-depth accident investigation cases from all the European countries.

Built on earlier pilot investigations conducted by previous projects, and following consultation with the range of stakeholders, an in-depth accident investigation system has been developed to standardise and harmonise the data to be collected during the investigations. Based on the new methodology, accident investigation teams from across Europe have been trained to systematically produce high quality research data. A comprehensive, secure, web-based database has been created to centralise the information collected and to analyse the results from the cases. To ensure the harmonisation of the data collected, a pilot study and subsequent data quality reviews were performed.

The DaCoTA project has developed a harmonised in-depth accident investigation methodology, openly available in an online manual. From 19 European countries, 22 organisations were trained in the DaCoTA accident investigation methodology. The web based database includes over 1,500 variables related to the road, vehicle, road-user, accident reconstruction and injury analysis. Over 450 of these variables are considered as essential "core variables".

In total, 99 on-scene and retrospective cases have been collected by 18 accident investigation teams using the standard methodology and these have been uploaded to the database for further analysis.

Good relationships have been established between the network teams and their local authorities, including the police and hospitals. In some countries, efforts to obtain the necessary permissions to gain access to the accident scenes and to acquire sensitive medical or forensic data is continued.

The DaCoTA project has developed the Pan-European in-depth accident investigation methodology, including a network of investigating teams, providing a viable means for the systematic collection of harmonised in-depth accident data for use by researchers, road and vehicle safety related industries and policy makers.

## INTRODUCTION

### Background

More than 30,000 people died in 2011 in the roads of the European Union [1]. These losses have an estimated socio-economic cost of around 2% of EU countries' gross domestic product, which means around 180 billion Euros [2].

In order to monitor trends, describe road safety problems and identify targets for interventions,

information on the state of road safety and factors influencing it is needed [3]. For this reason, improving the collection and analysis of data on accidents and injuries was one of the bullet points of the methodological network to identify and disseminate best practices pointed out by the European Commission [4].

Following this strategy, the DaCoTA project has built upon previous EU projects in in-depth accident investigation (as shown in Figure 1) with the intention of establishing the infrastructure for a future investigation system that will then be deployed beyond the completion of the project [5].

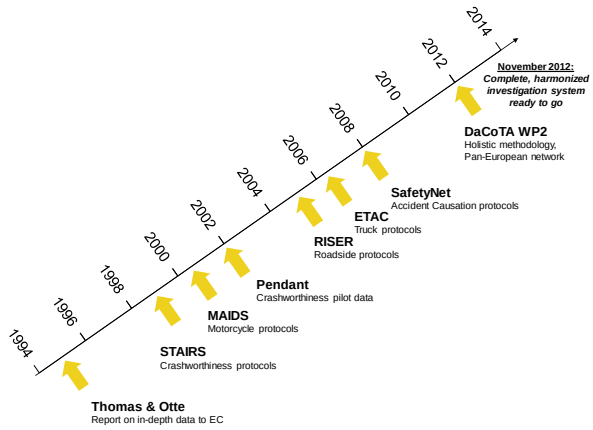


*Figure 1.* Key EU projects relating to in-depth data collection

The DaCoTA project [6] is a Collaborative Project developed as part of the European Commission's 7th Framework Programme. Led by the Transport Safety Research Centre at Loughborough University, 24 partners from 19 different countries were involved in the six different Work Packages which were focussed on policy-making and safety management processes, developing a pan-European in-depth accident investigation network, a data warehouse, decision support, safety and e-safety and driver behaviour monitoring through naturalistic driving.

## The need for in-depth data

In Europe, the main source of macroscopic road safety data is the European Road Safety Observatory (ERSO) which provides annual statistics and basic fact sheets to help to obtain national statistics, monitor trends or identify black spots. However, this macroscopic data cannot address the detailed circumstances of the accidents and lacks comparable injury data to identify the injury mechanisms.

Furthermore, in-depth accident data based on the road environment, vehicle analysis and the road user evaluation with road-user interviews and injury information can provide a case analysis with the impact speed and the accident and injury mechanisms as shown in Figure 2.

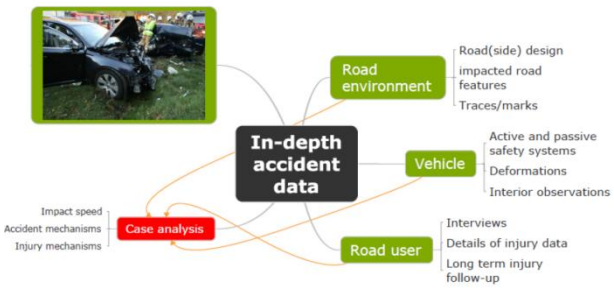


*Figure 2.* Example of information collected in the DaCoTA in-depth accident investigations.

Therefore, in order to develop new policies based on real evidence, we see that there is a fundamental need for in-depth data. In fact, in-depth accident data has been and continues to be used in road safety monitoring, in consumer testing, for setting standards and for research and development. It provides information about the accident and injury outcome in different collision scenarios, allows determination of injury mechanisms and provides valuable information for the design and development of new products.

## Objective of the DaCoTA project

The project aimed to enforce the strength and wealth of information in the Observatory (ERSO) by enhancing the existing data and adding new road safety information with the inclusion of new procedures and methods.

This paper is focused on Work Package 2, which was tasked with formulating a common methodology for research accident investigation and identifying and training new research teams across Europe.

The main goals for WP2 were:

- to identify research priorities requiring in-depth data
- to harmonise in-depth crash investigation methods at an EU level
- to identify and train crash investigation teams who will prepare to make investigations according to these harmonised methods.

The mainstay to reduce road casualties across Europe is to determine effective safety strategies by creating new knowledge based policies.

## METHODOLOGY

During an in-depth accident investigation, two processes can be differentiated: data collection and analysis [5]. These two stages of an investigation must be separately carried out but always connected. When an investigator gathers data from an accident they have to be aware of how the analysis will subsequently be performed to ensure that they get the required information and not less, but this analysis must be done afterwards because of the usual constraints of field work, especially for on-scene investigations.

The developed methodology will therefore cover both stages as separate processes but with a global vision of the accident investigation. More specifically, the methodology establishes a wide range of areas such as investigation routines, necessary equipment, suitable arrangements, safety and more. This paper intends to give an overview of how these areas were approached.

Before the development of the methodology and the database system, the current and future data needs were consulted with key stakeholders to ensure that the focus would be centred on current and future concerns in road safety. In order to carry out this consultation, a matrix of research questions was generated which were rated, based on the complexity and the type of data required providing answers. At this point the identification of causes of accidents in the high fatality rate countries was one of the recurrent issues identified in the different key research areas considered.

After the research survey, all the priorities voiced by DaCoTA partners, EU countries and European organisations and institutions were considered when developing the new in-depth investigation methods. Based on the results of the consultations, the methods were focussed on: on-scene information, vehicle data, road user injury data, human data, accident causation analyses and accident reconstructions [7].

In order to validate the methodology and identify possible improvements concerning the operability, a pilot study was carried out (explained in detail in the Results section of this paper and in [5]).

**The Network**

The culmination of the project was to establish a network of accident investigation teams with standardised methods and data gathering procedures. The Pan-European In-depth Accident Investigation Network consists of the investigating teams which participated in the pilot study (see Figure 3). The Network was composed of a core group including the ten partners in WP2 of DaCoTA and more teams across Europe were invited to participate in the Network.

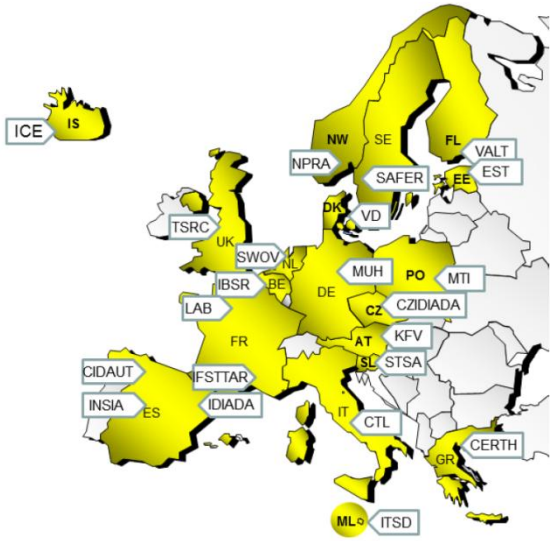


*Figure 3:* The participating teams

The different teams were divided into three different groups depending on the experience they had in in-depth accident investigation. This group division is considered in the methodology and the requirements for each team depend on this expertise classification.

However, all teams have a similar structure consisting of a team leader and multiple investigators. Other roles within the team are also defined, for example, case leader, on-scene investigator, interviewer, DREAM analyst, injury mechanism analyst. This role definition reflects the intention for the teams to be multi-disciplinary.

Another distinctive regard of the defined methodology is the differentiation between on-scene and retrospective investigations. On-scene work is carried out by accident investigators who arrive at the scene of the collision in time to record essential information before it is lost (ideally ≤ 30 minutes after the time when the collision occurred). Retrospective work includes any investigation activities carried out after the rescue of involved people is finished and the scene has been cleared from vehicles involved. Examples of retrospective

working include examining vehicles at a garage / recovery yard, interviewing people over the telephone or by using a postal questionnaire, and visiting the road location hours or days after the collision occurred. All teams can perform both types of investigations but the more experienced teams are encouraged to carry out the scene inspection on-scene.

**Database**

The DaCoTA database was built upon a web application originally developed by the SAFER consortium and was made available for the DaCoTA project. Making adaptations based on the needs and expectations of the DaCoTA project, CTL designed the database that was used in the Pilot study (see Figure A.1 in the Appendix).

The purpose of the final design of the database is to store in a harmonised way in-depth accident data, and to allow the partners to analyse and filter the accidents collected, securely exchange the data collected and share the analysis results. The database is designed to work on-line with a central secure server at CTL but it is also possible to store the data locally. The different operational systems of the database are detailed in Figure 4.

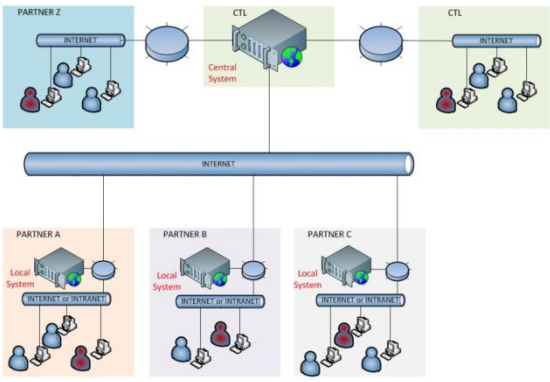


*Figure 4:* Database configured on-line or for local operation

The system is divided into two parts, one data collection section with mostly objective variables and one case analysis section with information on the conclusions of the collected data. After the data gathering, the teams have to fill in up to 1,500 variables per accident. However this number will typically be less depending on the nature of the accident (depending on the number and type of vehicles for example). The database tools and structure (see Figure A.2 in the Appendix) helps to insert the data in an organised and methodological way. The case analysis section provides helpful tools concerning the analysis causation analysis with the DREAM methodology [8] and coding tools for reconstruction and injury analysis.

The data introduction is divided into different items of an investigation (see Figure A.2 in the Appendix). A navigation menu on the left shows the structure of the data gathering and the completion of the information entered. This provides a structured and organised way to fill in all the information. Moreover, this structure leads the investigator to introduce first the observational data available such as from examination of cars or the scene features, and then more analytic points such as DREAM analysis or injury coding and analysis.

Then, depending on the predisposition and the legal limitation of each team, the cases can be made available for further analysis by other Network team members.

It must also be pointed out that, due to the high number of possible variables to be filled, a variable classification has been made. There are approximately 450 core variables which need to be filled in with the corresponding information, and the rest of variables, are considered essential for the completion of a full case by the most experienced teams. Finally, several pictures can be uploaded and classified according to the accident item they relate to. Also reconstruction data can be uploaded as the final analysis part of the accident. More detailed information about the database can be found in [9].

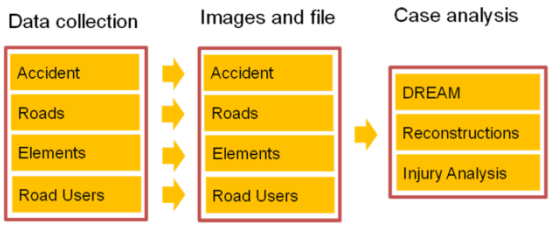


*Figure 5:* Database structure

The application is characterised by being internet accessible, the code is open source, multiplatform, and accessible from any web browser (that supports Adobe Flash). The data is securely stored either on a central or local data server.

Even for the more experienced teams, the database will introduce a new way to gather the data and perform the analysis. To provide all the needed support during the data insertion, all the variables in the database are linked with an openly available online manual to explain what information needs to be introduced for each field of interest to the user.

**The Online manual**

The online manual is the other component of the DaCoTA Crash Investigation System and works alongside the database as explained before. The purpose of the online manual is firstly to provide information about the scope, characteristics and practical requirements of the investigation methodology and secondly to provide detailed information on how to interpret each data variable that should be collected and/or analysed [10].

The on-line manual consists of the following sections:

- Introduction and Acknowledgements.
- DaCoTA Teams.
- Variables.
- Methodology outline.
- Detailed methodology.
- Forms and documents.

The 'DaCoTA teams' section describes all the established teams' features such as the structure and the roles of the investigators as stated before in this paper.

The 'Variables' section consists of a list of all the variables that should be collected within the DaCoTA methodology. These variables are also described in order to standardise the understanding and harmonise the methodology.

Then, the two following sections 'Methodology Outline' and 'Detailed Methodology' describe the methodology that all teams should follow.

Finally, the 'Forms and Documents' section provides all of the necessary material to gather the correct data and guides for use during the inspections and interviews (Figure 6).

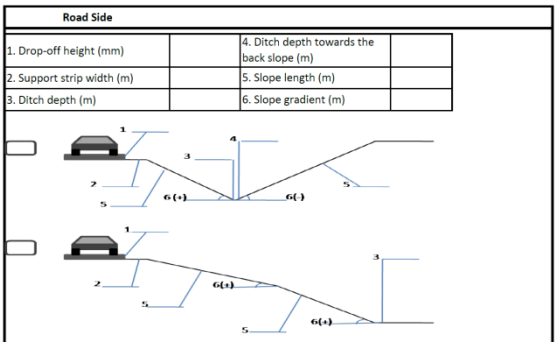

| Road Side | | | |
|---|---|---|---|
| 1. Drop-off height (mm) | | 4. Ditch depth towards the back slope (m) | |
| 2. Support strip width (m) | | 5. Slope length (m) | |
| 3. Ditch depth (m) | | 6. Slope gradient (m) | |

*Figure 6:* Partial view of the road inspection form

The on-line manual provides the DaCoTA Network or any other accident investigation team with complete guidance to carry out accident investigations with an accessible tool. The full manual is publically available at http://dacota-investigation-manual.eu.

**Training**

As explained before, the Network consists of teams from several EU or neighbouring countries with different experience in accident investigation. In order to reduce disparity in experience and provide the new teams with a valuable foundation in DaCoTA accident investigation methodology and tools, a training week was carried out at the IDIADA facilities. In March 2012, 48 delegates attended this training including 26 theoretical and practical sessions performed over 5 days. The theoretical sessions were presented by the experienced DaCoTA core teams in seminar design.

The practical sessions were carried out at IDIADA's proving ground where crashed cars and accident scene representations were examined. During these practical sessions, the delegates were given explanations of the guidelines of the DaCoTA methods and then were invited to collect the evidence that was made available for this purpose.

After the theoretical sessions and the data collection, the delegates were shown how to enter this data into the database. The mixture of theory and practice was greatly appreciated by the delegates. The training week aimed to explain and explore DaCoTA-specific methods to investigators of all experience levels, including the key investigation methods required for DaCoTA, DREAM causation analysis and DaCoTA database training [11].

The topics covered were:

- Preparing an investigation team, including safety at the accident scene.
- Scene examination, including recording visual evidence.
- Vehicle examination.
- Vulnerable road users.
- Collecting road user data.
- Medical/injury information.
- Interpreting the data.
- Using the DaCoTA database.

*Figure 7*: Picture of the vehicle examination practical session

This training week established the baseline to carry out a pioneering in-depth accident investigation pilot study across 18 European countries.

## RESULTS

**Pilot study & Review**

During the period from April to September 2012, the pilot study was carried out following the DaCoTA methodology.

The initial target for the pilot study was to collect 5 cases per partner, ideally collecting a range of collision and road user types at each centre. Although local needs were more specific in some cases - for instance, Italy and Spain focussed on vulnerable road user cases. After the collection, a review process was carried out by the core experienced teams. During this review, each core team revised one case from the other core Network teams and at least one from one of the new teams. After the revision, the conclusions on things that worked well, mistakes and difficulties during the study were pointed out and the possible solutions were determined. These possible improvements are described in the Final Report of the project [5].

Based on the revision parameters established, each core team reviewed up to 5 cases from the other Network teams, performing a quality review which confirmed that the training was beneficial and yielded a high quality database.

The teams participating in this pilot study were able to investigate 99 accident cases (Figure 8) and introduced 77 cases into the DaCoTA database by the end of December 2012. Out of these 77 cases, 46 were investigated on-scene and 31 retrospectively.

The feedback received from all the participants was very positive and provided valuable information to refine the methodology and the DaCoTA database system.

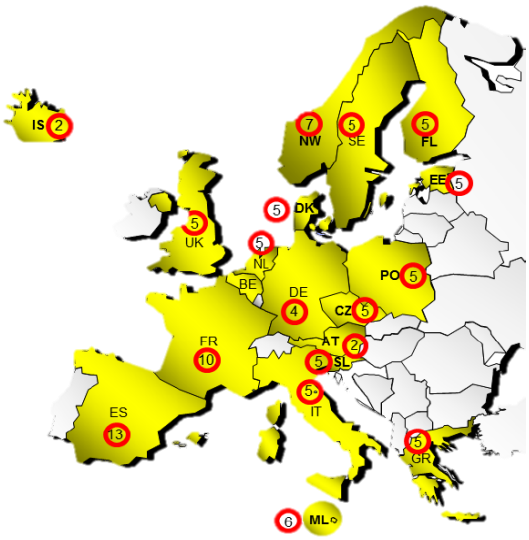


*Figure 8:* Cases collected by all the teams in the pilot study

The main challenges reported during the pilot studies involved the accident reconstructions, DREAM coding and collecting injury information.

About two thirds of the teams could complete the reconstruction information but only one third were able to insert the accident causation coding. After receiving the feedback from the participants, this difficulty was attributed to the unfamiliarity of the teams with the coding system.

The injury information is usually one of the most difficult types of information to collect due to the data protection, ethics or other legislation in many countries. Also the lack of experts able to code the injuries is one of the reasons.

The success of this pilot study is encouraging for a continuation and possible expansion of the Network in the future, especially considering the positive feedback received from the participating teams.

## CONCLUSIONS AND DISCUSSION

Previous EU projects focussed on accident investigation have already pointed out the importance of in-depth data in policy making but DaCoTA has proved that a programme of standardised data gathering across Europe is possible and has great potential.

An accident investigation Network team was created to carry out a pioneering pilot study to compile high quality data in several European countries. This proved that the creation and operation of a Pan-European in-depth accident investigation network and database is feasible and can provide valuable information for researchers and stakeholders.

The pilot study was performed during approximately five months gathering information on 99 new cases.

Continuing with this network and supporting the establishment of the tools developed is a priority for achieving the goal of enhanced road casualty reductions.

It is also encouraging for further developments remarking how 19 different countries worked in a coordinated way, overcoming the different natures of transport mobility and accidents to provide harmonised data across Europe.

A great effort must be focussed in overcoming the limitations in getting certain data like occupant injuries that represents key information for developing new policies and safety systems to prevent road injuries.

The project has achieved its aim to develop a common methodology, establish an investigating team network and overcome the key operational requirements. Beyond the project, a business model must be put in place to enable the continued data collection. It was encouraging to find out that when the partners were asked, only 3 out of 15 acknowledge having difficulties in finding funding to perform the pilot study. In conclusion, there was not just a need and an interest, but also now the willingness supported by a new system and network to carry out in-depth data collection activities across Europe.

## RECOMMENDATIONS

The pilot study yielded very encouraging feedback on the newly developed system and gave excellent ideas for further improvements.

It showed the need for on-going networking and team development activity to ensure the harmonisation of the data and improve the teams' knowledge, learning from each other and sharing the experiences when investigating the accidents.

Several participants have also pointed out the need for improvements in getting medical information based on the guarantee that all the data is anonymised before being added to the database. Personal information is of no interest in an accident investigation of these characteristics. However, during the pilot study it has been noticed that some information could be avoided (like geographical or accident time data) to reinforce the anonymisation of the data collected.

A lot of effort was focused on the creation of the database and the on-line manual, which are high essential, quality tools for carrying out accident investigations following the DaCoTA methods. However, these tools need maintenance and the future business model has to take this into account.

## ACKNOWLEDGMENTS

The DaCoTA project was co-funded by the European Commission within the Seventh Framework Programme. Special thanks go to the many individuals in addition to those named as authors who have contributed to this work from the following countries and institutions. Belgium: Belgian Road Safety Institute (IBSR). Germany: Medical University of Hannover (MUH). Greece: National Technical University of Athens (NTUA) and Hellenic Institute of Transport (HIT). Spain: Jefatura Central de Tráfico (DGT), Institute f. automobile Research (INSIA), Applus IDIADA, and Foundation for Transport and Energy Research and Development (CIDAUT). France: French Institute of science and technology for transport, development and networks (IFSTTAR) and Laboratoire d'Accidentologie (GIE RE PR). The

Netherlands: Institute for Road Safety Research (SWOV). Sweden: Vehicle and Traffic Safety Centre (SAFER), Chalmers University of Technology. United Kingdom: Transport Safety Research Centre (TSRC), Loughborough University.

We are very grateful to all organizations who contributed to the pilot study during 2012. The project partners were joined by other organizations to form the Pan-European In-Depth Accident Investigation Network. The partnership would like to extend our sincere thanks to colleagues from the following organizations for all their help and hard work: Austrian Road Safety Board; Austrian Institute of Technology; Technical University of Graz, Austria; IDIADA Czech Republic; Danish Road Traffic Accident Investigation Board; Estonian Investigation Team; Estonian Road Administration; Finnish Motor Insurers` Centre; Icelandic Road Accident Investigation Team; Transport Malta; Motor Transport Institute, Poland; Norwegian Accident Investigation Board; Norwegian Public Roads Administration; Slovenian Traffic Safety Agency and Volvo Car Corporation.

The DaCoTA partnership would like to acknowledge the contribution of SAFER at Chalmers University of Technology who developed the predecessor to the database and online manual which were given to DaCoTA for subsequent modification and use.

Mostafa Aldah and Rachel Talbot (TSRC, Loughborough University) are acknowledged for their considerable efforts in helping with the coordination of the final project reports and the contents that are reflected in this paper.

## REFERENCES

[1] EUROPEAN COMISSION. *Mobility and transport. Road safety. Trends.* (http://ec.europa.eu/transport/road_safety/specialist/statistics/index_en.htm, 5th March 2013)

[2] THOMAS, PETE, ET AL. *The New European Road Safety Observatory–SafetyNet*. 2006.

[3] INSTITUTE OF TRANSPORT ECONOMICS. *The need for data and evidence to support road safety policy*.**.** Athens : s.n., 2012. European Road Safety Conference on data and knowledge based road safety policy-making. p. 10.

[4] EUROPEAN COMMISSION**.** *Saving 20 000 lives on our roads. A shared responsibility*, 2003.

[5] HILL, J., ALDAH, M., TALBOT, R., MARTINSSON, J., FAGERLIND, H. *Final Updated Protocol with Updates from the Pilot Review*, Deliverable 2.4 of the EC FP7 project DaCoTA, 2012.

[6] DACOTA. *DaCoTA project website*, (http://www.dacota-project.eu/index.html, 5th March 2012)

[7] HAGSTROEM, L., FAGERLIND, H., DANTON, R., REED, S., HILL, J., MARTENSEN, H., MARGARITIS, D., JAHI, H, MORRIS, A. & THOMAS P. *Report on purpose of in-depth data and the shape of the new EU-infrastructure*, Deliverable 2.1 of the EC FP7 project DaCoTA, 2010.

[8] H. WALLÉN WARNER, M. LJUNG AUST, J SANDIN, E JOHANSSON & G. BJÖRKLUND, 2010. *Manual for DREAM 3.0* [online]. Chalmers University of Technology, Gothenburg. [viewed 7/02/2013] Avalaible from: http://www.dreamwiki.eu/

[9] GIUSTINIANI,G., CARROCCIA,R., ROBIBARO, M. *Specification of Data System*, Deliverable 2.2 of the EC FP7 project DaCoTA, 2012.

[10] HILL, J., ALDAH, M. TALBOT, R., GIUSTINIANI, G., FAGERLIND, H., JÄNSCH, M. *Final Report*, Deliverable 2.5 of the EC FP7 project DaCoTA, 2012.

[11] ATALAR, D., TALBOT, R., HILL, J., *Training Package including training manual and draft protocols*, Deliverable 2.3 of the EC FP7 project DaCoTA, 2012.

# APPENDIX

***Figure A.1.*** **View of the DaCoTA database tool.**

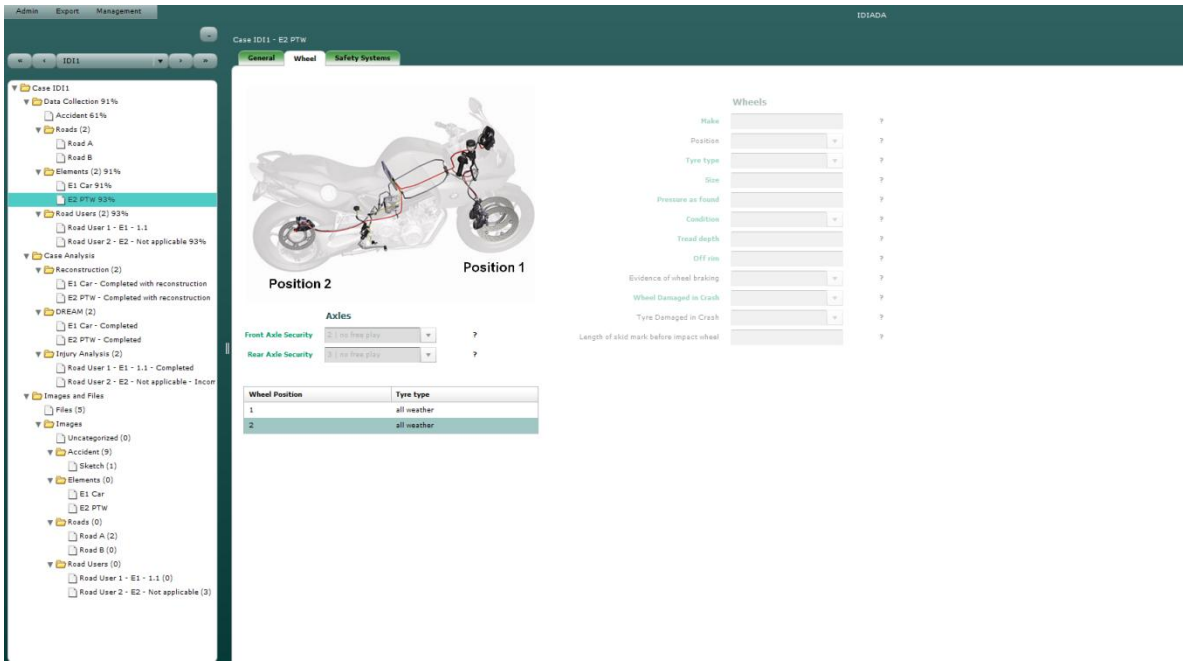


***Figure A.2. Welcome page of the On-line manual website***

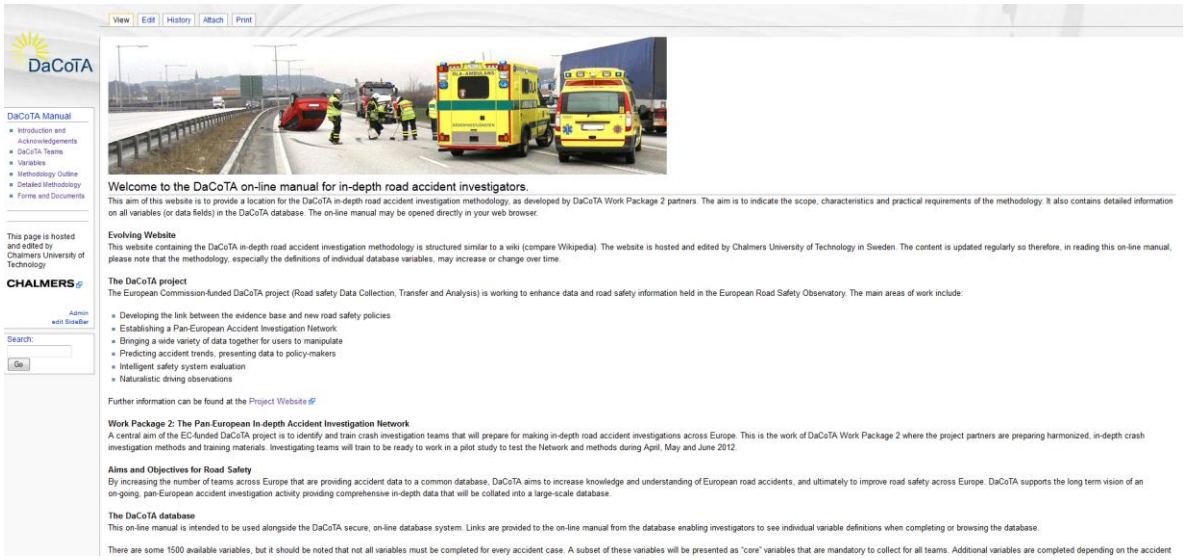

# PRECRASH DATA COLLECTION IN NHTSA'S CRASH DATABASES

**Mark Mynatt**
**Greg Radja**
National Highway Traffic Safety Administration
United States of America
Paper Number 13-0371

## ABSTRACT

The National Highway Traffic Safety Administration (NHTSA) has been gathering precrash information in its nationally representative crash data collection programs since the early 1980's. The various precrash elements, which describe the actions of a vehicle and driver leading up to a crash, will be a key source of data as focus on crash avoidance countermeasures and intelligent transportation systems increase in the automotive safety community. The purpose of this paper is to describe the evolution of precrash coding in NHTSA's crash databases and briefly explain the methodology that provides the basis for these elements. Additionally, the paper will offer an overview of the precrash detail available and differing data collection techniques used in the National Automotive Sampling System (NASS) General Estimates System (NASS-GES), the NASS Crashworthiness Data System (NASS-CDS), and the National Motor Vehicle Crash Causation Survey (NMVCCS). A set of crashes common to all three nationally representative programs will be examined, comparing the precrash element coding and discussing limitations to consider when using data from each of the programs.

## INTRODUCTION

NASS began in 1979 with a mission to provide nationally representative data on fatal and nonfatal motor vehicle traffic crashes for use in developing and evaluating federal motor vehicle safety standards and other safety countermeasures. In 1988 the program was re-evaluated and NASS was split into two components to focus more on crash protection performance: NASS-GES and NASS-CDS.

NASS-GES is designed to provide statistical information to monitor large scale trends on the general characteristics of the nation's police-reported traffic crashes. NASS-GES codes roughly 50,000 police accident reports (PARs) from 60 Primary Sampling Units (PSUs) across the country each year. Approximately 120 data elements are coded, some describing the precrash phase, from the information available on the PAR.

NASS-CDS begins with selection of the PAR. Researchers then conduct detailed investigations on light motor vehicle crashes at 24 PSU's, collecting data on vehicle damage, injury, injury mechanism, and the precrash phase of the crash. NASS-CDS averages about 4,500 cases annually with an emphasis on fatal and severe injury crashes. Trained researchers inspect the crash scene and vehicles, interview the involved drivers, and obtain occupant medical records. These follow-on investigations are typically initiated within 1-2 weeks of the crash.

The National Motor Vehicle Crash Causation Survey (NMVCCS) was a nationally representative survey of light vehicle crashes conducted by NHTSA from 2005-2007 using Emergency Medical Services (EMS) notification as the primary case initiation criteria. Trained researchers conducted on-scene investigations on nearly 7,000 crashes during the project, focusing on the precrash phase of the crash. Investigating the selected crashes on-scene, in most cases within minutes, allowed the researchers to make better assessments of the events that led up to the crash. The survey collected up to 300 data elements on the driver, vehicle, and environment.

In its early years NASS collected only limited information on the actions of the vehicle and driver leading up to the crash. From 1982-1984 any Avoidance Maneuvers taken and the Last Three Actions Prior to the Avoidance Maneuvers were coded in an initial attempt to add insight into the precrash phase [1]. A key element was added in 1985, Accident Type, which was based on the CALAX collision taxonomy developed by Kenneth Terhune [2, 3]. Accident Type was important because it offered a shorthand method for describing and communicating the essential features of the collision event, allowing analysts to group crashes for countermeasure development [4]. When NASS split into the two separate components in 1988, GES and CDS, Avoidance Maneuver and Accident Type were retained in both systems [5]. GES also included a

new variable, Vehicle Maneuver, which was a precursor to the the current Movement Prior to Critical Event element [6].

Precrash data collection in NASS-GES and CDS as we now know it began in 1992. The elements describe the precrash phase of the crash in further detail based on the concept of a critical crash envelope which was originally outlined by Kenneth Perchonok in the early 1970's [7]. It's important to note that when precrash was introduced in NASS, NHTSA elected not to use Perchonok and Terhune's methodologies in their purest forms, instead implementing adaptations of their ideas updated for use in crashworthiness-based systems.

The idea of a critical crash envelope is initially confusing to many; however, once a few key concepts are understood the precrash elements are relatively straightforward. The most important determination that must be made for each vehicle in the crash is identification of the crash envelope and the critical event. The critical crash envelope begins when the driver recognizes impending danger or when the vehicle is in an imminent path of collision. The envelope ends when the vehicle has an impact or when the driver has made a successful avoidance maneuver, has full steering control, and the vehicle is tracking. There are three types of critical crash envelopes: simple single, complex single, and multiple. The cornerstone of the critical crash envelope is the critical event. The critical event is the action or event that placed the vehicle on a course such that the collision was unavoidable. In other words, the critical event makes the crash inevitable.

A precrash method protocol commonly referred to as the "but for" test, which was borrowed from the Indiana Tri-Level Study [8], is used to assist in determining the critical event. One must ask what action by this vehicle, another vehicle, person, animal, or object was critical to this driver becoming involved in the crash? For example, "but for" the other vehicle going left-of-center, this vehicle would not have been involved in this crash. Or "but for" having entered into the intersection, this vehicle would not have been involved in this crash. Through the years, a set of ten precrash general rules have also been developed to offer guidance for coding consistency [9]. Once the critical crash envelope and critical event are identified, all the remaining precrash elements are coded relative to this selected critical event. It's essential to not consider culpability as a factor for determining precrash data. Many scenarios suggest fault, but this is considered coincidental rather than by design.

The precrash elements as a whole are designed to identify the following:

1. What was the vehicle doing just prior to the critical event?
2. What made the situation critical?
3. What was the avoidance response, if any, to this critical situation?
4. What was the movement of the vehicle just prior to impact? [10].

In an effort to collect more precrash information in its data collection systems, NHTSA elected to incorporate the seven basic precrash elements into the Fatality Analysis Reporting Sytem (FARS) in 2010 [11]. FARS is a nationwide census providing yearly data regarding fatal injuries suffered in motor vehicle traffic crashes. Similar to NASS-GES, the primary source of information in FARS is the police report.

Figure 1 shows the chronological order of the seven core elements used to describe a single crash envelope in NASS-GES, NASS-CDS, and FARS.

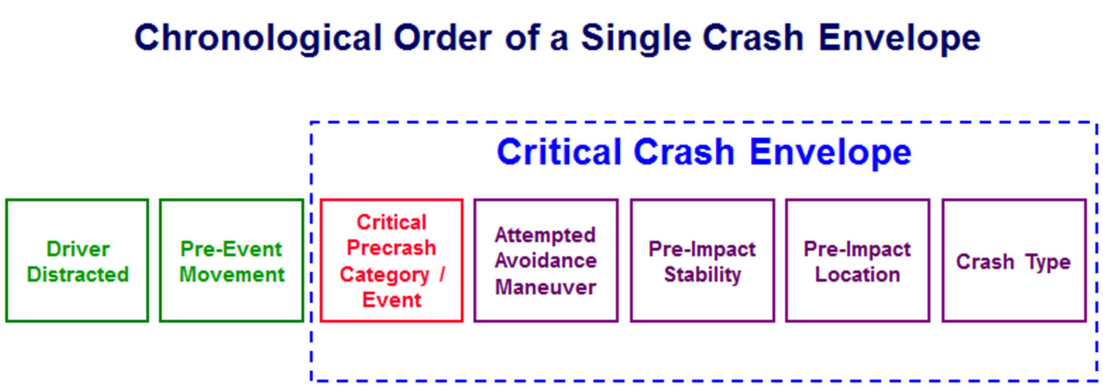


**Figure 1**

Two programs focusing on crash causation, the Large Truck Crash Causation Study (LTCCS) 2001-2003 and NMVCCS 2005-2007, expanded precrash coding to include more components of Perchonok's causal methodology such as the Critical Reason for the Critical Event and Associated Factors. The foundation of his approach is that there is no single specific cause of a given crash; rather, it views crashes as a process consisting of interrelated events and conditions [12]. This series of events leading to a crash is commonly referred to as the causal chain. Remove any one of the links in the chain, and a crash may not have occurred.

Due to the researchers' unique on-scene perspective in LTCCS and NMVCCS, the core precrash elements, as well as other important components of the casual chain, Critical Reason, and Associated Factors could be coded with a high degree of accuracy [13]. The Critical Reason is the immediate reason for the Critical Event and describes why the Critical Event occurred [14]. Although the Critical Event and Critical Reason are principal parts of the description of the crash, it should be noted that they do not imply the cause of the crash or assignment of fault. The primary purpose of these elements is to enhance the description of events and allow analysts to better categorize similar events [15]. Additionally, the two causation programs collected a multitude of information on the Associated Factors in the crash including the Driver's Condition, Recognition, Decision, Performance, and Emotional Factors. Factors associated with the vehicle, highway, and environment were collected as well.

Figure 2 shows the chronological order of the elements used to describe a single crash envelope in LTCCS and NMVCCS.

Here's a simple example to demonstrate precrash coding of the PAR-based and follow-on programs:

A teenage driver was on his way home from school after finals. He was tired from studying late the night before and decided to call a friend to see how they did on the test. When he looked down momentarily to begin dialing a cell phone the vehicle drifted off the right side of the road. The driver realized he departed the road and attempted to steer left just prior to striking a tree.

| | |
|---|---|
| Driver Distraction | Distracted/Dialing cell phone |
| Pre-Event Movement | Going straight |
| Critical Event | Off edge of road on right side |
| Avoidance Maneuver | Steering left |
| Pre-Impact Stability | Tracking |
| Pre-Impact Location | Departed roadway |
| Crash Type | Single driver/<br>Right roadside departure/<br>Drive off road |

Using the same example, in addition to the seven basic precrash elements, the on-scene programs would include the critical reason and associated factors in the crash.

| | |
|---|---|
| Critical reason | Internal distraction |
| Associated Factors | Fatigue<br>Inexperience<br>Internal distraction |

**Figure 2**

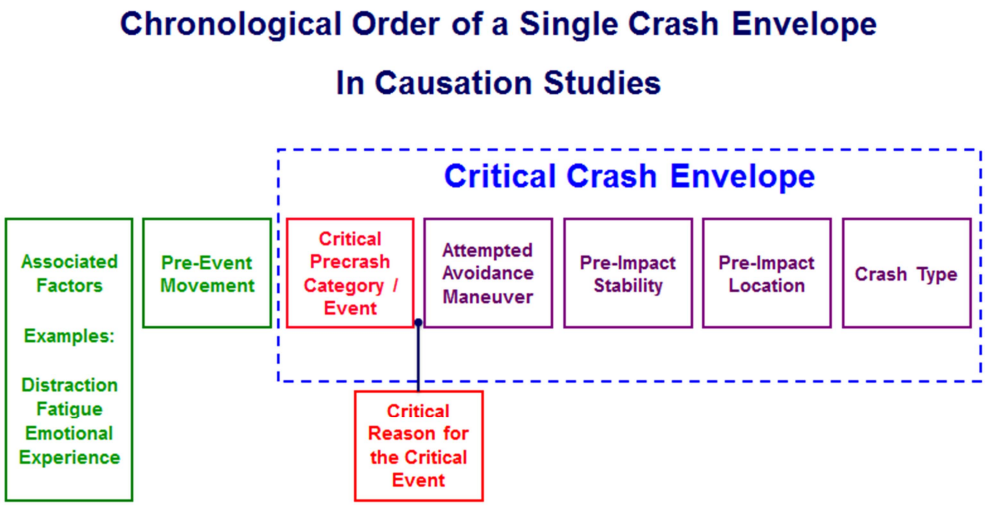

The LTCCS and NMVCCS approaches to causation data collection and analysis were discussed in depth by Dan Blower and Kenneth Campbell in a LTCCS analysis series paper sponsored by the Federal Motor Carrier Safety Administration (FMCSA). They describe that the methodology used in these two programs is based around the view of traffic crashes as probabilistic events and how the causation information collected is best analyzed using statistical associations of the aggregate data and not clinical methods. In the statistical method, causation is not determined by researchers at the data collection stage. In fact, the causes of specific crashes are not assigned at any point. Instead, crash cause is identified in terms of changes in risk. However, Blower and Campbell go on to mention that due to the extensive amount of objective information about precrash events collected, these types of programs can support clinical methods of assessing causation [16]. One such clinical review of NMVCCS fatalities was conducted by a NHTSA multi-disciplinary team in 2011. They found that the data available in the NMVCCS cases was sufficient to determine critical and secondary factors which contributed to the crash and possible crash prevention measures [17].

As a testament to their sound foundation, the precrash elements have seen very little change since their introduction in 1992. A history of the core precrash elements from NASS-GES, NASS-CDS, and NMVCCS is included in appendix A.

**METHOD**

During a three year period between 2005 and 2007 there were three nationally representative NHTSA programs with precrash information available being conducted concurrently at 24 sites across the country, NASS-GES, NASS-CDS, and NMVCCS. Although the three programs have very different purposes - NASS-GES (large scale statistical trends), NASS-CDS (detailed crashworthiness), and NMVCCS (causation data) – they are similar in that each collected the same basic precrash data elements. However, due to their separate objectives, a major difference in the programs is the sources with which to code the precrash elements. NASS-GES is limited to the police crash report. NASS-CDS uses follow-on vehicle and crash scene inspections and driver interviews along with the police report. NMVCCS collected data from the scene, vehicle, and drivers on-scene, usually within minutes of the crash. This paper compares the precrash data coding in common cases from each of the three programs to examine differences that may occur due to additional sources of information.

A query of NHTSA's internal databases was conducted to identify crashes common to the three programs. Cases were identified by matching the following:

1. Sites or Primary Sampling Units (PSUs),
2. Date and time,
3. Vehicle Year/Make/Model,
4. Vehicle identification number (VIN)

Each case was then evaluated individually to determine applicability to this review. There were unknown VINs from certain states in NASS-GES, but the cases were included in the study if all other matching criteria were met.

Five of the basic precrash elements were compared among all three programs:

Distraction/Inattention
Attempted Avoidance Maneuver
Pre-Impact Stability
Pre-Impact Location
Crash Type

Two of the precrash elements - Pre-Event Movement and Critical Event - could only be compared between NASS-GES and NASS-CDS due to subtle differences in their coding convention in NMVCCS. The different coding convention was tied to timing nuances in the crash configurations. In NMVCCS the Movement Prior to the Critical Crash Envelope was typically described as two stages prior to crash occurrence [18].

**RESULTS**

A total of 379 crashes involving 653 vehicles were eventually determined to be present in all three programs.

The first precrash element compared was Driver Distraction. In recent years distracted driving has been one of the areas most emphasized by the Department of Transportation and NHTSA with the development of guidelines, public awareness campaigns, and increased enforcement. In this review the elements and attributes used to determine the presence of a distraction were the same ones utilized in the NHTSA Traffic Safety Facts Research Note on distracted driving published in 2010 [19]. Table 1 shows the percentage of the common vehicles with a coded Distraction in each of the programs.

**Table 1**
**Common Vehicles with a Distraction Present**
**(Percentages rounded)**

| Distraction | NASS-GES | NASS-CDS | NMVCCS |
|---|---|---|---|
| Yes | 11% | 14% | 28% |
| No | 60% | 46% | 48% |
| Unknown | 30% | 40% | 24% |

As Table 1 indicates, in these same vehicles a Distraction was coded in the on-scene program twice as often as in the follow-on program; and 2½ times more often than in the PAR-based program. The on-scene based program also had a lower percentage of Unknown Distraction coding. Figure 3 displays the comparability of Distraction coding between the programs when grouping the various attributes in each data collection program into Yes, No, or Unknown.

**Figure 3**
**Distraction Coding Agreement**
**Between Programs**
**(Yes, No, or Unknown)**

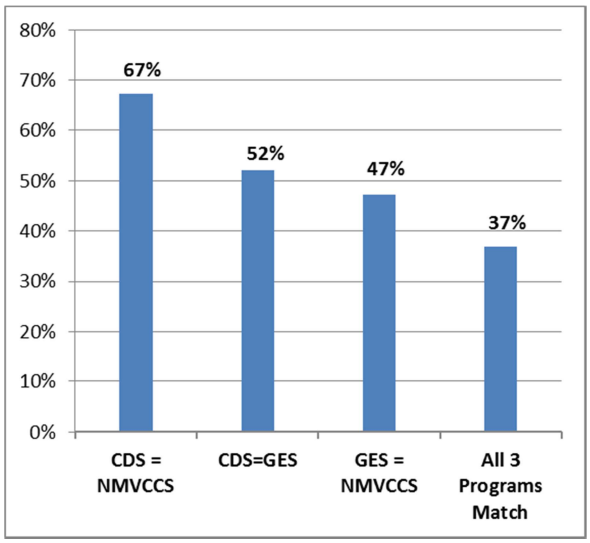


Attempted Avoidance Maneuver is another key precrash element in the NHTSA data collection programs that will be widely used in the future as the focus on crash avoidance becomes more prevalent in the industry. This element provides important information towards identifying the driver's actions leading up to a crash that are essential in development of new technologies such as auto/assisted braking and forward collision warning.

Table 2 presents the percentage of the vehicles common to the three programs with a coded Avoidance/Corrective Maneuver.

**Table 2**
**Common Vehicles with an Avoidance Action Present (Percentages rounded)**

| Avoidance | NASS-GES | NASS-CDS | NMVCCS |
|---|---|---|---|
| Yes | 16% | 35% | 40% |
| No | 17% | 40% | 51% |
| Unknown | 67% | 25% | 9% |

As Table 2 indicates, in these same vehicles an Avoidance Maneuver or Corrective Action was coded in the on-scene program 2½ times more often than in the PAR-based program, but only 5% higher than in the follow-on program. The on-scene based program had a much lower percentage of Unknown Avoidance coding than the other programs due their quick response to the scene and contact with the drivers. Figure 4 shows the percentage of cases between programs with the same Avoidance Maneuvers coded.

**Figure 4**
**Avoidance Coding Agreement**
**Between Programs**
**(Specific Maneuvers/Actions)**

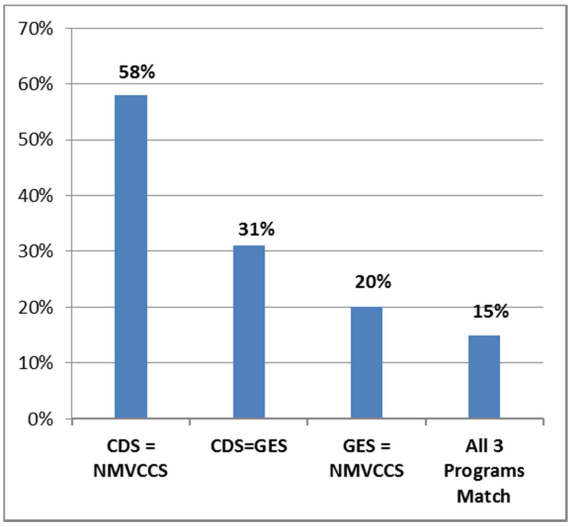


While the correlation between the programs in the first two elements presented was generally low, some of the precrash elements do have a very high degree of consistency between programs. Figures 5 and 6 respectively show the Pre-Impact Stability and Pre-Impact Location coding of the vehicles common to all three data collection programs.

**Figure 5**
**Pre-Impact Stability Coding Agreement Between Programs**

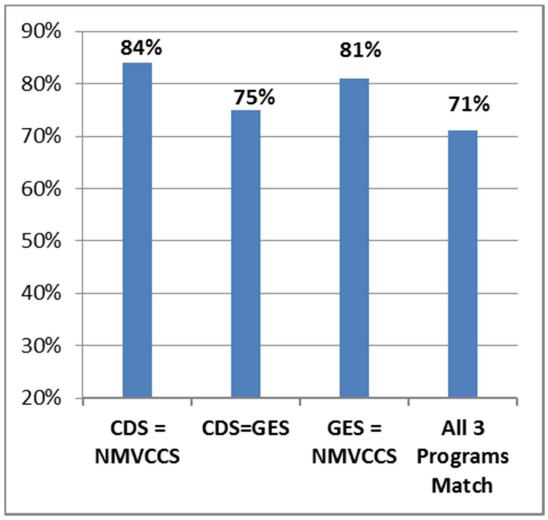


**Figure 6**
**Pre-Impact Location Coding Agreement Between Programs**

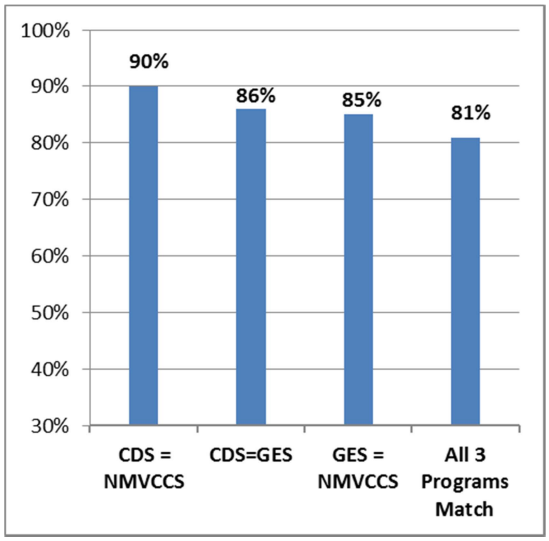


The Crash Type element will also be very important to data users as crash avoidance countermeasures and intelligent transportation system development continues. The element is particularly valuable when estimating potential safety benefits of technologies such as lane departure warning, forward collision warning, auto/assisted braking, blind spot detection, or electronic stability control. Figure 7 illustrates the Crash Type coding of the vehicles common to all three programs.

**Figure 7**
**Crash Type Coding Agreement Between Programs**

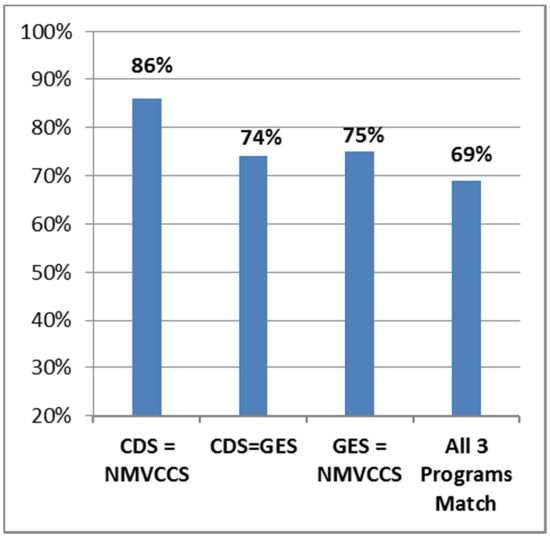


As mentioned earlier since there were subtle differences in the NMVCCS methodology of determining the Pre-Event Movement and Critical Event, NMVCCS was excluded from the evaluation of those elements. Other precrash data elements such as Critical Reason and Associated Factors were also not examined because they are not collected in NASS-CDS or GES. Figure 8 shows the Pre-Event Movement and Critical Event coding of the vehicles common to NASS-GES and NASS-CDS.

**Figure 8**
**Pre-Event Movement and Critical Event Coding Agreement Between Programs**

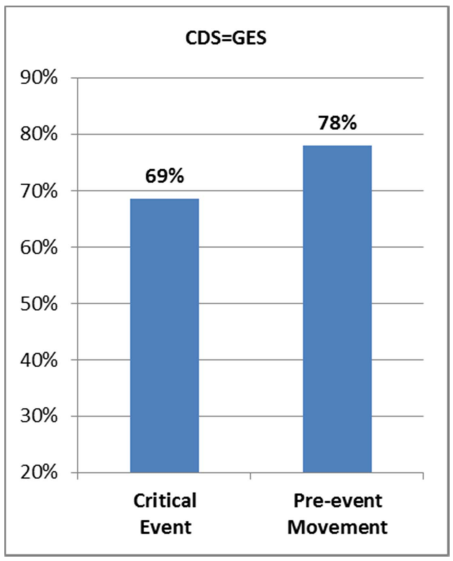

## DISCUSSION

The results suggest there are some differences in the precrash coding of the crashes common to all three data programs. Further examination revealed several issues likely responsible for these discrepancies. The most significant factor is the amount of information on the precrash phase of the crash available given the data collection method. PAR-based data collection used in NASS-GES has the least amount of data available to make precrash assessments. As discussed in the introduction, some of the information necessary to determine crash envelopes and other important precrash facts can be difficult to determine, particularly with limited materials. Although many states have elected to adopt NHTSA's Model Minimum Uniform Crash Criteria (MMUCC) for their police reports, only a handful of the MMUCC coded elements help with precrash coding [20]. Most of the precrash elements must be determined by NASS-GES coders using information from the coded boxes on a police report in conjunction with a crash narrative that may or may not have significant detail. The primary purpose of a police report is not an in-depth look at the actions of the vehicle and driver leading up to a crash.

Another difficulty faced by NASS-GES, and NASS-CDS to a lesser extent, is that several of the precrash elements depend on knowing actions taken by the driver and their intent. Not coincidently, these data elements - Distraction, Avoidance Maneuver, Critical Event and Crash Type - are the elements with the lowest amount of consistency between the programs. Driver actions and intentions are typically described on a limited basis in police reports; instead they normally require a driver interview to assess with a high confidence level. Experience has shown that the sooner a driver interview is conducted and the scene is inspected, the more reliable the information.

It's very important to acknowledge that due to extensive quality control efforts, in-depth training, and investigator/coder experience, each of the NHTSA data collection programs discussed have shown over the years to have very high coding reliability rates. In general, the precrash data in the cases is coded correctly based on the information they have available to them.

Of the three data collection methods discussed, there is no debate precrash data from on-scene causation-based programs give the most accurate portrayal of the events and actions of the driver leading up to a crash. This study also demonstrates that investigation-based programs utilizing follow-on methods achieve good results. However, these investigation-based methods have a much higher cost per case, require elevated degrees of local law enforcement cooperation, and need highly trained personnel to collect the data. Herein lies the advantage of PAR-based programs like NASS-GES. NASS-GES is able to produce a large number of cases at a fraction of the cost of more in-depth data collection methods. In addition, due to the larger sample size, statistically analyzing the NASS-GES data more closely approximates the represented population. The drawback to PAR-based programs is that some of the precrash elements could dramatically underestimate important details necessary for countermeasure development such as driver distraction and avoidance maneuver. In the 653 vehicles examined in this study Distraction and Avoidance Maneuvers were underreported by 2½ times compared to NMVCCS. There was also a large discrepancy in Critical Event coding, the cornerstone of the precrash methodology. As one would expect, unknown values in NASS-GES were much higher as well. To reiterate, precrash data is not a primary focus of police crash reporting.

Note that this study can only compare crashes common among the three systems, which are mostly severe in nature. Conclusions only represent the most stringent qualification criteria shared in these systems (towed light vehicle, etc.). Other, less severe crashes cannot be evaluated in this study. Therefore, conclusions made in this paper may not be representative of any of the three data programs as a whole.

## CONCLUSION

NHTSA's data collection programs have been collecting information on the events and factors leading up to a crash for many years. The precrash data available in the various data systems is based on sound methodologies widely accepted in the auto safety community. In the future the precrash elements will be used even more extensively as emphasis in the industry shifts from vehicle crashworthiness toward crash avoidance and intelligent transportation systems. The data collected by NHTSA will be crucial in identifying crash scenarios a given technology could potentially prevent or mitigate, as well as in the evaluation of their effectiveness once implemented.

Over the years precrash information has been collected by NHTSA's data programs using three different methods:

1. Gathering data from the police report (NASS-GES),
2. Follow-on vehicle and crash scene inspections and driver interviews along with the police report (NASS-CDS),
3. On-scene vehicle and scene inspections and driver interviews (NMVCCS)

Each of the collection methods has advantages and disadvantages: number of cases available, statistical strength, cost, level of detail, and how accurately the crash circumstances are portrayed.

Examining a set of cases with data collected using all three of these methods on the same crashes revealed significant differences in coding for some of the precrash elements. The disparities were largely attributed to the varying amounts of information available to the investigators and coders based on the data collection method. When analyzing NHTSA's precrash data, caution should be exercised to use data from the program that provides the level of detail and accuracy needed to achieve the objective.

**References**

[1] National Center for Statistics and Analysis, "National Automotive Sampling System (NASS) Analytical User's Manual 1982". U.S. Department of Transportation, National Highway Traffic Safety Administration, 1982.

[2, 4] Terhune, K. "CALAX: A Collision Taxonomy for Research and Traffic Records", Journal of Safety Research, Volume 14, pages 13-20, 1983.

[3] National Center for Statistics and Analysis, "National Automotive Sampling System (NASS) Analytical User's Manual 1985". U.S. Department of Transportation, National Highway Traffic Safety Administration, 1985.

[5] National Center for Statistics and Analysis, "National Automotive Sampling System (NASS) Crashworthiness Data Substem Analytical User's Manual 1988". U.S. Department of Transportation, National Highway Traffic Safety Administration, 1988.

[6] National Center for Statistics and Analysis, "National Automotive Sampling System (NASS) General Estimates System (GES) Analytical User's Manual 1988-2005". U.S. Department of Transportation, National Highway Traffic Safety Administration, 2005.

[7,12,14] Perchonok, K. "Accident Cause Analysis", Cornell Aeronautical Laboratory Inc., DOT HS 053-1-109, July 1972.

[8] Institute for Research in Public Safety School of Public and Environmental Affairs Indiana University. "Tri-Level Study of the Causes of Traffic Accidents: Interim Report Volume I Research Findings", Indiana University, DOT HS 034-3-535-73-TAC, August 1973.

[9,10] National Center for Statistics and Analysis, "National Automotive Sampling System (NASS) Crashworthiness Data Sytem (CDS) Coding and Editing Manual 2006". U.S. Department of Transportation, National Highway Traffic Safety Administration, 2006.

[11] National Center for Statistics and Analysis, "2010 FARS Coding and Validation Manual". U.S. Department of Transportation, National Highway Traffic Safety Administration, DOT HS 811 530, December 2011.

[15] Toth, G. et al, "Large Truck Crash Causation Study in the United States", ESV 2003, Paper Number 252.

[16] Blower, D., Campbell, K., "Large Truck Crash Causation Study Analysis Series", FMCSA –RI-05-035, February 2005.

[13, 17] Mynatt, M. "A Study of NMVCCS to Identify Critical Precrash Factors in Fatal Crashes", ESV 2011, Paper Number 11-0168.

[18] National Center for Statistics and Analysis, "NMVCCS Field Coding Manual". U.S. Department of Transportation, National Highway Traffic Safety Administration, DOT HS 811 051, December 2008.

[19] Traffic Safety Facts: Distracted Driving 2009, DOT HS 811 379, September 2010.

[20] MMUCC Guideline, Model Minimum Uniform Crash Criteria, Fourth Edition, DOT HS 811 631, August 2012.

**APPENDIX A**

**History of Core Precrash Elements in NASS and NMVCCS**
**[SAS DATASET.ELEMENT in brackets]**

**NASS (prior to 1988 separation of GES and CDS)**

1982-1984

Third to last action prior to avoidance maneuvers
[DRIVER.PRIORREAR]
Second to last action prior to avoidance maneuvers
[DRIVER.PRIORMID]
Last action prior to avoidance maneuvers
[DRIVER.PRIORLAT]
Attempted avoidance maneuvers
[DRIVER.AVOIDMAN]

1985-1987

Attempted avoidance maneuvers
[DRIVER.AVOIDMAN]
Accident type
[DRIVER.ACCTYPE]

**NASS-GES**

1988-1989

Vehicle maneuver
[VEHICLE.MANEUVER]
Accident type
[VEHICLE.ACC_TYPE]

1990-1991

Driver distracted by
[VEHICLE.DR_DSTRD]
Vehicle maneuver
[VEHICLE.MANEUVER]
Accident type
[VEHICLE.ACC_TYPE]

1992-1995

Driver distracted by
[VEHICLE.DR_DSTRD]
Movement prior to critical event
[VEHICLE.P_CRASH1]
Critical precrash event
[VEHICLE.P_CRASH2]
Corrective action attempted
[VEHICLE.P_CRASH3]
Vehicle control after corrective action
[VEHICLE.P_CRASH4]
Vehicle path after corrective action
[VEHICLE.P_CRASH5]
Accident type
[VEHICLE.ACC_TYPE]

**NASS-GES (continued)**

1995-2011

Driver distracted by
[VEHICLE.DR_DSTRD]
2002-[DISTRACT.MDRDRSTRD]
Movement prior to critical event
[VEHICLE.P_CRASH1]
Critical precrash event
[VEHICLE.P_CRASH2]
Corrective action attempted
[VEHICLE.P_CRASH3]
2002-[MANEUVER.MDRMANAV]
Precrash vehicle control
[VEHICLE.P_CRASH4]
Precrash location
[VEHICLE.P_CRASH5]
Accident type (Crash type Beginning 2011)
[VEHICLE.ACC_TYPE]

**NASS-CDS**

1988-1991

Attempted avoidance maneuver
[GV.MANEUVER]
Accident type
[GV.ACCTYPE]

1992-1995

Pre event movement
[GV.PRMOVE]
Critical precrash event
[GV.PREEVENT]
Attempted avoidance maneuver
[GV.MANEUVER]
Precrash stability after avoidance maneuver
[GV.PRESTAB]
Precrash directional consequences of avoidance maneuver
[GV.CONSEQ]
Accident type
[GV.ACCTYPE]

**NASS-CDS (continued)**
1995-2010
Drivers distraction/inattention to driving
[GV.DRIVDIST]
Pre event movement
[GV.PRMOVE]
Critical precrash event
[GV.PREEVENT]
Attempted avoidance maneuver
[GV.MANEUVER]
Pre impact stability
[GV.PREISTAB]
Pre impact location
[GV.PREILOC]
Accident type
[GV.ACCTYPE]

**NMVCCS**
2005-2007
Driver distraction (multiple associated factor elements are used)
[PCA.OTDRACT]
[PCA.CONVERSE]
[PCA.EXTFA]
[PCA.INATTEN]
Movement Prior To Critical Crash Envelope
[PCA.PREMOVE]
Critical precrash event
[PCA.PREEVENT]
Critical reason for the critical precrash event
[PCA.CRITREASON]
Attempted avoidance maneuver
[PCA.AVMAN]
Pre impact stability of vehicle
[PCA.PREISTAB]
Pre impact location on trafficway
[PCA.PREILOC]
First harmful event crash type
[PCA.ACCTYPE]

# EVALUATION METHOD OF THE EFFECTIVENESS OF ACTIVE SAFETY TECHNOLOGIES IN LIGHT GOODS VEHICLES BASED ON REAL WORLD ACCIDENTS RECONSTRUCTION

**Francisco Javier, Páez Ayuso**
**Arturo, Furones Crespo**
University Institute of Automobile Research (INSIA) – Technical University of Madrid (UPM)
Spain
Paper Number 13-0480

## ABSTRACT

There are limited data in Europe on light goods vehicles (LGVs) crashes. The project IMPROVER shows that the country of the EU-25 with the highest number of fatalities in accidents involving LGVs is Spain (2002).

The aim of this paper is the evaluation of the accident reduction which could be achieved by incorporating active safety technologies to LGVs involved in crashes, based on a reconstruction evaluation method.

The methodology is based on a retrospective analysis of the accident technical reports from the Spanish Traffic Directorate (DGT). It comprises 254 fatal accidents with LGVs involved, occurred in rural roads during 2009 and 2010. This information has been analysed to identify the most significant stages (independent variables) during the pre-crash phase based on the HFF method. Afterwards a classification tree has been created using those independent variables and their interactions to describe and quantify their influences on LGV accidents.

Accidents have been analyzed and evaluated considering the assumed effect of each specific active safety system proposed –ABS, BAS and ESP-. Every case has been simulated using the PC-Crash® software. Two crash situations have been modelled: the first one is a reconstruction of the real accident and the second one is a simulation in which the operation of the active systems is emulated modifying the collision parameters and its potential consequences.

This study makes the identification of critical parameters easier and it simplifies the development of practical solutions by quantifying their potential impact on future actions to improve LGVs safety. Reconstructions of these accidents were performed using software techniques to estimate multiple parameters from the collision, the pre- and post-impact phases. The gathered information has been used for the evaluation of the effectiveness of the Antilock Brake System (ABS), the Brake Assist System (BAS) and the Electronic Stability Programme (ESP). The performance of these systems has been simulated in reconstructions, so it is possible to assess their capacity for the avoidance of the analysed accidents.

The implementation of active safety technologies in all new vehicles will lead to achieve reductions in LGVs-involved accidents or to decrease their severity. In order to assess the safety performance of these vehicles it is necessary to be able to identify these vehicles data relating to accident involvement, vehicle registration and vehicle usage. It would improve any future evaluations of LGVs safety performance or help to monitor the effects of any policy decisions.

For many years numerous studies have conducted to estimate the effectiveness of safety systems for vehicles. However, the most of these ones has been focused on passenger cars and clear gaps were detected in the case of specific studies on LGVs.

Although the performance of active safety technologies explains basically their behaviour in test conditions, they are not enough to assess their success in each real world scenario. A full forecast of their potential is only possible by modelling the driver-vehicle-system-environment. The reconstruction of real world accidents is the core tool of the proposed method.

## INTRODUCTION

There are limited data in Europe on light goods vehicles (LGVs) crashes. In-depth work has been carried out in Britain (Lenard, J. et al., 2000 [5]) and Germany (Niewohner, W et al., 2001 [6]). These investigations indicate that while LGVs do not have a higher crash rate than other motor vehicles, crashes tend to occur in predominantly urban environments.

The growing problem of accidents in the transport of goods in light vehicles has been undertaken in some studies in Europe. The project IMPROVER (Höhnscheid et al., 2006 [2]) shows that the country of the EU-25 with the highest number of

fatalities in accidents involving LGVs is Spain (2002).

In Spain, accidents involving LGVs account for 9,5 % of the total accidents (average value in the period 2000 - 2010). The evolution of road accidents in this period of time (*Figure 1*) draws: a low variation in 2000 - 2003; a reduction in 2003 - 2005; and a high increase in 2005 - 2007 especially in accidents involving LGVs.

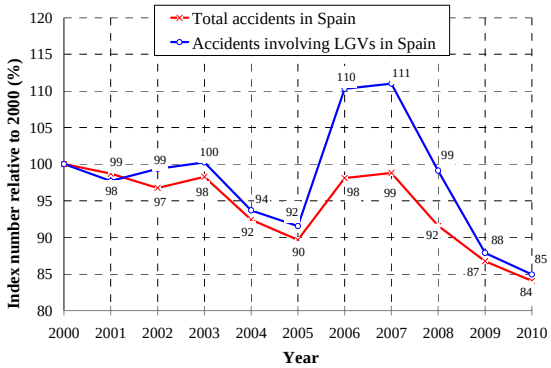


*Figure 1*. Evolution of accidents involving LGVs in Spain per year (2000 - 2010).

In order to assess the safety performance of LGVs it is necessary to identify data of these vehicles in accident databases. Many EU Member States do not collect information on goods vehicles of this size and many use different definitions of smaller goods vehicles that could not be made to fit the European definitions. The type of vehicle "LGV" as considered in this paper includes two categories:

- Category 1 (C1): N1, vehicles designed and constructed for the carriage of goods and having a maximum mass not exceeding 3,5 tonnes (extracted from 2007/46/EC [7]). This definition is consistent with "Light Goods Vehicle, LGV" or "Light Commercial Vehicle, LCV".

- Category 2 (C2): car-derived LGV, a variant of a passenger car design that has been adapted to carry goods.

The aim of this paper is the evaluation of the accidents reduction which could be achieved by incorporating active safety technologies to LGVs involved in crashes, based on a reconstruction evaluation method. The methodology proposed identifies the most significant stages (independent variables) during the pre-crash phase based on the HFF method (Van Elslande, P. et al., 2007 [8]). Afterwards it creates a classification tree using those independent variables and their interactions to describe and quantify their influence on LGV accidents.

## SOURCES AND METHODS

### Accident database and reconstruction tool

The model developed to study collisions with LGVs involved uses information from an accident database compiled by the Accidentology and Vehicle Dynamics Department of INSIA within the FURGOSEG project (INSIA, 2011 [3]).

The methodology was established to carry out a retrospective in-depth analysis of Accident Reports. These reports came from two different sources, the Spanish Traffic Police and the Spanish Traffic Directorate (DGT), and contained detailed information about real-world fatal accidents involving LGVs and occurred in Spanish rural roads between 2009 and 2010.

Fully detailed scene plans were drawn to be used in the reconstruction process. The plans condensed as much information as possible covering all events that took place before, during and after the collision, illustrating positions, distances, marks and most plausible paths for the vehicles involved. The scaled plans were used as backgrounds on the computer simulations.

Next the corresponding vehicle was selected in each case and loaded from the vehicle database available in the computer program; its characteristics were set up according to the real vehicle.

All available information and data investigated have been analyzed and were used to simulate the accidents with the PC-Crash® software.

### Simulation of ABS, BAS and ESP systems operation

Every single case has been simulated twice using the PC-Crash® software: the first is a reconstruction of the real accident and the second is a simulation in which the operation of the active systems –ABS, BAS and ESP- is emulated modifying the collision parameters and its potential consequences. A common simulation procedure with simplified hypotheses about the driver reactions and the active systems operation was previously adopted, considering the functional criteria of these systems:

- The Antilock Brake System (ABS) is an automobile safety system that allows the wheels on vehicle to continue interacting with the road surface as directed by driver steering inputs while braking, preventing the wheels from locking up. The ABS generally offers improved vehicle control and decreases

stopping distances on dry and slippery surfaces for many drivers.

- The Brake Assist System (BAS) combined with the Antilock Brake System (ABS), measures the speed and force of brake application to determine whether the driver is attempting an emergency stop. If such an emergency is determined, the system applies additional brake pressure to allow the driver to take full advantage of the Antilock Brake System (ABS) which prevents wheel lock up.

- The Electronic Stability Program (ESP) is a technology that improves the vehicle stability by detecting and reducing the loss of traction. When it detects loss of steering control, it automatically applies the brakes to drive the vehicle where the driver intends to go and it also reduces the engine power until the control is regained.

Both real reconstructions and ABS/BAS/ESP-simulation outputs were compared by pairs. Examples of such comparison are presented in figure 2 and figure 3 which illustrate some key sequences. The possible perception point (PPP) is the same for both cases as also is the reaction time of the driver

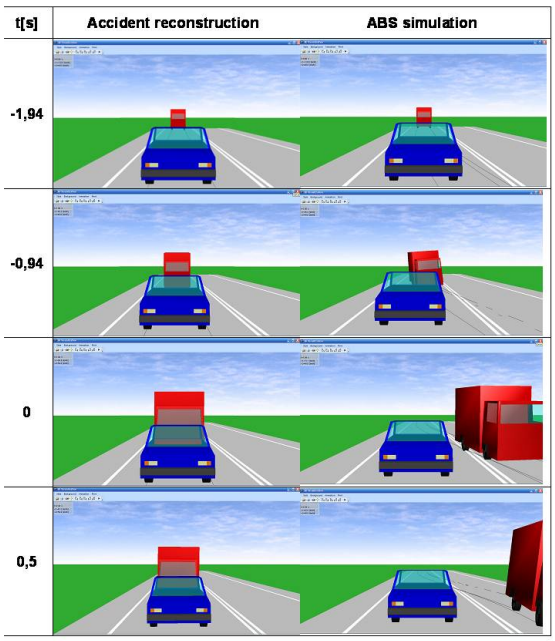


*Figure 2*. Time-line comparison between the real accident reconstruction and the ABS simulation.

Figure 2 shows a simulation of a rear-end collision and in which the braking system of the involved LGV does not contain ABS system. During the real situation and when the driver applies an emergency braking action the wheel is locked up; after that, the vehicle does not react to steering wheel inputs.

When the ABS is simulated, the vehicle develops combined manoeuvres (braking and steering) and the collision avoidance action is possible.

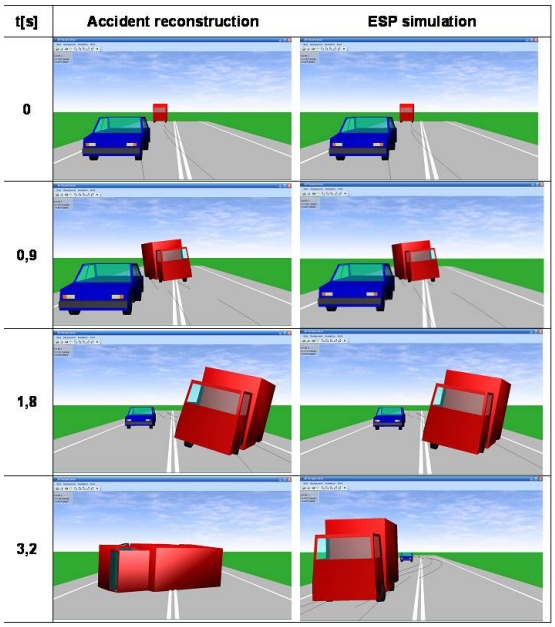


*Figure 3*. Time-line comparison between the real accident reconstruction and the ESP simulation.

Figure 3 shows a simulation of a LGV overtaking another moving vehicle and driving along the same lane. The real LGV does not include an ESP system. During the real situation and when the driver tries to return to his lane after the overtaking manoeuvre, the LGV rolls over onto its side due to the inadequate velocity. When the ESP is simulated, it helps the driver and the vehicle finishes the manoeuvre successfully.

**Method for analysis of accident causation**

An operational method of accident causation analysis is necessary to reach the definition of more appropriate measures, involving notably electronic safety functions, possibly able at preventing it. Along this objective, the HFF method (Human Functional Failures) (Van Elslande, P. et al., 2007 [8]) has been applied to the investigated accidents. It presents several operational grids of analysis along the accident process production, in line with theoretical models, which offer a means of progressing in the conceptions regarding the human role in accident generation.

The first stage of analysis consists in drawing up the accident scenario in terms of the sequence of events along: the driving phase, the rupture phase, the emergency phase and the collision phase, and, in particular, describing the initial system status, identifying the triggering event and reconstructing the emergency manoeuvre.

The second stage is to identify the mechanisms that contribute to the production of this sequence of events: these mechanisms are found in the system component interaction.

The coding process of the HFF method involves 11 steps supported by corresponding coding sheets. One interest of the method is that it offers both the possibility to process each step in a disaggregated manner, so giving the opportunity to provide quantitative results for each category of data; and it also offers the capacity to provide aggregated results through the definition of typical HFF producing scenarios. The 11 steps of analysis are the following:

- Step 1: define the pre-accident priving Situations (with the HFF_Sheet1).
- Step 2: define the initiating factors (with the HFF_Sheet2).
- Step 3: define the pivotal human functional failure (with the HFF_Sheet3).
- Step 4: define the triggering factors (with the HFF_Sheet2).
- Step 5: define the typical HFF generating scenarios (with the HFF_Sheet4).
- Step 6: define the involvement level of the driver (with the HFF_Sheet5).
- Step 7: define the emergency failure (with the HFF_Sheet6)
- Step 8: define the emergency limiting factors (with the HFF_Sheet2)
- Step 9: define the crash configuration (with the HFF_Sheet7)
- Step 10: define the crash aggravating factors (with the HFF_Sheet8)
- Step 11: define the crash pictograms (with the HFF_Sheet9).

### Classification model

The tool of classification trees was used to find the most influential accident causation mechanisms that contribute to the accidents reduction achieved by incorporating active safety technologies. This is an effective technique for studying complex systems with many variables.

Classification and regression trees (Breiman et al., 1984 [1]) are hierarchical statistical techniques suitable for exploring the data set, detecting all significant interactions and developing chart models that illustrate how the response variable depends on the explanatory variables.

The potential effectiveness of each active safety technology (ABS+BAS, ESP) was the dichotomous response variable for the classification tree. The two possible values (effective=1 or ineffective =0), were estimated in each accident by the simulation of their operation in real scenarios.

The SPSS statistical program was used to create the classification tree. The following explanatory variables were initially introduced as input:

- No_vehicles: number of vehicles involved in the accident.
- LGV_category: category of the LGV, as previously defined.
- The eleven steps contained in the method of accident causation analysis (HFF).

The method used to create the tree was CHAID (Kass, 1980 [4]). This method considers the gain of each variable and iteratively includes the most relevant. Of the explanatory variables introduced in the initial model, the algorithm kept only the most significant two, which had the largest influence on the response variable. The CHAID algorithm splits the independent variables into discrete intervals for classification.

## RESULTS

### Descriptive statistics of the accidents database

According to the LGVs categories as defined previously, the figure 4 shows the distribution of LGVs involved in real-world fatal crashes by category. It comprises 266 LGVs involved in 254 fatal accidents occurred in rural roads during 2009 and 2010.

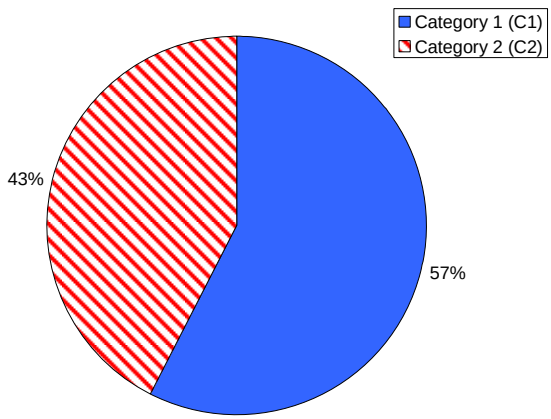


*Figure 4*. Distribution of LGVs involved in real-world fatal crashes by category (2009 and 2010).

The distribution of these accidents by crash configuration and by category is drawn in figure 5.

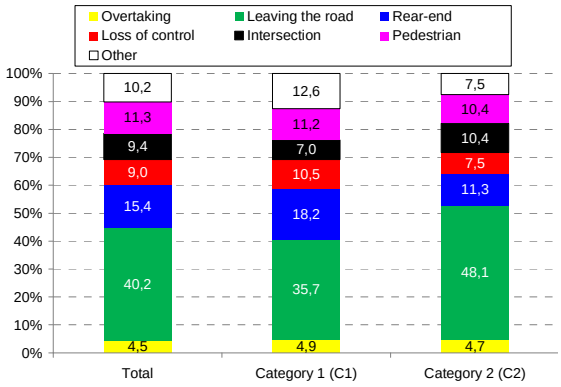


*Figure 5*. Distribution of LGVs involved in real-world fatal crashes by crash configuration and by category. (2009 and 2010).

**Potential effectiveness of active safety technologies**

The potential effectiveness of the analysed systems in LGVs involved in accidents is shown in figure 6, figure 7 and figure 8.

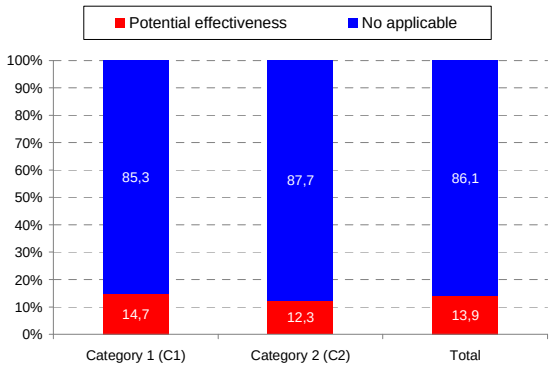


*Figure 6*. Potential effectiveness of the ABS system in LGVs involved in real accidents (2009 and 2010).

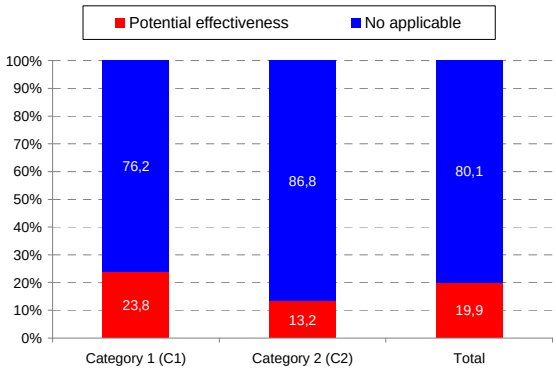


*Figure 7*. Potential effectiveness of the ABS+BAS system in LGVs involved in real accidents (2009 and 2010).

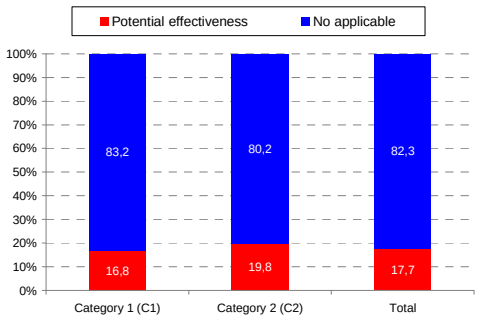


*Figure 8*. Potential effectiveness of the ESP system in LGVs involved in real accidents (2009 and 2010).

**Variable interactions and classification. ABS+BAS system**

The resulting classification tree grew into three depth levels (Figure 9). The first splitting criterion was the primary crash configuration (HFF_Sheet7_1). This first branching clearly differentiates between two branches (nodes) of this variable:

- Node 1: LGV is impacted on lateral or back side. In these 56 cases, the ABS+BAS system is effective in 3,6 % of cases.
- Node 2: LGV is impacted on front or it rolls over. In these 210 cases, the ABS+BAS system is effective in 26,7 % of cases.

Node 2 contains an important population of both cases, so it had to be further developed with another criterion. The CHAID algorithm performed a new split on this node through the variable "involvement level of the driver" (HFF_Sheet5). The split from HFF_Sheet5 classifies cases into two new groups:

- Node 3: the LGV driver provokes the disturbance. In these 111 cases, the ABS+BAS system is effective in 18,0 % of cases.
- Node 4: the LGV driver is not at the origin of the disturbance which precipitates the conflict. In these 99 cases, the ABS+BAS system is effective in 36,4 % of cases.

From a statistical standpoint, the tree has a good response. *Table 1* contains the gains of the nodes. As it shows, all of the gains of the tree are in the terminal nodes (leaves): 1, 3, and 4.

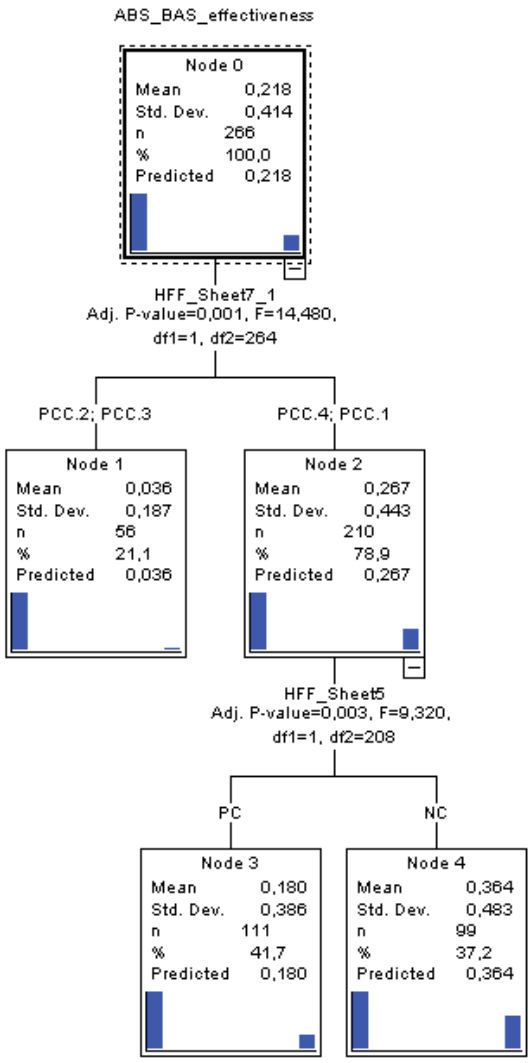


*Figure 9*. Classification tree for ABS +BAS system (CHAID method).

**Gain Summary for Nodes**

| Node | N | Percent | Mean |
|---|---|---|---|
| 4 | 99 | 37,2% | ,36 |
| 3 | 111 | 41,7% | ,18 |
| 1 | 56 | 21,1% | ,04 |

Growing Method: CHAID
Dependent Variable:
ABS_BAS_effectiveness

*Table 1*. Gain summary table for nodes. Growing method: CHAID. Dependent Variable: ABS+BAS effective/ineffective.

**Variable interactions and classification. ESP system**

The resulting classification tree grew into three depth levels (Figure 10). The first splitting criterion was the emergency failure of the LGV driver (HFF_Sheet6). This first branching clearly differentiates between two branches (nodes) of this variable:

- Node 1: the choice of the maneuver that the road user decided to put forward is not suitable, or the conditions are too short to allow for achieving a successful avoidance. In these 190 cases, the ESP system is effective in 4,2 % of cases.

- Node 2: the intention of maneuver is appropriate but the execution carried out is incorrect or not successful, as a result of a decision forced by the situation constraints. In these 76 cases, the ABS+BAS system is effective in 51,3 % of cases.

Node 1 contains an important population of both cases, so it had to be further developed with another criterion. The CHAID algorithm performed a new split on this node through the variable "involvement level of the driver" (HFF_Sheet5). The split from HFF_Sheet5 classifies cases into two new groups:

- Node 3: the LGV driver provokes the disturbance. In these 77 cases, the ESP system is effective in 7,8 % of cases.

- Node 4: the LGV driver is not at the origin of the disturbance which precipitates the conflict. In these 113 cases, the ESP system is effective in 1,8 % of cases.

From a statistical standpoint, the tree has a good response. *Table 2* contains the gains of the nodes. As it shows, all of the gains of the tree are in the terminal nodes (leaves): 2, 3, and 4.

**Gain Summary for Nodes**

| Node | N | Percent | Mean |
|---|---|---|---|
| 2 | 76 | 28,6% | ,51 |
| 3 | 77 | 28,9% | ,08 |
| 4 | 113 | 42,5% | ,02 |

Growing Method: CHAID
Dependent Variable: ESP_effectiveness

*Table 2*. Gain summary table for nodes. Growing method: CHAID. Dependent Variable: ESP effective/ineffective.

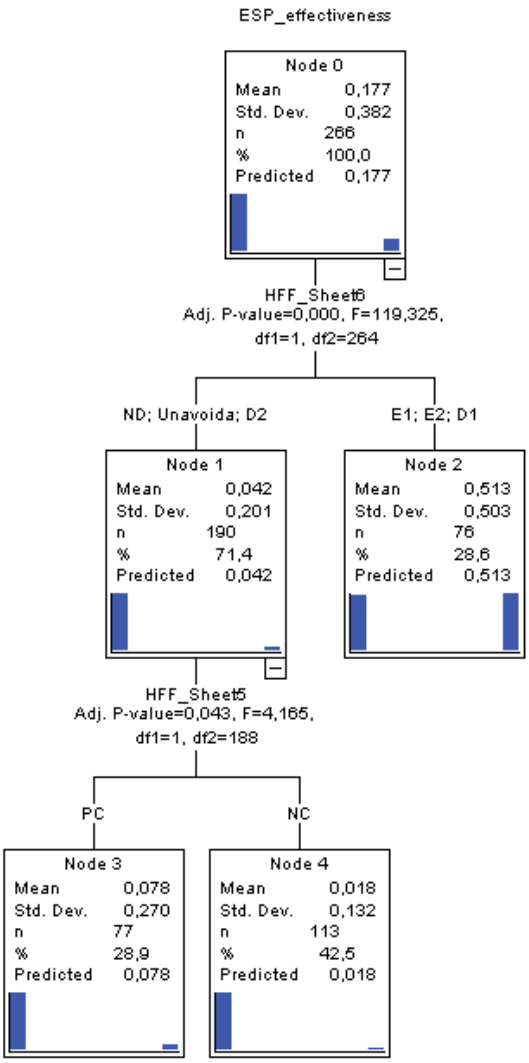


*Figure 10*. Classification tree for ESP system (CHAID method).

## CONCLUSIONS

For many years numerous studies have conducted to estimate the effectiveness of safety systems for vehicles. However, most of these have been focused on passenger cars and clear gaps were detected in the case of specific studies on vans.

Multi-disciplinary approaches such as this study make the identification of critical parameters easier and simplify the development of practical solutions by quantifying their potential impact on future actions to improve van safety. Using this methodology, a database comprising 254 fatal accidents with LGVs involved was created, including information of the vehicle and scene. Reconstructions of these accidents were performed using advanced techniques to accurately estimate multiple parameters from the collision, the pre- and post-impact phases.

The gathered information has been used for the evaluation of the effectiveness of the Antilock Brake System (ABS), the Brake Assist System (BAS) and the Electronic Stability Programme (ESP). The performance of these systems has been simulated in reconstructions, so it was possible to assess their capacity for the avoidance of the analysed accidents. The considered active systems proved to be efficient for avoiding the accidents in a percentage of the studied cases.

The classification model developed through a concurrent approach was used to find the most influential accident causation mechanisms that contribute to the accidents reduction achieved by incorporating active safety technologies. This model performs several functions: variable filtering, classification, interaction detection and quantification of variable influence.

The implementation of active safety systems in all new vehicles will lead to achieve reductions in LGV-involved accidents or to decrease their severity. So, it is recommended to influence on the generalization of ABS, BAS and ESP as standard equipment in all new LGVs.

Finally and in order to assess the safety performance of LGVs it is necessary to be able to identify data related to their accident involvement, vehicle registration and vehicle usage. It would improve any future evaluations of LGV safety performance or help to monitor the effects of any policy decisions.

## ACKNOWLEDEGEMENTS

This research was partially supported by the Ministry of Public Works and Transport (FURGOSEG: “Desarrollo y aplicación de una metodología integrada para el estudio de los accidentes de tráfico con implicación de furgonetas”, P24/08) and the Community of Madrid (SEGVAUTO: “SEGuridad de Vehículos AUTOmóviles”). The authors would like to thank the experts of the Spanish Traffic Police and the Spanish Traffic Directorate (DGT) for their contribution.

## REFERENCES

[1] Breiman, L., Friedman, J., Olshen, R. and Stone, C. (1984). Classification and Regression Trees. Wadsword International. Group. CRC Press. Belmont. California.

[2] Hohnscheid D, K. J. and others. 2006. “Impact assessment of measures concerning the improvement of road safety of light goods vehicles (LGV)”. Final report of Subproject 2, IMPROVER Project.

[3] INSIA. 2011. “Desarrollo y aplicación de una metodología integrada para el estudio de los accidentes de tráfico con implicación de furgonetas. FURGOSEG ”. Nº 2008-2011 - P24/08. Madrid.

[4] Kass, G. (1980). An exploratory technique for investigating large quantities of categorical data. J. Royal Statistical Society. Series C (Applied Statistics) 29, 2, 119−127.

[5] Lenard, J., Frampton, R., Kirk, A., Morris, A., Newton, R, Thomas, P. and Fay P. 2000. “An overview of accidents and safety priorities for light goods vehicles”. IMechE paper.

[6] Niewohner, W; Berg, F. A. and Froncz, M. 2001. “Accidents with Vans and Box-type Trucks (Transporters); Results from Official Statistics and Real-life Crash Analyses”. In Proceedings of Enhanced Safety in Vehicles (ESV) Conference, 2001.

[7] The European Parliament and the Council of the European Union. 2007. “Directive 2007/46/EC on establishing a framework for the approval of motor vehicles and their trailers, and of systems, components and separate technical units intended for such vehicles”. Official Journal of the EU, L 263, September 2007.

[8] Van Elslande, P., Fouquet, K. (INRETS). 2007.“Analyzing 'human functional failures' in road accidents”. D5.1. from Project No. 027763 – TRACE.

# SIMILARITIES AND DIFFERENCES BETWEEN JAPAN AND THE U.S. DISTRIBUTION OF FACTORS INFLUENCING INJURIES IN FRONTAL COLLISIONS USING FIELD ACCIDENT DATA

**Hiroshi Kuniyuki**
Institute for Traffic Accident Research and Data Analysis
Japan
Paper Number 13-0094

## ABSTRACT

Traffic accident analysis using accident database can indicate important causes and useful countermeasures. Japan has an in-depth accident investigation database: Institute for Traffic Accident Research and Data Analysis (ITARDA) Micro Data; however, the number of investigated accidents is limited. On the contrary, the National Automotive Sampling System/Crashworthiness Data System (NASS/CDS) in the U.S. is the largest and many researchers utilize it. In this study, research questions are clarified by studying similarities and differences between Japan and the U.S. distribution of factors influencing occupant injuries in frontal collisions using these databases, and presenting new utilization of the NASS/CDS for accident analysis.

Accident types compared are head-on collisions and frontal single-vehicle collisions occurred in 2000-2009. Appropriate eleven variables on occupant injuries in frontal collisions are selected, and Mahalanobis distance (MD) of discriminant analysis shows the similarities for each accident database. In this analysis, the variables are classified into four groups: injury prediction factors, vehicles factors, occupant factors, and injury outcome factors; furthermore, the multidimensional distribution is compared using these groups.

In results, the NASS/CDS data has similar distribution of MD to the ITARDA Micro Data in the injury prediction factors such as delta-V, seat belt use, multiple impact, occupant age etc.; however, conditions which include vehicle factor such as vehicle curb weight, and occupant factors such as occupant height have different distribution. Therefore, the NASS/CDS is useful for statistical analysis such as injury prediction for Japan; however, it cannot be utilized as it is for small vehicles crashes, or short statured occupants because of the differences in vehicle factors and occupant factors. It is necessary to consider these differences in case of using these factors. Furthermore, new weighting method for the NASS/CDS using the MD can create closer weighted database to traffic accidents in Japan. This method needs further improvements; however, it is useful in Japan for analyses using the NASS/CDS.

## INTRODUCTION

In Japan, the numbers of traffic accident fatalities are 4,612 occurring within 24 h; furthermore, 859,105 casualties occurred in 2011. The casualties have decreased over the past decade; however, the rate in a few years has slowed down over the past few years. The Japanese government has set a new target for traffic accidents, 3,000 fatalities or fewer and 700,000 casualties or fewer by 2015, with the aim of achieving the safest road traffic in the world. To achieve these targets, more contributory aspects for traffic accidents need to be identified and studied, and more effective countermeasures are needed.

Accident analyses using accident database can indicate priority issues and validate effects of countermeasures. The National Automotive Sampling System/Crashworthiness Data System (NASS/CDS) is the largest and the most utilized database of crash outcomes. Many researchers produce statistical accident analysis such as injury prediction analysis [1, 2] because of its abundant number. However, the outcomes basically represent field accident data in the U.S.

There are two major traffic accident databases in Japan. One is the Institute for Traffic Accident Research and Data Analysis (ITARDA) Macro Data which is the police reported database for all traffic accidents that occur throughout Japan. The other is in-depth accident investigation database (ITARDA Micro Data). The ITARDA Macro Data has many accident data; however, the detailed information is limited such as AIS (Abbreviated Injury Scale) code and delta-V. On the contrary, the ITARDA Micro Data has detailed information of accidents; however, the number of investigated accidents is limited. The ITARDA Micro Data may have bias issues and errors in statistical analyses; therefore, analyses using the ITARDA Micro Data are utilized with the validation by the ITARDA Macro Data [3, 4], or lack of information is covered by additional analyses using the NASS/CDS [5].

In the NASS/CDS, there is a weighting factor for each accident case to estimate accident attributes for national data in the U.S [6]. The U.S. has in-depth accident investigation database: Crash Injury Research and Engineering Network (CIREN). For the

CIREN, the similarity to the NASS/CDS is discussed [7]; furthermore, pseudo-weighting method is studied to countermeasure the bias issue between the CIREN and the NASS/CDS [8]. In these ways, there are many studies to deal with bias issues using weighting methods.

This study investigates similarities and differences of influential factors between the ITARDA Micro Data in Japan and the NASS/CDS in the U.S. using statistical analysis. Moreover, points of attention and the effectiveness using the NASS/CDS data for Japanese accident analyses are indicated, and new utilization of the NASS/CDS for Japan is presented. Accident types are frontal crashes of head-on collisions and frontal single-vehicle collisions. Drivers in front seats are analyzed in this study.

## METHODS

### Flow of the Study

The goal of this study is to clarify the similarities and differences between Japan and the U.S. distribution of factors influencing injuries in frontal collisions. That indicates points of attention when analyzing accidents occurring in other areas, and new utilization of accident database in other countries. In this study, databases compared are the ITARDA Micro Data for Japan, and the NASS/CDS for the U.S. The flow of the study used is as follows: first, sampling accidents from each database. Second, the evaluated factors are selected and grouped into a few groups. Third, Mahalanobis distance (MD) of discriminant analysis indicates the similarities of multidimensional distribution for each database in combinations of the groups. Fourth, uncommon accidents are extracted from each database using MD. These show the differences, and these accidents should be excluded in analyses for the other countries. Finally, a new weighting method to create similar distribution of MD between the two presents new utilization of accident database.

### Data Sources

Object data sources are 2000-2009 accidents, involving small and regular passenger vehicles, vans, SUVs and pickup trucks. For Japan, they include Kei cars (light vehicles with an engine displacement of 660 cc or less), and Kei trucks (light trucks with an engine displacement of 660 cc or less), which are standards unique to Japan. The analyzed accident types are head-on collisions (H-on) and frontal single-vehicle collisions (f-SVC) with the impact direction of Collision Deformation Classification (CDC) codes: 11F, 12F, and 01F. The analyzed occupants are drivers in frontal seats.

The author examines the injury prediction model using the ITARDA Micro Data, and the model can correspond to the documented accident data in the ITARDA Macro Data [3, 4]. Therefore, in this study, the ITARDA Micro Data is used as the representative accidents in Japan. The total sampling number without missing values is 216. The numbers of each accident type are shown in Table 1.

In the NASS/CDS, there is weighting variable called the *ratio inflation factor* for each case sample, which estimates the converted number of accidents as national data in the U.S. In this study, the NASS/CDS weighted is used as the representative accidents in the U.S. The total sampling number is 2,104 sample, which, when weighted, becomes 486,680 without missing values. The numbers of each accident type are also shown in Table 1.

**Table 1.**
**Data sources of Japan and the U.S.**

| | ITARDA Micro Data 2000-2009 | | NASS/CDS 2000-2009 | | |
|---|---|---|---|---|---|
| | CDC code | unweighted | CDC code | unweighted | weighted |
| H-on | 11F – 01F | 108 | 11F – 01F | 585 | 79,410 |
| f-SVC | 11F – 01F | 108 | 11F – 01F | 1,519 | 407,270 |
| Total | | 216 | | 2,104 | 486,680 |

### Analysis of Mahalanobis Distance

The MD is a distance measure in statistics. It is used in discriminant analysis, which discriminate the attributes using the nearness of stochastic distance in multidimensional distributions. The MD is based on correlations between variables and inclines to the average of variables, and defined as follows:

$$D^2 = (\boldsymbol{x} - \boldsymbol{\mu})^T \mathbf{S}^{-1} (\boldsymbol{x} - \boldsymbol{\mu}) \qquad (1).$$

where D is Mahalanobis distance, $\boldsymbol{x}$ is multivariate vector of variables, $\boldsymbol{\mu}$ is mean vector of $\boldsymbol{x}$, and $\mathbf{S}$ is variance-covariance matrix.

For instance, when Dj and Du represent the MD from group Japan and group the U.S. in case of two dimensional variables x1 and x2, the curves with equal MD show ellipses in Figure 1. An accident case is discriminated into the group with the minimum of Dj and Du. If the data conform to k-dimensional multivariate normal distribution, the distribution of $D^2$ fits the chi-squared distribution with degree of freedom k [9]. As valuables have different measurements in this study, all the valuables are standardized by their means and standard deviations.

### Explanatory Variables and Grouping

In this study, fifteen explanatory variables are selected, and grouped into four groups. These

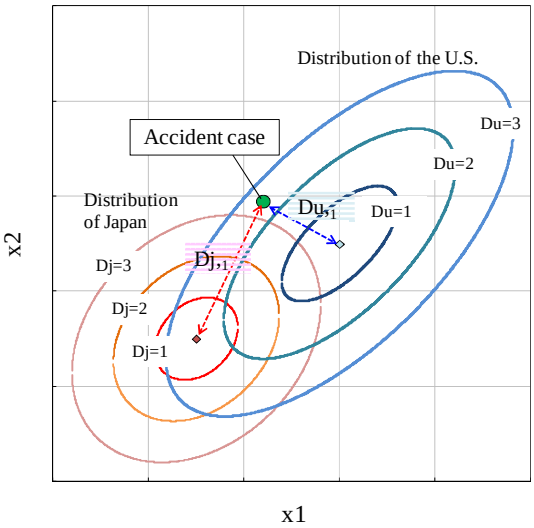


*Figure 1.* Image of distributions of MD for two databases.

variables are considered to evaluate occupant injuries in frontal collisions refer to injury prediction methods [1–4]. These variables and groups are shown in Table 2. Group A consists of major injury prediction factors used in URGENCY algorithm etc [2, 3]. Group B consists of vehicle factors indicating vehicle attributes and performance. Group C consists of occupant factors indicating occupant attributes. Group D consists of injury outcome factors indicating injury severity. Category data are converted into dummy variables of 0 or 1.

Prior to performing the MD analysis, variables that have multicollinearity are excluded using Pearson's product-moment correlation coefficients. The standard of exclusion is a multicollinearity coefficient greater than 0.5. EBS, occupant gender, occupant weight, and ISS are excluded by this standard; therefore, eleven variables are analyzed in combinations of the groups for each database.

### Japanese Weighting Method to the NASS/CDS

The MD of accident cases indicates the nearness from each database. The NASS/CDS accident cases with small MD from the ITARDA Micro Data are similar accident cases to the ITARDA Micro Data, in other words, these accident cases in the NASS/CDS frequently occur in Japan. Moreover, the distribution of MD basically fits the chi-squared distribution with degree of freedom k. As a consequence, the weighting method that selects accident cases with nearness in the NASS/CDS and distribute them to fit the chi-squared distribution can create new weighted database with similar distribution to Japan.

At first, accident cases in the NASS/CDS within 95% distribution of MD from the ITARDA Micro Data are selected. In case of degree of freedom k = 11, it means $D^2$ is less than 19.7 by the chi-squared

**Table 2.**
**Explanatory variables and grouping**

| Group | | Factors | Categories |
|---|---|---|---|
| A | Injury prediction factor | Delta-V, km/h | |
| | | Seat belt use | Belted/Unbelted |
| | | Multiple impact | Yes/No |
| | | Rollover | Yes/No |
| | | Extent of damage code | 1–9 |
| | | Occupant age, yrs | |
| B | Vehicle factor | Vehicle curb weight, kg | |
| | | Vehicle registration year | |
| | | EBS[a)], km/h | |
| C | Occupant factor | Occupant gender | Male/Female |
| | | Occupant height, cm | |
| | | Occupant weight, kg | |
| | | Occupant BMI[b)] | |
| D | Injury outcome factor | MAIS | 1–6 |
| | | ISS[c)] | 1–75 |

a) EBS: Equivalent Barrier Collision Speed
b) BMI: Body Mass Index
c) ISS: Injury Severity Score

distribution. Secondly, the weight for each accident case is determined so that the distribution of $D^2$ from the ITARDA Micro Data corresponds to the chi-squared distribution. In this process, case weight is the average of five steps to smoothen the weight. Finally, the distribution of $D^2$ is compared to the ITARDA Micro Data, and validated as new weighted accident database for Japan using the NASS/CDS data. It is called "J-weighted" to the NASS/CDS.

## RESULTS

### Comparison of Mahalanobis Distance

Figure 2–4 show the comparison of MD from the ITARDA Micro Data for each combination of groups. In these figures, Dj means the MD from the ITARDA Micro Data. For A+D group in Figure 2, which injury prediction factors and injury outcome factor, the distributions of MD between the ITARDA Micro Data and the NASS/CDS data are same in each crash type. Therefore, the NASS/CDS data are similar to the ITARDA Micro Data, that is, the NASS/CDS data are useful for accidents in Japan on statistical analysis such as injury prediction. The discriminant efficiency (DE), which means the distance between the each mean of MD, are 1.26 for head-on collision, and 0.68 for frontal single-vehicle collision. The discriminant efficiency is smaller, these databases are more similar.

For A+B+D group in Figure 3, which is added vehicle factors to A+D groups, the distribution of MD are somewhat different between the two. The DE

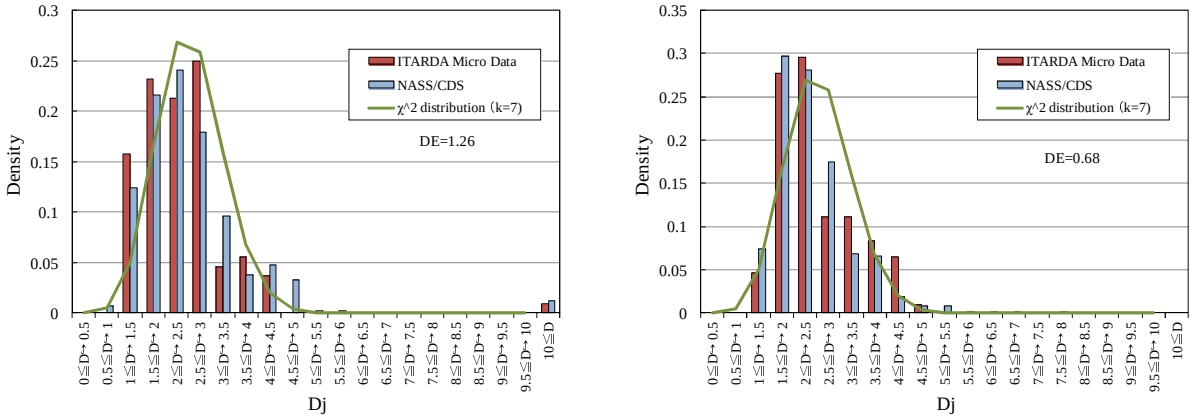


(a) Head-on collisions (b) Frontal single-vehicle collisions

*Figure 2*. Distributions of MD from the ITARDA Micro Data, A+D factors (k=7).

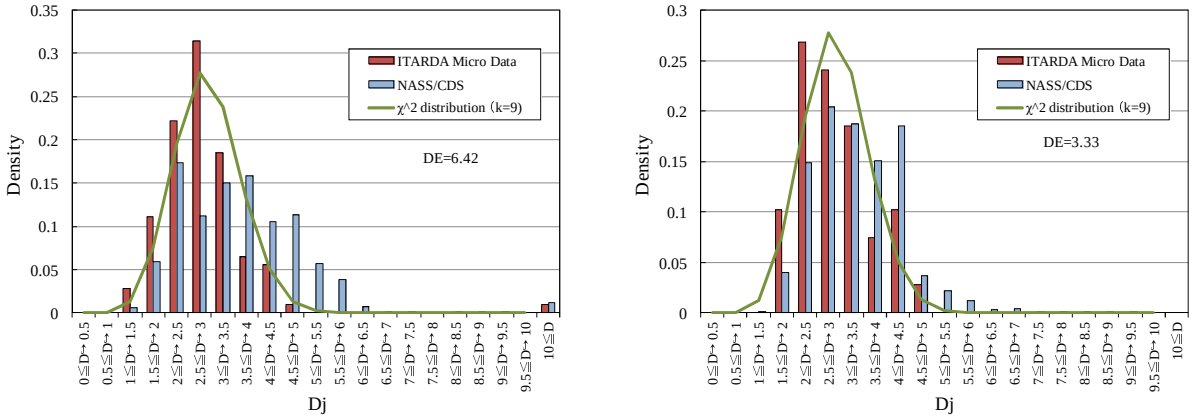


(a) Head-on collisions (b) Frontal single-vehicle collisions

*Figure 3*. Distributions of MD from the ITARDA Micro Data, A+B+D factors (k=9).

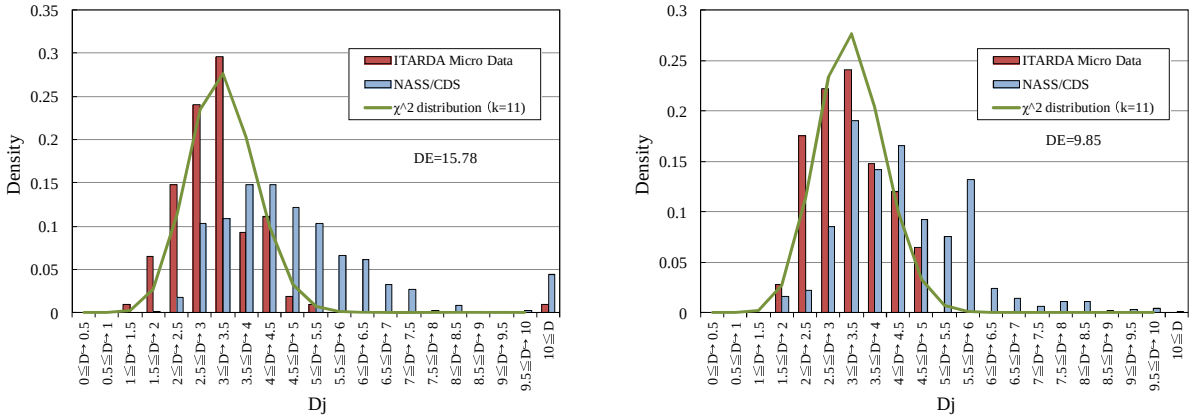


(a) Head-on collisions (b) Frontal single-vehicle collisions

*Figure 4*. Distributions of MD from the ITARDA Micro Data, A+B+C+D factors (k=11).

are 6.42 for head-on collision, and 3.33 for single-vehicle collision. These values are higher than that in A+D group. Furthermore, for A+B+C+D group (all factors) in Figure 4, the distribution of MD is different between the two. The DE is 15.78 for head-on collision, and 9.85 for single-vehicle collision. This means that the NASS/CDS data cannot be utilized as it is in case of analyses using vehicle factors such as vehicle weight and occupant factors such as occupant height as Japanese traffic accidents.

Figure 5 shows the distributions of MD from each database using A+B+C+D group. The Dj means the MD from the ITARDA Micro Data, and the Du means the MD from the NASS/CDS. For the NASS/CDS, each area of a circle means weight value. On the contrary, for the ITARDA Micro Data, each

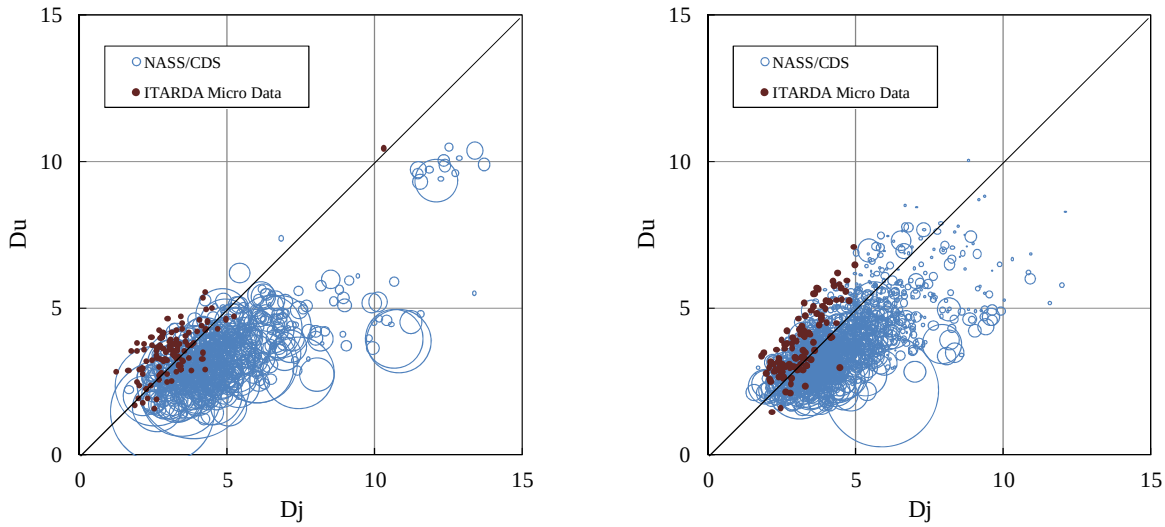


(a) Head-on collisions (b) Frontal single-vehicle collisions

*Figure 5.* Distributions of MD from the ITARDA Micro Data (Dj) and the NASS/CDS (Du), A+B+C+D factors (k=11).

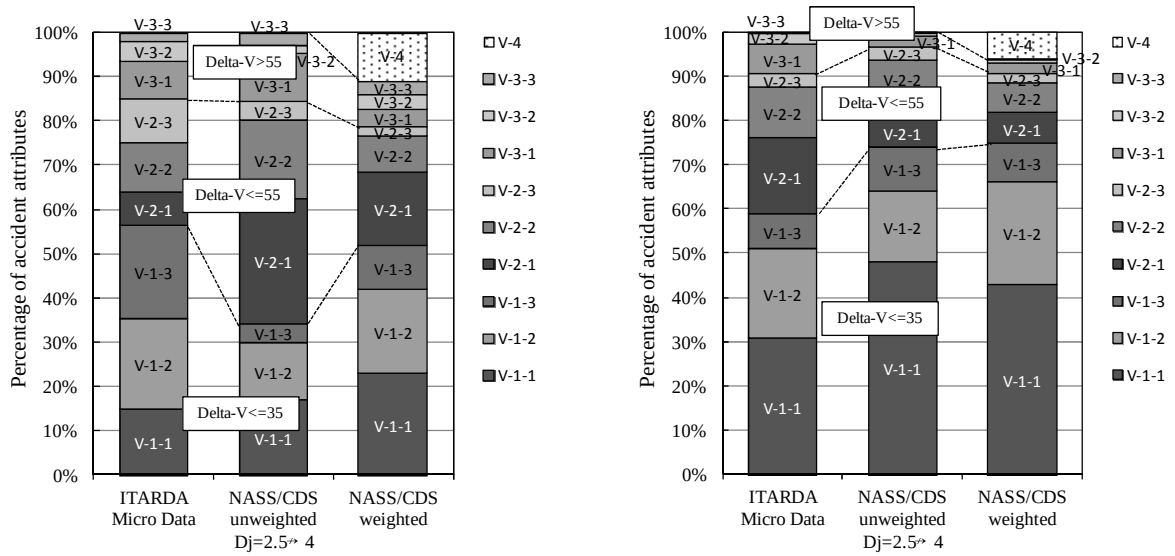


(a) Head-on collisions (b) Frontal single-vehicle collisions

*Figure 6.* Percentage of accident attributes in the ITARDA Micro Data and the NASS/CDS.

circle means an accident case. The ITARDA Micro Data are involved in part of the NASS/CDS data; however, The ITARDA Micro Data does not occupy the center of the NASS/CDS. In case of using the NASS/CDS data for analyses of Japan, it is important for the analyses to exclude the far accident cases from Japanese distribution.

**Validation of Accident Cases with Same Mahalanobis Distance**

The accident cases with small Dj in the NASS/CDS are similar accidents in Japan. In Figure 4, majority of Dj in the ITARDA Micro Data is in the range 2.5<= Dj< 4.0; therefore, the accident cases with 2.5<= Dj< 4.0 are selected, and analyzed on the accident attributes. Figure 6 shows the comparison

**Table 3.**
**Codes of accident attributes in Figure 6**

| Code | Delta-V | Occupant age | BMI |
|---|---|---|---|
| V-1-1 | <=35km/h | <30 | <35 |
| V-1-2 | | <55 | <35 |
| V-1-3 | | >=55 | <35 |
| V-2-1 | <=55km/h | <30 | <35 |
| V-2-2 | | <54 | <35 |
| V-2-3 | | >=55 | <35 |
| V-3-1 | >55km/h | <30 | <35 |
| V-3-2 | | <55 | <35 |
| V-3-3 | | >=55 | <35 |
| V-4 | ALL | ALL | >=35 |

between the ITARDA Micro Data and the NASS/CDS with 2.5<= Dj< 4.0. The codes in Figure 6 are defined in Table 3. The NASS/CDS with 2.5<= Dj< 4.0 are removed high BMI occupants (BMI >=35) from the original NASS/CDS weighted data, and the balance of each delta-V range is similar to that in the ITARDA Micro Data. In these results, the nearness of Dj means the similarity to accidents in Japan. However, the balance of occupant age is different between the two. The ITARDA Micro Data have higher rate of elderly occupants (55 yrs or older); on the contrary, The NASS/CDS with 2.5<= Dj< 4.0 data have higher rate of younger occupants (under 30 yrs). A weighting method is required to create closer database to Japanese accidents.

**The Accident Cases in the U.S. Far from Japan**

The accident cases in the NASS/CDS with long MD from the ITARDA Micro Data are uncommon for Japanese accidents. These accident cases are called as "far accident cases from Japanese distribution". Figure 7 shows the accident cases with long MD over 6 (out of 99.98 %) from the ITARDA Micro Data, i.e. far accident cases in the U.S. from Japanese distribution. In head-on collisions, there are multiple impacts with rollover in high delta-V (>75km/h) (M.R.D>75), multiple impacts with rollover in lower delta-V (<=75km/h) (M.R.D75–), high BMI (50+) drivers in low delta-V (<=35km/h) (B50+.D35–), high BMI (35+) drivers in low delta-V (<=35km/h) (B35+.D35–), high BMI (35+) drivers in higher delta-V (>35km/h) (B35+.D>35), and tall (185cm+) drivers (H185+). In frontal single-vehicle collisions, there are the same accident cases as head-on collisions except for high delta-V (>75km/h) (D>75), which are not limited of multiple impacts and rollover. These far accident cases should be noted in case of analyses for Japan using the NASS/CDS.

**The Accident Cases in Japan Far from the U.S.**

On the contrary, the accident cases in the ITARDA Micro Data with long MD from the NASS/CDS are uncommon for accidents in the U.S. These accident cases are called as "far accident cases from the U.S. distribution". Figure 8 shows the accident cases with long MD over 5 (out of 99.10 %) from the NASS/CDS, i.e. far accident cases in Japan from the U.S. distribution. In head-on collisions, there are light vehicle (900kg–, including Kei car) by short statured persons (<155cm) (LV.H<155), and high delta-V (>90 km/h) impact with heavy duty truck (D>90). In frontal single-vehicle collisions, there are other crash types i.e. light vehicle (900kg–, including Kei car) by taller drivers (155cm+) (LV), low delta-V (<=10km/h) impact (D10–), and short statured persons (<155cm) (H<155). It is difficult to analyze these far accident cases from the U.S. using the NASS/CDS. These cases need inherent accident

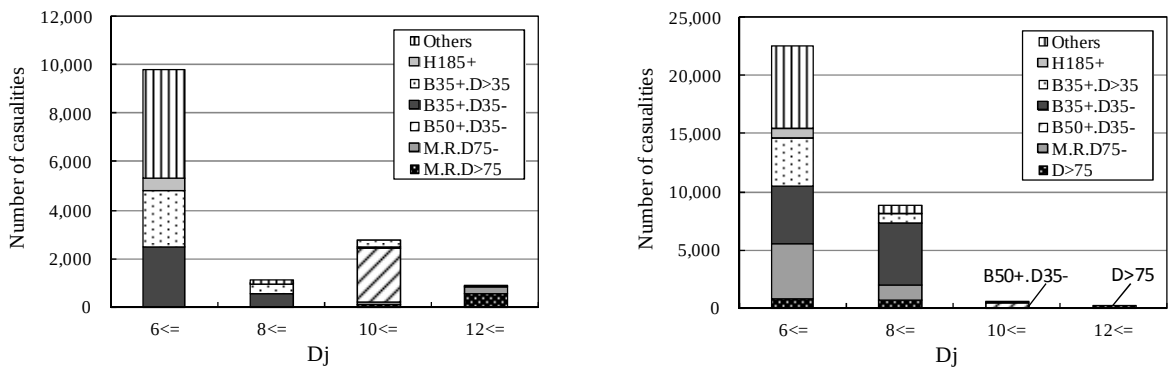


(a) Head-on collisions (b) Frontal single-vehicle collisions

*Figure 7*. The far accident cases in the NASS/CDS from the ITARDA Micro Data using A+B+C+D factors.

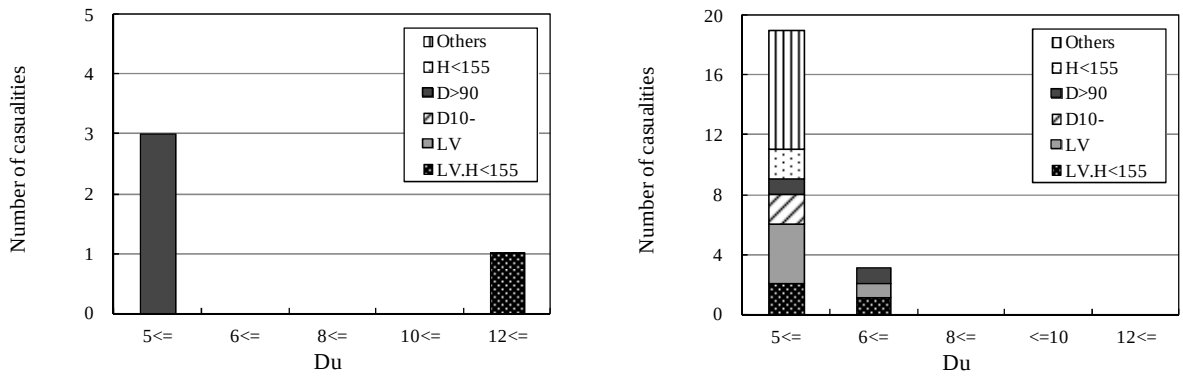


(a) Head-on collisions (b) Frontal single-vehicle collisions

*Figure 8.* The far accident cases in the ITARDA Micro Data from the NASS/CDS using A+B+C+D factors.

analyses using Japanese in-depth accident investigations.

### Japanese Weight to the NASS/CDS

The NASS/CDS data are processed using the "J-weighted" method. Figure 9 shows the comparison of distribution between the NASS/CDS J-weighted and the ITARDA Micro Data using A+B+C+D group (k=11). These data have good agreement between the two, and correspond to the chi-squared distribution. This result indicates the NASS/CDS J-weighted are similar to the ITARDA Micro Data.

Figure 10 shows the comparison of percentage between the NASS/CDS J-weighted and the ITARDA Micro Data. The components of the NASS/CDS J-weighted data are improved, and have good balance; in addition, the NASS/CDS J-weighted data are more similar to the ITARDA Micro Data especially for frontal single-vehicle collisions. However, there are some differences of occupant age balance in head-on collisions. This method can stand further improvements.

## DISCUSSION

### Distribution of Each Accident Database

The MD shows the multidimensional distributions for each database. The database which has near MD is similar to the other database which has the same MD comprehensively. However, each factor has somewhat different distribution in each database respectively. In this discussion, the further detail distributions for delta-V and occupant age, which are major injury prediction factors, are investigated.

**Delta-V** Figures 11–12 show the histograms of delta-V for each database respectively. Also the NASS/CDS J-weighted is compared in Figures 11–12. The ITARDA Micro Data have many cases

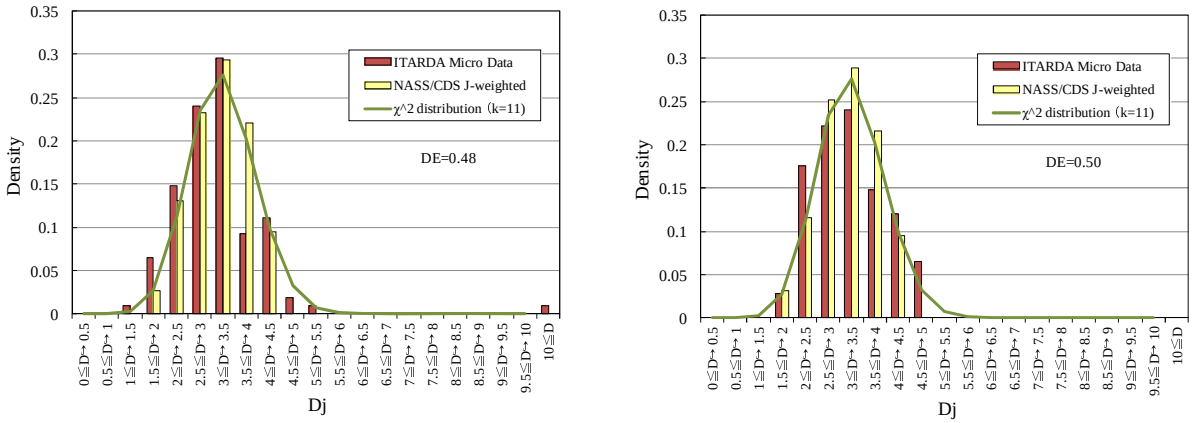


(a) Head-on collisions (b) Frontal single-vehicle collisions

*Figure 9.* Comparison of distribution between the NASS/CDS J-weighted and the ITARDA Micro Data, A+B+C+D factors (k=11).

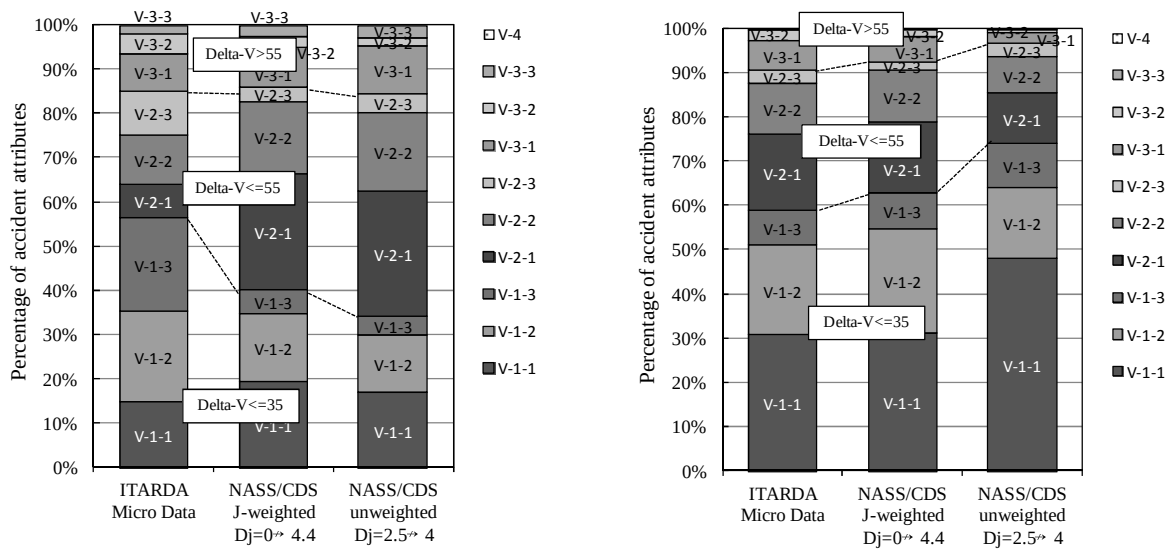


(a) Head-on collisions (b) Frontal single-vehicle collisions

*Figure 10.* Comparison of percentage between the NASS/CDS J-weighted and ITARDA Micro Data.

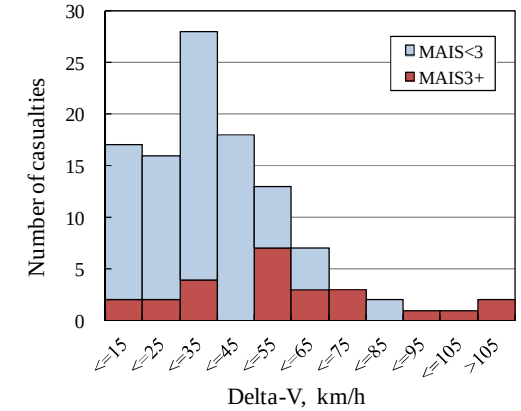


(a) ITARDA Micro Data

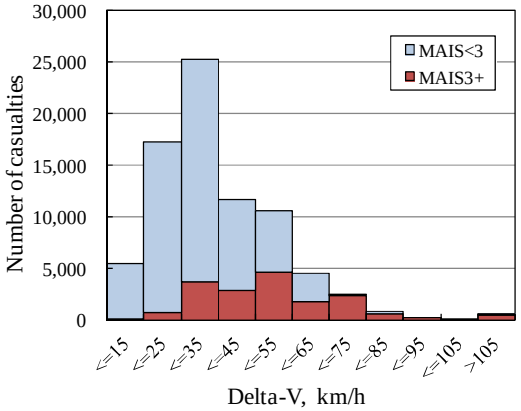


(b) NASS/CDS weighted

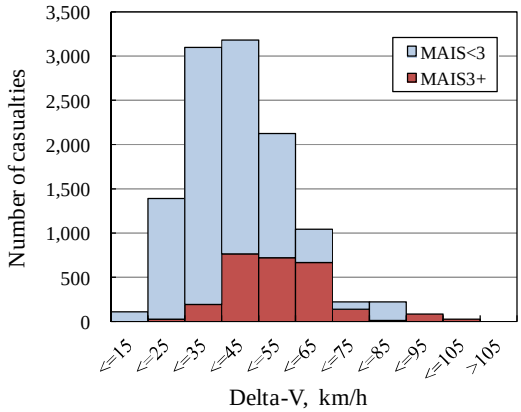


(c) NASS/CDS J-weighted

*Figure 11*. Histogram of delta-V, head-on collisions.

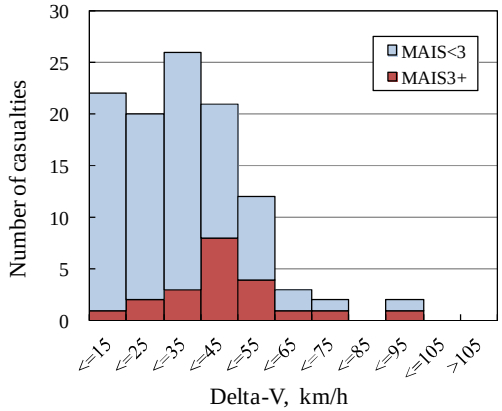


(a) ITARDA Micro Data

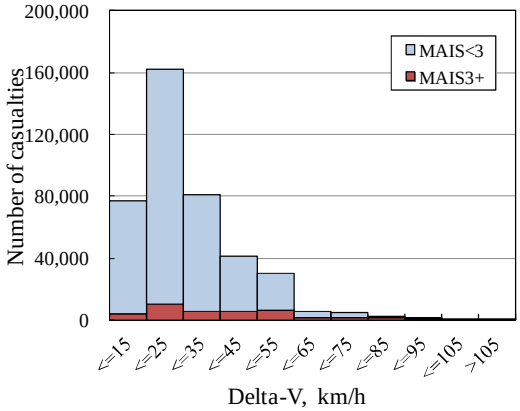


(b) NASS/CDS weighted

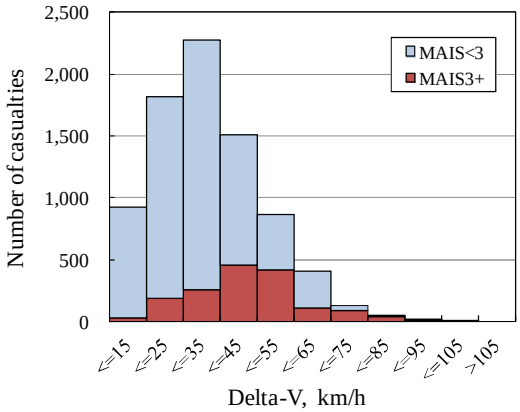


(c) NASS/CDS J-weighted

*Figure 12*. Histogram of delta-V, frontal single-vehicle collisions.

with delta-V under 15 km/h. The delta-Vs in Japan are lower than that in the U.S. This indicates the impact speed in the U.S. is higher than that in Japan. The delta-Vs in the NASS/CDS J-weighted are lower than that in the original NASS/CDS weighted; however, the percentage of lower delta-V cannot be improved sufficiently.

**Occupant age** Figures 13–14 show the histograms of occupant age for each database respectively, also the NASS/CDS J-weighted. The ITARDA Micro Data have two peaks of distribution. One is younger occupants and the other is elderly occupants. On the contrary, the NASS/CDS weighted data has many teenagers and not so many elderly occupants in relative rates. It is hard to fit the NASS/CDS J-weighted to the ITARDA Micro Data because of this distribution of the NASS/CDS weighted. There are limitations of similarities for the factors which have large different distribution. Furthermore, the MD analysis in this study basically assumes the normal distribution for every factor. In this point of view, further improvements for this method need to study.

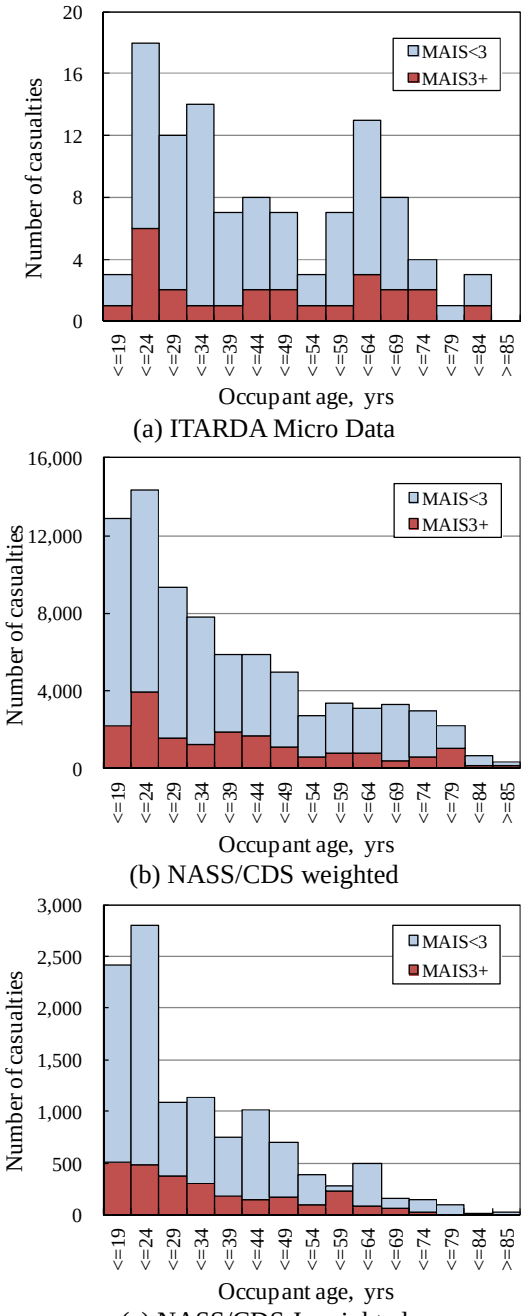


(a) ITARDA Micro Data

(b) NASS/CDS weighted

(c) NASS/CDS J-weighted

*Figure 13.* Histogram of occupant age, head-on collisions.

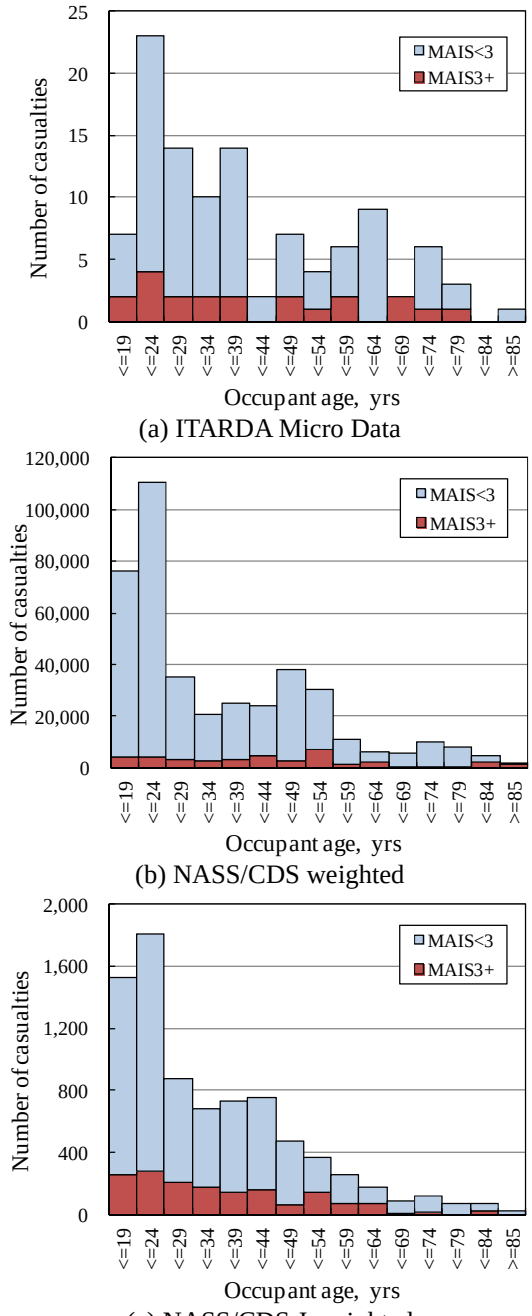


(a) ITARDA Micro Data

(b) NASS/CDS weighted

(c) NASS/CDS J-weighted

*Figure 14.* Histogram of occupant age, frontal single-vehicle collisions.

**Comparison of Odds Ratio**

Figures 15−17 show the comparison of log odds ratio for each factor between Japan and the U.S. The references of each factor are set at majority conditions or conditions with lower odds ratios. The factors are compared in each group. For injury prediction factors: group A, the odds ratios in Japan are almost similar to those in the U.S. (Figure 15). In this point of view, the NASS/CDS data are useful on statistical analyses such as injury prediction for accidents in Japan.

On the other hand, for vehicle factors: group B, there are some differences (Figure 16). Vehicle curb weight factor has different odds ratio between Japan and U.S. especially in light vehicles less than 900kg (V-weight <900kg). The U.S. log odds ratio is higher than Japan log odds ratio for vehicle curb weight less than 900kg.

In occupant factors: group C, occupant height factor has different odds ratio between the two (Figure 17). The U.S. log odds ratio is higher than Japan odds ratio for occupant height less than 155cm (O-height <155cm). These factors can be found in the differences of MD distributions. The analyses on the

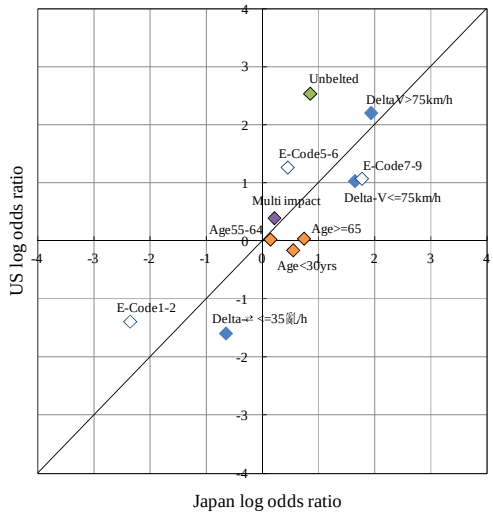


(a) Head-on collisions

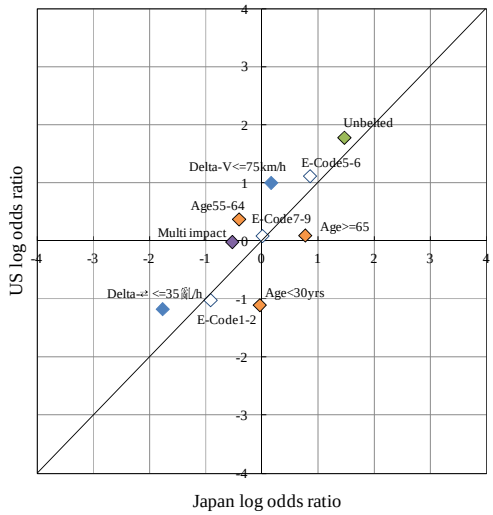


(b) Frontal single-vehicle collisions

*Figure 15.* Comparison log odd ratio on group A factors. E-code: Extent of damage code.

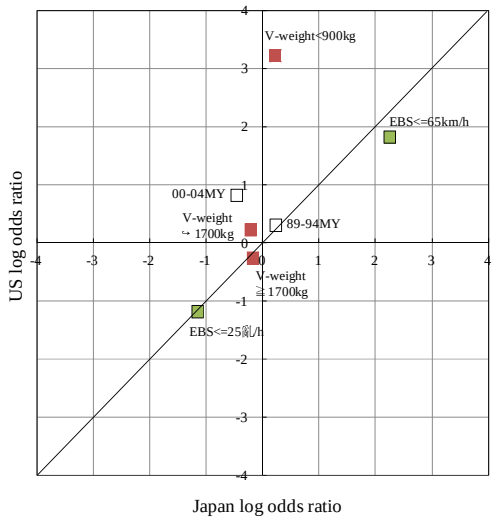


(a) Head-on collisions

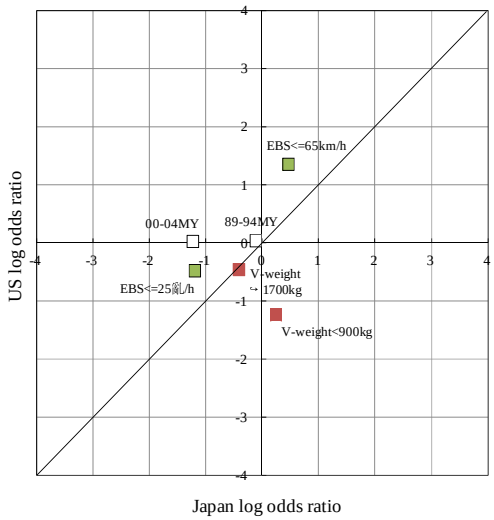


(b) Frontal single-vehicle collisions

*Figure 16.* Comparison log odd ratio on group B factors. V-weight: Vehicle curb weight, MY: Vehicle registration year.

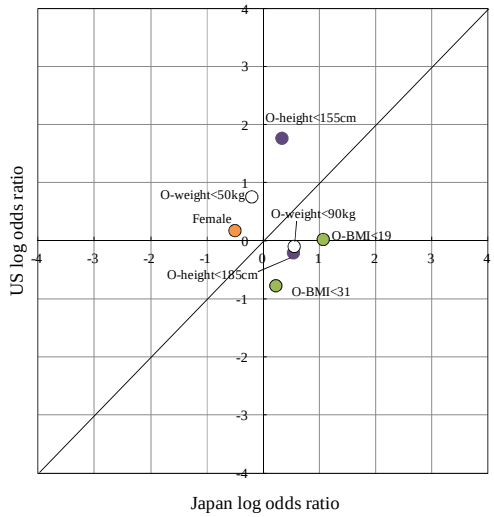


(a) Head-on collisions

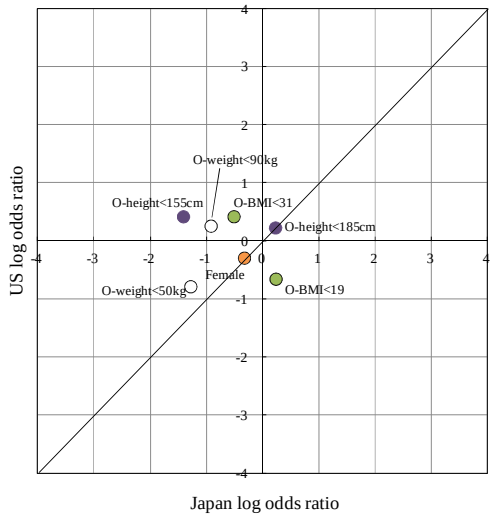


(b) Frontal single-vehicle collisions

*Figure 17.* Comparison log odd ratio on group C factors. O-height: Occupant height, O-BMI: Occupant BMI.

vehicle weight or occupant height should be noted using the NASS/CDS; moreover, should be added Japanese in-depth accident investigations.

## CONCLUSIONS

This study presents the evaluation method of similarities for traffic accident databases using Mahalanobis distance (MD), and shows the similarities and differences between Japan and the U.S. distribution of factors influencing injuries in frontal collisions. Furthermore, the points of attention and useful utilization using the NASS/CDS in analyses for Japanese traffic accidents are indicated. The conclusions of this study are as follows:

(1) The NASS/CDS data has similar distribution of MD to the ITARDA Micro Data in the injury prediction factors: delta-V, seat belt use, multiple impact, rollover, extent of damage code and occupant age. Therefore, the NASS/CDS can be utilized as it is for Japanese statistical analyses such as injury prediction for Japan.
(2) Conditions which include vehicle factors such as occupant height have different distribution of MD. Therefore, the NASS/CDS cannot be utilized as it is for Japan in case of using these factors.
(3) The accident cases in the U.S. far from Japanese distribution indicate uncommon accidents in Japan such as high delta-V (over 75km/h) with multiple impacts and rollover, or high BMI (50+) drivers in low delta-V (<=35km/h) etc. These far accident cases should be noted in case of analyses for Japan using the NASS/CDS.
(4) The accident cases in Japan far from the U.S. distribution indicate characteristic accidents in Japan such as light vehicle (900kg–, including Kei car) by short statured persons (<155cm) etc. These cases need inherent accident analyses using Japanese in-depth accident investigations.
(5) New weighting method for the NASS/CDS which fits the distribution of MD to Japan presents useful utilization of the analyses in Japan using the NASS/CDS. However, it needs further improvements on occupant age balance.

## ACKNOWLEDGMENTS

The author would like to thank NISSAN Motor Co. ltd. for providing support for the NASS/CDS data and many pieces of valuable advice.

## REFERENCES

[1] Malliaris, A.C., Digges, K.H., and DeBlois, J.H. 1997. "Relationship Between Crash Casualties and Crash Attributes," SAE Technical Paper 970393
[2] Augenstein, J., Perdeck, E., Stratton, J., Digges, K., Bahouth, G., Borchers, N., and Baur, P. 2003. "Methodology for the Development and Validation of Injury Predicting Algorithms," Proc. of the 18th ESV Conference, No. 467
[3] Kuniyuki, H. 2012. "A Study on Injury Prediction Method and Influential Factors in Frontal Collision Using Accident Data,"Transactions of the JSAE, Vol. 43, No. 2:261–267
[4] Kuniyuki, H. 2012. "A Study on Injury Prediction Method and Influential Factors in Frontal Collision Using Accident Data (Second Report) –Analysis of Frontal Pole Collision –," Transactions of the JSAE, Vol. 43, No. 6:1359–1364
[5] Katagiri, M. et al. 2011. "Occupant Injury Prediction Based on Frontal Collision Accident Simulations Using A Human Model –consideration of age and gender–," Proc. of the JSAE Annual Congress (Spring), No. 78–11:15–18
[6] NHTSA. "National Automotive Sampling System (NASS) Crashworthiness Data System Analytical User's Manual 2009"
[7] Stitzel, J., Kilgo, P., Schmotzer, B., Gabler, C., and Meredith, J.W. 2007. "Comparing CIREN and NASS Cases: A Multivariate Similarity Approach," SAE Government Industry Meeting
[8] Elliott, M.R., Resler, A., Flannagan, C.A., Rupp, J.D. 2010. "Appropriate Analysis of CIREN Data: Using NASS-CDS to Reduce Bias in Estimation of Injury Risk Factors in Passenger Vehicle Crashes," Journal of Accident Analysis and Prevention, 42:530–539
[9] B. Flury, H.Riedwyl. 1988. "Multivariate Statistics –A Practical Approach–," Chapman and Hall, London

# A COMPARATIVE STUDY BETWEEN GMLAN SPEED AND GPS REPORTED VEHICLE SPEED BY VEHICLE MANEUVER

**Eugene, Won**
**Jinwon, Kim**
**Sung-gi, Kang**
**Dongseok Kim**
General Motors
Republic of Korea

Paper Number 13-0127

## ABSTRACT

Some GM (General Motors) vehicles are using a GMLAN (General Motors Local Area Network) communication protocol for control and diagnostics. The airbag control module uses vehicle speed information from the GMLAN to record the vehicle speed as pre-crash information. In order to use the vehicle speed information for crash reconstruction purposes, it helps to be able to understand the accuracy of the data. The actual vehicle speed is not expected to be the same as the GMLAN indicated speed in some situations like a spin or if there is hard braking. This paper compares the actual vehicle speed and vehicle speed information during specific vehicle maneuvers. Actual vehicle speed is calculated from a GPS sensor, while GMLAN vehicle speed is calculated from transmission output sensor by the Engine control module (ECM). Vehicle maneuvers defined as Mode #1, Mode #2, Mode #3. The Mode #1 maneuver simulates wheel lock-up and skidding during Hard-braking at a specific speed. The Mode #2 maneuver simulates a 90degree turn using a J-turn maneuver at a specific speed. The Mode#3 maneuver simulates a 180 degree turn using a spin type of maneuver at a specific speed. The study then compares the GMLAN speed and GPS speed to see what speed difference exists between them. The results of this paper are applicable to GM vehicles only. This paper catalogs the performance and limitations of two vehicles as useful reference for crash reconstructions where there is a need to understand the speed indicated in the pre-crash section of the SDM data.

## INTRODUCTION

Vehicular crash reconstruction is used to determine how a crash happened. An understanding of the vehicle status during the crash is important factor for the crash reconstruction. At General Motors (GM) the internal term for an airbag control module is Sensing and Diagnostic Module (SDM). The SDM controls the crash sensing and deployable restraints. The SDM also records crash and deployment information when a deployment level crash occurs as well as for some non-deployment events. Also, the SDM records a limited amount of vehicle status information as pre-crash information. This pre-crash information could be important data to understand. At GM, the internal term for the recording function is Event Data Recorder(EDR). The SDM records vehicle status information for a short period of time prior to and during the crash. Such information as accelerator pedal position, brake switch circuit status, engine speed, throttle Position, and vehicle speed are recorded. This paper focused on vehicle speed information. When a SDM records vehicle speed in the EDR, the SDM receives vehicle speed data from the ECM (Engine Control Module) through the GMLAN bus which is one of the electric communication protocols of GM vehicles. Vehicle speed represents longitudinal speed of vehicle for the tire rotation because the ECM calculates vehicle speed from transmission output sensor. So, if vehicle is skidding due to wheel lock-up during hard braking or skidding in a lateral direction, the vehicle speed may not be same as vehicle longitudinal movement.

### Reconstruction

Vehicle speed can be calculated through physical evidence on the roadway such as brake marks, skid marks or other clues at the incident scene for crash reconstruction. But sometimes it may be hard to get this information from the incident scene due to scene conditions erasing skid marks and other evidence. In the case of ABS braking, the witness marks are faint to begin with and can be erased, misinterpreted, or be nonexistent for the entire length of applied braking. In this case EDR data becomes an important information source for crash reconstruction. Accident reconstructionists use the EDR as another piece of information to verify their calculations and

assumptions. Understanding the limitations of the pre-crash data is important to accident reconstruction. Moreover, understanding the accuracy of this information and how the data recorded is more important to improve the accuracy of the crash reconstruction effort.

### Pre-crash data of EDR

The SDM records to the EDR when the record condition is met. For example, if delta velocity is over 8km/h or when safety protection devices like a belt pre-tensioner or an airbag is deployed EDR recorded data includes parameters such as restraint system data and vehicle data. Restraint system data such as, seat belt status, airbag status, deployment status, SDM status, DTC (Diagnostic Trouble Code), etc., is recorded(Table 1). Vehicle data - such as accelerator pedal position, brake switch circuit status, engine speed, throttle position, vehicle speed, etc. (Table 2), is recorded for a brief period of time prior to the crash.

**Table1. Example of restraint system data**

| | |
|---|---|
| Driver 1st Stage Deployment Loop Commanded | Yes |
| Passenger 1st Stage Deployment Loop Commanded | Yes |
| Driver 2nd Stage Deployment Loop Commanded | No |
| Passenger 2nd Stage Deployment Loop Commanded | No |
| Driver Pretensioner Deployment Loop #1 Commanded | Yes |
| Passenger Pretensioner Deployment Loop #1 Commanded | Yes |
| Driver Pretensioner Deployment Loop #2 Commanded (If Equipped) | Yes |
| Passenger Pretensioner Deployment Loop #2 Commanded (If Equipped) | Yes |
| Driver Thorax Loop Commanded (If Equipped) | No |
| Passenger Thorax Loop Commanded (If Equipped) | No |
| Driver Row 2 Thorax Loop Commanded (If Equipped) | No |
| Passenger Row 2 Thorax Loop Commanded (If Equipped) | No |
| Driver Row 1 Roof Rail/Head Curtain Loop Commanded (If Equipped) | No |
| Passenger Row 1 Roof Rail/Head Curtain Loop Commanded (If Equipped) | No |
| Driver Row 2 Roof Rail/Head Curtain Loop Commanded (If Equipped) | No |
| Passenger Row 2 Roof Rail/Head Curtain Loop Commanded (If Equipped) | No |
| Driver Row 3 Roof Rail/Head Curtain Loop Commanded (If Equipped) | No |
| Passenger Row 3 Roof Rail/Head Curtain Loop Commanded (If Equipped) | No |
| Driver Knee Deployment Loop Commanded (If Equipped) | No |
| Passenger Knee Deployment Loop Commanded (If Equipped) | No |
| Driver Row 2 Pretensioner Deployment Loop Commanded (If Equipped) | No |
| Passenger Row 2 Pretensioner Deployment Loop Commanded (If Equipped) | No |
| Center Row 2 Pretensioner Deployment Loop Commanded (If Equipped) | No |
| Battery Cutoff Loop Commanded (If Equipped) | No |
| Driver Roll Bar Loop Commanded (If Equipped) | No |
| Passenger Roll Bar Loop Commanded (If Equipped) | No |
| Steering Column Energy Absorbing Loop Commanded (If Equipped) | No |
| Driver Head Rest Loop Commanded (If Equipped) | No |
| Passenger Head Rest Loop Commanded (If Equipped) | No |
| Driver Row 2 Head Rest Loop Commanded (If Equipped) | No |
| Passenger Row 2 Head Rest Loop Commanded (If Equipped) | No |
| Center Row 2 Head Rest Loop Commanded (If Equipped) | No |
| High Voltage Battery Cutoff Loop Commanded (If Equipped) | No |

**Table2. Example of vehicle data**

| Seat Belt Status | |
|---|---|
| Passenger Seatbelt Buckle Switch | *Data Not Available* |
| Driver Seatbelt Buckle Switch | *Buckled* |

| Brake Pedal Status | |
|---|---|
| Brake Pedal Status Current | *OFF* |
| Brake Pedal Status 0.5 seconds prior | *OFF* |
| Brake Pedal Status 1.0 seconds prior | *OFF* |
| Brake Pedal Status 1.5 seconds prior | *OFF* |
| Brake Pedal Status 2.0 seconds prior | *OFF* |

| Vehicle Speed Data | |
|---|---|
| Vehicle Speed Current | *24km/h* |
| Vehicle Speed 0.5 seconds prior to current | *22km/h* |
| Vehicle Speed 1.0 seconds prior to current | *20km/h* |
| Vehicle Speed 1.5 seconds prior to current | *19km/h* |
| Vehicle Speed 2.0 seconds prior to current | *17km/h* |

Among the above vehicle status information, vehicle speed is obtained from the GMLAN communication bus. Vehicle speed is calculated by the ECM from the signal off of the transmission output sensor. This vehicle speed shows the longitudinal velocity or speed of vehicle along the wheel rotation. The BCM receives vehicle speed from the ECM and then transmits it to the GMLAN communication bus. The ECM and BCM each have a 100ms time interval to transmit vehicle speed information. For this reason, vehicle speed information on the GMLAN has time lag up to a 200ms.

## VEHICLE SPEED MEASURING AND ANALYSIS USING VEHICLE MANEUVER TEST

### Test schematic

Vehicle testing was conducted to get speed data using a Chevrolet CRUZE with ABS (Anti-lock Brake System) and an AVEO without ABS. There were three test modes. Mode #1 intended to simulate hard braking on a dry asphalt road at a speed of 40kph and 80kph. Mode #2 intended to simulate lateral skidding by using a J-turn maneuver (90 degree rotation) on a dry asphalt road at a speed of 40kph and 80kph. Mode #3 intended to simulate lateral skidding by using a spin turn (180 degree rotation) on a dry asphalt road at a speed of 40kph and 80kph. GMLAN speeds and GPS speeds were collected to compare speed differences between the EDR speed and the actual vehicle speed. Extra testing was performed at other speed condition such as 20kph, 60kph, 100kph. But this paper only discussed 40kph and 80kph data only because these data show a clear speed trend.

### Test Mode

**Mode #1** Hard braking test was conduct at 40km/h and 80km/h (table 3).

**Mode # 2** J-turn test was conduct at 40km/h and 80km/h (table 3).

**Mode # 3** Spin turn test was conduct at 40km/h and 80km/h (table 3).

**Table3. Test mode**

| Speed[km/h] | Hard braking | J-turn | Spin turn |
|---|---|---|---|
| 40 | X | X | X |
| 80 | X | X | X |

**Test conditions**

**Test site** Test was conducted at Chung-na proving ground of GM Korea. Surface condition was dry asphalt.

**Test Vehicle** The AVEO (Picture 1) and CRUZE (Picture 2) were chosen for the vehicle maneuver tests. The Vehicle Identification Number (VIN) of AVEO is 'KLATA48EDCB000327'and CRUZE is 'KLAJA695DDK006345'. These vehicles use the GMLAN for the electric communication. The AVEO had no ABS and was equipped with KUMHO tires (P205/55/R16, 35psi). The CRUZE had ABS and was equipped with HANKOOK tires (P205/65/R16, 35psi).

Picture1. AVEO without ABS

Picture2. CRUZE with ABS

**Instrument** GMLAN bus data and GPS data from the GPS signal measurement system (picture 4) was recorded by a DEWE3010 data acquisition instrument. The GMLAN bus data was accessed through the DLC (Data Link Control) connector. The DEWE3010 instrument has a 32 bit data transfer rate at 33Mhz and 16 Analog input channels, with 16 bit resolution, and 200kS/s sampling rate (picture 3). Speed data from the GMLAN and GPS was recorded to every 10ms (0.01 sec) by the DEWE3010. GPS speed was measured by a RT4100 (picture 4) with external GPS antenna AT575-70 (picture 5) that has 0.1 km/h RMS speed precision, and 250Hz refresh rate.

Picture3. DEWE3010 – Data acquisition system

Picture4. RT4100 - GPS signal measurement system

Picture5. AT575-70 - External GPS antenna
(Installed on the roof center of vehicle.)

**TEST RESULT**

For discussion, the GPS speed represents actual vehicle speed. The GMLAN speed represents EDR speed. Vehicle speed differences between the GPS

speed and GMLAN speed during a straight run was about ±1km/h. GPS speed and GMLAN speed was recorded at a 10ms sample rate by the data acquisition system. GMLAN speed was recorded at a 100ms step due to BCM provides vehicle speed as 100ms periodic message rate. Unit of Vehicle speed for EDR is 1km/h. Therefore both the GMLAN and GPS speed data recorded from maneuver tests were truncated to the nearest tenth decimal point to match the EDR recording specification. Also GMLAN speed data was modified to compensate for the 200ms time lag caused by ECU and BCM communication the GMLAN. For these reason, time of GMLAN speed shifted 200ms ahead.

**Result of mode #1 (Hard braking test)**

For the AVEO with non-ABS, the GMLAN speed recorded as '0' while the GPS speed decreased continually (Figure 1, 2). In figure 1, the non-ABS vehicle will lock the wheels and the transmission output shaft stops. So the vehicle speed input to the GMLAN would be zero around 0.8 msec. In reality, the vehicle is still moving and stops about a second later. In ABS vehicles, the wheels tend not to lock up so you expect to see the data trend closer with the ASB activated.

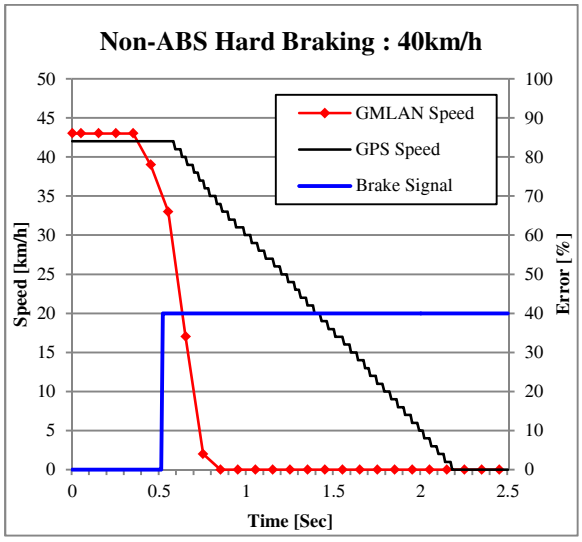


*Figure1*. Speed comparison of Non-ABS(AVEO) hard braking test at 40km/h

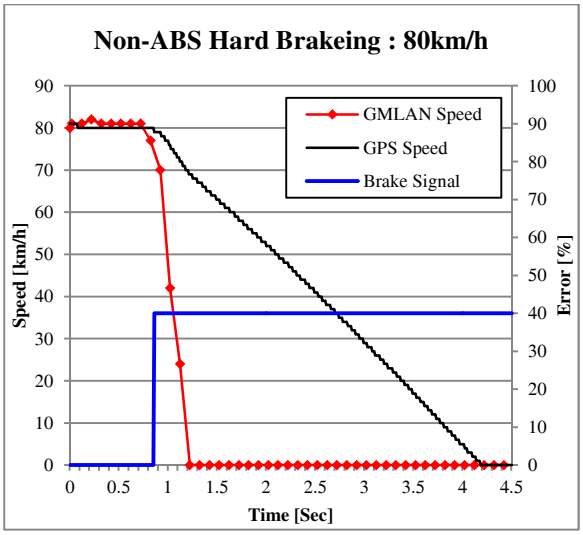


*Figure2*. Speed comparison of Non-ABS(AVEO) hard braking test at 80km/h

For the CRUZE with ABS, the GMLAN speed recorded lower than the GPS speed. The GMLAN speed of CRUZE with ABS showed fluctuation due to ABS operation during the maneuvers. This trend is more clearly indicated at 40km/h test (Figure 3). That trend decreased at 80km/h test but fluctuation was still indicated (Figure4).

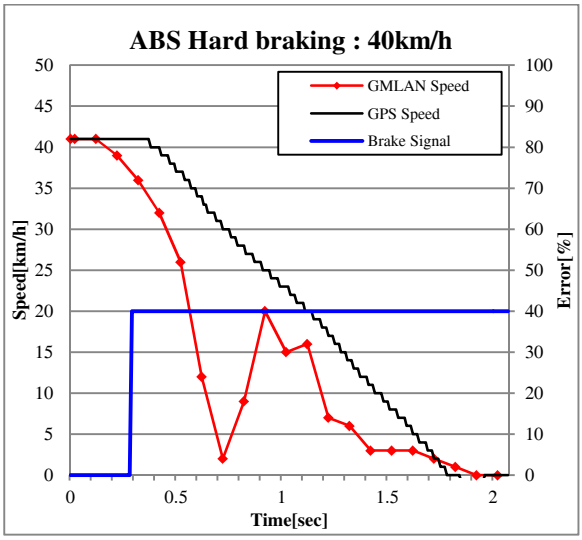


*Figure3*. Speed comparison of ABS(CRUZE) hard braking test at 40km/h

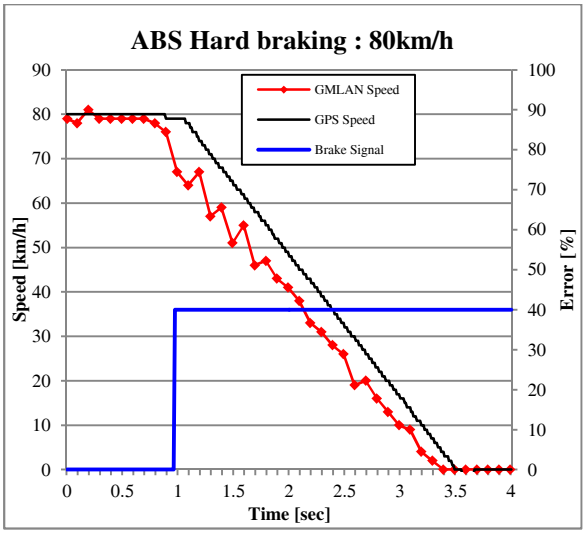


*Figure4*. Speed comparison of ABS(CRUZE) hard braking test at 80km/h

**Result of mode #2(J-turn test)**

The trend of speed differences between the GMLAN speed and GPS speed is similar from the result of test mode #1(Figure 5, 7, 8) except for fluctuation trend. GMLAN speed fluctuation was only indicated at the 80km/h test of Non-ABS AVEO due to brake pedal application during the maneuver. The Brake signal still recorded as 'ON' at fluctuation of the 80km/h test of Non-ABS AVEO, but the driver released the brake pedal slightly to maintain vehicle control in the maneuver. (Figure 6). The Brake signal is not matched to the decline start point in all of J-turn test results because test driver used the parking brake prior to brake pedal to make the J-turn.

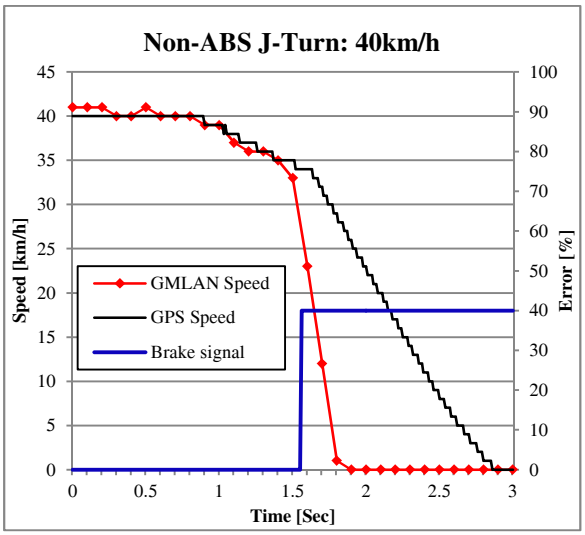


*Figure5*. Speed comparison of Non-ABS(AVEO) J-turn test at 40km/h

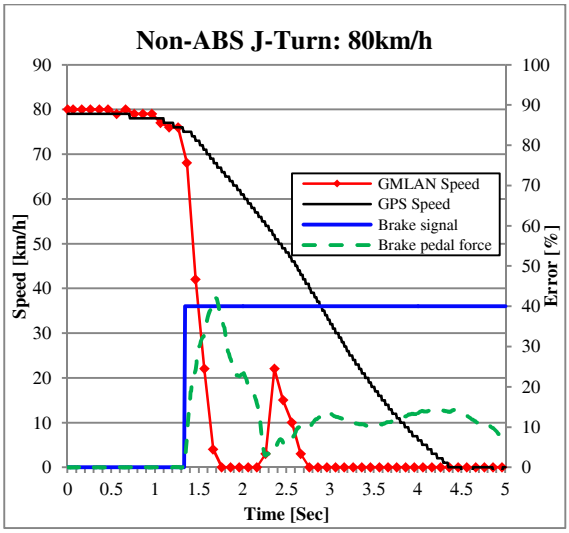


*Figure6*. Speed comparison of Non-ABS(AVEO) J-turn test at 80km/h

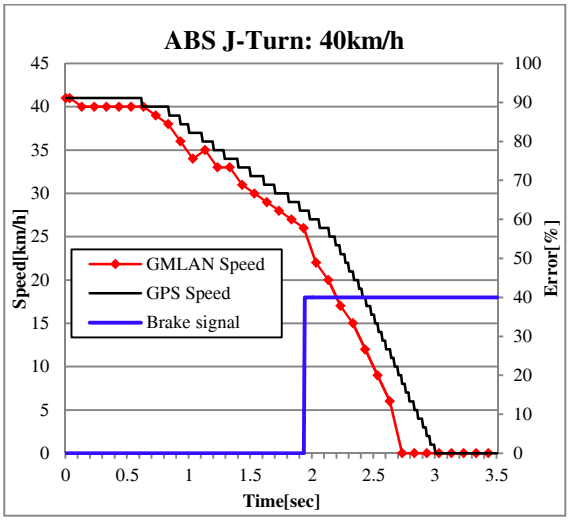


*Figure7*. Speed comparison of ABS(CRUZE) J-turn test at 40km/h

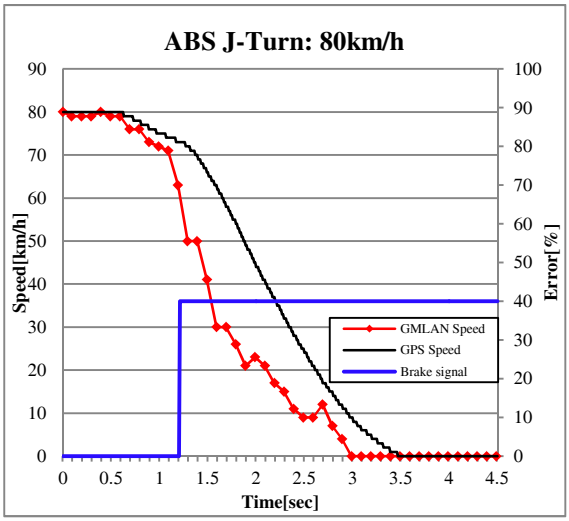


*Figure8*. Speed comparison of ABS(CRUZE) J-turn test at 80km/h

**Result of mode #3 (Spin turn test)**

For the AVEO with Non-ABS, the test result of mode #1 and mode #2 was shown as '0' GMLAN speed while the GPS speed decreased continually. The result of mode #3 does not show the same characteristic. Speed does not go to zero in mode #3 because the front wheels of vehicle still rotate during the turning maneuver due to the test driver using the parking brake prior to using the pedal brake to make the spin turn (Figure 9, 10, 11, 12). Fluctuation of the GMLAN Speed was not shown for the test result of the CRUZE with ABS because the test driver did not use brake pedal(Figure 11, 12). In the 80km/h test, the GPS speed of CRUZE with ABS and the AVEO with Non-ABS reached '0' then showed a negative movement due to vehicle moving backward at near 110 degree of rotation (Figure 10, 12). The Rotation trend of the 80km/h spin turn test for the AVEO and CRUZE can be found in Appendix A. in the 80km/h test of the AVEO with Non-ABS, the GMLAN speed recorded '0' while the GPS speed indicated a negative because the test driver used the brake pedal.(Figure 10). In the 80km/h test result of CRUZE with ABS, the GMLAN speed recorded as '0' then indicated a negative while GPS speed indicated a negative because test driver did not use the brake pedal(Figure 12).

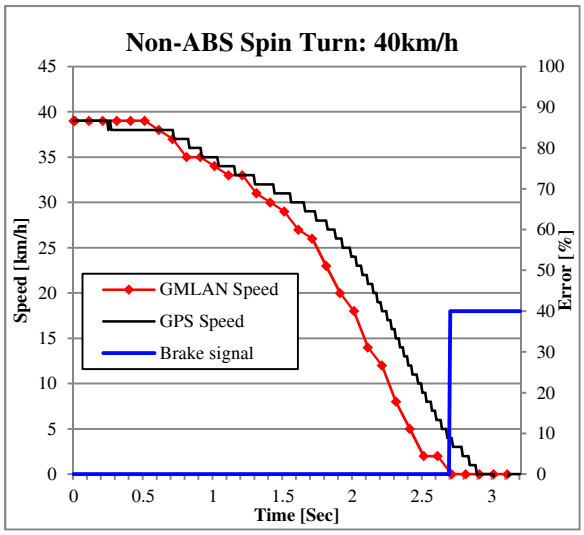


*Figure9*. Speed comparison of AVEO with Non-ABS Spin-turn test at 40km/h

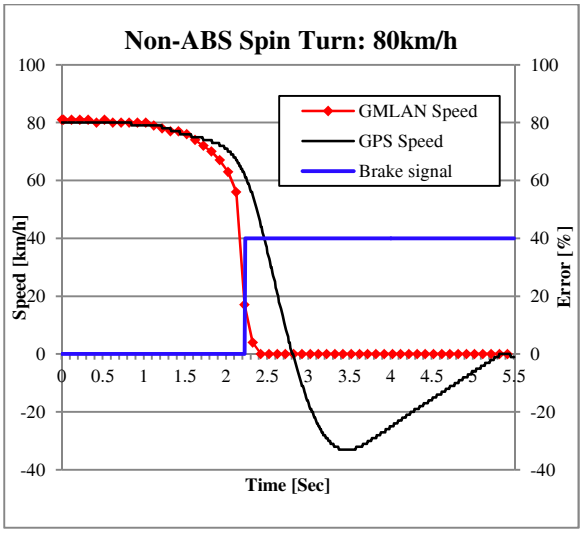


*Figure10*. Speed comparison of Non-ABS(AVEO) Spin-turn test at 80km/h

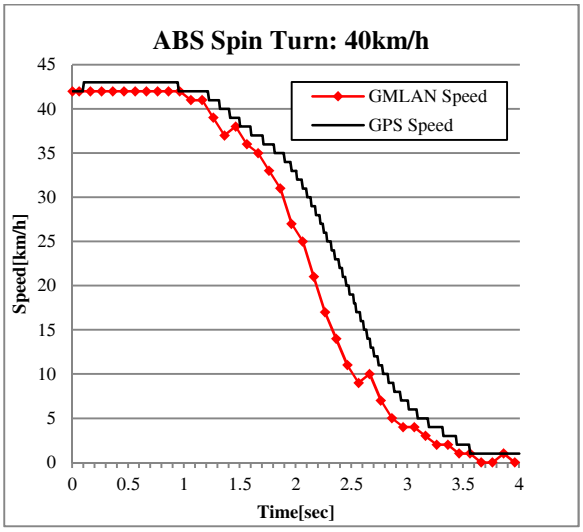


*Figure11*. Speed comparison of ABS(CRUZE) Spin-turn test at 40km/h

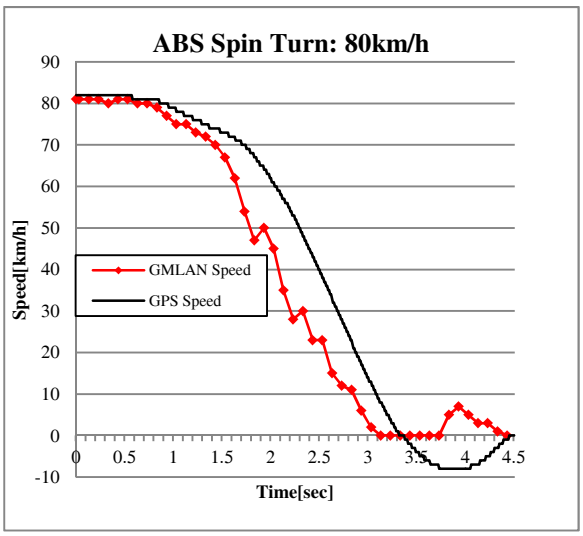


*Figure12*. Speed comparison of ABS(CRUZE) Spin-turn test at 80km/h

## CONCLUSIONS

### Hard braking test

- The GMLAN speed of the AVEO with Non-ABS was recorded as '0' while actual vehicle speed decreased continually. The non-ABS vehicle will lock the wheels and the transmission output shaft stops. The vehicle speed input to the GMLAN would be zero around 0.8 msec. In reality, the vehicle is still moving and stops about a second later. In ABS vehicles, the wheels tend not to lock up so you expect to see closer data trends when the ASB is activated.

- Fluctuation appeared on the GMLAN speed of the ABS vehicle. ABS releases brake pressure on a wheel when wheel lock-up is detected during braking and then repeats braking and releasing. For these reasons the GMLAN vehicle speed would show a fluctuation trend as evidenced in the test result of this paper.

- The Speed difference of a Non-ABS vehicle is higher than an ABS vehicle. Detail figures of speed differences are shown as below table4.

**Table4. Speed differences of hard braking test**

(*Speed difference = GPS speed - GMLAN speed, [km])

| Non-ABS : AVEO<br>ABS : CRUZE | Hard braking | | | |
|---|---|---|---|---|
| | 40km/h test | | 80km/h test | |
| | Non-ABS | ABS | Non-ABS | ABS |
| 0 sec<br>(After maneuver) | 9 | 5 | 9 | 12 |
| 0.5 sec | 32 | 29 | 67 | 9 |
| 1 sec | 22 | 5 | 59 | 8 |
| 1.5 sec | 12 | 5 | 50 | 9 |
| 2 sec | 2 | 2 | 41 | 10 |
| 2.5 sec | - | - | 32 | 7 |
| 3 sec | - | - | 22 | 4 |
| 3.5 sec | - | - | 7 | 0 |

### J-turn test

- The GMLAN speed of the AVEO with Non-ABS was recorded as '0' while the actual vehicle speed decreased continually due to the same reasons as discussed for hard brake test result.

- Fluctuations did not appear in GMLAN speed regardless of an ABS vehicle or non-ABS vehicle except in the 80km/h test of the AVEO with Non-ABS. GMLAN speed fluctuation was only indicated for the 80km/h test of Non-ABS AVEO due to brake pedal application during the maneuver.

- Speed difference of Non-ABS vehicle is higher than ABS vehicle. Detail figures of speed differences are shown as below table5.

**Table5. Speed differences of J-turn test**

(*Speed difference = GPS speed - GMLAN speed, [km]

| Non-ABS : AVEO<br>ABS : CRUZE | J-turn | | | |
|---|---|---|---|---|
| | 40km/h test | | 80km/h test | |
| | Non-ABS | ABS | Non-ABS | ABS |
| 0 sec<br>(After maneuver) | 0 | 2 | 0 | 1 |
| 0.5 sec | 0 | 2 | 32 | 2 |
| 1 sec | 19 | 2 | 65 | 11 |
| 1.5 sec | 20 | 2 | 52 | 32 |
| 2 sec | 9 | 6 | 41 | 22 |
| 2.5 sec | 0 | 8 | 31 | 17 |
| 3 sec | 0 | 1 | 19 | 7 |
| 3.5 sec | - | - | 6 | 2 |

### Spin turn test

- The GMLAN speed does not indicate as '0' while actual vehicle speed decreased continually regardless ABS vehicle and non-ABS vehicle.

- Fluctuations did not appear for GMLAN speed. Test driver use parking brake prior to use brake pedal for non-ABS vehicle and does not use brake pedal for ABS vehicle.

- GPS speed of ABS vehicle and non-ABS vehicle reached '0' then indicated negative movement in the 80km/h test. For the 80km/h test of AVEO with Non-ABS, the GMLAN speed recorded '0' while the GPS speed indicated a negative because the test driver used the brake pedal.(Figure 10). For the 80km/h test result of CRUZE with ABS, The GMLAN speed recorded as '0' then indicated a positive while the GPS speed indicated a negative because the test driver did not use the brake pedal.

- Detail figures of speed difference are shown as below table6.

**Table6. Speed differences of spin turn test**

(*Speed difference = GPS speed - GMLAN speed, [km])

| Non-ABS : AVEO<br>ABS : CRUZE | Spin turn | | | |
|---|---|---|---|---|
| | 40km/h test | | 80km/h test | |
| | Non-ABS | ABS | Non-ABS | ABS |
| 0 sec<br>(After maneuver) | 0 | 0 | 0 | 1 |

| | | | | |
|---|---|---|---|---|
| 0.5 sec | 1 | 3 | 5 | 4 |
| 1 sec | 1 | 3 | 50 | 4 |
| 1.5 sec | 5 | 8 | 9 | 21 |
| 2 sec | 7 | 8 | -25 | 25 |
| 2.5 sec | 4 | 3 | -33 | 18 |
| 3 sec | 0 | 2 | -27 | 10 |
| 3.5 sec | - | - | -16 | -7 |
| 4 sec | - | - | -6 | -11 |
| 4.5 sec | - | - | -1 | 0 |

**REFERENCES**


Timothy J. Reust and James M. Morgan, "Commercial Vehicle Event Data Recorders and the Effect of ABS Brakes During Maximum Brake Application" SAE 2006-01-1129

Richard R. Ruth, Sgt. Timothy Brown, James Lau, "Accuracy of EDR during Rotation on Low Friction Surfaces" SAE 2010-01-1001

Cleve Bare, Brian Everest and Donald Floyd, Douglas Nunan "Analysis of Pre-Crash Data Transferred over the Serial Data Bus and Utilized by the SDM-DS Module" SAE 2011-01-0809

Richard Ruth, Wade Bartlett, Jeremy Daily "Accuracy of Event Data in the 2010 and 2011 Toyota Camry During Steady State and Braking Conditions" SAE 2012-01-0999

Timothy J. Ruth, James M. Morgan " The Accuracy of Speed Recorded by an SDM and The Effects of Brake, Yaw and Other Factors" Collision Magazine Volume 1, Issue 1, page 8

Appendix A. Rotation trend of 80km/h spin turn test of AVEO and CRUZE

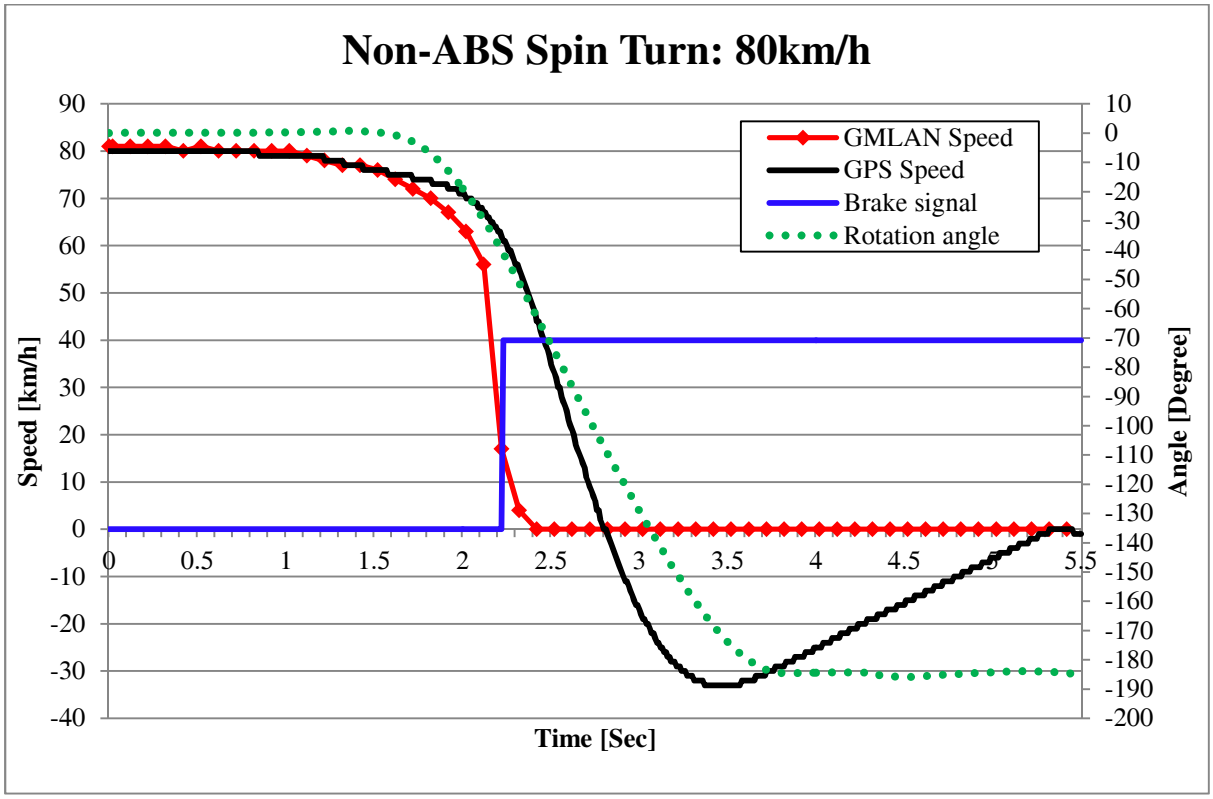


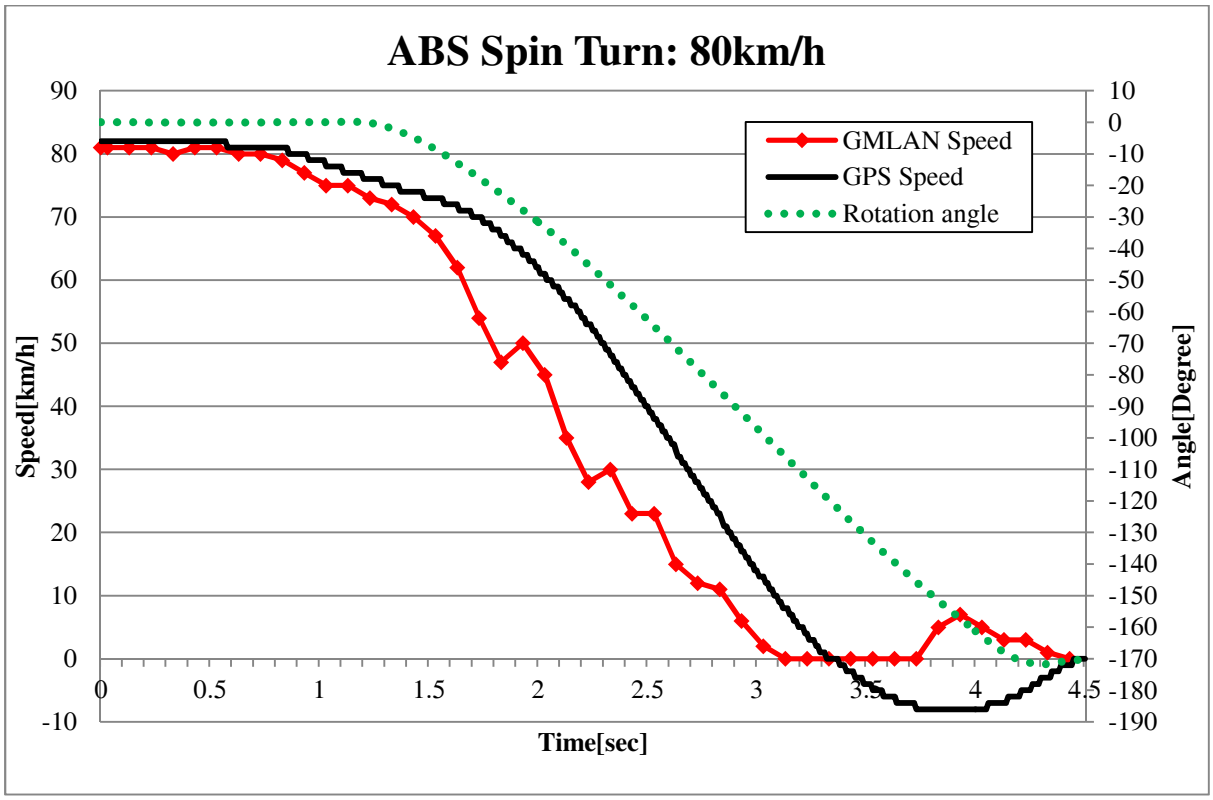

# PRE-CRASH SCENARIOS FOR DETERMINING TARGET POPULATIONS OF ACTIVE SAFETY SYSTEMS

**Kristofer D. Kusano**
**Hampton C. Gabler**
Virginia Tech
Blacksburg, VA, USA

Paper Number 13-0078

## ABSTRACT

The of active safety systems is to prevent or mitigate collisions. A critical component in the design of active safety systems is to identify the target population for a proposed system. The target population for an active safety system is that set of crashes that a proposed system could prevent or mitigate. Target crashes have scenarios in which the sensors and algorithms would likely activate. For example, the rear-end crash scenario, where the front of one vehicle contacts another vehicle traveling in the same direction and in the same lane as the striking vehicle, is one scenario in which Forward Collision Warning (FCW) would be most effective in mitigating or preventing. This paper presents novel pre-crash scenarios based upon coded variables from NHTSA's nationally representative crash databases. Using three databases the scenarios developed in this study can be used to quantify the number of police reported crashes, seriously injured occupants, and fatalities that are applicable to proposed systems. In this paper, we use the pre-crash scenarios to identify the target populations for FCW, Lane Departure Warning (LDW), and Vehicle-to-Vehicle (V2V) or Vehicle-to-Infrastructure (V2I) systems. This study found that these three systems could potentially mitigate or prevent 59% of both seriously injured occupants and fatalities.

## INTRODUCTION

The target population for an active safety system is that set of crashes that a proposed system could prevent or mitigate. These crashes have scenarios in which the sensors and algorithms would likely activate. For example, the rear-end crash scenario, where the front of one vehicle contacts another vehicle traveling in the same direction and in the same lane as the striking vehicle, is one scenario in which a Forward Collision Avoidance System (FCAS) would activate. Many of FCAS systems utilize forward-facing sensors, e.g. radar. Because the vehicle is in view of the sensors prior to the crash, rear-end collision are likely to be detected. In other forward crash scenarios, such as intersection or turning crashes, a struck vehicle may come in view of the sensors too late to activate. This is especially true for the warning component, which needs longer times to be maximally effective.

Another important aspect of the target population is the societal cost which a proposed active safety system could potentially mitigate. These societal costs of crashes can be measured by the costs associated with injured occupants including the costs of medical treatment, lost wages, and long-term disability. Because active safety systems have tremendous equipment and development costs for automakers, the systems that can potentially mitigate the most injuries should be prioritized based on cost reduction. Therefore, systems that can potentially mitigate the most injuries should be prioritized.

An important tool in identifying target populations for countermeasures is examining the crash population in terms of crash scenarios. Crash scenarios group similar crashes in real-world crash databases using the variables coded for each case. Previous researchers have developed crash scenarios for nationally representative crash databases, such as those by Eigen and Najm [1]. The approach in Eigen and Najm was to use variables that described the pre-crash phase of the collision to group scenarios. We will adapt these scenarios for the current study and

use them to examine the target population of forward collision avoidance systems as an example.

The objective of this study is to develop crash scenarios for use in identifying the target population for active safety systems.

## METHODOLOGY

### Data Sources

Three data sources were used for this study: the National Automotive Sampling System (NASS) General Estimates System (GES), the NASS Crashworthiness Data System (CDS), and the Fatality Analysis Reporting Systems (FARS). GES is a representative sample of all police reported crashes in the U.S. CDS is a representative sample of crashes which involve passenger vehicles towed from the scene due to damage. FARS is a census of all traffic related fatalities in the U.S. All three databases are funded and maintained by the National Highway Traffic Safety Administration (NHTSA) and are released to the public on an annual basis.

Each data base represents a different population of crashes. The GES sample is an estimate of all crash exposure in the U.S. There are approximately 50,000 crashes per year that make up the GES sample. The CDS database is similar, but is restricted to tow-away crashes only. Unlike GES that collects data from police accident reports only, CDS has trained crash investigation teams that gather in-depth information on each crash. The CDS investigators photograph and diagram the crash scene, prepare scene diagrams, measure vehicle damage, conduct interviews with occupants involved, and collect injury information from medical sources. FARS is similar to GES in that most of the data is gathered from police accident reports. GES and CDS are probability samples of police reported crashes that are weighted to represent all crashes. FARS is meant to be a census of all fatal traffic crashes.

Because these three data sources are all maintained by NHTSA, some of the key variables are similar. Of interest when defining pre-crash scenarios are those coded variables that pertain to the pre-crash period of the event. In the last several years of data collection, i.e. 2010 and 2011, the pre-crash variables in GES and FARS have been standardized so that they match the CDS definitions [2]. The standardization of these pre-crash variables across all three databases allows for the comparison of these data sources. Such a comparison prior to year 2010 would have not been possible. For this study, the last 5 years of NASS/CDS (2007 to 2011) were used. For GES and FARS years 2010 and 2011 were used. Previous years of FARS and GES either do not have pre-crash variables or they were drastically changed for the 2010 standardization and could not be used for this study. In order to be included in the CDS database, at least one passenger vehicle must have been towed from the scene due to damage. To facilitate comparisons between data sources, cases from FARS and GES were restricted to those involving at least one passenger vehicle. The variable definitions for passenger vehicles, including cars, light utility, light vans, and light trucks, are included in the appendix.

The data are provided by NHTSA to the public via download (ftp://ftp.nhtsa.dot.gov/). Files are sometimes modified from their original release, to correct mistakes in the data. GES 2010 files were dated October 11, 2011 and 2011 files were dated December 9, 2012. CDS 2007 files were dated August 15, 2008, 2008 files were dated December 1, 2011, 2009 files were dated September 20, 2010, 2010 files were dated September 11, 2011, and 2011 files were dated December 18, 2012. FARS 2010 files were dated July 31, 2012 and 2011 files were dated August 14, 2012.

### Crash Scenarios

Figure 1 shows photographs taken as part of a fatal rear-end collision involving a 2010 Ford Fusion (right of Figure 1) which struck a 2007 Subaru Impreza (left), which was stopped in traffic. This case is an example of a crash that would be applicable to FCAS. The driver of the Impreza, a 37-year-old male, was fatally injured (brain stem transection) while a 3-year-old female in a child seat in the middle position of the back seat only suffered moderate injuries (a foot fracture and lung contusion). The driver of the Fusion was a 49-year-old male who had a 0.0 blood alcohol concentration as measured by a police administered test. The driver of the striking vehicle was seriously injured with

bilateral rib fractures that required a 9-day hospitalization.

*Figure 1.* Photograph from NASS/CDS Investigation of a Fatal Rear-end Collision (Case 2010-82-137).

In the three NHTSA databases, the critical pre-crash event, pre-crash movement, and accident type variables provide information about the configuration and driver maneuvers in each crash. Figure 2 shows the approach developed for this study to classify collisions using database variables. Example values for each variable are provided below for the striking vehicle of the rear-end shown above. The critical pre-crash event is the event that made the crash imminent as determined by the investigator. The databases in our study had 92 critical event categories. The accident type variable describes the configuration of the crash for the first harmful event and has approximately 100 values. Finally, the pre-crash maneuver describes the vehicle's activity prior to the crash, such as decelerating in lane, passing, or going straight. Together these three variables were used to assign every vehicle in each database a pre-crash scenario. All crashes in the database were assigned a single crash scenario. Each crash was assigned a scenario based upon the crash scenarios of the two vehicles involved in the first harmful event in the crash. If there was only one vehicle involved in the crash, this vehicle was used to determine the scenario.

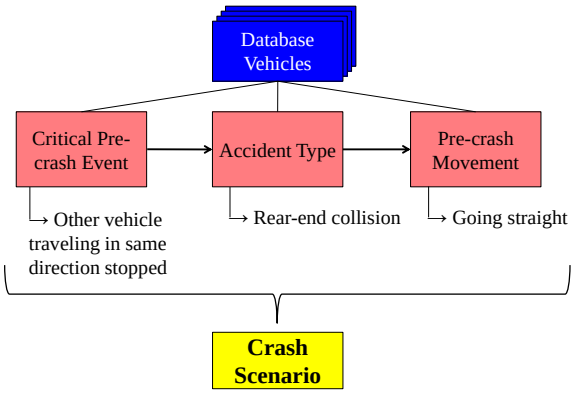


*Figure 2.* Approach for Determining Pre-Crash Scenario from NASS/CDS Variables.

In many cases the critical pre-crash event and accident type variables indicate very similar information, such as in the example rear-end crash above. The accident type variable must correspond to the first impact in a crash whereas the critical pre-crash event describes what made the first pre-crash event unavoidable. In some scenarios this can lead to meaningful differences with regard to if an active safety system would activate. Consider NASS/CDS case 2011-41-116 whose scene diagram is shown in the left of Figure 3. Vehicle 1, a 2001 Mercedes Benz E-class departed its lane and struck vehicle 2, which was stopped. The pre-crash critical event for the striking vehicle was "this vehicle traveling over the left lane line" and the accident type was a rear-end collision. The pre-crash maneuver of the striking vehicle was going straight, not changing lanes or avoiding another critical event. For the study of active safety systems, this crash would most likely be mitigated by a Lane Departure Warning (LDW) system that could have warned the driver he was exiting his lane. Compare this rear-end crash with the one involving the Fusion and Impreza, shown in the right of Figure 3. FCAS could more likely be applicable to this crash because the struck vehicle would have been in view of the front-facing sensors in time to either deliver a warning or take action. In

our approach to assign pre-crash scenarios, pre-crash critical event was prioritized over accident type because it described the portion of the pre-crash phase where active safety systems would activate more completely.

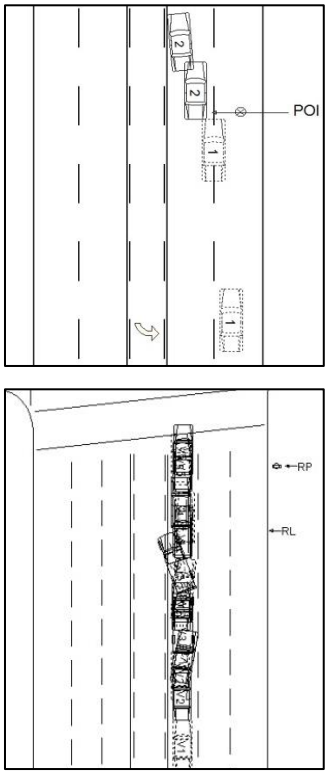


*Figure 3.* Scene Diagram Prepared by Investigator for NASS/CDS Cases 2011-41-116 (Top) and 2010-82-137 (Bottom).

Figure 4 shows the single vehicle crash scenarios: single vehicle crashes with fixed objects on the roadside, control loss, caused by an animal in the road, caused by a pedestrian or cyclist in the road, object in the road, and other. Similarly, scenarios for multiple vehicle collision are shown in Figure 5. For target population analysis, many of these crashes can be broken down further into subgroups based on pre-crash maneuver (e.g. turning, going straight) or object struck.

**Measure of Injury and Harm**

In addition to examining the frequency of crashes, the number of injuries is also an important measure of the target population. NASS/CDS codes individual injuries using the Abbreviated Injury Scale (AIS). The AIS is a one to six score that measures the threat to life an injury poses [3]. A score of one corresponds to a minor injury and a score of six corresponds to an unsurvivable injury. NASS/CDS includes AIS codes for each injury suffered by occupants. AIS scores are derived from medical records and coded by a trained AIS coding specialist. Other crash databases, such as GES, often use less exact injury scales, e.g. the KABCO scale, that are designed to be assigned by non-medical staff, e.g. police officers filling out police accident reports. These less exact injury measures assign either no injury, possible injury, moderate injury, incapacitating injury, or fatal injury to each occupant. This assessment is often made at the crash scene, is not based on medical records, and is less reliable [4].

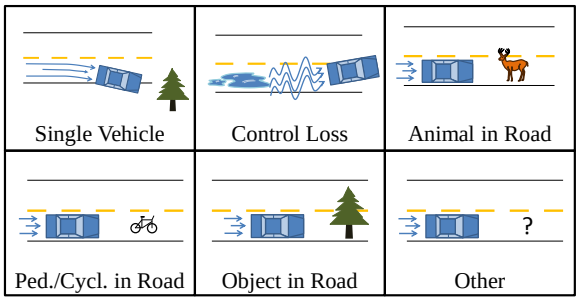


*Figure 4.* Single Vehicle Crash Scenario Categories.

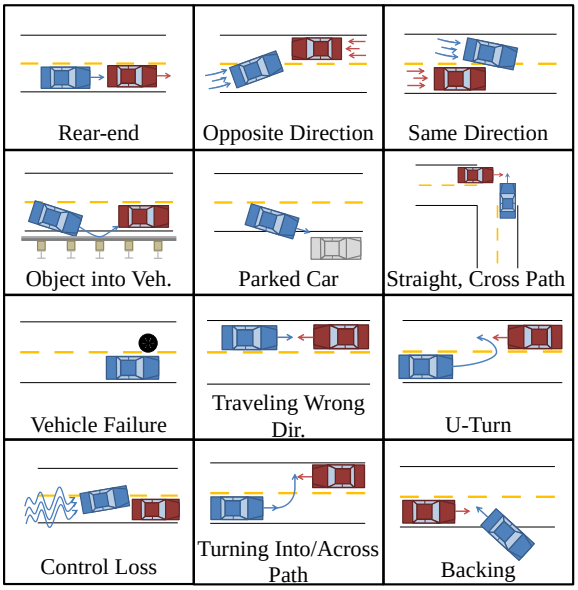


*Figure 5.* Multi-Vehicle Crash Scenario Categories.

In this study a serious injury to a body region was considered as those with AIS level 3 and above (AIS3+). Occupants were considered seriously to

fatally injured if the maximum of their body region AIS (MAIS) was of level 3 or greater (MAIS3+) or if the occupant was fatally injured. The AIS is a threat to life scale. Another measure, known as Harm, attempts to place a socioeconomic cost on injuries sustained from a crash. The Harm metric is based on medical costs, lost wages, and long term disability from an injury and is often measured with a monetary value. Each body region (e.g. head, chest, lower extremity) is assigned a representative cost for each AIS level of injury. Next, the costs of all injuries to an occupant are summed to find the Harm cost of a crash. In this study we used Harm values presented by Fildes *et al.* [5]-[7].

### Target Populations for Active Safety Systems

The target population for an active safety system is the set of collisions that would be most likely mitigated by a system. To demonstrate the utility of the scenarios developed for this study, we will examine the target populations for several systems becoming available or being developed: Forward Collision Warning (FCW), Lane Departure Warning (LDW), and Vehicle-to-Vehicle (V2V) and Vehicle-to-Infrastructure (V2I) systems. FCW and LDW warn drivers of impending frontal collisions and inadvertent lane departures, respectively. FCW and LDW are available as optional or standard equipment many on production vehicles. V2V and V2I are communication systems where vehicle safety data, e.g. position, speed, and heading, are shared between vehicles and infrastructure. This information can be used in safety applications similar to FCW and LDW. One advantage of V2V and V2I is that they are not restricted by line of sight of the sensors. FCW use radar and/or cameras to sense other vehicles and LDW systems often use cameras to track lane lines. The systems will fail if the objects being tracked are occluded, such as in intersection situations.

Table 1 summarizes the applicable crash scenarios for each of these systems. Rear-end collisions, where the driver was not maneuvering before the crash, are the most applicable scenario for FCW. The vehicles in front of the equipped vehicle must be tracked well before the crash in order to deliver an effective warning early enough. This is the case in rear-end collisions but might not be true for crash scenarios such as opposite direction crashes. LDW is applicable to road departure, opposite direction, and same direction crashes when the driver of the departing vehicle is lane keeping, i.e. going straight, prior to the departure. V2V and V2I systems could mitigate intersection and turning crashes. Drivers could be warned if they are about to enter an intersection at the same time as another vehicle as well as advise drivers when it is safe to turn across opposing lanes of traffic. V2V could also be used to accomplish the same goals as FCW. Rear-end crashes were not included in the V2V/V2I target population so that the systems' target populations are mutually exclusive.

**Table 1.**
**Applicable Crash Scenarios for Three Active Safety Systems**

| System | Crash Scenarios |
|---|---|
| Forward Collision Warning (FCW) | • Rear-end, no maneuvers |
| Lane Departure Warning (LDW) | • Road departures, lane keeping<br>• Opposite direction, lane keeping<br>• Same direction, lane keeping |
| V2V/V2I | • Straight crossing paths (SCP)<br>• Left turn across path, Opposite Direction (LTAP/OD)<br>• Left turn across path, Perpendicular<br>• Turn into path, Same Direction |

## RESULTS

### Crash Scenarios

Table 2 shows the number of crashes from GES, CDS, and FARS. GES and CDS are weighted samples of crashes. Each crash in the database is assigned a weight that describes the number of similar collisions that occurred nationally during the sample time. On average, there were 5.2 million police reported crashes, 2.1 million tow-away crashes, and 28,373 fatal crashes per year involving at least one passenger vehicle. The total number of involved occupants, both in motor vehicles and non-

motorists, was tabulated from all GES crashes. There are approximately 37.6 million persons exposed to traffic related crashes involving at least one passenger vehicle per year. The number of seriously injured occupants (MAIS3+) was tabulated from CDS and totals approximately 70,129 persons per year. Finally, there was an average of 30,960 fatalities annually, tabulated from FARS. NASS/CDS focuses on crashes that involve injury that occurs to passengers in motor vehicle crashes. Because at least one passenger vehicle must have been towed from the scene due to damage in NASS/CDS cases, there are very few crashes that involve non-motorists, i.e. pedestrians and cyclists. To aid comparison with CDS, GES and FARS were restricted to crashes involving at least one passenger vehicle. This restriction accounted for 96% of GES crashes and 94% of FARS crashes.

**Table 2.**
**Number of Crashes and Persons involving at least one Passenger Vehicle from GES 2010-2011, CDS 2007-2011, and FARS 2010-2011**

| | Total | | Annual Average | |
|---|---|---|---|---|
| **Category** | **n** | **Frequency** | **n** | **Frequency** |
| GES Crashes | 97,975 | 10,404,563 | 48,988 | 5,202,281 |
| CDS Crashes | 24,464 | 10,267,849 | 4,893 | 2,053,570 |
| FARS Crashes | 56,745 | 56,745 | 28,373 | 28,373 |
| | | | | |
| Total Occupants (GES) | 652,854 | 75,239,504 | 326,427 | 37,619,752 |
| MAIS3+ Occupants (CDS) | 4,733 | 350,645 | 947 | 70,129 |
| Fatalities (FARS) | 61,919 | 61,919 | 30,960 | 30,960 |

Figure 6 shows the number of occupants (GES), seriously injured (MAIS3+) occupants (CDS), and fatalities (FARS) for single and multiple vehicle crashes. Only 20% of occupants were involved in single vehicle crashes, yet 46% of seriously injured occupants and 56% fatalities were in single vehicle crashes. Of fatal single vehicle crashes, however, almost 1 in 5 were vehicles striking pedestrians or cyclists, almost all of which were fatalities involving occupants not in a motor vehicle. Of all fatalities, 45% were single vehicle crashes excluding pedestrian and cyclist crashes, almost equaling the proportion of seriously injured occupants involved in single vehicle crashes. Approximately 43% of Harm was in single vehicle crashes, which agrees with the number of seriously injured drivers (not shown in graph).

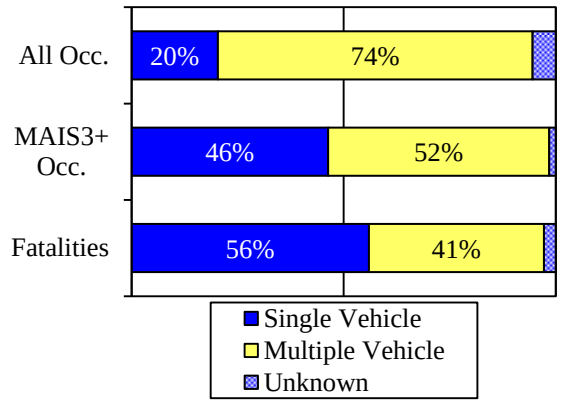


*Figure 6.* Number of Occupants, Seriously Injured (MAIS3+) Occupants, and Fatalities in Single and Multiple Vehicle Crashes involving at least one Passenger Vehicles.

The number of seriously injured occupants (MAIS3+) and fatalities vs. the total number of occupants for the most frequent crash scenarios is shown in Figure 7 and Figure 8. Points that fall above the diagonal line are overrepresented in injury or fatality frequency with respect to their exposure and *vice versa* for those points that fall below the diagonal line. Opposite direction, single vehicle control loss, and single vehicle crashes were the most overrepresented crash scenarios. Straight crossing path (SCP) and turning into/across path crashes were slightly overrepresented in injured drivers and fatalities. Rear-end collisions were the single most frequent crash mode (35% of occupants) but accounted for only 7.2% of MAIS33+ occupants and 6.8% of fatalities. The number of crashes and occupants for all pre-crash scenario are tabulated in the appendix.

**Active Safety Applicable Crashes**

Figure 9 summarizes the number of occupants, seriously injured occupants, and fatalities applicable to FCW, LDW, and V2V/V2I systems. FCW is

applicable to the most number of exposed occupants, but is applicable to a smaller proportion of injured occupants and fatalities compared to LDW and V2V/V2I. In total, these three systems could potentially mitigate 59% of both seriously injured occupants and fatalities. Annually the three systems could potentially mitigate 3,256,150 crashes, 41,625 seriously injured occupants, and 18,366 fatalities.

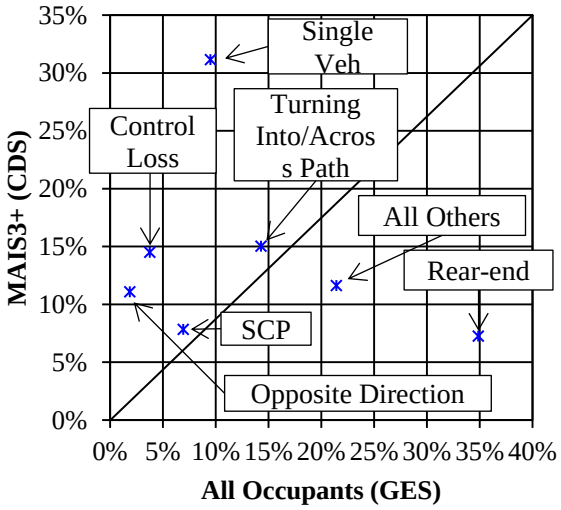


*Figure 7.* Number of Seriously Injured Occupants (MAIS3+) vs. Number of Occupants by Crash Scenario for Crashes involving at least one Passenger Vehicle.

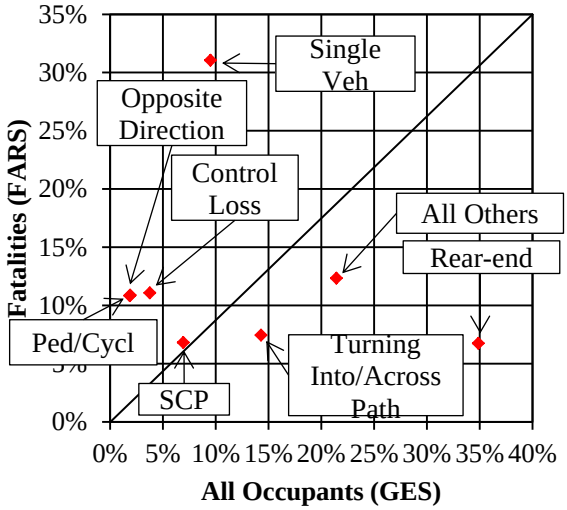


*Figure 8.* Number of Fatalities vs. Number of Occupants by Crash Scenario for Crashes involving at least one Passenger Vehicle.

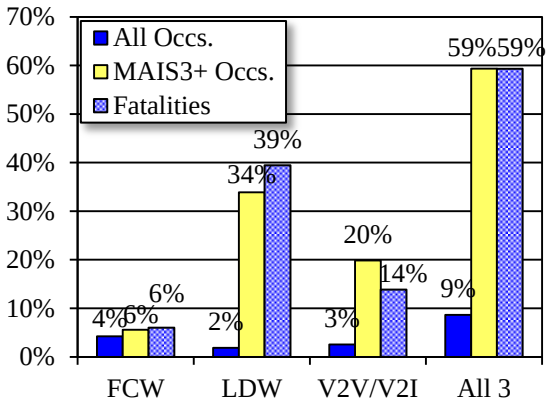


*Figure 9.* Proportions of Occupants, Seriously Injured Occupants (MAIS3+), and Fatalities Applicable to Active Safety Systems.

## CONCLUSIONS

This paper presented novel pre-crash scenarios that describe the pre-crash scenarios in crashes from real-world crash databases. These scenarios can be applied to these databases to identify the target populations for active safety systems. We identified the target population for three emerging active safety systems: FCW, LDW, and V2V/V2I systems. FCW was applicable to the largest number of exposed occupants, but was not applicable to as many seriously injured occupants and fatalities as compared to LDW and V2V/V2I. In total, these three systems could potentially mitigate 59% of both seriously injured occupants and fatalities, representing 3.3 million crashes and 18,366 fatalities anually. These crash scenarios are unique to past efforts in that they are comparable between the three major NHTSA databases, GES, CDS, and FARS. This comparison is only possible for GES and FARS 2010 due to major changes in pre-crash variables that resulted from harmonization of pre-crash variables among these databases.

## ACKNOWLEDGEMENTS

The authors would like to thank Toyota Motor Corporation (TMC), Toyota Engineering & Manufacturing North America, Inc. (TEMA), and the Toyota Collaborative Safety Research Center (CSRC) for funding this research. The authors would also like to thank Chuck Gulash and Rini Sherony of TEMA and Masami Aga, Katsuhiko Iwazaki, and

Hiroyuki Takahashi of TMC for their feedback and assistance in preparing this manuscript.

## REFERENCES

[1] Eigen, A. M., Najm, W. G. Problem Definition for Pre-Crash Sensing Advanced Restraints. DOT HS 811 114, U.S. Department of Transportation, National Highway Traffic Safety Administration. April 2009.

[2] "2010 FARS/NASS GES Standardization," National Highway Traffic Safety Administration, Washington, D.C., Report Number DOT HS 811 564, 2011.

[3] Gennarelli, T. A., Wodzin, E. AIS 2005. Association for the Advancement of Automotive Medicine: Barrington, IL, 2005.

[4] Compton, C. P. "Injury Severity Codes: A Comparison of Police Injury Codes and Medical Outcomes as Determined by NASS CDS Investigators," *Journal of Safety Rsearch – Traffic Records Forum proceedings*, 36, 483-484, 2005.

[5] Fildes, B. N., Lane, J. C., Lenard, J., and Vulcan, A. P. "Passenger Cars and Occupant Injury: Side Impact Crashes." Report CR 134, Federal Office of Road Safety, Canberra, Australia, 1994.

[6] "Feasibility of Occupant Protection Measures," Monash University Accident Research Centre, Clayton, Australia, Report CR 100, June 1992.

[7] Gabler, H. C., Digges, K., Fildes, B. N., Sparke, L. "Side Impact Injury Risk for Belted Far Side Passenger Vehicle Occupants," SAE International Technical Paper Series, Warrendale, PA, Paper Number 2005-01-0287, 2005.

## APPENDIX

**Table A2.**
**Body Style Codes for GES, CDS, and FARS**

| Group | Codes between | and | Excluding |
|---|---|---|---|
| Cars | 1 | 13 | |
| Light Utility Vehicle | 14 | 19 | |
| Light Van | 20 | 29 | |
| Light Truck | 30 | 49 | 42 |
| Bus | 50 | 59 | |
| Heavy Vehicle | 60 | 79 | 65 and 73 |
| Motor Home | 42, 65, 73 | | |
| Motorcycle/Moped | 80 | 89 | |
| Other Vehicle (e.g. ATV, construction equipment, golf cart) | 90 | 97 | |
| Not Reported | 98 | | |
| Unknown | | | |

**Table A2.**
**Number of Crashes per Pre-Crash Scenario Category**

| | Crashes | | | % Crashes | | |
|---|---|---|---|---|---|---|
| **Scenario** | **GES** | **CDS** | **FARS** | **GES** | **CDS** | **FARS** |
| No Scenario | 449,717 | 175,211 | 1,507 | 4.3% | 1.7% | 2.7% |
| Sing Veh - Departure | 1,246,953 | 1,775,040 | 18,041 | 12.0% | 17.3% | 31.8% |
| Sing Veh - Control Loss | 766,695 | 1,161,477 | 6,278 | 7.4% | 11.3% | 11.1% |
| Sing Veh - Animal in Road | 566,055 | 198,867 | 667 | 5.4% | 1.9% | 1.2% |
| Sing Veh - Ped/Cyclist in Road | 173,224 | 9,950 | 6,682 | 1.7% | 0.1% | 11.8% |
| Sing Veh - Object in Road | 38,114 | 52,368 | 73 | 0.4% | 0.5% | 0.1% |
| Sing Veh - Other | 168,383 | 60,468 | 980 | 1.6% | 0.6% | 1.7% |
| Mult Veh - Rear-end | 3,386,482 | 2,536,117 | 3,779 | 32.5% | 24.7% | 6.7% |
| Mult Veh - Opp Dir, no turning | 136,744 | 236,813 | 5,548 | 1.3% | 2.3% | 9.8% |
| Mult Veh - Same Dir, no turning | 655,103 | 268,560 | 1,033 | 6.3% | 2.6% | 1.8% |
| Mult Veh - Control Loss | 154,836 | 265,596 | 1,791 | 1.5% | 2.6% | 3.2% |
| Mult Veh - Object into Vehicle | 6,753 | 26,967 | 272 | 0.1% | 0.3% | 0.5% |
| Mult Veh - Parked Car | 425 | 207,750 | 12 | 0.0% | 2.0% | 0.0% |
| Mult Veh - Crossing Path, Both Straight | 667,587 | 894,554 | 3,750 | 6.4% | 8.7% | 6.6% |
| Mult Veh - Turning Into/Across Path | 1,540,901 | 2,126,451 | 4,343 | 14.8% | 20.7% | 7.7% |
| Mult Veh - Wrong Direction | 11,520 | 29,396 | 809 | 0.1% | 0.3% | 1.4% |
| Mult Veh - U-turn | 41,092 | 61,157 | 118 | 0.4% | 0.6% | 0.2% |
| Mult Veh - Backing | 166,675 | 30,074 | 49 | 1.6% | 0.3% | 0.1% |
| Vehicle Failure | 74,029 | 107,784 | 530 | 0.7% | 1.0% | 0.9% |
| Multiple/Conflicting Scenarios | 147,690 | 39,232 | 394 | 1.4% | 0.4% | 0.7% |
| No Driver | 5,585 | 4,018 | 89 | 0.1% | 0.0% | 0.2% |
| **Total** | **10,404,563** | **10,267,849** | **56,745** | **100.0%** | **100.0%** | **100.0%** |

**Table A3.**
**Number of Occupants, MAIS3+ Occupants, Harm, and Fatalities**

| | Frequency | | | | % | | | |
|---|---|---|---|---|---|---|---|---|
| **Scenario** | **Total Occ.** | **MAIS3+** | **Harm** | **Fatalities** | **GES** | **MAIS3+** | **Harm** | **Fatalities** |
| No Scenario | 4,097,882 | 5,321 | 2,688 | 1,629 | 5.4% | 1.5% | 1.4% | 2.6% |
| Sing Veh - Departure | 7,150,105 | 109,263 | 58,885 | 19,234 | 9.5% | 31.2% | 29.8% | 31.1% |
| Sing Veh - Control Loss | 2,831,220 | 50,826 | 24,186 | 6,859 | 3.8% | 14.5% | 12.2% | 11.1% |
| Sing Veh - Animal in Road | 2,153,844 | 1,332 | 890 | 687 | 2.9% | 0.4% | 0.5% | 1.1% |
| Sing Veh - Ped/Cyclist in Road | 1,428,716 | 0 | 5 | 6,741 | 1.9% | 0.0% | 0.0% | 10.9% |
| Sing Veh - Object in Road | 80,534 | 0 | 56 | 80 | 0.1% | 0.0% | 0.0% | 0.1% |
| Sing Veh - Other | 1,643,124 | 1,034 | 1,104 | 1,048 | 2.2% | 0.3% | 0.6% | 1.7% |
| Mult Veh - Rear-end | 26,237,454 | 25,415 | 19,307 | 4,182 | 34.9% | 7.2% | 9.8% | 6.8% |
| Mult Veh - Opp Dir, no turning | 1,402,784 | 38,883 | 19,500 | 6,706 | 1.9% | 11.1% | 9.9% | 10.8% |
| Mult Veh - Same Dir, no turning | 6,941,534 | 6,243 | 3,395 | 1,158 | 9.2% | 1.8% | 1.7% | 1.9% |
| Mult Veh - Control Loss | 1,157,907 | 18,190 | 9,257 | 2,083 | 1.5% | 5.2% | 4.7% | 3.4% |
| Mult Veh - Object into Vehicle | 36,463 | 2,417 | 1,788 | 320 | 0.0% | 0.7% | 0.9% | 0.5% |
| Mult Veh - Parked Car | 1,041 | 2,444 | 1,241 | 16 | 0.0% | 0.7% | 0.6% | 0.0% |
| Mult Veh - Crossing Path, Both Straight | 5,212,537 | 27,460 | 17,292 | 4,220 | 6.9% | 7.8% | 8.8% | 6.8% |
| Mult Veh - Turning Into/Across Path | 10,754,450 | 52,693 | 32,254 | 4,610 | 14.3% | 15.0% | 16.3% | 7.4% |
| Mult Veh - Wrong Direction | 55,965 | 3,181 | 2,001 | 991 | 0.1% | 0.9% | 1.0% | 1.6% |
| Mult Veh - U-turn | 378,652 | 1,301 | 840 | 125 | 0.5% | 0.4% | 0.4% | 0.2% |
| Mult Veh - Backing | 1,228,872 | 177 | 156 | 53 | 1.6% | 0.1% | 0.1% | 0.1% |
| Vehicle Failure | 272,519 | 4,023 | 2,321 | 636 | 0.4% | 1.1% | 1.2% | 1.0% |
| Multiple/Conflicting Scenarios | 2,171,653 | 442 | 272 | 448 | 2.9% | 0.1% | 0.1% | 0.7% |
| No Driver | 2,245 | 0 | 1 | 93 | 0.0% | 0.0% | 0.0% | 0.2% |
| **Total** | **83,344,310** | **350,470** | **197,305** | **65,252** | **100.0%** | **100.0%** | **100.0%** | **100.0%** |

# An Application of Weibull Analysis to Determine Failure Rates in Automotive Components

Jingshu Wu, PhD, PE, Stephen McHenry, Jeffrey Quandt
National Highway Traffic Safety Administration (NHTSA)
U.S. Department of Transportation
Paper No. 13-0027

## 1. Abstract

This paper focuses on the automotive component failure rate detection using Weibull analysis and other survival analysis techniques. Detailed attention is paid to three areas: 1) overall failure rates are described statistically first, and data cleaning and definitions of 'failed' and 'censored' data within the research time or warranty period are made; 2) Kaplan-Meier life curves and Log-rank tests are used to compare the component reliability over time and explore risks factor related to the component failure; 3) Weibull regressions, with two and three parameters, are applied to fit real-world reliability data from different test conditions, and to predict the automotive component failure trend over future time. The analysis results agree well with real-world test data, and provide reasonable prediction of future failure trends.

## 2. Introduction

Automotive components fail over time, especially beyond the warranty time period. It is important to study the reasons why automotive components fail, and to predict the component reliability trends, associated with various manufacturing, environmental and testing conditions.

For effective use of a predictive failure analysis of automotive components, all of the failures within a specific driving time period need to be captured. Because any repairs to failed components are free to the owner and paid by the manufacturer during the manufacturer's *basic warranty* coverage period (usually 36 months or 36,000 miles), most repair records are kept well. These are available to investigators and provide information on what components have been repaired or replaced at specific mileages and time in service. However, as soon as the basic warranty (free repair) period is over, and owners are required to pay for the repairs, there is no central repository to collect comprehensive information on failures due to data availability, which may lead to limited or incomplete analysis beyond the relatively short basic warranty window. In order to overcome this obstacle and to capture more insightful failure information within a relatively longer period, a data analysis technique was developed to utilize the manufacturer's *extended warranty* data to create a richer and more representative sample, from which the data analysis could be efficiently utilized, although it is not easy to completely avoid data bias when the extended warranty programs are slected. Most manufacturers will offer an extended service plan to an owner that provides coverage for a specified period beyond the basic warranty. For example the *extended warranty plan* may be for 5 years from purchase and 60,000 miles, or 5 years/75,000 miles, or 5 years/100,000 miles, or for 4 years/75,000 miles, etc. and that there are typically extended service plans offering different levels of coverage on different components (e.g., Gold Plan, Platinum Plan, Powertrain Plan). The driver may choose a plan that best fits his/her need. The data technique developed here requires that 1) all vehicles sold with all extended service plans be identified, 2) the plan(s) that cover repairs on the subject component be identified, 3) that a calculation is made to determine average miles per month driven for the subject vehicles using records of warranty repairs, which provide time in service and mileage at the time of repair. All detailed records of repairs associated with time and mileages are then used for data analysis.

For example, one powertrain component under consideration has a population sample size of over 200,000, the component failures starts around 30,000 miles, with extended service plans for 60 months, or 100,000 miles (warranty period or agreements), whichever comes first, the data set is termed as '*Old K60'* data of type-1 in this study. Second type of test data of this same component may have a different failure mode or with a mix of failure modes. For this type-2 test, there are three new data sets of interest – first new data set has the capture information of 60 months and 100,000 miles, i.e., the maximum month to failure is 60 months, and maximum mileage of 100,000 miles ('*New K60' data*); Similarly, 2nd new data set has the information of 48 month/100,000 mile capture, i.e., the maximum month to failure is 48, and with maximum mileage of 100,000 ('*New K48*'); The third contains the info of 72 month/100,000 mile capture ('*New K72'*). In total, there are four sets of data for type 1 and type 2 tests of this same component, which are summarized in Table 1.

Most reliability test data are closely time-related, and failures happened within the warranty time window or beyond, a technique of 'time-to-event' or survival analysis is very suitable for such reliability data, especially Weibull model is a well established tool to fit the test data and to predict the future failure trend beyond the available test duration. The main goals of this project are to apply a Weibull model to the automotive component reliability analysis, and then explore the failure rate over service time or mileage, and to provide some statistically-based insights into the component failures by the following process:

- Provide descriptive summary of available failure data of a component;
- Verify the reliability difference over time of the component under two different conditions;
- Explore the component failure probability over test time, and compare the failure rates of the same component from a few different data sets;
- Improve the data fitting and prediction by using a three-parameter Weibull model, and compare with real-world test results.

## 3. Descriptive Summary of Data Sample

The focused automotive component test data, with service plan for 60 months, or 100,000 miles ('Old K60' of Type-1), can be divided into two sub-groups: The first group is "failed event" data (234 failures as following Table 1); The second group, 'Suspension' or 'Censored' group, has 4483 observations and has no failures within 60 months, further, their future failure behavior beyond 60 months are unknown. The service time of the 'censored' group, at least, all passed the 'Cut-Off' line of 60 months. Figure 1 on next page is helpful to explain the failures within and beyond a warranty time, or research time window.

The similar descriptive summaries of three new data sets (New K60, New K48, and New K72) are also listed in following Table 1, with the failure data descriptive summary.

**Table1: Descriptive Statistics for Failed Components**

| | **mean** | **Std Dev.** | **Min** | **Max** | **failure/ all %** |
|---|---|---|---|---|---|
| Type-1: **Old K6**0 Data (234 failures, 4483 censors) | | | | | |
| Month | 44.3 | 9.92 | 19.0 | 60 | 5.0% |
| Type-2: **New K60** Data (280 failures & 4474 censors) | | | | | |
| Month | 43.3 | 10.14 | 14.0 | 60 | 5.89% |
| Mile | 70,597 | 17,326 | 27,920 | 126,288 | |
| Type-2: **New K72** Data (164 failures & 2282 censors) | | | | | |
| Month | 42.24 | 13.68 | 9.0 | 68 | 6.70% |
| Mile | 60,097 | 17,513 | 21,290 | 98,958 | |
| Type-2: **New K48** Data (54 failures and 871 censors) | | | | | |
| Month | 32.3 | 10.3 | 10.0 | 48.0 | 5.80% |
| Mile | 69,798 | 20,370 | 28,888 | 97,687 | |

The ratio of 'failures /all %' (all=failures + censors)' in the last column in Table 1 is an important parameter that gives the overall failure rate at the end of service time, and will be used later to compare with the failure rate predicted by a Weibull model at the same time. For example, the failure rate at the time of 60 months is 5%, for data 'Old K60', or 5.89% for 'New K60' data.

## 4. Methods of Modeling Survival and Failure Rates

It is of great interest to observe the component failure rate, F(t), or from an opposite point of view, the survival probability varying over a test time, S(t), while there is a simply relationship between the two: 'S(t)= 1 – F(t)', i.e., 20% failures means 80% survival rate among a fixed sample.

One of the most useful tools to compare the survival probability over time is a method proposed by

Kaplan and Meier [1]. The Kaplan-Meier survival curve is described by the following formula:

$$\hat{S}(t) = \prod_{t_i <= t} (1 - \frac{d_i}{n_i}) = \prod_{t_i <= t} (\frac{s_i}{n_i}) \qquad (1)$$

Where '$d_i$' is 'deceased' subject or failed automotive component, and '$s_i$' is the 'survivor' or 'alive' component, and '$n_i$ ' is the total (both failed and suspension components) in the study at any moment beyond time zero.

Or, turning the problem around, the failure probability over test time, F(t), equal to '1-S(t)', it can be further expressed by following Eq. (2) in Weibull model [2]:

$$F(t) = 1 - e^{-(t/\eta)^{\beta}} \qquad (2)$$

Or, equivalently it can be visualized by the following *'linear'* transformation, as Eq. (3): [2]

$$\log(-\log(S(t)) = \beta \log(t) - \beta \log(\eta) \qquad (3)$$

In the above Eq.(3), S(t) is survival function, which can be estimated from the Kaplan-Meier curve discussed earlier, and F(t) of Eq. (2) is the accumulation of failure probability as time increases, here '**β**' is regarded as the 'Slope' of the 'linear' plot, or 'Shape' parameter, and '**η**' is a 'Scale' parameter and is related to the intercept of the 'linear' plot.

When a plot of test data is not visualized as a *'linear'* plot as Eq. (3), especially at the earlier time stage, a Weibuull with three parameters, as Eq. (4), provides a better data fitting, where a time shift, or threshold, $t_0$, is included as Eq. (4) -

$$F(t) = 1 - e^{-((t - t_0)/\eta)^{\beta}} \qquad (4)$$

Three cases are studies in details using above Eq. (1) to (4), from some investigation data and examples, as shown as following Sections 5, where Case1 compares the reliability curves over time of two different conditions; and Cases 2-3 applies Weibull models, with two or three parameters, for data fitting and future trend predictions.

Computing procedures by SAS Institute, *'LifeTest', 'LifeReg', and 'Reliability'*, are used for calculations [3]. Some extra attentions should be paid to - how to clean the time data using SAS program; to determine the test interval from start to end; to convert the time data from calendar time (with different starting time each) to study time where all subjects have the same starting time; and to determine the relative status of 'censor' over time. [1,3]

## 5. Case Studies of Modeling Survival and Failure Rates

### ***Case 1***: *Compare Survival Rates Over Time of Two different Conditions*

It is often required to investigate automotive component reliability or survival rates over time under two different conditions, either manufactured during different time periods, or, by two different designs, or being used under different environmental conditions.

Here is one example of discussing 'failed event' and 'censor' within the research time window and beyond – there are 234 failures from data set of 'Old K60' within the study time of 60 months, however, the 'Suspension' or 'Censored' 4483 observations have service time beyond the 'Cut-Off' line of 60 months, and their future statuses beyond 60 months are unknown (see Figure 1).

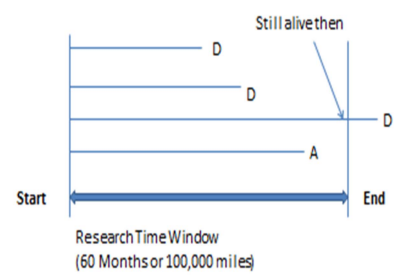


**Figure 1**: **Research Time Window, censor & failures**

In this project, the research time frame is '0-60' months (warranty duration or other agreement), some components have test time less than 60 months without failures, and they are treated as 'censored' data; all 'suspension' data are still 'alive' without failures beyond 60 months ('Censors', or '0'), and their service time are all assumed to be at least 60 months. On the other hand, all 'failed' data (234 failures, coded as '1') have specific time of failures for each, prior to 60 months (Figure 1).

The following Kaplan-Meier life curves (Figure 2), using 'Old K60' failed data only, are studied in detail to verify if the reliability of products built during 'Period A' might be different from the reliability of products built at other time.

Figure 2 indicates that no significant difference of reliability is observed between the products built during 'Period-A' (orange color) and other dates ('blue' or '0'). The log-rank test, which compares two survival rate curves over time, provides a p-value of 21% for the two Kaplan-Meier plots of Figure 2, where 'X-axis' has a unit of 'month' and 'Y-axis' displays the probability from zero to 1.0.

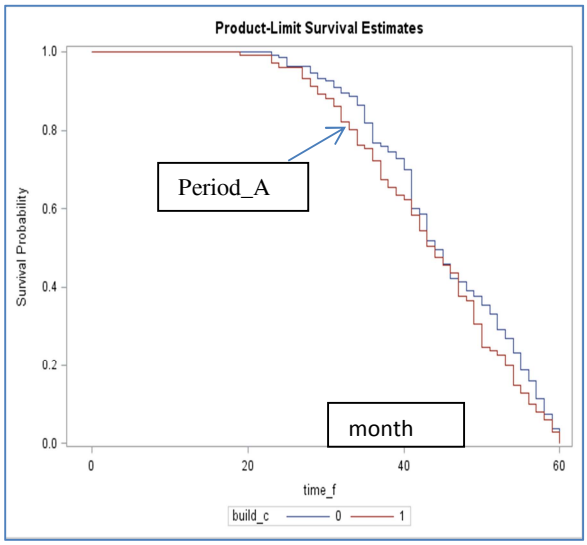


**Figure 2: Survival Plots of Component built during 'Period_A' (Orange Color) vs. Other Dates.**

On the other hand, a significant difference (p-value <0.0001) of reliability is observed (Figure 3), from the failed data of another automotive component whose mileage (X-axis) information for each is available, under two different using conditions (1673 failures under Condition-A, and 531failures under Condition-B).

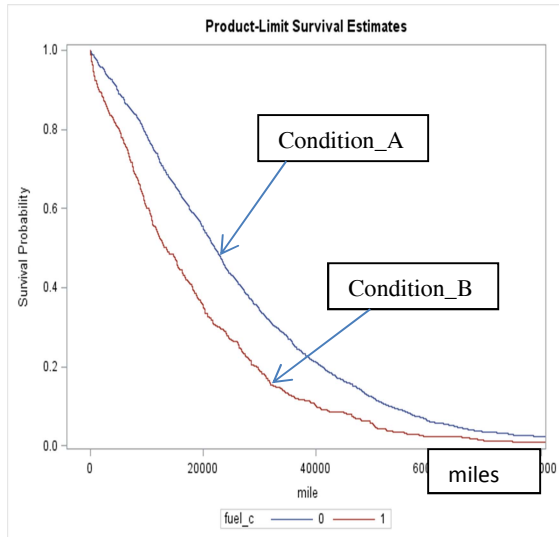


**Figure 3: Survival Plots of Two Groups with two Using Conditions, p-value<0.0001**

One useful feature of the Kaplan-Meier life curve is to permit comparison of the survival rates over time between two different conditions, and evaluate the effect of one single factor (such as manufacturing time as Figure 2, or using condition as Figure 3) on reliability, if more risk factors are considered simultaneously, the Cox proportional hazard model is a better tool to evaluate multiple risk factors [3].

## ***Case 2**: Weibull Modeling with 'Linear' Plot using Different Data Sets*

One specific automotive component can be tested under different conditions, and the different tests (such as load or temperature) may lead to different failure modes. A 'linear' Weibull model, based on Eq. (2) –(3), is used first to plot the failure rates over time. For various tests of this same component, the similar approach of treating 'failed' events ('1') and 'censor' data ('0'), as Figure 1 of Case 1, is applied to all data sets: 'Old K60', 'New K60', 'New K72' and 'New K48'.

Figure 4 shows the 'linear' plots of Weibull modeling of failure probability from data set of 'Old K60', where 'X-axis' has a unit of 'month' and 'Y-axis' displays the probability from zero to 1.0.

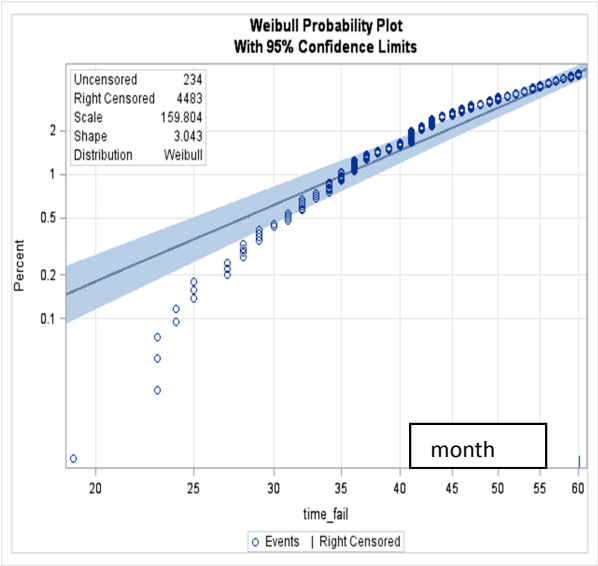


**Figure 4: Weibull Plot with Data of 'Old K60', where 234 are failures and 4483 are "suspension"**

In Figure 4, the failure rate will reach approximately 5 percent afters 60 months, and this prediction agrees very well with the test result as Table 1 (the last column and 3rd row). On the other hand, the 'linear' Weibull model with only two parameters of '**β**' ('Slope' or 'Shape') and '**η**' ('Scale') does not fit the earlier time data very well (under 30 months), more discussions will be given later in 'Case 3', where the 'non-linear' plot under 30 months will be described further.

The data fitting results from using all data ('failed' and 'censored' data) and from 'failed' data only are listed in Table 2.

**Table 2**: Weibull Parameters and Failure Prediction (Two Samples out of 'Old K60' Data)

| Parameter | 'Failed, (1)' and 'Suspension, (0)' | Failed data ('1') Only |
|---|---|---|
| **β** (slope/shape) | 3.04 | 5.24 |
| **η** (scale) | 159.8 | 48.2 |
| 5% failure | 60 months (*) | 23 months |

When a few test data sets of the same component are available, it is of interest to compare the failure rates from using old data (Old K60), together with the results using new data (New K60, New 72K, and New 48K), as shown in Table 3. The failure rate from the shortest warranty program (48 months) is slightly faster, which reflects the reality of components in use.

**Table 3: Weibull Parameters and Failure Prediction (One Old & Three New Data Samples)**

| parameter | Old 60K | New 60K | New 72K | New 48K |
|---|---|---|---|---|
| **β** (shape) | 3.04 | 2.84 | 1.79 | 2.20 |
| **η** (scale) | 159.8 | 161.1 | 311.9 | 172.4 |
| 5% fail. | 60 mo | 56 Mo | 59 Mo | 45 mo |
| 10% fail | 76 mo | 73 mo | 88 mo | 62 mo |

Figure 5 provides the Weibull modeling results using two data sets of 'Old K60' and 'New K60' (with the same warranty program) as one example. The predictions from the two different data sets agree well, and indicates that the same component fails at a similar rate although under two slightly different test modes and conditions.

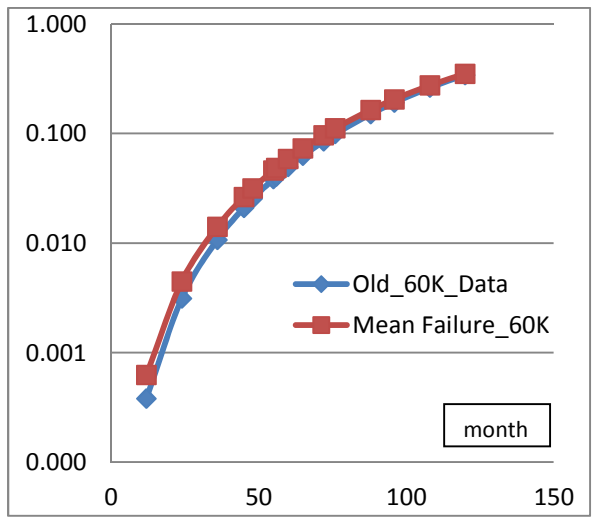


**Figure 5**: **Compare Mean Failures (Y-axis) vs. Month (X-axis) from Old Data (Old K60) vs. New Data (New K60).**

## ***Case 3:*** *Improving Data Fitting and Prediction by Considering the Time Shift*

The Weibull 'linear' plot with only two parameters, as Figure 4, is not fitting data well enough, especially at the earlier time stage (time <30 months). A Weibull model with three parameters, shown as Eq. (4), provides a better fit. The data fitting parameters displayed in Figure 6 are for the'Old K60' data.

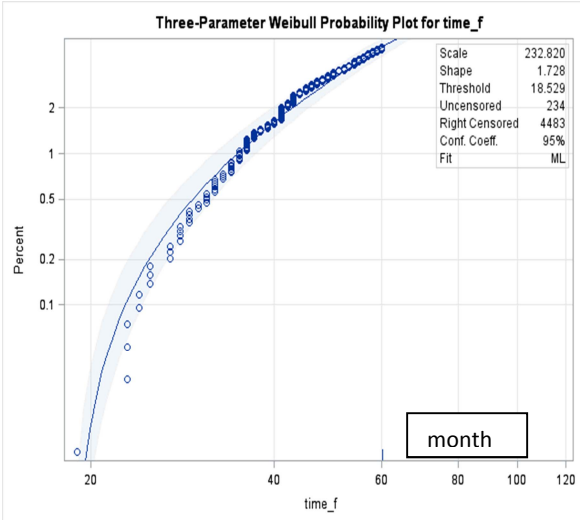


**Figure 6**: **Failure (Y-axis) vs. Month (X-axis) using Eq (4), 'Old 60K' data**

Furthermore, the three parameters of Figure 6 (Slope $\beta$=1.728, Scale $\eta$=232.82, and threshold or time-shift $t_0$=18.529) are used in Eq. (4), and provides the future trend prediction as Figure 7.

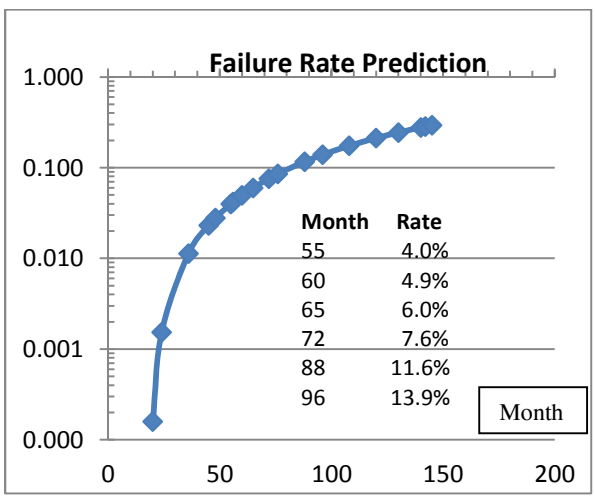


**Figure 7**: **Mean Failure Prediction vs. Month using Results of Figure 6, by Eq(4), with Slope (1.728), Scale ( 232.82), and time-shift (18.529), 'Old 60K' data.**

A similar Weibull curve as Figure 6 but using 'mileage' for the 'X-axis' is also plotted from a data set 'New K60', and the plot of failure against mileage can be more intuitive and realistic sometimes than the similar curve of failure against time (a car can be kept in a garage for a long time).

## 6. Conclusion

- Modeling of automotive component reliability is a data mining and learning process at NHTSA. From the simple statistical description, to estimation of a reliability curve over time, to a proper mathematical model to fit the test data and to predict the future component failure trend.

- Employing the Kaplan-Meier life curve permits us to compare the component reliability over time between two different conditions, and to evaluate the effect of one single factor with statistical reliability.

- A Weibull model with two parameters (slope, $\beta$, and scale, $\eta$) can reasonably predict the mean failure with a 'linear' model, while a Weibull model with three parameters can treat some 'nonlinearity' at earlier time stage much better. For example, about 5 percent of products fail when service time has reached 60 months, and this prediction agrees well with the known test.

- The modeling results from using a few different test data sets from a same component provide meaningful comparisons, and such comparisons permit insights into component failure modes under different manufacturing regimes.

## 7. References


1. Kaplan, E. L. and Meier, P. (1958), "Nonparametric Estimation from Incomplete Observations", J. of the American Statistical Association, 261, 719-724.
2. Abernethy, Robert, *The New Weibull Handbook*, (3rd Edition), 1999
3. Allison, P. (1999), *Survival Analysis using SAS: A Practical Guide*, SAS Publishing.

# LAPLACE DOMAIN ANALYSIS OF THE COLLINEAR VEHICLE-TO-VEHICLE COLLISION UNDER LINEAR FORCE-DEFLECTION CONSTRAINTS COUPLED WITH NET EXTERNALLY APPLIED LOADS

**Jai Singh**
Biomechanical Engineering Analysis & Research Inc.
United States
Paper Number 13-0016

## ABSTRACT

The focus of the subject study was on the development of the closed-form solutions for displacement, velocity and acceleration, based upon the utilization of the Laplace transform, experienced by each collision partner involved in a collinear collision under the constraints of linearity in the force-deflection response during closure and separation and while subject to any number of net externally applied loads for which an analytic Laplace transform was determinable. Starting from the basic expression of Newton's Second Law, the coupled equations of motion were developed in standard matrix-vector form by the introduction of the definitions of structural deflections in terms of the displacements of the center of mass of each collision partners and the massless common collision interface. The solution for the equations of motion was determined by applying the Laplace Transform and determining the solution for the dynamic stiffness matrix and transfer function by means of an Eigendecomposition. The closed-form analytic for the Laplace domain displacement was readily amenable to the inverse Laplace Transform and thereby provided a closed-form analytic solution for displacement in the time domain. The first and second time derivatives of this solution provided the closed form solution for velocity and acceleration, respectively. The reduced forms of each of these three equations, addressing the specific limits of the achievement of common velocity at the terminus of closure and the achievement of zero acceleration due to the collision force at the terminus of separation, were then developed.

The use of the residue theorem, instead of a partial fraction expansion, for the evaluation of the transfer function, coupled with the reduction in the complexity of the general problem secondary to both the complex conjugate nature of the solutions for the Eigenvalue problem and the reduction of the same to only complex roots for the solution to the characteristic polynomial of the dynamic stiffness matrix for the undamped problem, revealed a solution set comprised of a rigid body mode and a solution based upon the circular frequency of the effective system mass and stiffness. Depending on the nature of the net externally applied forces, the solution for the time of terminus of closure could be determined from basic trigonometric relationships or from equating the velocities of the collision partners in the Laplace domain, solving for the Laplace variable and then performing an inverse Laplace transform to obtain the solution in the time domain. The terminus of the separation could be solved for in a similar manner through the use of the acceleration of either collision partner.

## INTRODUCTION

Collinear vehicle-to-vehicle collisions, either in full actuality or reductive in the case of minimal vehicle rotation or lateral translation during the collision phase, thereby reducing the collision phase to that of global uniaxiality, represent a common situation encountered in the field of motor vehicle accident reconstruction. The analysis of such collisions, as with a substantial number of vehicle-to-vehicle collisions, is predicated upon the treatment of the collision partners, during the duration of the collision, as being a single system subject solely to the collision force, generated internally, within the system. Forces applied external to the system (e.g. braking, acceleration, drag, etc.) are typically neglected as their magnitude is substantially smaller than that of the magnitude of the collision force. There are two general situations in which such an approach may lead to the substantive underestimation of the collision severity. The first case is when one or both of the collision partners is interacting with at least one additional partner during the collision phase. The second is in the case of exceedingly low velocity collisions. There are a number of empirical studies within the scientific literature that detail the collision response for the latter case [1-5] or for relatable events [2, 6-8].

From the modeling perspective, the focus of the extant scientific literature has been within the context of modeling the effects of brake application during the collision phase. Emori and Horiguchi [1] and Siegmund et al. [2] modeled the effects of braking by

adding impulse terms to the post-collision side of the one dimensional conservation of linear momentum equation. This was combined with the definition of the coefficient of restitution to derive paired equations for the change in velocity of each collision partner in relation to the velocity of the striking vehicle under the case of the struck vehicle being at rest at the start of closure. Anderson et al. [4] expanded this formulation in terms of closing speed. Mastandrea and Vangi [9] approached the problem by separating the closure and separation phases. The separation force-deflection response was modeled as being bilinear with the inflection point being defined by the collision force magnitude corresponding to the collision force magnitude on loading associated with the linear bumper stiffness. The authors implemented a discretized form of the equations of motion and braking force, over each sequential time step, was taken as the average value between the time step. The cited literature has focused on the use of time domain techniques for modeling the collinear vehicle-to-vehicle problem, under global uniaxial constraints, and with net externally applied forces present.

The objective of the subject study was to apply an integral transform method, specifically the Laplace transform method, to the subject problem, under strict linear force-deflection modeling constraints.

## THEORY

Collinearity with global uniaxiallity greatly simplifies the collision problem by reducing the rotation matrices associated with orientation to identity matrices and by reducing the degrees of freedom for each collision partner to unity. We consider the case of an aligned collinear collision between two collision partners. For ease of reference, the collision partners and their relevant parameters are referenced using the subscript notation of one and two, respectively. Two limiting factors are emplaced in regards to the subject theoretical development. The first is that the collision force is a function of the structural deflection of the collision partners. The second is that scope of externally applied unbalanced forces applied to each collision partner are either constant or temporally varying without the explicit inclusion of being functions of displacement. Terms in boldface type represent vector quantities.

The collision is temporally manifested by the start of closure, denoted as $t = t_o$, the terminus of closure/start of separation, denoted as $t = t_c$ and the terminus of separation, denoted as $t = t_s$. The structural deflection experienced by the contacted regions of the first and second collision partner, are denoted as $\boldsymbol{\delta}_1(t)$ and $\boldsymbol{\delta}_2(t)$, respectively. The peak deflection experienced by each collision partner, under the modeling limits, occurs at $t = t_c$ and is denoted as $\boldsymbol{\delta}_1(t_c) = \boldsymbol{\delta}_{1d}$ and $\boldsymbol{\delta}_2(t_c) = \boldsymbol{\delta}_{2d}$, respectively. The residual deformation (i.e. crush – a purely static parameter) for each collision partner, under the modeling limits, occurs at $t = t_s$ and is denoted as $\boldsymbol{\delta}_1(t_s) = \boldsymbol{\delta}_{1s}$ and $\boldsymbol{\delta}_2(t_s) = \boldsymbol{\delta}_{2s}$, respectively. The center of mass displacement experienced by each collision partner, measured with respect to an inertial frame of reference, is denoted by $\mathbf{u}_1(t)$ and $\mathbf{u}_2(t)$, respectively. The displacement of the common collision interface between the two collision partners, measured with respect to an inertial frame of reference, is denoted as $\mathbf{u}_{IF}(t)$. The single and double dot notation is used for velocity and acceleration, respectively. The collision force is denoted as $\mathbf{F}_c(t)$ and has a peak magnitude $|\mathbf{F}_{cp}|$ at $t = t_c$ and zero magnitude at $t = t_s$. Figure 1 depicts the collinear collision under consideration.

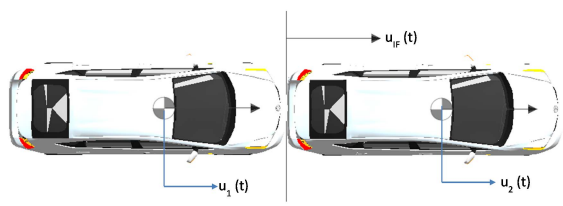


*Figure 1.* Collinear collision under consideration

### Equations of motion for the collinear collision

The second order differential equation of motion for each collision partner can be written through the direct implementation of Newton's Second Law [10].

$$m_1\ddot{\mathbf{u}}_1(t) = -\mathbf{F}_c(t) + \mathbf{F}_{1ext} \qquad (1).$$

$$m_2\ddot{\mathbf{u}}_2(t) = \mathbf{F}_c(t) + \mathbf{F}_{2ext} \qquad (2).$$

As noted previously, the form of the externally applied unbalanced forces on either collision partner are in the form of a constant force $F_{jext} = F_{jconstant}$, a time varying force $F_{jext} = F_{jext}(t)$ or a combination of the two.

### Linear loading and unloading models

The simplest method for modeling the force-deflection response is that of a linear relationship between force and deflection. In this case, each collision partner has a structural response defined as

$k_1$ and $k_2$, which differ from each other during closure (loading) and separation (unloading) and which differ for each collision partner during loading and unloading. The limitations of the linear-linear model have been detailed elsewhere [11-12]. We consider the time parametric force deflection response between time $t = t_a$ and time $t = t_b$ such that $t_b > t_a$. Figure 2 depicts a plot of the magnitude of the collision force as a function of the deflection for each collision partner between $t_a$ and $t_b$.

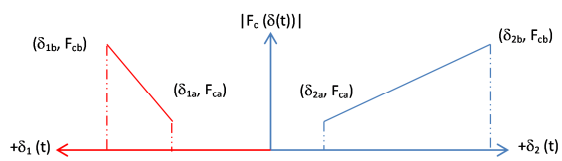


*Figure 2*. Magnitude of collision force plotted as a function of deflection for each collision partner for the linear force-deflection model.

The structural stiffness of each collision partner is simply the slope of the response between $t_a$ and $t_b$. The force values shown in equation (3) represent the magnitude of the collision force and the subscripts "a" and "b" denote evaluation at $t = t_a$ and $t = t_b$ respectively.

$$k_1 = \frac{\mathbf{F}_{cb} - \mathbf{F}_{ca}}{\boldsymbol{\delta}_{1b} - \boldsymbol{\delta}_{1a}} \quad k_2 = \frac{\mathbf{F}_{cb} - \mathbf{F}_{ca}}{\boldsymbol{\delta}_{2b} - \boldsymbol{\delta}_{2a}} \qquad (3).$$

Each of the equations shown in (3) can be solved for $\mathbf{F}_{cb}$.

$$\mathbf{F}_{cb} = \mathbf{F}_{ca} + k_1\left(\boldsymbol{\delta}_{1b} - \boldsymbol{\delta}_{1a}\right) \quad \mathbf{F}_{cb} = \mathbf{F}_{ca} + k_2\left(\boldsymbol{\delta}_{2b} - \boldsymbol{\delta}_{2a}\right) \quad (4).$$

The magnitude of the collision force is equal, as determined from either vehicle, at all points in time during the collision. As a result, the two equations shown in (4) can be set equal to each other at $t_b$ and $\mathbf{F}_{ca}$ can be eliminated from both sides of the equality.

$$k_1\left(\boldsymbol{\delta}_{1b} - \boldsymbol{\delta}_{1a}\right) = k_2\left(\boldsymbol{\delta}_{2b} - \boldsymbol{\delta}_{2a}\right) \qquad (5).$$

The structural deflections can be readily defined in terms of the center of mass displacements of each collision partner and in terms of the displacement of the common contact interface.

$$\begin{aligned} \boldsymbol{\delta}_1(t) &= \mathbf{u}_1(t) - \mathbf{u}_{IV}(t) \\ \boldsymbol{\delta}_2(t) &= \mathbf{u}_{IV}(t) - \mathbf{u}_2(t) \end{aligned} \qquad (6).$$

Defining the deflections for both collision partners at $t_a$ and $t_b$, in terms of the displacements and substituting into equation (5) leads to a solution for $\mathbf{u}_{IFb}$.

$$\mathbf{u}_{IVb} = \mathbf{u}_{IVa} + \frac{\left(k_1\mathbf{u}_{1b} - k_1\mathbf{u}_{1a} + k_2\mathbf{u}_{2b} - k_2\mathbf{u}_{2a}\right)}{k_1 + k_2} \qquad (7).$$

A closed-form analytic solution for the displacement of the common collision interface at $t = t_b$ is one that is generally not developable in cases in which the force-deflection response is non-linear. Substitution of equation (7) into either of the equations shown in (4) results in a solution for the collision force in terms of the center of mass displacements at $t_a$ and $t_b$.

$$\begin{aligned} \mathbf{F}_{cb} = \mathbf{F}_{ca} &+ \left(\frac{k_1k_2}{k_1+k_2}\right)\mathbf{u}_{1b} - \\ &\left(\frac{k_1k_2}{k_1+k_2}\right)\mathbf{u}_{2b} + \left(\frac{k_1k_2}{k_1+k_2}\right)\left(\mathbf{u}_{2a} - \mathbf{u}_{1a}\right) \end{aligned} \qquad (8).$$

Substitution of equation (8) into equations (1) and (2) provides for the form of the equations of motion for the specific linear force-deflection modeling methodology under consideration.

$$\begin{aligned} m_1\ddot{\mathbf{u}}_1 &+ \left(\frac{k_1k_2}{k_1+k_2}\right)\mathbf{u}_{1b} - \left(\frac{k_1k_2}{k_1+k_2}\right)\mathbf{u}_{2b} = \\ -\mathbf{F}_{ca} &- \left(\frac{k_1k_2}{k_1+k_2}\right)\left(\mathbf{u}_{2a} - \mathbf{u}_{1a}\right) + \mathbf{F}_{1ext} \end{aligned} \qquad (9).$$

$$\begin{aligned} m_2\ddot{\mathbf{u}}_2 &- \left(\frac{k_1k_2}{k_1+k_2}\right)\mathbf{u}_{1b} + \left(\frac{k_1k_2}{k_1+k_2}\right)\mathbf{u}_{2b} = \\ \mathbf{F}_{ca} &+ \left(\frac{k_1k_2}{k_1+k_2}\right)\left(\mathbf{u}_{2a} - \mathbf{u}_{1a}\right) + \mathbf{F}_{2ext} \end{aligned} \qquad (10).$$

The constant term, for each phase, defined by the quotient of the product of the individual stiffnesses to the sum of the stiffnesses, is termed the effective stiffness, $k_{eff}$. Equations (9) and (10) can be written in vector-matrix form.

$$\mathbf{M}\ddot{\mathbf{u}}(t) + \mathbf{K}\mathbf{u}(t) = \mathbf{F}_{ca} + \mathbf{F}_{\Delta ua} + \mathbf{F}_{ext} \qquad (11).$$

Where:

$$\mathbf{M} = \begin{bmatrix} m_1 & 0 \\ 0 & m_2 \end{bmatrix} \quad \mathbf{K} = \begin{bmatrix} k_{eff} & -k_{eff} \\ -k_{eff} & k_{eff} \end{bmatrix} \qquad (12).$$

$$\mathbf{F}_{ca} = \begin{bmatrix} -\mathbf{F}_{ca} \\ \mathbf{F}_{ca} \end{bmatrix} \quad \mathbf{F}_{\Delta ua} = \begin{bmatrix} -k_{eff}\left(\mathbf{u}_{2a} - \mathbf{u}_{1a}\right) \\ k_{eff}\left(\mathbf{u}_{2a} - \mathbf{u}_{1a}\right) \end{bmatrix}$$
$$\mathbf{F}_{ext} = \begin{bmatrix} \mathbf{F}_{1ext} \\ \mathbf{F}_{2ext} \end{bmatrix} \qquad (13).$$

$$\mathbf{u}(t) = \begin{bmatrix} \mathbf{u}_1(t) \\ \mathbf{u}_2(t) \end{bmatrix} \quad \dot{\mathbf{u}}(t) = \begin{bmatrix} \dot{\mathbf{u}}_1(t) \\ \dot{\mathbf{u}}_2(t) \end{bmatrix}$$
$$\ddot{\mathbf{u}}(t) = \begin{bmatrix} \ddot{\mathbf{u}}_1(t) \\ \ddot{\mathbf{u}}_2(t) \end{bmatrix} \qquad (14).$$

For the analysis of the closure phase, the subscript "o" denoting the start of closure replaces the general subscript "a." The initial displacement conditions are generally taken as being zero. The column vectors $\mathbf{F}_{co}$ and $\mathbf{F}_{\Delta ua}$ are both $\mathbf{0}$. The initial velocities of the collision partners are defined as:

$$\dot{\mathbf{u}}_o = \begin{bmatrix} \dot{\mathbf{u}}_{1o} \\ \dot{\mathbf{u}}_{2o} \end{bmatrix} \qquad (15).$$

The effective stiffness during closure is derived from the loading stiffness values of both collision partners.

$$k_{eff} = \frac{k_{1load} k_{2load}}{k_{1load} + k_{2load}} \qquad (16).$$

The initial conditions for separation are the terminus conditions for closure. The constant valued forcing terms become:

$$\mathbf{F}_{ca} = \begin{bmatrix} -\mathbf{F}_{cp} \\ \mathbf{F}_{cp} \end{bmatrix} \quad \mathbf{F}_{\Delta ua} = \begin{bmatrix} -k_{eff}\left(\mathbf{u}_{2c} - \mathbf{u}_{1c}\right) \\ k_{eff}\left(\mathbf{u}_{2c} - \mathbf{u}_{1c}\right) \end{bmatrix} \qquad (17).$$

The effective stiffness in (17) is the effective stiffness for the unloading phase and is defined as:

$$k_{eff} = \frac{k_{1unload} k_{2unload}}{k_{1unload} + k_{2unload}} \qquad (18).$$

The initial conditions for the unload phase, using $t^* = t - t_c$, are:

$$\mathbf{u}_o = \begin{bmatrix} \mathbf{u}_{1c} \\ \mathbf{u}_{2c} \end{bmatrix} \quad \dot{\mathbf{u}}_o = \begin{bmatrix} \dot{\mathbf{u}}_{1c} \\ \dot{\mathbf{u}}_{2c} \end{bmatrix} \qquad (19).$$

The velocities of the collision partners, at the terminus of closure, are equal.

**Laplace transform and Eigensolution for the undamped equations of motion**

The unilateral Laplace transform for a time domain function f(t) that is integrable over the domain $[0, \infty)$ is defined as:

$$F(s) = \mathcal{L}\{f(t)\} = \int_0^\infty e^{-st} f(t)\,dt \qquad (20).$$

Taking the Laplace transform of equation (11) converts the differential equations of motion in the time domain into algebraic equations in the Laplace domain.

$$\mathbf{M}\left(s^2\mathbf{u}(s) - s\mathbf{u}_o - \dot{\mathbf{u}}_o\right) + \mathbf{K}\mathbf{u}(s) = \frac{\mathbf{F}_{ca}}{s} + \frac{\mathbf{F}_{\Delta ua}}{s} + \mathcal{L}\left(\mathbf{F}_{ext}\right) \qquad (21).$$

Rearranging equation (21):

$$\left(s^2\mathbf{M} + \mathbf{K}\right)\mathbf{u}(s) = s\mathbf{M}\mathbf{u}_o + \mathbf{M}\dot{\mathbf{u}}_o + \frac{\mathbf{F}_{ca}}{s} + \frac{\mathbf{F}_{\Delta ua}}{s} + \mathcal{L}\left(\mathbf{F}_{ext}\right) \qquad (22).$$

The dynamic stiffness matrix $\mathbf{D}(s)$ and the transfer function $\mathbf{H}(s)$ are defined as:

$$\mathbf{D}(s) = \mathbf{H}^{-1}(s) = s^2\mathbf{M} + \mathbf{K} \qquad (23).$$

For a complex valued function with characteristic polynomial of the order m and degrees of freedom N, $m = 2N + p$; $p \geq 0$. For a complex valued non-zero square matrix under the case of having m Eigenvalues appearing in 2N complex conjugate pairs, the Eigenvalues are $s_j$ and $\bar{s}_j$ with corresponding Eigenvectors $\mathbf{z}_j$ and $\bar{\mathbf{z}}_j$ for $\forall j = 1, \ldots, 2N$. This holds for the undamped problem. The Eigenproblem for any such matrix $\mathbf{X}(s)$, $s \in \mathbb{C}$, can be expressed in the following manner where $\nu_k(s)$ is the distinct $k^{th}$ Eigenvalue with corresponding distinct Eigenvector $\phi_k(s)$.

$$\mathbf{X}(s)\phi_k(s) = \nu_k(s)\phi_k(s) \quad \forall k = 1, \ldots, N \qquad (24).$$

Because the Eigenvalues, $\nu_k(s)$, are distinct, the Eigenvectors are orthogonal and the following relationship holds:

$$\phi_j^T(s)\phi_k(s) = \delta_{kj} \quad \forall k, j = 1, \ldots, N \qquad (25).$$

Equation (24) can then be rewritten as:

$$\begin{aligned} \phi_j^T(s)\mathbf{X}(s)\phi_k(s) &= \nu_k(s)\delta_{kj} \\ \mathbf{\Phi}^T(s)\mathbf{X}(s)\mathbf{\Phi}(s) &= \boldsymbol{\nu}(s) \end{aligned} \qquad (26).$$

Equation (26) is the Eigendecomposition of **X**(s). Substitution of the dynamic stiffness matrix **D**(s) for **X**(s) results in the following solutions for **D**(s) and **H**(s).

$$\begin{aligned} \mathbf{D}(s) &= \mathbf{\Phi}(s)\boldsymbol{\nu}(s)\mathbf{\Phi}^T(s) \\ &= \sum_{k=1}^{N}\left(\phi_k(s)\nu_k(s)\phi_k^T(s)\right) \\ \mathbf{H}(s) &= \mathbf{D}^{-1}(s) \\ &= \mathbf{\Phi}(s)\boldsymbol{\nu}^{-1}(s)\mathbf{\Phi}^T(s) \\ &= \sum_{k=1}^{N}\left(\phi_k(s)\nu_k^{-1}(s)\phi_k^T(s)\right) \end{aligned} \qquad (27).$$

The use of the residue theorem allows for the transfer function to be written in the form shown by equation (28),which avoids the necessity for a partial fraction expansion of the transfer function.

$$\mathbf{H}(s) = \sum_{j=1}^{m}\left(\frac{\mathbf{R}_j}{s - s_j}\right) \qquad (28).$$

When $s = s_j$, the $r^{th}$ Eigenvalue, $\nu_r$, is $\nu_r(s_j)$, which equals zero, while all other Eigenvalues are non-zero and the corresponding Eigenvector $\phi_r(s_j) = \mathbf{z}_j$. Adhikari [13] has shown that the residue $\mathbf{R}_j$ and the transfer function **H**(s) may be written as:

$$\mathbf{R}_j = \frac{\mathbf{z}_j\mathbf{z}_j^T}{\mathbf{z}_j^T\dfrac{\partial\mathbf{D}(s_j)}{\partial s_j}\mathbf{z}_j} = \gamma_j\mathbf{z}_j\mathbf{z}_j^T \qquad (29).$$

The transfer function **H**(s) then becomes:

$$\mathbf{H}(s) = \sum_{j=1}^{m}\left(\frac{\gamma_j\mathbf{z}_j\mathbf{z}_j^T}{s - s_j}\right) \qquad (30).$$

Adhikari [13] has also shown that for the case in which there exists 2N eigenvalues in complex conjugate form, among the m Eigenvalues, equation (30) can be written as:

$$\mathbf{H}(s) = \sum_{j=1}^{N}\left(\frac{\gamma_j\mathbf{z}_j\mathbf{z}_j^T}{s - s_j} + \frac{\overline{\gamma}_j\overline{\mathbf{z}}_j\overline{\mathbf{z}}_j^T}{s - \overline{s}_j}\right) + \sum_{j=2N+1}^{m}\left(\frac{\gamma_j\mathbf{z}_j\mathbf{z}_j^T}{s - s_j}\right) \qquad (31).$$

For the undamped case such that the characteristic polynomial of **D**(s) of second order and zero order terms in s, m = 2N and p = 0. The second term to the right of the equality in (31) becomes zero secondary to the limits on the summation operator. The partial derivative of the dynamic stiffness matrix, evaluated at $s_j$, with respect to $s_j$ becomes:

$$\frac{\partial\mathbf{D}(s)}{\partial s_j} = 2s_j\mathbf{M} \qquad (32).$$

Correspondingly:

$$\gamma_j = \frac{1}{\mathbf{z}_j^T\dfrac{\partial\mathbf{D}(s_j)}{\partial s_j}\mathbf{z}_j} = \frac{1}{2s_j\mathbf{z}_j^T\mathbf{M}\mathbf{z}_j} \qquad (33).$$

The transfer function then becomes:

$$\mathbf{H}(s) = \frac{1}{2}\sum_{j=1}^{N}\left(\frac{\mathbf{z}_j\mathbf{z}_j^T}{s_j\mathbf{z}_j^T\mathbf{M}\mathbf{z}_j(s - s_j)} + \frac{\overline{\mathbf{z}}_j\overline{\mathbf{z}}_j^T}{\overline{s}_j\overline{\mathbf{z}}_j^T\mathbf{M}\overline{\mathbf{z}}_j(s - \overline{s}_j)}\right) \qquad (34).$$

For the undamped system, the characteristic polynomial of **D**(s) results in a solution for the Eigenvalue problem where $s_j = a_j + jb_j = jb_j$, where $b_j \in \mathbb{R}, s_j \in \mathbb{C}$ for $\forall j$. As a result:

$$s_j = jb_j \quad \overline{s}_j = -jb_j = -s_j \qquad (35).$$

The Eigenvalues of **D**(s) are determined by taking the determinant of **D**(s) and solving for the values of $s_j$ such that det[**D**(s)] is equal to zero.

$$\det\left[\mathbf{D}(s)\right] = \det\left[s^2\mathbf{M} + \mathbf{K}\right] = 0 \qquad (36).$$

Substitution of the terms from **M** and **K** into equation (36) results in the following form of the characteristic polynomial.

$$s^2\left(m_1m_2s^2 + k_{eff}(m_1 + m_2)\right) = 0 \qquad (37).$$

The Eigenvalues are the roots of equation (37)

$$s_1 = 0 \quad s_2 = \pm j\sqrt{\left(\frac{m_1 + m_2}{m_1 m_2}\right)k_{eff}} \qquad (38).$$

Correspondingly:

$$b_1 = 0 \quad b_2 = \sqrt{\left(\frac{m_1 + m_2}{m_1 m_2}\right)k_{eff}} \qquad (39).$$

The Eigenvector problem for **D**(s) is given as:

$$\mathbf{D}\left(s_j\right)\mathbf{z}_j = 0 \qquad (40).$$

Substitution for the positions of $\mathbf{D}(s_j)$ in terms of the components of **M** and the positions of **K** results in the following:

$$\begin{bmatrix} s_j^2 m_1 + k_{eff} & -k_{eff} \\ -k_{eff} & s_j^2 m_2 + k_{eff} \end{bmatrix}\begin{bmatrix} z_{j1} \\ z_{j2} \end{bmatrix} = \begin{bmatrix} 0 \\ 0 \end{bmatrix} \qquad (41).$$

Normalizing the solution such that $z_{j2}$ is unity:

$$\mathbf{z}_j = \begin{bmatrix} z_{j1} \\ z_{j2} \end{bmatrix} = \begin{bmatrix} \dfrac{k_{eff}}{\left(s_j^2 m_1 + k_{eff}\right)} \\ 1 \end{bmatrix} \qquad (42).$$

For the conjugate of $s_j$:

$$\overline{\mathbf{z}}_j = \begin{bmatrix} \overline{z}_{j1} \\ \overline{z}_{j2} \end{bmatrix} = \begin{bmatrix} \dfrac{k_{eff}}{\overline{s}_j^2 m_1 + k_{eff}} \\ 1 \end{bmatrix} \qquad (43).$$

From equation (35), it can be seen that the square of the Eigenvalue $s_j = jb_j$ and its complex conjugate are equal. Therefore, the Eigenvector $\mathbf{z}_j$ and its complex conjugate are equal for the undamped case.

$$\mathbf{z}_j = \begin{bmatrix} z_{j1} \\ z_{j2} \end{bmatrix} = \begin{bmatrix} \dfrac{k_{eff}}{\left(k_{eff} - b_j^2 m_1\right)} \\ 1 \end{bmatrix} = \begin{bmatrix} \overline{z}_{j1} \\ \overline{z}_{j2} \end{bmatrix} = \overline{\mathbf{z}}_j \qquad (44).$$

The Eigenvectors corresponding to $s_1$ and $s_2$ thus become:

$$\mathbf{z}_1 = \begin{bmatrix} 1 \\ 1 \end{bmatrix} \quad \mathbf{z}_2 = \begin{bmatrix} -m_1^{-1} m_2 \\ 1 \end{bmatrix} \qquad (45).$$

Equation (34) requires the evaluation of the scalars $\mathbf{z}_j^T \mathbf{M} \mathbf{z}_j$ and $\overline{\mathbf{z}}_j^T \mathbf{M} \overline{\mathbf{z}}_j$.

$$\begin{aligned} \mathbf{z}_j^T \mathbf{M} \mathbf{z}_j &= \begin{bmatrix} z_{j1} & z_{j2} \end{bmatrix}\begin{bmatrix} m_1 & 0 \\ 0 & m_2 \end{bmatrix}\begin{bmatrix} z_{j1} \\ z_{j2} \end{bmatrix} \\ &= \begin{bmatrix} m_1 z_{j1} & m_2 z_{j2} \end{bmatrix}\begin{bmatrix} z_{j1} \\ z_{j2} \end{bmatrix} \\ &= m_1 z_{j1}^2 + m_2 z_{j2}^2 \end{aligned} \qquad (46).$$

$$\begin{aligned} \overline{\mathbf{z}}_j^T \mathbf{M} \overline{\mathbf{z}}_j &= \begin{bmatrix} \overline{z}_{j1} & \overline{z}_{j2} \end{bmatrix}\begin{bmatrix} m_1 & 0 \\ 0 & m_2 \end{bmatrix}\begin{bmatrix} \overline{z}_{j1} \\ \overline{z}_{j2} \end{bmatrix} \\ &= \begin{bmatrix} m_1 \overline{z}_{j1} & m_2 \end{bmatrix}\begin{bmatrix} \overline{z}_{j1} \\ \overline{z}_{j2} \end{bmatrix} \\ &= m_1 \overline{z}_{j1}^2 + m_2 \overline{z}_{j2} \\ &= m_1 z_{j1}^2 + m_2 z_{j2}^2 \end{aligned} \qquad (47).$$

Terms of the form $\mathbf{z}_j \mathbf{z}_j^T$ and $\overline{\mathbf{z}}_j \overline{\mathbf{z}}_j^T$ are matrices:

$$\begin{aligned} \mathbf{z}_j \mathbf{z}_j^T &= \overline{\mathbf{z}}_j \overline{\mathbf{z}}_j^T \\ &= \begin{bmatrix} z_{j1} \\ z_{j1} \end{bmatrix}\begin{bmatrix} z_{j1} & z_{j1} \end{bmatrix} = \begin{bmatrix} z_{j1}^2 & z_{j1} z_{j2} \\ z_{j1} z_{j2} & z_{j2}^2 \end{bmatrix} \end{aligned} \qquad (48).$$

Equation (34) can then be rewritten as:

$$\begin{aligned} \mathbf{H}(s) &= \sum_{j=1}^{N}\left(\frac{\begin{bmatrix} z_{j1}^2 & z_{j1} z_{j2} \\ z_{j1} z_{j2} & z_{j2}^2 \end{bmatrix}}{m_1 z_{j1}^2 + m_2 z_{j2}^2}\left(\frac{1}{s^2 + b_j^2}\right)\right) \\ &= \sum_{j=1}^{N}\left(\mathbf{c}_j\left(\frac{1}{s^2 + b_j^2}\right)\right) \end{aligned} \qquad (49).$$

From equation (45), the values of $\mathbf{c}_1$ and $\mathbf{c}_2$ are:

$$\mathbf{c}_1 = \frac{\begin{bmatrix} 1 & 1 \\ 1 & 1 \end{bmatrix}}{m_1 + m_2} \quad \mathbf{c}_2 = \frac{\begin{bmatrix} m_1^{-2} m_2^2 & -m_1^{-1} m_2 \\ -m_1^{-1} m_2 & 1 \end{bmatrix}}{m_1^{-1} m_2^2 + m_2} \qquad (50).$$

Substitution of equation (49) into equation (22) yields the solution for the displacement of the collision partners in the Laplace domain.

$$\mathbf{u}(s)=\left[\sum_{j=1}^{N}\left(\mathbf{c}_j\left(\frac{s}{s^2+b_j^2}\right)\right)\right]\mathbf{M}\mathbf{u_o}+\left[\sum_{j=1}^{N}\left(\mathbf{c}_j\left(\frac{1}{s^2+b_j^2}\right)\right)\right]\mathbf{M}\dot{\mathbf{u}}_\mathbf{o}+\left[\sum_{j=1}^{N}\left(\mathbf{c}_j\left(\frac{1}{s\left(s^2+b_j^2\right)}\right)\right)\right]\left(\mathbf{F}_{ca}+\mathbf{F}_{\Delta ua}\right)+\mathbf{H}(s)\mathcal{L}\{\mathbf{F}_{ext}\} \quad (51).$$

The inverse Laplace transform of equation (51) yields the time domain displacement solution. The first and second derivatives, with respect to time, yield the velocity and acceleration solution, respectively, in the time domain.

$$\mathbf{u}(t)=\sum_{j=1}^{N}\left(\mathbf{c}_j\mathbf{M}\mathbf{u_o}\cos\left(b_jt\right)\right)+\sum_{j=1}^{N}\left(\mathbf{c}_j\mathbf{M}\dot{\mathbf{u}}_\mathbf{o}\frac{\sin\left(b_jt\right)}{b_j}\right)+\sum_{j=1}^{N}\left(\mathbf{c}_j\left(\mathbf{F}_{ca}+\mathbf{F}_{\Delta ua}\right)\left(\frac{1-\cos\left(b_jt\right)}{b_j^2}\right)\right)+\mathcal{L}^{-1}\left\{\mathbf{H}(s)\mathcal{L}\{\mathbf{F}_{ext}\}\right\} \quad (52).$$

$$\dot{\mathbf{u}}(t)=-\sum_{j=1}^{N}\left(\mathbf{c}_j\mathbf{M}\mathbf{u_o}b_j\sin\left(b_jt\right)\right)+\sum_{j=1}^{N}\left(\mathbf{c}_j\mathbf{M}\dot{\mathbf{u}}_\mathbf{o}\cos\left(b_jt\right)\right)+\sum_{j=1}^{N}\left(\mathbf{c}_j\left(\mathbf{F}_{ca}+\mathbf{F}_{\Delta ua}\right)\left(\frac{\sin\left(b_jt\right)}{b_j}\right)\right)+\frac{d}{dt}\left(\mathcal{L}^{-1}\left\{\mathbf{H}(s)\mathcal{L}\{\mathbf{F}_{ext}\}\right\}\right) \quad (53).$$

$$\ddot{\mathbf{u}}(t)=-\sum_{j=1}^{N}\left(\mathbf{c}_j\mathbf{M}\mathbf{u_o}b_j^2\cos\left(b_jt\right)\right)-\sum_{j=1}^{N}\left(\mathbf{c}_j\mathbf{M}\dot{\mathbf{u}}_\mathbf{o}b_j\sin\left(b_jt\right)\right)+\sum_{j=1}^{N}\left(\mathbf{c}_j\left(\mathbf{F}_{ca}+\mathbf{F}_{\Delta ua}\right)\cos\left(b_jt\right)\right)+\frac{d^2}{dt^2}\left(\mathcal{L}^{-1}\left\{\mathbf{H}(s)\mathcal{L}\{\mathbf{F}_{ext}\}\right\}\right) \quad (54).$$

For the case in which a rigid body mode of motion is indication (i.e. $s_j = 0$), the terms associated with j = 1 can be separated from the summation operator in equation (51) and evaluated separately.

**Specific issues regarding closure**

Using the initial conditions, described previously, for a typical closure scenario, equation (51) reduces to the following form:

$$\mathbf{u}(s)=\left[\sum_{j=1}^{N}\left(\mathbf{c}_j\left(\frac{1}{s^2+b_j^2}\right)\right)\right]\mathbf{M}\dot{\mathbf{u}}_\mathbf{o}+\mathbf{H}(s)\mathcal{L}\left(\mathbf{F}_{ext}\right) \quad (55).$$

Applying the summation operator and substituting for the constituent terms results in the following form of the displacement solution in the Laplace domain.

$$\mathbf{u}(s)=\frac{1}{m_1+m_2}\cdot\left(\begin{bmatrix}m_1\dot{u}_{1o}+m_2\dot{u}_{2o}\\ m_1\dot{u}_{1o}+m_2\dot{u}_{2o}\end{bmatrix}\left(\frac{1}{s^2}\right)+\begin{bmatrix}m_2\left(\dot{u}_{1o}-\dot{u}_{2o}\right)\\ m_1\left(\dot{u}_{2o}-\dot{u}_{1o}\right)\end{bmatrix}\left(\frac{1}{s^2+b_2^2}\right)\right)+\mathbf{H}(s)\mathcal{L}\{\mathbf{F}_{ext}\} \quad (56).$$

The time domain solutions are obtained as before.

$$\mathbf{u}(t)=\frac{1}{m_1+m_2}\cdot\left(\begin{bmatrix}m_1\dot{u}_{1o}+m_2\dot{u}_{2o}\\ m_1\dot{u}_{1o}+m_2\dot{u}_{2o}\end{bmatrix}t+\begin{bmatrix}m_2\left(\dot{u}_{1o}-\dot{u}_{2o}\right)\\ m_1\left(\dot{u}_{2o}-\dot{u}_{1o}\right)\end{bmatrix}\left(\frac{\sin\left(b_2t\right)}{b_2}\right)\right)+\mathcal{L}^{-1}\left\{\mathbf{H}(s)\mathcal{L}\{\mathbf{F}_{ext}\}\right\} \quad (57).$$

$$\dot{\mathbf{u}}(t)=\frac{1}{m_1+m_2}\cdot\left(\begin{bmatrix}m_1\dot{u}_{1o}+m_2\dot{u}_{2o}\\ m_1\dot{u}_{1o}+m_2\dot{u}_{2o}\end{bmatrix}+\begin{bmatrix}m_2\left(\dot{u}_{1o}-\dot{u}_{2o}\right)\\ m_1\left(\dot{u}_{2o}-\dot{u}_{1o}\right)\end{bmatrix}\cos\left(b_2t\right)\right)+\frac{d}{dt}\left(\mathcal{L}^{-1}\left\{\mathbf{H}(s)\mathcal{L}\{\mathbf{F}_{ext}\}\right\}\right) \quad (58).$$

$$\ddot{\mathbf{u}}(t) = -\frac{b_2}{m_1+m_2}\begin{bmatrix} m_2(\dot{u}_{1o}-\dot{u}_{2o}) \\ m_1(\dot{u}_{2o}-\dot{u}_{1o}) \end{bmatrix}\sin(b_2 t) + \frac{d^2}{dt^2}\left(\mathcal{L}^{-1}\{\mathbf{H}(s)\mathcal{L}\{\mathbf{F_{ext}}\}\}\right) \quad (59).$$

In the case in which there are no externally applied unbalanced forces on either collision partner, the time at which closure terminates can readily be found as $t_c = \pi / (2b_2)$. An analytical closed form solution for $t_c$ can also be found for cases in which $\mathbf{F_{ext}}$ is not zero and for which the time domain velocity solution includes other functions of time besides $\cos(b_2 t)$. The solution in such cases is determined by taking the Laplace transform of equation (58), setting the velocities of the collision partners equal to each other and solving for s. The inverse Laplace transform of s yields the solution $t_c\,\boldsymbol{\delta}(t_c)$ where $\boldsymbol{\delta}$ is the Dirac Delta function and $\boldsymbol{\delta}(t_c)$ has a value of unity at $t_c$ and zero elsewhere. With the value of $t_c$ known, the displacements at the terminus of closure can be solved for using equation (57) and the velocities at the terminus of closure can be solved for using equation (58) The displacement of the common collision interface at the terminus of closure can then be solved for using equation (7) The peak deflections can then be determined from equation (6) and the magnitude of the peak collision force can be determined from equation (5)

**Specific issues regarding separation**

As noted previously, the terminus conditions regarding closure represent the initial conditions for separation. Furthermore, the equations defined in (17) become operative. Because the time shift of $t^* = t - t_c$ is being used, the conjoined loading and unloading solutions, require the substitution of the latter for the former for a complete solution in terms of t. The tilde notation is employed to distinguish parameters associated with the unload (separation) phase from those associated with the load (closure) phase. We sequentially expand the three terms to the right of the equality of equation (51)

$$\left[\sum_{j=1}^{N}\left(\mathbf{c}_j\left(\frac{s}{s^2+\tilde{b}_j^{\,2}}\right)\right)\right]\mathbf{M}\mathbf{u}_\mathbf{c} = \frac{1}{m_1+m_2}\left(\begin{bmatrix} m_1 u_{1c}+m_2 u_{2c} \\ m_1 u_{1c}+m_2 u_{2c} \end{bmatrix}\left(\frac{1}{s}\right) + \begin{bmatrix} m_2(u_{1c}-u_{2c}) \\ m_1(u_{2c}-u_{1c}) \end{bmatrix}\left(\frac{s}{s^2+\tilde{b}_2^{\,2}}\right)\right) \quad (60).$$

$$\left[\sum_{j=1}^{N}\left(\mathbf{c}_j\left(\frac{1}{s^2+\tilde{b}_j^{\,2}}\right)\right)\right]\mathbf{M}\dot{\mathbf{u}}_\mathbf{c} = \frac{1}{m_1+m_2}\left(\begin{bmatrix} m_1 \dot{u}_{1c}+m_2 \dot{u}_{2c} \\ m_1 \dot{u}_{1c}+m_2 \dot{u}_{2c} \end{bmatrix}\left(\frac{1}{s^2}\right) + \begin{bmatrix} m_2(\dot{u}_{1c}-\dot{u}_{2c}) \\ m_1(\dot{u}_{2c}-\dot{u}_{1c}) \end{bmatrix}\left(\frac{1}{s^2+\tilde{b}_2^{\,2}}\right)\right) \quad (61).$$

$$\left[\sum_{j=1}^{N}\left(\mathbf{c}_j\left(\frac{1}{s\left(s^2+b_j^{\,2}\right)}\right)\right)\right]\left(\mathbf{F_{ca}}+\mathbf{F_{\Delta ua}}\right) = \frac{\left(F_{cp}+k_{eff}(u_{2c}-u_{1c})\right)}{m_1+m_2}\cdot\left(\begin{bmatrix} -1+1 \\ -1+1 \end{bmatrix}\left(\frac{1}{s^3}\right) + \begin{bmatrix} -m_1^{-1}m_2-1 \\ m_1 m_2^{-1}+1 \end{bmatrix}\left(\frac{1}{s\left(s^2+\tilde{b}_2^{\,2}\right)}\right)\right) \quad (62).$$

In equation (61), the second term within the parenthesis on the right of the equality is zero as the differences in the velocities of the collision partners at closure is zero. In equation (62), the first term within the parenthesis on the right of the equality is clearly zero (i.e. -1+1 = 0). Taking the inverse Laplace transform of equations (60) through (62) and summing the resultants (along with the general form for the externally applied unbalanced forces) gives the specific form of the displacement solution in the time domain.

$$\mathbf{u}\left(t^*\right)=\frac{1}{m_1+m_2}\cdot\left(\begin{array}{l}\begin{bmatrix}m_1u_{1c}+m_2u_{2c}\\ m_1u_{1c}+m_2u_{2c}\end{bmatrix}+\\ \begin{bmatrix}m_2\left(u_{1c}-u_{2c}\right)\\ m_1\left(u_{2c}-u_{1c}\right)\end{bmatrix}\cos\left(\tilde{b}_2t^*\right)+\\ \begin{bmatrix}m_1\dot{u}_{1c}+m_2\dot{u}_{2c}\\ m_1\dot{u}_{1c}+m_2\dot{u}_{2c}\end{bmatrix}t^*+\\ \begin{bmatrix}-m_1^{-1}m_2-1\\ m_1m_2^{-1}+1\end{bmatrix}\cdot\\ \left(\dfrac{1-\cos\left(\tilde{b}_2t^*\right)}{\tilde{b}_2^{\,2}}\right)\cdot\\ \begin{pmatrix}F_{cp}+\\ k_{eff}\left(u_{2c}-u_{1c}\right)\end{pmatrix}\end{array}\right)+\mathcal{L}^{-1}\left(\mathbf{H}(s)\mathcal{L}\left(\mathbf{F_{ext}}\right)\right) \quad (63).$$

The solutions for the velocity and acceleration are:

$$\dot{\mathbf{u}}\left(t^*\right)=\frac{1}{m_1+m_2}\left(\begin{array}{l}-\begin{bmatrix}m_2\left(u_{1c}-u_{2c}\right)\\ m_1\left(u_{2c}-u_{1c}\right)\end{bmatrix}\cdot\\ \tilde{b}_2\sin\left(\tilde{b}_2t^*\right)+\\ \begin{bmatrix}m_1\dot{u}_{1c}+m_2\dot{u}_{2c}\\ m_1\dot{u}_{1c}+m_2\dot{u}_{2c}\end{bmatrix}+\\ \begin{bmatrix}-m_1^{-1}m_2-1\\ m_1m_2^{-1}+1\end{bmatrix}\cdot\\ \left(\dfrac{\sin\left(\tilde{b}_2t^*\right)}{\tilde{b}_2}\right)\cdot\\ \left(F_{cp}+k_{eff}\left(u_{2c}-u_{1c}\right)\right)\end{array}\right)+\frac{d}{dt}\mathcal{L}^{-1}\left(\mathbf{H}(s)\mathcal{L}\left(\mathbf{F_{ext}}\right)\right) \quad (64).$$

$$\ddot{\mathbf{u}}\left(t^*\right)=\frac{1}{m_1+m_2}\left(\begin{array}{l}-\begin{bmatrix}m_2\left(u_{1c}-u_{2c}\right)\\ m_1\left(u_{2c}-u_{1c}\right)\end{bmatrix}\cdot\\ \tilde{b}_2^{\,2}\cos\left(\tilde{b}_2t^*\right)+\\ \begin{bmatrix}-m_1^{-1}m_2-1\\ m_1m_2^{-1}+1\end{bmatrix}\cos\left(\tilde{b}_2t^*\right)\cdot\\ \left(F_{cp}+k_{eff}\left(u_{2c}-u_{1c}\right)\right)\end{array}\right)+\frac{d^2}{dt^2}\mathcal{L}^{-1}\left(\mathbf{H}(s)\mathcal{L}\left(\mathbf{F_{ext}}\right)\right) \quad (65).$$

The time at which separation occurs is the time at which the accelerations of the collision partners due to the collision force alone, drops to zero. By the form of equation (65), this occurs at $t_s^* = \pi / (2b_2)$.

## ANALYSIS

We first consider the case in which no net externally applied forces are present to develop a reference. We define the constant terms $\mathbf{A}_m \forall m$, which are readily defined in the following development. From equation (39), $b_{11} = b_{12} = 0$ while $b_{21}$ and $b_{22}$, where the second subscript represents loading and unloading, respectively, are non-zero.

During closure, from the form of equation (57), with the term associated with the external forces set to zero, the displacement for each collision partner may be written as

$$\mathbf{u}_j(t)=\mathbf{A}_o t+\mathbf{A}_{1j}\sin\left(b_{21}t\right) \quad (66).$$

The velocity and acceleration during closure are:

$$\begin{aligned}\dot{\mathbf{u}}_j(t)&=\mathbf{A}_o+\mathbf{A}_{1j}b_{21}\cos\left(b_{21}t\right)\\ \ddot{\mathbf{u}}_j(t)&=-\mathbf{A}_{1j}b_{21}^{\,2}\sin\left(b_{21}t\right)\end{aligned} \quad (67).$$

The displacement of the common collision interface during closure is (where the stiffness values are the loading stiffnesses):

$$\mathbf{u}_{IV}(t)=\mathbf{A}_o t+\frac{\sum_j k_j\mathbf{A}_{1j}}{\sum_j k_j}\sin\left(b_{21}t\right) \quad (68).$$

The structural deflection experienced by each collision partner during closure is:

$$\begin{aligned}\boldsymbol{\delta}_1(t)&=\left(\mathbf{A}_{11}-\frac{\sum_j k_j\mathbf{A}_{1j}}{\sum_j k_j}\right)\sin\left(b_{21}t\right)\\ \boldsymbol{\delta}_2(t)&=\left(\frac{\sum_j k_j\mathbf{A}_{1j}}{\sum_j k_j}-\mathbf{A}_{12}\right)\sin\left(b_{21}t\right)\end{aligned} \quad (69).$$

As noted before, the terminus of closure is at $t = t_c = 0.5\pi b_{21}^{-1}$. The common velocity reached at the terminus of closure, $\mathbf{v}_{com}$ is equal to $\mathbf{A}_o$ and the peak acceleration for each collision partner is $-\mathbf{A}_{1j}b_{21}^{\,2}$.

The peak displacements for each collision partner and the common collision interface are:

$$\mathbf{u}_j\left(t_c\right) = \mathbf{u}_{jc} = 0.5\mathbf{A}_o\pi b_{21}^{-1} + \mathbf{A}_{1j}$$
$$\mathbf{u}_{IV}\left(t_c\right) = \mathbf{u}_{IVc} = 0.5\mathbf{A}_o\pi b_{21}^{-1} + \frac{\sum_j k_j\mathbf{A}_{1j}}{\sum_j k_j} \quad (70).$$

The peak deflections are:

$$\boldsymbol{\delta}_1\left(t_c\right) = \boldsymbol{\delta}_{1d} = \left(\mathbf{A}_{11} - \frac{\sum_j k_j\mathbf{A}_{1j}}{\sum_j k_j}\right)$$
$$\boldsymbol{\delta}_2\left(t_c\right) = \boldsymbol{\delta}_{2d} = \left(\frac{\sum_j k_j\mathbf{A}_{1j}}{\sum_j k_j} - \mathbf{A}_{12}\right) \quad (71).$$

Finally, the magnitude of the peak collision force is:

$$\left|\mathbf{F}_{cp}\right| = k_1\left(\mathbf{A}_{11} - \frac{\sum_j k_j\mathbf{A}_{1j}}{\sum_j k_j}\right)$$
$$= k_2\left(\frac{\sum_j k_j\mathbf{A}_{1j}}{\sum_j k_j} - \mathbf{A}_{12}\right) \quad (72).$$

During separation, $t^* = t - t_c$. From equation (63) it is evident that the form of the displacement for each collision partner during unloading is:

$$\mathbf{u}_j\left(t^*\right) = \mathbf{u}_{jc} + \mathbf{A}_o t^* + \mathbf{A}_{2j}\cos\left(b_{22}t^*\right) \quad (73).$$

The solutions for the velocity and acceleration are:

$$\dot{\mathbf{u}}_j\left(t^*\right) = \mathbf{A}_o - \mathbf{A}_{2j}b_{22}\sin\left(b_{22}t^*\right) \quad (74).$$

$$\ddot{\mathbf{u}}_j\left(t^*\right) = -\mathbf{A}_{2j}b_{22}^2\cos\left(b_{22}t^*\right) \quad (75).$$

The displacement of the common collision interface during separation is (the stiffness values are the unloading stiffnesses):

$$\mathbf{u}_{IV}\left(t^*\right) = \mathbf{A}_o t^* + \frac{\sum_j k_j\left(u_{jc} + A_{2j}\cos\left(b_{22}t^*\right)\right)}{\sum_j k_j} \quad (76)$$

The deflection experienced by each collision partner during separation is:

$$\boldsymbol{\delta}_1\left(t^*\right) = \mathbf{u}_{1c} + \mathbf{A}_{21}\cos\left(b_{22}t^*\right) - \frac{\sum_j k_j\left(u_{jc} + A_{2j}\cos\left(b_{22}t^*\right)\right)}{\sum_j k_j} \quad (77).$$

$$\boldsymbol{\delta}_2\left(t^*\right) = \frac{\sum_j k_j\left(u_{jc} + A_{2j}\cos\left(b_{22}t^*\right)\right)}{\sum_j k_j} - \mathbf{u}_{2c} - \mathbf{A}_{22}\cos\left(b_{22}t^*\right) \quad (78).$$

The terminus of separation, as noted previously, occurs when the collision force drops to zero magnitude. This occurs at $t^* = 0.5\pi b_{22}^{-1}$. The displacements at the terminus of separation are:

$$\mathbf{u}_j\left(t_s^*\right) = \mathbf{u}_{jc} + 0.5\mathbf{A}_o\pi b_{22}^{-1} \quad (79).$$

$$\mathbf{u}_{IV}\left(t_s^*\right) = 0.5\mathbf{A}_o\pi b_{22}^{-1} + \frac{\sum_j k_j u_{jc}}{\sum_j k_j} \quad (80).$$

The residual damage depths are:

$$\boldsymbol{\delta}_1\left(t_s^*\right) = \mathbf{u}_{1c} - \frac{\sum_j k_j u_{jc}}{\sum_j k_j} \quad (81).$$

$$\boldsymbol{\delta}_2\left(t_s^*\right) = \frac{\sum_j k_j u_{jc}}{\sum_j k_j} - \mathbf{u}_{jc} \quad (82).$$

**Linear net external forces**

We define the net externally applied force on the striking vehicle as $\mathbf{F}_{ext1}(t) = \mathbf{g}_{o1} + \mathbf{g}_{11}t$. When this force is time invariant (i.e. $\mathbf{g}_{11} = \mathbf{0}$) then the model reduces to a simple constant force model (i.e. $\mathbf{g}_{01} = -f\mu m_1 g$ for constant braking). The external force vector, in the Laplace domain, in equation (51), becomes:

$$\mathcal{L}\{\mathbf{F}_{ext}\} = \begin{pmatrix} \frac{\mathbf{g}_{o1}}{s} + \frac{\mathbf{g}_{11}}{s^2} \\ \frac{\mathbf{g}_{o2}}{s} + \frac{\mathbf{g}_{12}}{s^2} \end{pmatrix} \quad (83).$$

Multiplying the external force vector, in the Laplace domain, by the transfer function and taking the inverse Laplace transform results in the following time domain solution (using the subscript notation as before):

$$\mathcal{L}^{-1}\{\mathbf{H}(s)\mathcal{L}\{\mathbf{F}_{ext}\}\} = \left(6b_2^3 m_j (m_1 + m_2)\right)^{-1} \cdot \begin{pmatrix} b_2 \begin{pmatrix} 6(g_{oj}m_k - g_{ok}m_j) + \\ 6t(g_{1j}m_k - g_{1k}m_j) + \\ b_2^2 m_j t^3 (g_{11} + g_{12}) + \\ 3b_2^2 m_j t^2 (g_{o2} + g_{o1}) \end{pmatrix} + \\ 6b_2 (g_{ok}m_j - g_{oj}m_k)\cos(b_2 t) + \\ 6(g_{1k}m_j - g_{1j}m_k)\sin(b_2 t) \end{pmatrix} \quad (84).$$

As expected, substitution of t = 0 into equation (84) results in zero displacement due to the externally applied loads. The corresponding first and second time derivatives, required for the velocity and acceleration solution, respectively, are:

$$\frac{d}{dt}\mathcal{L}^{-1}\{\mathbf{H}(s)\mathcal{L}\{\mathbf{F}_{ext}\}\} = \left(6b_2^3 m_j (m_1 + m_2)\right)^{-1} \cdot \begin{pmatrix} b_2 \begin{pmatrix} 6(g_{1j}m_k - g_{1k}m_j) + \\ 3b_2^2 m_j t^2 (g_{11} + g_{12}) + \\ 6b_2^2 m_j t (g_{o2} + g_{o1}) \end{pmatrix} - \\ 6b_2^2 (g_{ok}m_j - g_{oj}m_k)\sin(b_2 t) + \\ 6b_2 (g_{1k}m_j - g_{1j}m_k)\cos(b_2 t) \end{pmatrix} \quad (85).$$

$$\frac{d^2}{dt^2}\mathcal{L}^{-1}\{\mathbf{H}(s)\mathcal{L}\{\mathbf{F}_{ext}\}\} = \left(6b_2^3 m_j (m_1 + m_2)\right)^{-1} \cdot \begin{pmatrix} b_2 \begin{pmatrix} 6b_2^2 m_j t (g_{11} + g_{12}) + \\ 6b_2^2 m_j (g_{o2} + g_{o1}) \end{pmatrix} - \\ 6b_2^3 (g_{ok}m_j - g_{oj}m_k)\cos(b_2 t) - \\ 6b_2^2 (g_{1k}m_j - g_{1j}m_k)\sin(b_2 t) \end{pmatrix} \quad (86).$$

The time at which closure occurs can be readily obtained by setting the velocities of the collision partners equal to each other and solving for $t = t_c$. For zero initial displacement conditions the solution is determinate in closed form but is of such length as to preclude its inclusion herein.

The solutions for the displacement and acceleration of each collision partner at the terminus of closure are obtained, directly, by substitution of the time at which closure terminates into equations (84) and (86) respectively. Using the terminus of closure conditions as the initial conditions for the separation phase, the time domain displacement solution is:

$$\mathbf{u}_j(t^*) = \frac{1}{6}(m_1 + m_2)^{-1} \cdot \left(c_1 + \frac{1}{(\tilde{b}_2^2 m_j)c_2}\right) \quad (87).$$

Where:

$$c_1 = 6\begin{pmatrix} (\dot{\mathbf{u}}_{1c}m_1 + \dot{\mathbf{u}}_{2c}m_2)(t^* + 1) + \\ (-1)^j \begin{pmatrix} \mathbf{F}_{cp} + \\ \tilde{k}_{eff}(\mathbf{u}_{2c} - \mathbf{u}_{1c}) \end{pmatrix} \cdot \\ (\cos(b_2 t^*) - 1) + \\ m_j (\mathbf{u}_{jc} - \mathbf{u}_{kc})\cos(b_2 t^*) \end{pmatrix} \quad (88).$$

$$c_2 = b_2 \begin{pmatrix} 6(\mathbf{g}_{oj}m_k - \mathbf{g}_{ok}m_j) \\ +6(\mathbf{g}_{1j}m_k - \mathbf{g}_{1k}m_j)t^* \\ +3b_2^2(\mathbf{g}_{o1}m_j + \mathbf{g}_{o2}m_j)t^{*2} + \\ b_2^2(\mathbf{g}_{11}m_j + \mathbf{g}_{12}m_j)t^{*3} \end{pmatrix} + (-1)^k 6b_2(\mathbf{g}_{o2}m_1 - \mathbf{g}_{o1}m_2)\cos(b_2 t^*) + 6(\mathbf{g}_{1k}m_j - \mathbf{g}_{1j}m_k)\sin(b_2 t^*) \quad (89).$$

The velocity of each collision partner during separation is:

$$\dot{\mathbf{u}}_j\left(t^*\right)=\frac{1}{6}\left(m_1+m_2\right)^{-1}\cdot\left(\frac{3c_3}{\left(b_2{}^2m_j\right)}+6c_4\right) \quad (90).$$

Where:

$$\begin{aligned} c_3 = {} & 2\left(\mathbf{g}_{1j}m_k-\mathbf{g}_{jk}m_j\right)+2b_2{}^2m_j\left(\mathbf{g}_{o1}+\mathbf{g}_{o2}\right)t^*+ \\ & b_2{}^2m_j\left(\mathbf{g}_{11}+\mathbf{g}_{12}\right)t^{*2}+ \\ & 2\left(g_{1k}m_j-g_{1j}m_k\right)\cos\left(b_2t^*\right)+ \\ & 2b_2\left(\mathbf{g}_{oj}m_k-\mathbf{g}_{ok}m_j\right)\sin\left(b_2t^*\right)+ \end{aligned} \quad (91).$$

$$c_4=\begin{pmatrix} \dot{\mathbf{u}}_{1c}m_1+\dot{\mathbf{u}}_{2c}m_2+ \\ (-1)^j\,\tilde{b}_2m_k\left(\mathbf{u}_{1c}-\mathbf{u}_{2c}\right)\sin\left(\tilde{b}_2t^*\right)+ \\ (-1)^j\left(\dfrac{m_1+m_2}{\tilde{b}_2m_j}\right)\cdot \\ \left(\mathbf{F}_{cp}+\tilde{k}_{eff}\left(\mathbf{u}_{2c}-\mathbf{u}_{1c}\right)\right)\sin\left(\tilde{b}_2t^*\right) \end{pmatrix} \quad (92).$$

Finally, the acceleration of each collision partner during separation is:

$$\ddot{\mathbf{u}}_j\left(t^*\right)=b_2{}^{-1}m_k{}^{-1}\left(m_1+m_2\right)^{-1}\cdot\left(c_5+c_6\right) \quad (93).$$

Where:

$$c_5=b_2\begin{pmatrix} \mathbf{g}_{o1}m_j+\mathbf{g}_{o2}m_k+m_j\left(\mathbf{g}_{11}+\mathbf{g}_{12}\right)m_jt+ \\ \left(\mathbf{g}_{o1}m_k-\mathbf{g}_{o2}m_j\right)\cos\left(b_2t\right) \end{pmatrix} \quad (94).$$

$$\begin{aligned} c_6 = {} & (-1)^j\,b_2\cdot \\ & \begin{pmatrix} \mathbf{F}_{cp}\left(m_1+m_2\right)- \\ \begin{pmatrix} -\tilde{b}_2{}^2m_1m_2+ \\ \tilde{k}_{eff}\left(m_1+m_2\right) \end{pmatrix}\left(\mathbf{u}_{1c}-\mathbf{u}_{2c}\right) \end{pmatrix}\cos\left(\tilde{b}_2t\right)+ \\ & \left(\mathbf{g}_{1j}m_k-\mathbf{g}_{1k}m_j\right)\sin\left(b_2t\right) \end{aligned} \quad (95).$$

The time at which separation terminates can be determined in closed form as before. The solution, however, is exceedingly lengthy and precluded from inclusion due to space limitations. Substitution of the solution for the time at which separation terminates into equation (87) yields the solution for the displacement at the terminus of closure. Similarly, substitution into equation (90) yields the velocity of each collision partner at separation.

**EXAMPLE**

As a hypothetical example, we consider the inline collision between two collision partners with the following parameters: $m_1$ = 1500 kg, $m_2$ = 1900 kg, $k_1$ (loading phase) = $5 \cdot 10^5$ $Nm^{-1}$, $k_2$ (loading phase) = $1.9 \cdot 10^5$ $Nm^{-1}$, $k_1$ (unloading phase) = $3 \cdot 10^6$ $Nm^{-1}$, $k_2$ (unloading phase) = $5 \cdot 10^6$ $Nm^{-1}$, zero magnitude initial displacement and with initial velocities of 15 and 4 $msec^{-1}$. The circular frequency for the load phase, using equation (39), is 12.8 $sec^{-1}$. The load phase displacement response, under no net external forces, for each collision partner and the common collision interface, respectively, are:

$$\begin{aligned} \mathbf{u}_1\left(t\right) &= 8.85t+0.48\sin\left(12.8t\right) \\ \mathbf{u}_2\left(t\right) &= 8.85t-0.38\sin\left(12.8t\right) \\ \mathbf{u}_{IV}\left(t\right) &= 8.85t+0.24\sin\left(12.8t\right) \end{aligned} \quad (96).$$

The load phase velocity and acceleration is obtained by the simple first and second time derivatives of the equations shown in (96). The structural deflection, during the load phase, for each collision partner, is:

$$\begin{aligned} \boldsymbol{\delta}_1\left(t\right) &= 0.24\sin\left(12.8t\right) \\ \boldsymbol{\delta}_2\left(t\right) &= 0.62\sin\left(12.8t\right) \end{aligned} \quad (97).$$

The time at which closure occurs is 0.123 sec with peak displacements of 1.56 m and 0.71 m for each collision partner and with peak deflections of 0.24 m and 0.62 m, respectively. The common velocity at the terminus of closure is 8.85 $msec^{-1}$ and the peak collision force is $1.18 \cdot 10^6$ N. For the unload phase, the circular frequency is 47.3 $sec^{-1}$. The displacement for each collision partner and the common collision interface, respectively, are:

$$\begin{aligned} \mathbf{u}_1\left(t^*\right) &= 1.53+8.85t^*+0.035\cos\left(47.3t^*\right) \\ \mathbf{u}_2\left(t^*\right) &= 0.73+8.85t^*-0.028\cos\left(47.3t^*\right) \\ \mathbf{u}_{IV}\left(t^*\right) &= 1.33+8.85t^*-0.0042\cos\left(47.3t^*\right) \end{aligned} \quad (98).$$

Separation terminates at $t^*$ = 0.033 sec ($t_s$ = 0.156 sec) with terminus displacement values of 1.83 m and 1.03 m, respectively, and peak deflections of 0.20 m and 0.59 m, respectively. The separation velocity of each collision partner is 7.19 and 10.2 $msec^{-1}$, respectively. Figure 3 depicts the kinematic response for both collision partners.

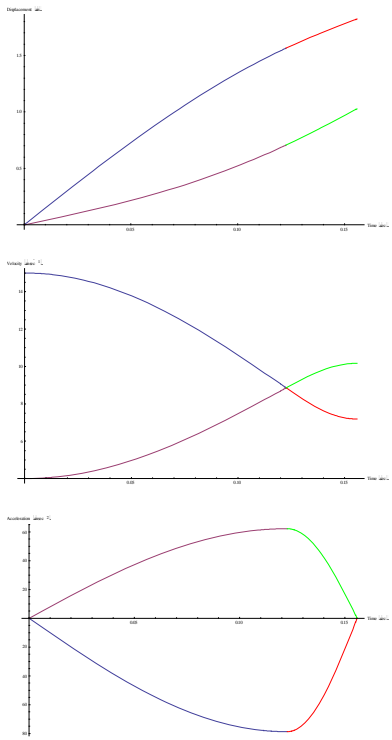

*Figure 3*. Displacement, velocity and acceleration time histories for the subject example.

Figure 4 depicts the parametric in time force-deflection response for both collision partners.

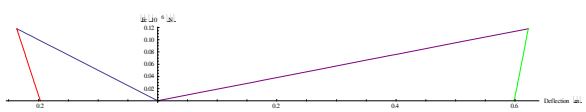

*Figure 4*. Collision force magnitude as a function of structural deflection for each collision partner.

We consider this problem, again, but with the following externally applied forces acting on each collision partner throughout the collision duration (with $\mu_1$ = -0.9 and $\mu_2$ = 0.3):

$$\begin{aligned} \mathbf{F}_{ext1} &= -\mu_1 m_1 g + 0.1t \\ \mathbf{F}_{ext2} &= \mu_2 m_2 g - 0.05t \end{aligned} \qquad (99).$$

The loading phase displacement response for the collision partners and the common collision interface are:

$$\begin{aligned} \mathbf{u}_1(t) &= -4.00\cdot 10^{-2} + 8.85t - \\ &\quad 1.13t^2 + 2.45\cdot 10^{-6} t^3 \\ &\quad +4.00\cdot 10^{-2}\cos(12.8t) \\ &\quad +0.480\sin(12.8t) \\ \mathbf{u}_2(t) &= 3.16\cdot 10^{-2} + 8.85t - \\ &\quad 1.13t^2 + 2.45\cdot 10^{-6} t^3 \\ &\quad -3.16\cdot 10^{-2}\cos(12.8t) \\ &\quad -0.379\sin(12.8t) \\ \mathbf{u}_{IV}(t) &= -2.03\cdot 10^{-2} + 8.85t - \\ &\quad 1.13t^2 + 2.45\cdot 10^{-6} t^3 \\ &\quad +2.03\cdot 10^{-2}\cos(12.8t) \\ &\quad +0.243\sin(12.8t) \end{aligned} \qquad (100).$$

The velocity and acceleration solutions are obtained, as before, by the simple first and second time derivatives. Closure terminates at 0.116 sec with a resultant peak displacement of 1.45 m, 0.663 m and 1.24 m, respectively for the collision partners and the common collision interface. The common velocity at closure is 8.59 msec$^{-1}$. The structural deflection experienced by each collision partner, during closure, is:

$$\begin{aligned} \boldsymbol{\delta}_1(t) &= -2.03\cdot 10^{-2} + 8.85t - \\ &\quad 1.13t^2 + 2.45\cdot 10^{-6} t^3 + \\ &\quad 2.03\cdot 10^{-2}\cos(12.8t) \\ &\quad +0.243\sin(12.8t) \\ \boldsymbol{\delta}_2(t) &= -1.97\cdot 10^{-2} + 8.85t - \\ &\quad 1.13t^2 + 2.45\cdot 10^{-6} t^3 + \\ &\quad 2.03\cdot 10^{-2}\cos(12.8t) \\ &\quad +0.243\sin(12.8t) \end{aligned} \qquad (101).$$

The peak deflection for each collision partner is 0.217 m and 0.572m, respectively. The peak collision force is 1.09 · $10^6$ N. The time at which separation occurs is $t^* = 3.49\cdot 10^{-2}$ sec. The unload displacement response of the collision partners and the common collision interface are:

$$
\begin{aligned}
\mathbf{u}_1\left(t^*\right) &= 1.38 + 8.59t^* - \\
&\quad 1.13t^{*2} + 2.45\cdot 10^{-6}\, t^{*3} \\
&\quad +4.00\cdot 10^{-2}\cos\left(12.8t^*\right) \\
&\quad +3.24\cdot 10^{-2}\cos\left(47.3t^*\right) \\
&\quad -2.47\cdot 10^{-8}\sin\left(12.8t^*\right) \\
\mathbf{u}_2\left(t^*\right) &= 0.72 + 8.59t^* - \\
&\quad 1.13t^{*2} + 2.45\cdot 10^{-6}\, t^{*3} \\
&\quad -3.16\cdot 10^{-2}\cos\left(12.8t^*\right) \\
&\quad -2.56\cdot 10^{-2}\cos\left(47.3t^*\right) \\
&\quad +1.95\cdot 10^{-8}\sin\left(12.8t^*\right) \\
\mathbf{u}_2\left(t^*\right) &= 1.25 + 8.59t^* - \\
&\quad 1.13t^{*2} - 2.45\cdot 10^{-6}\, t^{*3} \\
&\quad -4.74\cdot 10^{-3}\cos\left(12.8t^*\right) \\
&\quad -3.84\cdot 10^{-3}\cos\left(47.3t^*\right) \\
&\quad +2.95\cdot 10^{-9}\sin\left(12.8t^*\right)
\end{aligned}
\qquad (102).
$$

The displacements at separation for the collision partners and the common collision interface are 1.72 m, 0.994 m and 1.54 m, respectively. The residual deflections for each collision partner are 0.174 m and 0.546 m with the corresponding deflection-time histories being:

$$
\begin{aligned}
\boldsymbol{\delta}_1\left(t^*\right) &= 0.137 + 3.53\cdot 10^{-7}\, t^* \\
&\quad -2.22\cdot 10^{-16}\, t^{*2} + 4.48\cdot 10^{-2}\cos\left(12.8t^*\right) \\
&\quad +3.62\cdot 10^{-2}\cos\left(47.3t^*\right) \\
&\quad -2.76\cdot 10^{-8}\sin\left(12.8t^*\right) \\
\boldsymbol{\delta}_2\left(t^*\right) &= 0.524 + 2.12\cdot 10^{-7}\, t^* \\
&\quad +2.69\cdot 10^{-2}\cos\left(12.8t^*\right) \\
&\quad +2.17\cdot 10^{-2}\cos\left(47.3t^*\right) \\
&\quad -1.66\cdot 10^{-8}\sin\left(12.8t^*\right)
\end{aligned}
\qquad (103).
$$

The kinematic response is shown in Figure 5.

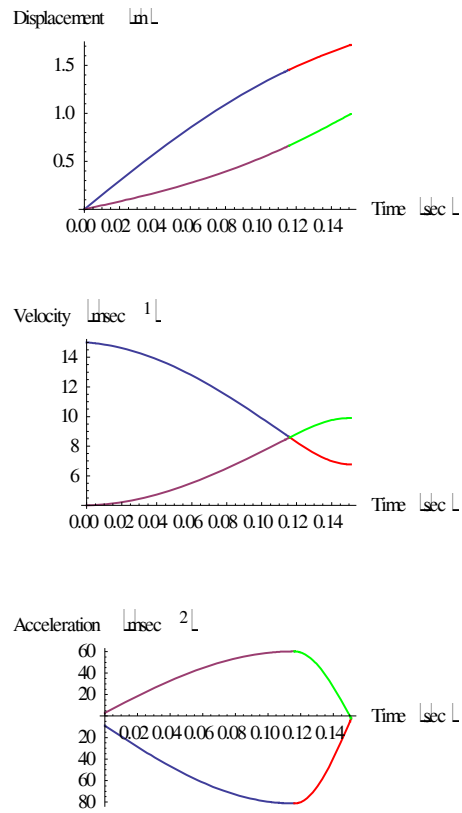


*Figure 5.* Kinematic response for the subject example with net unbalanced externally applied loads.

The force-deflection response follows that shown in Figure 4, but with the terminus of closure occurring at a lower peak collision force magnitude and with correspondingly lower magnitude peak and residual deflection magnitudes.

## DISCUSSION

Net unbalanced externally applied loads, with respect to the system comprised of collision partners, are generally neglected when considering a collision phase analysis. This approach is generally apt in that the collision force magnitude and its impulse are generally the dominant factors in most collisions except for those that are classifiable as exceedingly minor severity collisions. Higher severity collisions involving a substantively disabled collision partner or collisions in which significant snagging is present during the collision phase represent exceptions to this generality. The typical case, however, involves collisions in which the net unbalanced externally applied loads, consisting of tire forces acting upon the collision partners during the impact, are of sufficient magnitude as to warrant their effects. The

approach taken in the subject study, in regards to the inclusion of such forces, was through the use of the Laplace transform of the second order coupled differential equations of motion. In this regard, two fundamental limitations are present. The first is that the collision partner structural modeling approach, for both closure and separation, is predicated on the linear elastic model. This approach, while allowing for the relatively simple decomposition of the undamped equations of motion, would require further modification in cases in which proportional damping is included in the structural response model. The linear load-linear unload model, while limited, can be utilized in certain appropriate cases [11]. The second limitation is that the set of externally applied loads must have a determinate Laplace transform and must not alter the dynamic stiffness matrix, $\mathbf{D}(s)$. Correspondingly, the framework developed herein can readily handle the temporally diminishing, operator-mediated, brake force that arises from the occupant kinematic response for a vehicle impacted in the rear and with the foot of the operator initially depressing the brake pedal if such force is defined on a purely temporal basis. However, if such an unbalanced load is defined in terms of struck vehicle forward displacement, the dynamic stiffness matrix will be altered. The worked example, while limited to the first two terms of a polynomial representation of the net externally applied force model, readily shows the utility of the subject modeling methodology. Future work will focus on expanding the subject model for modeling chain-reaction collinear collisions and upon including the effects of proportional damping with respect to the structural response model.

## REFERENCES


1. Emori, R. and Horiguchi, J., "Whiplash in low speed vehicle collisions," SAE Technical Paper 900543, 1990.
2. Siegmund, G., Bailey, M., King, D., "Characteristics of specific automobile bumpers in low-velocity impacts," SAE Technical Paper 940916, 1994.
3. Bailey, M., Wong, B., Lawrence, J., "Data and methods for estimating the severity of minor impacts," SAE Technical Paper 950352, 1995.
4. Anderson, R., Welcher, J., Szabo, T., et al., "Effect of braking on human occupant and vehicle kinematics in low speed rear-end collisions," SAE Technical Paper 980298, 1998.
5. Ivory, M., Furbish, C., Hoffman, M., et al., "Brake pedal response and occupant kinematics during low speed rear-end collisions," SAE Technical Paper 2010-01-0667, 2010.
6. Vehicle Research and Test Center, National Highway Traffic Safety Administration, United States Department of Transportation, "Vehicle characterization and performance study of Toyota Camrys," VRTC Report DCD9157-1, 2011.
7. Rast, P., Stearns, R., Allison, M., et al., "Acceleration factors and maximum speeds under conditions of idle acceleration," *Accident Investigation Quarterly*, Summer: 16-17, 2000.
8. Bailey, M., "Reconstructing minor collisions," Presented at the Society of Automotive Engineers Low Speed Topical Technical (TOPTEC) Conference, Richmond (Vancouver), British Columbia, Canada, August 19-20, 1996.
9. Mastandrea, M. and Vangi, D., "Influence of braking force in low-speed vehicle collisions," *Proc. IMechE, Part D: J. Automobile Eng.*, 219:151-164, 2005.
10. Carpenter, N. and Welcher J., "Stiffness and crush energy analysis for vehicle collision and its relationship to barrier equivalent velocity (BEV)," SAE Technical Paper 2001-01-0500, 2001.
11. Singh, J., "A fundamental reconsideration of the CRASH3 damage analysis algorithm: the case against uniform ubiquitous linearity between BEV, peak collision force magnitude and residual damage depth," *Traffic Injury Prevention*, In Press, 2013.

# TRAFFIC ACCIDENTS IN SHANGHAI - GENERAL STATISTICS AND IN-DEPTH ANALYSIS

**Bing Deng**
General Motors Safety Electronics & Innovation
U.S.A.
**Hongyan Wang and Junyi Chen**
Shanghai United Road Traffic Safety Scientific Research Center
China
**Xuesong Wang and Xiaohong Chen**
Tongji University, School of Transportation Engineering
China
Paper Number 13-0182

## ABSTRACT

In China, traffic accident data is published annually by the Traffic Management Research Institute of the Ministry of Public Security [1]. Accidents without casualties are usually not included. To gain a complete understanding and reliable insight of Shanghai traffic accidents, the project team collected the original accidents records on 192 Shanghai roads between 1-1-2009 and 12-31-2009. The overall traffic accident statistics, the temporal distributions, and the spatial distributions of crashes, crash modes, and crash severity were analysed for different road categories, including freeways, classified highways, urban expressways, and surface roads.
In-depth accident cases were obtained from Shanghai United Road Traffic Safety Scientific Research Center, a research consortium conducting accident investigation in Shanghai. Each case was reconstructed using PC-Crash. The impact speed was estimated and studied for different crash modes.

## INTRODUCTION

Today, about half of the people in the world live in urban areas. In 20 more years, 60% of the world's population, and 80% of the wealth, will be concentrated in cities [2]. With such a trend, cities around the world are actively looking for smart and safe driving. In China, roads are classified as highways (freeway, Class I highway, Class II highway, Class III highway, and Class IV highway), and urban streets (urban expressways, arterial roads, minor arterial roads, and branch roads) [3]. This research studied the current traffic safety situation on different roads in Shanghai, China. The objective is to understand traffic accident characteristics on typical city roads in a megacity, like Shanghai, and to help develop safety priorities for vehicles driving in cities.

## METHODOLOGY

The original accidents' records on 192 Shanghai roads (from the whole geographic area), between 1-1-2009 and 12-31-2009 were collected from traffic police stations. The general traffic accidents were analyzed on different roads.

Shanghai United Road Traffic Safety Scientific Research Center has been conducting in-depth accident investigation in Jiading, one of 19 districts in Shanghai, since 2005. This research consortium only investigates severe accidents involving passenger vehicles which meet one of following three criteria:

1. At least one of the involved persons sustained severe injury or fatal injury; or
2. At least one air bag deployed; or
3. The total damage is $3500 or above

"Severe injury" refers to non-life-threatening injuries, such as bone fracture.

A total of 404 cases collected between 2005 and 2011 were obtained and analyzed. Each case has a detailed report with many photos and measurements. There is information about accident time, location, weather, road surface condition, lighting condition, traffic condition, vehicles involved, and vulnerable road users, if any. The accident scene was generated to detail the crash event, the initial contact position, and final positions of involved accident participants (Figure 1). Vehicles were measured or scanned for exterior deformation and interior deformation (Figure 2). The restraint system performance was investigated (Figure 3). The injury descriptions were obtained from the traffic police and/or the hospital. Accident sketches were created using Auto-CAD, accurately scaled according to the accident scene investigation (Figure 4). The developed sketch was used for accident reconstruction in PC-Crash (Figure 5). Vehicle impact speeds were estimated by validating the vehicles' trajectory and final landing position.

*Figure 1.* An accident scene to detail the crash event

*Figure 2.* Vehicle deformation measurements

*Figure 3.* Restraint system performance investigation

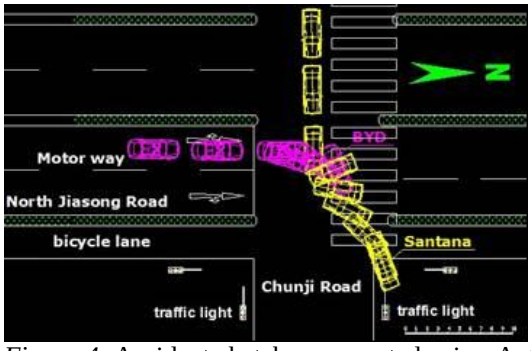


*Figure 4.* Accident sketch was created using Auto-CAD with accurate scale

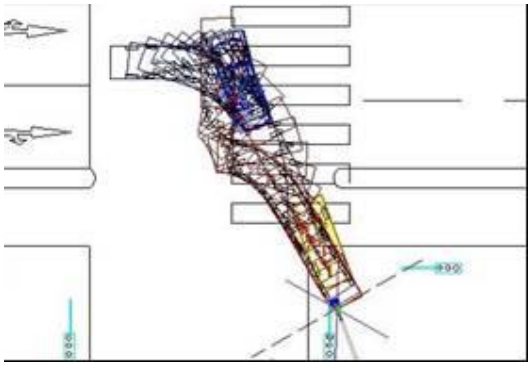

*Figure 5.* Vehicle impact speed estimation using accident reconstruction in PC-Crash

## RESULTS

### General Statistics

The number of accidents per kilometer was used to compare the collision frequency among different roads (Figure 6). Using a freeway as a reference, the relative number of accidents on the urban expressways, classified highways, and surface roads are 2.8, 2.2, and 5.5, respectively. Surface roads have the highest number of accidents per unit length. Surface roads are designed for mixed road users, including motor vehicles, non-motorized vehicles, and pedestrians. Since they have the most frequent accidents, arterial roads and signalized intersections were separated out from surface roads when studying injuries and crash modes. Accidents occurred within 15 meters of a signalized intersection were excluded from surface roads and included for signalized intersection. Figure 7 shows the injury distribution. On all roads, the majority of accidents had no casualty (more than 74.6%). Accidents with minor injuries were the second most frequent accidents on all roads, followed by fatal accidents and accidents with severe injuries. The highest fatal accident probability is on freeway (0.7%).

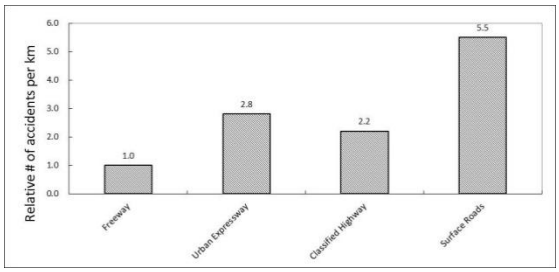


*Figure 6.* Relative number of accidents per kilometer on different roads

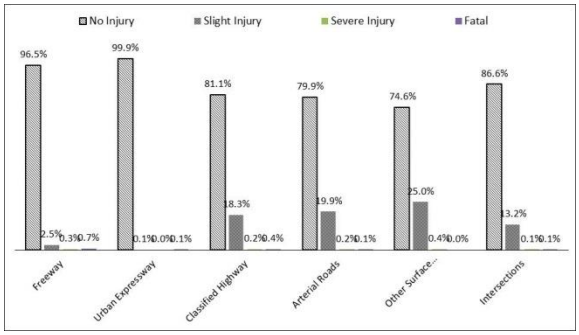


*Figure 7.* Accident injury severities

Figure 8 shows the crash modes distribution recorded in the accident reports. Freeway and surface roads (including intersections) had a large number of unknown crash type accidents (47.3% for freeway, 39.1% for arterial roads, 36.2 for other surface roads, and 43.6% for intersections). Such a large number of unknown crash types in the accident reports showed the need to improve the

data recording method. The unknown crash modes are only 8.1% and 12.6% for classified highways and urban expressways, respectively. Among all known crash modes, side collisions, followed by rear-end collisions, and “hit fixed objects” were the most frequent crashes on freeways, on classified highways, and on surface roads. Rear-end collisions followed by side collisions were the two dominant crash modes on urban expressway. It is interesting to note that less than 1.3% recorded accidents on all roads were “hit pedestrian”. One explanation could be that all crash cases were collected from traffic police records. Many pedestrian collisions may not even be recorded by the traffic police, unless severe injuries occurred.

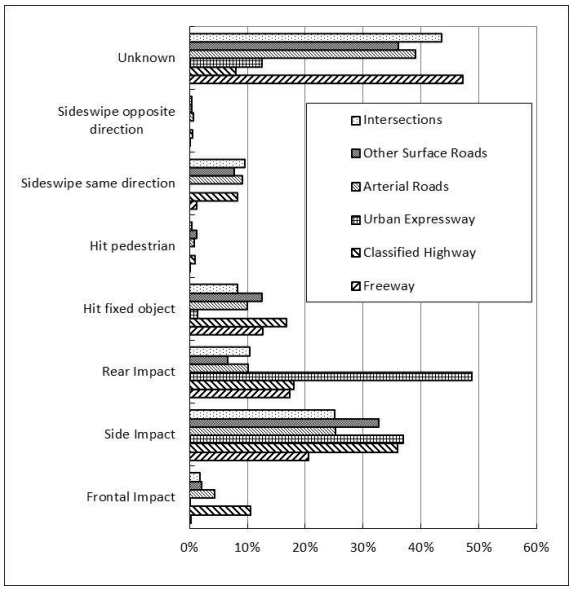


*Figure 8.* Crash modes as recorded in the accident reports

Figure 9 shows the causes of accidents that were recorded in the accident reports. More than 55% of accidents had unknown causes. Such a high percentage of unknown causes shows the urgent need to improve data quality. All the identified causes are related to driver behaviors. On freeway and urban expressway, where only motorized vehicles are allowed, and there is no traffic light, “illegal lane change” is the only dominant cause. On surface roads and classified highways, where mixed traffic participants are expected, including vehicles, two wheelers, and pedestrians, and there are traffic lights at intersections, “illegal lane change” and “fail to yield” are the two dominant causes of accidents.

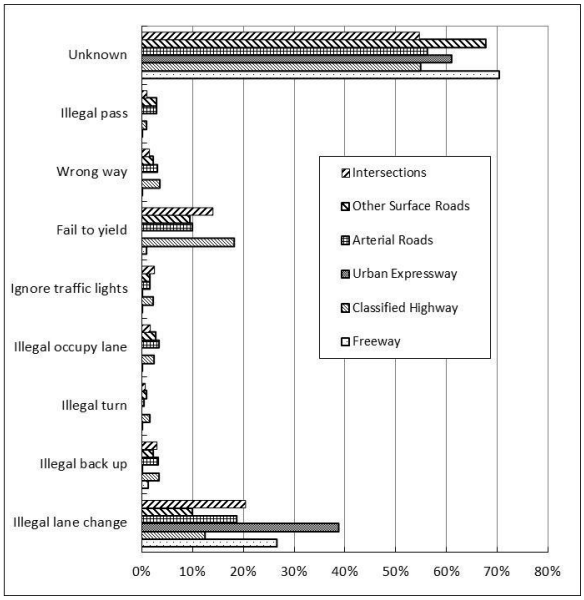


*Figure 9.* Cause of accident as recorded in the accident reports

## In-Depth Analysis

The general statistics showed that side collisions and rear-end collisions were the top two most frequent crashes on Shanghai roads, a megacity with more than 19 million registered residents [3]. A total of 404 in-depth accident cases were obtained from Shanghai United Road Traffic Safety Scientific Research Center. Those cases were studied to understand how accidents happened and what the impact speeds were. Among those severe cases, only 231 cases were capable of being reconstructed using PC-Crash. The impact speeds were obtained from those 231 cases and studied for different crash modes.

**Side Collision** The impact direction of each passenger vehicle is identified according to the 12 o’clock scheme (Figure 10). The struck locations at 2, 3, 4, 8, 9, and 10 o’clock are grouped as side collisions. All side collision cases happened on surface roads. The struck vehicles were passenger cars. There were a total of reconstructed 67 side collisions. Those collisions involved 132 occupants. Figure 11 shows the estimated vehicle impact speed distribution.

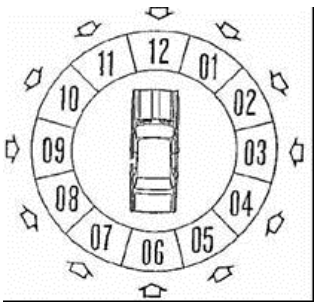


*Figure 10.* 12 o’clock scheme for impact direction

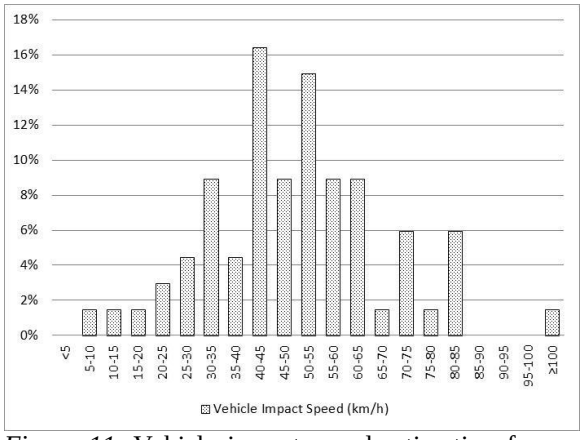


*Figure 11.* Vehicle impact speed estimation from reconstructed 67 severe side collisions

**Rear-end Collision** There were a total of 19 rear-end collisions reconstructed using PC-Crash. Six cases happened on freeway or classified highway. Thirteen cases happened on surface roads. Those collisions involved at least one passenger car and a total of 46 passenger car occupants. Figure 12 shows the estimated vehicle impact speed distribution.

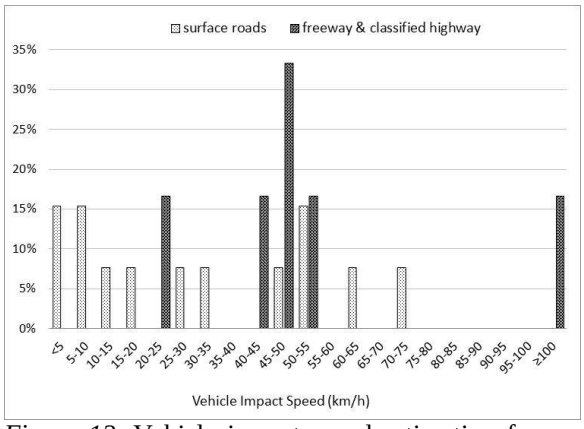


*Figure 12.* Vehicle impact speed estimation from reconstructed 19 severe rear-end collisions

**Car to Two Wheelers Collision** It is interesting to note that, among those severe in-depth cases in Jiading (a remote district of Shanghai), 47% cases were passenger car to two wheeler collisions. The two wheelers include motor bikes, electric bikes, and bicycles. Those collisions all happened on surface roads. All severe injuries were sustained by the vulnerable road users. There was no injury to the car occupants. A total of 110 car to two wheeler collisions were reconstructed. Those collisions involved at least one passenger car and a total of 139 vulnerable road users. Figure 13 shows the estimated vehicle impact speed distribution.

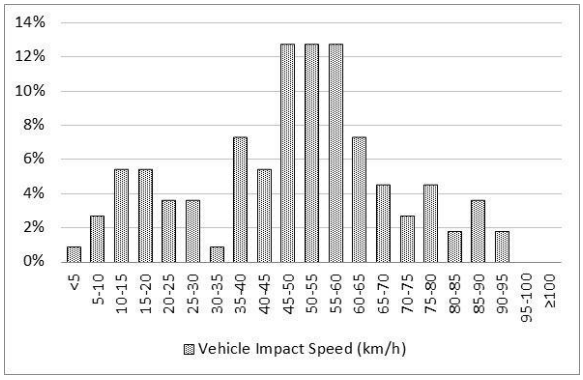


*Figure 13.* Vehicle impact speed distribution from reconstructed 110 severe passenger car to two wheeler collisions.

## CONCLUSIONS

In a megacity like Shanghai, the majority of accidents recorded by traffic police, had no casualties. Surface roads have the highest number of accidents per unit length. As surface roads are designed for mixed road users, including motor vehicles, non-motorized vehicles, and pedestrians, improving megacity traffic safety would need to consider all road users.

Side collisions and rear-end collisions are the top two most frequent crashes on Shanghai roads. Technologies mitigating those types of crashes may be desirable.

All identified accident causes in the traffic police reports are related to driver behaviors. “Illegal lane change” is the only dominant cause on freeway and urban expressway. “Illegal lane change” and “fail to yield” are the two dominant causes of accidents on surface roads and classified highways. Traffic safety education and traffic law enforcement could improve road user behavior.

The high percentage of unknown crash types and unknown accidents causes also shows the need of using scientific method to accurately record traffic accidents.

Vehicle impact speeds were estimated by reconstructing in-depth accident cases. A wide range of impact speeds were observed. Detailed injury descriptions are needed for further study.

## REFERENCES

[1] Blue books by Traffic Management Research Institute of the Ministry of Public Security (2000 to 2010)

[2] William J. Mitchell, Christopher E. Borroni-Bird, and Lawrence D. Burns, “Reinventing the Automobile - Personal Urban Mobility for the 21st Century”, 2010.

[3] Shanghai Urban Planning Institute, “The Fourth Shanghai Traffic Survey”, 2009.

# NEAR-CRASH SCENARIO IN CHINA BASED ON SHANGHAI DRIVING DATA

**Bing Deng**
General Motors Safety Electronics & Innovation
U.S.A.
**Jiaqi Li, Yin Yang, Xiaofei Dong, Xichan Zhu, Zhixiong Ma**
Tongji University, Automotive Engineering College
China
**J.T. Wang**
General Motors Vehicle Systems Research Laboratory
U.S.A.
Paper Number 13-0187

## ABSTRACT

In 1995, there were 1.4 million automobiles in China. In 2010, the number of automobiles reached 18.27 million, including 9.576 million passenger vehicles [1]. With such rapidly growing capacity, traffic safety is becoming increasingly important. In 2010, there were 3,906,173 accidents, 65,225 fatalities, and 254,075 injuries reported by the Chinese official statistics [2].

Crash scenario typologies have been widely used in support of identifying crash intervention opportunities, setting research priorities and direction in safety technology development, and evaluating the effectiveness of selected crash countermeasure systems. The objective of this study is to collect data and to develop a list of representative near-crash scenarios. The developed frequency distribution of typical near-crash scenario can help identifying intervention technology development opportunities for collision avoidance.

## INTRODUCTION

Real-world accidents and near-crash cases provide the necessary data to develop control algorithms to avoid accidents, as well as to prepare vehicles for inevitable crashes. Crashes typology in the U.S. has been developed by General Motors (GM) and adopted by automakers for the design, development, and benefits assessment of potential crash countermeasure technologies [3]. Near-crash scenario typologies have been gaining strong research interests in recent years. A near-crash is referred to a successful crash avoidance event, where a successful, last-second evasive maneuver is required to avoid a crash. Near-crash studies can provide unique insight into the elements and factors associated with successful crash avoidance maneuvers for comparison to unsuccessful or crash circumstances. The 100-Car Naturalistic Driving Study completed by the Virginia Tech Transportation Institute, is the first instrumented-vehicle study undertaken with the primary purpose of collecting near-crash, pre-crash, crash, and naturalistic driving data [4].

This study instrumented ten taxis with drive recorder (Horiba TWINs) to collect naturalistic driving data. The data collected between February 2011 and July 2012 were combined with data collected from four taxis with Video Drive Recorder (Horiba VDR) between September 2008 and September 2009. The top six near-crash scenarios are presented in this paper.

## METHODOLOGY

Two sets of data were used in the analysis. Both sets of data were from taxis travelled in Jiading District in Shanghai under normal driving conditions. No special instructions were given to the drivers. The first set of data was collected from four taxis with Video Drive Recorder (VDR) between September 2008 and September 2009 (Figure 1). Each VDR had one camera focusing on the road in front. The forward image, vehicle traveling velocity, and vehicle accelerations in the longitudinal, lateral, and vertical directions were monitored continuously and recorded for a 20 second period, 15 seconds prior to the trigger and 5 seconds after the trigger. The second set of data was collected from ten taxis with drive recorder TWINs between February 2011 and July 2012. Each TWIN had two cameras, one focusing on the road in front, and the other focusing on the driver (Figure 2). The additional data from TWINs included the vehicle interior image focusing on the driver and the GPS data. The trigger for data collection was set at 0.4 g in any direction. This conservative approach is to avoid missing any near-crash cases. After carefully viewing the logged data video images, vehicle velocity, and the specific driving environment, cases without any inherent collision potential were excluded from the near-crash cases. The events requiring a rapid, evasive maneuver to avoid a crash were considered as a near-crash case.

To identify all common pre-crash scenarios of all police-reported crashes involving at least one light vehicle, NHTSA defined and statistically described a pre-crash scenario typology for light vehicles based on the 2004 General Estimates System (GES) crash database [2]. Single-vehicle and two-vehicle crashes of common crash types were analyzed and produced the list of 37 representative pre-crash scenarios [2]. These 37 pre-crash scenario definitions developed by NHTSA were used to characterize near-crash cases collected in the current study. The top most frequent scenarios were compared.

*Figure 1.* Horiba VDR instrumentation. Data included forward image, vehicle traveling velocity, and vehicle accelerations in the longitudinal, lateral, and vertical directions.

*Figure 2.* Horiba TWIN instrumentation. Data included forward image, interior image focusing on the driver, vehicle traveling velocity, vehicle accelerations in the longitudinal, lateral, and vertical directions, and GPS data.

## RESULTS

There were a total of 1,420 cases collected from VDR instrumented taxies and TWIN instrumented taxies. Of them, 11 cases were actual crashes. After carefully reviewing each of those non-crash cases, 430 cases were judged as near-crash cases and were further analyzed. Table 1 shows the comparison of six most frequent scenarios. In NHTSA's analysis, the six most frequent scenarios accounted for 51% of all police-reported light-vehicle crashes. In current Shanghai analysis, the six most frequent scenarios accounted for 70% of all near crashes. The most frequent scenarios from both studies include "Lead Vehicle Decelerating" and "Vehicle(s) Changing Lanes - Traveling in Same Direction". Two types of single vehicle crashes were in NHTSA's top six of the most frequent scenarios ("Control Loss Without Prior Vehicle Action" and "Road Edge Departure Without Prior Vehicle Maneuver"). Three out of six most frequent Shanghai scenarios included vulnerable road users ("Two Wheeler Crash – Vehicle Going Straight", "Two Wheeler Crash – Vehicle Turning", "Pedestrian Crash - Vehicle Going Straight").

The top six most frequent Shanghai near-crash scenarios involve either two vehicles or one vehicle with a vulnerable road user. There was no single vehicle near crash in the analyzed 430 cases. A typical "Lead Vehicle Decelerating" scenario can be described as: vehicle is going straight and following another lead vehicle on a surface road, in daylight, under clear weather conditions, at a non-junction with a posted speed limit ranging from 30 km/h to 60 km/h; and the lead vehicle suddenly decelerates. A typical "Two Wheeler Crash - Vehicle Going Straight" scenario can be described as: vehicle is going straight on a surface road, in daylight, under clear weather conditions, with a posted speed limit ranging from 30 km/h to 60 km/h and encounters a two wheeler at a non-junction location. Two wheelers include motor bikes, electric bikes, and bicycles. A typical "Two Wheeler Crash – Vehicle Turning" scenario can be described as: vehicle is turning right or left on a surface road, in daylight, under clear weather conditions, with a posted speed limit ranging from 30 km/h to 60 km/h; and encounters a two wheeler at an intersection. A typical "Vehicle(s) Changing Lanes - Traveling in Same Direction" scenario can be described as: vehicle is changing lane on a surface road, in daylight, under clear weather conditions, with a posted speed limit ranging from 30 km/h to 60 km/h; and encroaches into another vehicle traveling in the same direction. A typical "Vehicle(s) Drifting - Traveling in Same Direction" scenario can be described as: vehicle is going straight on a surface road, in daylight, under clear weather conditions, at a non-junction with a posted speed with a posted speed limit ranging from 30 km/h to 60 km/h; and then drifts into an adjacent vehicle traveling in the same direction. A typical "Pedestrian Crash - Vehicle Going Straight" scenario can be described as: vehicle is going straight on a surface road, in daylight, under clear weather conditions, with a posted speed limit ranging from 30 km/h to 60 km/h; and encounters a pedestrian at a non-junction location. Figure 3 depicts the top six common scenarios.

Table 1. Top six pre-crash scenarios comparison between NHTSA's study and current study

| Top 6 pre-crash scenarios based on US 2004 GES crash database [2] | | Top 6 pre-crash scenarios based on 430 near-crash cases in Jiading, Shanghai | |
|---|---|---|---|
| **Scenario** | **Frequency** | **Scenario** | **Frequency** |
| Lead Vehicle Stopped | 16.41% | Lead Vehicle Decelerating | 20.50% |
| Control Loss Without Prior Vehicle Action | 8.90% | Two Wheeler Crash - Vehicle Going Straight | 20.08% |
| Vehicle(s) Turning at Non-Signalized Junctions | 7.32% | Two Wheeler Crash - Vehicle Turning | 13.46% |
| Lead Vehicle Decelerating | 7.20% | Vehicle(s) Changing Lanes - Traveling in Same Direction | 7.25% |
| Vehicle(s) Changing Lanes - Traveling in Same Direction | 5.69% | Vehicle(s) Drifting - Traveling in Same Direction | 4.76% |
| Road Edge Departure Without Prior Vehicle Maneuver | 5.62% | Pedestrian Crash - Vehicle Going Straight | 4.35% |

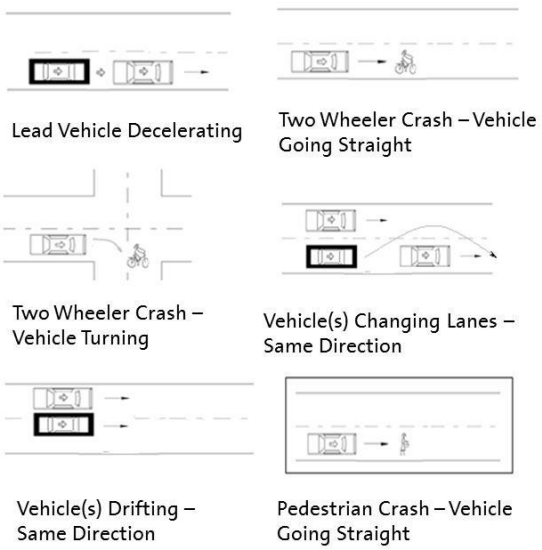


*Figure 3.* The top six common scenarios from current study.

The recorded velocities were studied as vehicle kinematics for the top six common scenarios. The data frequency is only 30 Hz for current instrumentation. Figure 5 shows the velocity vs. time for a number of vehicles that experienced the "Two Wheeler Crash - Vehicle Going Straight" scenario.

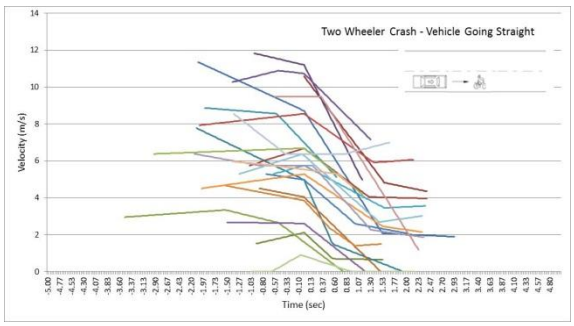


*Figure 4.* Vehicle velocity for a number of vehicles experienced the "Two Wheeler Crash Without Prior Vehicle Maneuver" scenario.

A critical braking phase was observed from every one of these cases. Following such critical braking (defined as highest deceleration), the studied vehicle successfully avoided the potential collisions (Figure 5).

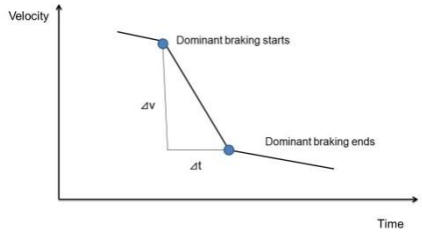


*Figure 5.* A representative critical braking phase in near crashes

The time duration and the velocity change were analyzed during the critical braking phase for all six scenarios. Table 2 shows the average time duration and the average velocity change during the critical braking for the top six most frequent scenarios.

Table 2. The average time duration and the average velocity change during the critical braking

| Scenario | ⊿t (sec) | ⊿v (m/s) |
|---|---|---|
| Lead Vehicle Decelerating | 1.53 | 4.43 |
| Two Wheeler Crash - Vehicle Going Straight | 1.28 | 3.76 |
| Two Wheeler Crash - Vehicle Turning | 0.86 | 2.40 |
| Vehicle(s) Changing Lanes - Traveling in Same Direction | 1.20 | 3.82 |
| Vehicle(s) Drifting - Traveling in Same Direction | 1.33 | 3.22 |
| Pedestrian Crash - Vehicle Going Straight | 1.58 | 3.68 |

For the near-crash scenarios in the same motor lane, including "Lead Vehicle Decelerating", "Two Wheeler Crash - Vehicle Going Straight", and "Pedestrian Crash - Vehicle Going Straight"), the conflicts with two wheelers showed the shortest braking time, and the conflict with a vehicle showed the highest velocity change. For the near-crash scenarios involving two wheelers, the conflicts at intersections ("Two Wheeler Crash – Vehicle Turning") showed shorter braking time and lower velocity change. The near-crash scenarios involving lane change ("Vehicle Changing Lane" and "Vehicle Drafting") showed similar braking characteristics.

Data from ten taxis with drive recorder TWINs had the vehicle interior image focusing on the driver. The driver images were analyzed together with the forward road images to study driver and environment risky factors which may lead to near-

crashes. Of the 100 cases we analyzed, forty-six cases were due to unexpected opponent movements, such as leading vehicle decelerating, unexpected two wheelers getting into path, etc. Twenty-three cases involved aggressive movements of both objects, such as lane hovering. Twenty-one cases were caused by the subject vehicle itself, such as changing lanes, driver inattention. Ten cases had blocked opponent, such as pedestrians coming out of a light pole.

The results from the current study were compared to a previous study in Beijing [5]. The Beijing study concluded that rear-end conflicts were the most common type (41%). The current study revealed similar trend (Table 1, 20.5% "Lead Vehicle Decelerating"). The current study also revealed that two wheeler conflicts while a vehicle is going straight or turning, are very common (33.46%, Table 1). However, since both studies only used data from a small sample of taxis in a mega city like Beijing or Shanghai, the results may not be generalized to represent the characteristic of all near-crashes in China.

## CONCLUSIONS

Four hundred thirty near crash cases were analyzed from a two and a half years' data collection of instrumented taxis in Jiading district of Shanghai. The previously developed 37 pre-crash scenarios definitions by NHTSA were used to study near-crash cases collected in the current study. The six most frequent scenarios accounted for 70% of all near crashes. Three out of six of the most frequent Shanghai scenarios included vulnerable road users. There was no single vehicle near-crash in the studied 430 near crash cases. The most frequent Shanghai near-crash scenarios involve either two vehicles or one vehicle with a vulnerable road user.

All vehicles exhibited a critical braking phase and successfully avoided the potential collisions. The braking characteristics were studied for each scenario and quantified using braking time duration and the velocity change.

Using the vehicle interior images together with the forward road images, we found that an unexpected opponent movement is the leading cause of near-crashes.

## REFERENCES

[1] China Statistic Yearbook http://www.stats.gov.cn/
[2] Blue books by Traffic Management Research Institute of the Ministry of Public Security (2010)
[3] NHSTA, "Pre-Crash Scenario Typology for Crash Avoidance Research", DOT HS 810 767 (2007)
[4] Knipling, "The 100-car naturalistic driving study: Phase II-Results of the 100-car field experiment", 2005
[5] Qingfeng Lin, Ruijia Feng, and Bo Cheng, "Analysis of Causes of Rear-end Conflicts using Naturalistic Driving Data Collected by Video Drive Recorders", 2008

# DEVELOPMENT OF OCCUPANT INJURY PREDICTION ALGORITHMS FOR ADVANCED AUTOMATIC COLLISION NOTIFICATION BY NUMERICAL CRASH RECONSTRUCTIONS

**Maika, Katagiri**
**Yusuke, Miyazaki**
Tokyo Institute of Technology
Japan
**Jonas, Pramudita**
Niigata University
Japan
**Sadayuki, Ujihashi**
Nippon Bunri University
Japan
Paper Number 13-0149

## ABSTRACT

Prediction of injured body regions and injury severity from available accident data can lead to more appropriate and hastier emergency care in automotive accidents. The existing prediction method was based on statistical analysis of a massive amount of real-world accident data. However, numerical crash simulations were also considered to provide a virtual injury database in a relatively short time. Therefore, the purpose of this study was to develop and to evaluate a new method to obtain injury prediction algorithm by utilizing virtual database of numerous computer simulation results.

Occupant and cabin were modeled as multi-bodies. The occupant models have geometries of typical Japanese adult males. The cabin model consists of safety restraint systems and interior panels. Acceleration and intrusion of the door panels during side impact were delivered to the occupant in the simulations. Hundreds of crash simulations were performed where crash parameters were changed systematically. The injury prediction algorithms were developed by logistic regression analysis of the database constructed from the results of the simulations.

The algorithms correctly predicted more than half of the head, thorax, and thigh injuries in 48 accidents. However, this study neglected cabin deformation in frontal crash, break of door-window, as well as occupant's age and gender, which may affect on the occupant responses and injury severities. These limitations might be the cause of the miss predictions of injury severity in the simulations.

In this study, possibility of developing injury prediction algorithms by using numerical crash reconstructions was presented as a different approach from existing method that used real-world accident data. For more accurate predictions, improvement of the simulation models and consideration of occupant characteristics are required.

## INTRODUCTION

Advance in active and passive safety technology has contribution on reducing casualties in automotive accidents. For "Zero Death", a multidisciplinary approach at post crash stage is required. Advanced Automatic Collision Notification (AACN), which is a notification system associated with injury prediction based on the accident data, is expected to optimize Emergency Medical Service (EMS) and reduce trauma deaths. In frontal crashes, the ratio of deaths or severe injuries to the number of accidents was siginificant, while in lateral crashes, severe injuries occured under relatively low impact velocity [1]. Therefore, AACN is required in particular for frontal and lateral crashes.

URGENCY Algorithm [2] which was statistically built from a massive amount of field data was proposed to be used in predicting the probability of injury occurrence from several accident parameters. However, it is difficult and costly to collect lots of reliable field accident information which is necessary for developing a valid algorithm. Furthermore, the algorithm does not consider the injury mechanism, because field data can not provide any information regarding injury process during the accidents.

Simulations of various types of accidents using computer models of occupant and vehicle interior can be used to easily develop a huge accident database. In this study, we suggest a new method to develop

injury prediction algorithm for frontal and lateral crashes by using multi-body models.

## NUMERICAL CRASH SIMULATIONS

Occupant and vehicle interior were modeled as multi-bodies. Only acceleration was delivered to the occupant in frontal crash simulations, while intrusion of the door panels was also simulated in addition to acceleration in near-side impact simulations. MADYMO ver. 7.1 (TASS) was used as an analysis solver.

### Occupant Model [3]

The occupant models consist of 15 segments and have geometries of typical Japanese adult males. The body sizes can be divided into three: $5^{th}$ , $50^{th}$ , and $95^{th}$ percentile in body stature and weight. The geometries were based on the database of three dimensional measurement of Japanese subjects. The passive resistance of the joints and contact stiffness of body segments were determined according to references.
The responses of these occupant models to frontal and side impact had been validated in numerical reconstruction of a volunteer experiment. As a result of numerical reconstruction in frontal impact test [4], the behavior of the model was generally similar to that of the volunteers [5]. In a case of side impact, a volunteer test which simulated side impact on shoulder [6] was numerically reconstructed, and it was found that result of the reconstruction simulation coincided well with the test result [7].

### Cabin Model

The cabin model for frontal crashes [3] consists of safety restraint systems and simplified interior panels. The airbag and seat-belt were modeled as finite elements. For side impact crashes, the model did not have airbag, and the seat was modeled as finite elements [7].

### Crash Simulation Models

The occupant and cabin models were combined, and impacts were imposed on it as shown in Figure 1. In a frontal crash simulation, posterior-anterior translational acceleration, which was obtained from measured crash acceleration of vehicle during rigid barrier crash, was given to the occupant model. In a side impact crash simulation, left-right translational acceleration was given to occupant model, and enforced displacement was also given to the two inferior panel of the three-segmented door panel model in order to simulate the door intrusion. The top panel represents door window, which was considered to has no significant displacement during a crash.

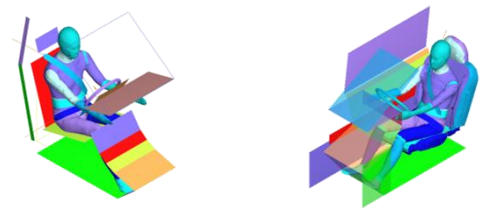

(a) Frontal (b) Lateral

*Figure 1.* Crash simulation models

### Validation against JNCAP tests

The crash simulation models had been validated against JNCAP full-wrap frontal and side impact crash tests [5][7] . In the validations, accelerations measured during the tests and estimated door panel displacement were given to the simulation model. The kinematic behavior, the resultant acceleration of head, thorax, and pelvis, as well as the compressive force on thigh matched qualitatively to that of crash dummy. Moreover, The gaps between two responses were not quantitatively significant.

## INJURY DATABASE

Injury occurrence was evaluated by relevant injury criteria. Simulations of 324 frontal and 162 near-side impact crashes were performed. Severity of injuries was found to increase along with the increase of crash velocity.
To create an injury database, parametric studies using the crash simulation models were carried out. In an accident, crash parameters, such as collision velocity, collision angle, and driver stature must be varied. Therefore, it should be considered during simulation. Practically, it can be obtained or estimated by in-vehicle devices, such as EDR. Systematically changes on those crash parameters were made during the parametric studies.

### Crash Parameters

**Frontal Crash** The crash parameters for frontal crash simulations, including airbag, seat-belt, driver stature, vehicle type, collision speed, and

collision angle, were altered into two or three levels as shown in Table 1. Vehicle accelerations, which depend on the collision speed, collision angle, and vehicle type, were created as an input for simulation. A minivan, a compact-vehicle and a light-vehicle were selected as representatives from JNCAP full-wrap crash tests data respectively. Figure 2 shows the time histories of crash acceleration of each vehicle measured in the tests. The time integration corresponded with rigid barrier collision at speed of 55 km/h. Under an assumption that the waveform features of crash acceleration is independent from collision speed, crash accelerations at 30 and 80 km/h were created by scaling the waveform as presented in Figure 2. In case of oblique crashes, the waveform was resolved into anterior-posterior and lateral components.

**Side Crash** The crash parameters for side impact crash simulations, including seat-belt, vehicle type, seat height, driver stature, and collision speed were altered into two or three levels as shown in Table 2. Time histories of vehicle acceleration were created depending on the collision speed and vehicle type. A minivan, a compact-vehicle and a light-vehicle were selected from JNCAP side impact tests data respectively. Figure 3 shows the time histories of acceleration of each vehicle measured in the tests. As in frontal crashes, the acceleration waveforms were scaled to create acceleration waveforms for crash simulation at 30 and 70 km/h. Moreover, time histories of the door displacement were created as shown in Figure 4. It was reported that the deformation behavior of door panel is independent of vehicle type [8], and the spring back is less than 25% [9]. Therefore, the maximum displacement was set to be 1.25 times of the residual deformation. The maximum and the residual deformation were assumed to occur at the same time with the maximum acceleration and a time when the relative velocity between the vehicle and the striking barrier became zero respectively. Deformation at Belt Line and H-Point were given to the middle and bottom segment of the door model respectively. Under an assumption that collision speed correlates with the degree of deformation but not with the deformation characteristics, door displacement behavior at 30 and 70 km/h were created based on that at 55 km/h.

**Table 1.**
**Parameters in frontal crash simulations**

| | Parameter | Level | Value |
|---|---|---|---|
| 1 | Airbag | 2 | 1: on, 0: off |
| 2 | Seat belt | 2 | 1: on, 0: off |
| 3 | Driver stature [m] | 3 | 1.58: 5%, 1.71: 50%, 1.85: 95% |
| 4 | Vehicle type | 3 | 1: minivan, 2: compact, 3: light |
| 5 | Collision speed [km/h] | 3 | 30, 55, 80 |
| 6 | Collision angle [degree] | 3 | -30, 0, 30 |

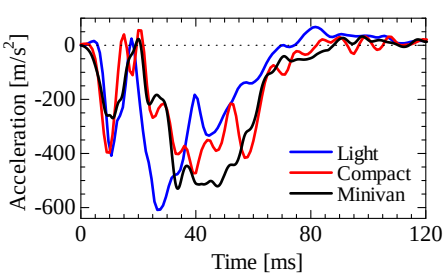


*Figure 2.* Frontal crash accelerations at 55 km/h

**Table 2.**
**Parameters in side impact crash simulations**

| | Parameter | Level | Value |
|---|---|---|---|
| 1 | Seat belt | 2 | 1: on, 2: off |
| 2 | Vehicle type | 3 | 1: light, 2: compact, 3: minivan |
| 3 | Seat height [mm] | 3 | 230, 255, 280 |
| 4 | Driver stature [m] | 3 | 1.58: 5%, 1.71: 50%, 1.85: 95% |
| 5 | Collision speed [km/h] | 3 | 30, 55, 70 |

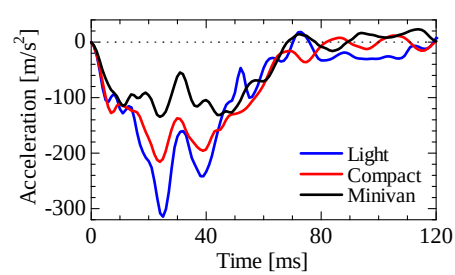


*Figure 3.* Side impact crash accelerations at 55 km/h

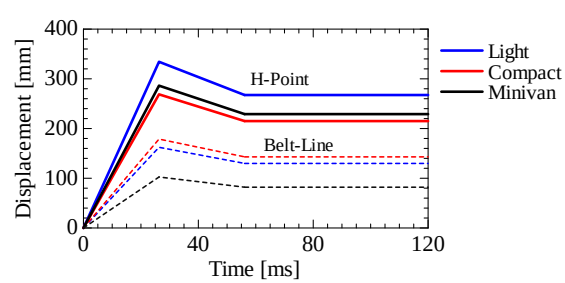


*Figure 4.* Door panel displacements at 55 km/h

### Conversion to Abbreviated Injury Scale

From the occupant model responses, injuries on head, thorax, and thigh were evaluated. Injury criteria for head, thorax, and thigh were Head Injury Criterion (HIC), cumulative maximum resultant acceleration in 3 ms, and maximum compression load on femur respectively.

In EMS, severity of injury is important rather than the value of injury criterion, because this information is required to decide treatment method. Abbreviated Injury Scale (AIS) is an anatomical-based scoring system classifying each injury by body region according to its severity into a six-level ordinal scale (from minor:1 to maximum:6). Proposed injury risk curves [10][11][12], which were developed based on the experiments, provide the relationships between probability of AIS level and value of injury criteria. Under an assumption that 50% of probability was the threshold for injury occurence, the relationships between the value of injury criteria and AIS level were determined as shown in Table 3. According to this relationships, values of injury criteria obtained from the simulations were then converted into injury severities (AIS).

**Table 3.**
**Relationships between Injury Criteria and AIS**

| AIS | Head | Thorax | Thigh |
|---|---|---|---|
| | HIC | max. res. acc. in 3ms [G] | comp. load [kN] |
| 1+ | 330 – 585 | < 21 | < 11 |
| 2+ | 586 – 966 | 21 – 50 | 11 – 15 |
| 3+ | 967 – 1435 | 51 – 69 | >16 |
| 4+ | 1436 – 1847 | 70 – 133 | |
| 5+ | 1848 – 2182 | > 133 | |
| 6+ | > 2182 | | |

## INJURY PREDICTION ALGORITHMS

### Logistic Regression Analysis

Prediction algorithms for head, thoracic and thigh injury probability were derived from ordinal logistic regression analysis of the injury database where the crash parameters and the injury outcome are related each other. Equation 1 shows the relationships between occurrence probability of over a level of AIS, $P_{\mathrm{AIS}*+}$, and an explanatory variable, $Z$, whose value was defined by values of crash parameters and their regression coefficients. $P_{\mathrm{AIS}*+}$ become larger along with the increase of $Z$. Algorithms for frontal and side impact crashes have six and five parameters respectively. Airbag, seat-belt, and vehicle type were categorical, while driver stature, seat height, collision velocity, and collision angle were continuous variables. PASW Statistics ver. 17 (SPSS) was used for the statistical analysis.

$$P_{\mathrm{AIS}*+} = \frac{1}{1+\exp(-Z)} \qquad (1)$$

$$Z_{\mathrm{frontal}} = \beta_0 + \beta_1 + \beta_2 + \beta_3 + \beta_4 x_4 + \beta_5 x_5 + \beta_6 x_6$$
$$Z_{\mathrm{side}} = \beta_0 + \beta_1 + \beta_2 + \beta_3 x_3 + \beta_4 x_4 + \beta_5 x_5$$

$\beta_j$: regression coefficients, $x_j$: parameter values

$j$ for frontal crashes
0: intercept, 1: airbag, 2: seat-belt, 3: vehicle type, 4: driver stature, 5: collision velocity, 6: collision angle

$j$ for side impact crashes
0: intercept, 1: seat-belt, 2: vehicle type, 3: seat height, 4: driver stature, 5: collision velocity

### Algorithms for Head, Thorax, and Thigh Injury

Generally, in vehicle safety performance evaluations, injury threshold of AIS 3+ was used for head and thorax, while AIS 2+ was used for thigh [13]. In this study, the algorithms for head and thorax AIS 3+ injuries, and for lower limb AIS 2+ injury were developed through the logistic regression analysis.

Table 4 shows the regression coefficients, chi-square value, significance level, and Nagelkerke's coefficient for each prediction algorithm. The injury prediction algorithms showed high goodness-of-fit. The regression coefficients were different among body segments, which means that injury probability has different correlations with the crash parameters according to the body segments. In frontal crashes, $\beta_1$ for without airbag deployment was positive and negative for head and thorax respectively, which indicates that airbag was effective to reduce risk of head injury but not for thoracic injury. These correlations were supported by reported injury mechanisms, indicating that the crash simulation models were appropriate to build a virtual accident database.

**Table 4.**
**Coefficients of the injury prediction algorithms**

(i) Frontal crash

| | | Head (AIS3+) | Thorax (AIS3+) | Thigh (AIS2+) |
|---|---|---|---|---|
| $\beta_1$ | on: 1 | 0 | 0 | 0 |
| | off: 0 | 0.069 | -0.027 | 0.173 |
| $\beta_2$ | on: 1 | 0 | 0 | 0 |
| | off: 0 | 1.241 | 1.502 | 5.026 |
| $\beta_3$ | 3 | 0 | 0 | 0 |
| | 2 | -0.776 | -1.137 | -0.883 |
| | 1 | -0.425 | -0.604 | -0.630 |
| $\beta_4$ | | 4.709 | 0.798 | 7.009 |
| $\beta_5$ | | 0.123 | 0.124 | 0.102 |
| $\beta_6$ | | -0.006 | -0.002 | 0.006 |
| $\beta_0$ | | -14.429 | -5.473 | -24.659 |
| $\chi^2$ | | 312.730 | 322.839 | 253.157 |
| $p$ | | <0.001 | <0.001 | <0.001 |
| Nagelkerke $R^2$ | | 0.646 | 0.672 | 0.664 |

(ii) Side impact crash

| | | Head (AIS 3+) | Thorax (AIS 3+) |
|---|---|---|---|
| $\beta_1$ | on: 1 | 0 | 0 |
| | off: 0 | 4.075 | -3.619 |
| $\beta_2$ | 1 | 5.537 | 7.165 |
| | 2 | 4.836 | 6.567 |
| | 3 | 0 | 0 |
| $\beta_3$ | | 0.022 | -0.015 |
| $\beta_4$ | | 4.998 | -10.237 |
| $\beta_5$ | | 0.245 | 0.298 |
| $\beta_0$ | | -29.713 | -5.974 |
| $\chi^2$ | | 252.490 | 231.906 |
| $p$ | | <0.001 | <0.001 |
| Nagelkerke $R^2$ | | 0.826 | 0.869 |

## PREDICTION ACCURACY

Accuracy of each algorithm was evaluated by comparing the prediction results to field accident data. Micro data collected in Japan and USA were used for frontal and side impact crashes respectively.

### Real World Accident Data

**Frontal Crash** From accident analysis reports [14][15], 14 car-to-car accidents (28 cases) including two crash test data reconstructing real world accidents and 12 real world accident data were selected. Table 5(i) shows the detail of each case including crash parameters and injury severity of the driver. Equivalent Barrier Speed (EBS) was adopted as collision velocity during the injury prediction. In the reference [15], driver statures were not mentioned, therefore male and female driver were uniformly assumed to be similar to 50th percentile and 5th percentile Japanese male occupant model respectively.

**Side Impact Crash** From the CIREN database [16], 20 accidents were selected. Since light vehicle is common only in Japan, this vehicle type was excluded during the accuracy evaluation. Table 5(ii) shows the detail of each case. Seat heights, which were not informed in the database, were assumed as the lowest value, 255 mm. Collision velocities were assumed as the velocity difference between struck and striking vehicles, and were calculated by Equation 2. Vehicle stiffness for striking and struck vehicle were apparent stiffness of Moving Deformable Barrier and the subject vehicle respectively. These values were estimated from the JNCAP test results.

$$V_{\mathrm{B}} = \sqrt{\frac{k_2}{k_1 + k_2}\frac{m_2}{m_1 + m_2}}\,|V_1 - V_2| \qquad (2)$$

$V_{\mathrm{B}}$: EBS, $V_i$: vehicle velocity
$k_i$: vehicle stiffness, $m_i$: vehicle mass,
$i$ =1: struck vehicle, 2: striking vehicle

### Predicting Injuries in Real World Accidents

Probabilities of injury occurrence in the accidents were calculated by substituting the values of crash parameters into Equation 1, and then compared with the actual injury circumstances. In this study, the threshold for injury was assumed to be 50% of probability. When $P_{\mathrm{AIS3+}}$ for an AIS 3 injury was predicted as over 50% of probability, the prediction was correct. Moreover, the prediction was also correct when $P_{\mathrm{AIS3+}}$ for an AIS 1 injury was predicted as less than 50% of probability.

**Frontal Crash** Severe injuries in the 28 cases of frontal crashes were predicted as shown in Table 5(i). The agreement ratios for head, thorax and thigh injuries were 85, 50 and 71% respectively.
$P_{\mathrm{AIS3+}}$ for head injuries were less than 50% except for four cases. This trend matched with the actual injury circumstances where severe injuries did not occur.

**Table 5.**
**Predicted AIS 3+ probability and accident data (wrong predictions are marked: over, under-estimated.)**

(i) Frontal

| Case | Vehicle | Seat -belt | Air -bag | height [m] | EBS [km/h] | Head AIS | Head $P_{AIS3+}$ | Thorax AIS | Thorax $P_{AIS3+}$ | Thigh AIS | Thigh $P_{AIS2+}$ |
|---|---|---|---|---|---|---|---|---|---|---|---|
| Test 1 | V1: minivan | on | off | 1.42 | 35 | 0 | 2.3 | 1 | 35.0 | 0 | 0.00 |
| | V2: light | on | on | 1.63 | 40 | 0 | 6.7 | 0 | 41.1 | 3 | 0.00 |
| No.36 | V1: compact | on | on | 1.73 | 60 | 0 | 60.9 | 0 | 90.5 | 3 | 0.06 |
| | V2: compact | on | on | 1.60 | 60 | 0 | 45.7 | 0 | 89.5 | 3 | 0.02 |
| No.40 | V1: light | off | on | 1.70 | 40 | 0 | 44.9 | 3 | 91.4 | 2 | 2.42 |
| | V2: light | on | on | 1.47 | 25 | 0 | 1.2 | 3 | 23.5 | 1 | 0.00 |
| Test 2 | V1: light | on | on | 1.62 | 45 | 1 | 21.0 | 0 | 79.9 | 1 | 0.02 |
| | V2: compact | on | on | 1.70 | 40 | 0 | 13.4 | 1 | 56.5 | 0 | 0.01 |
| No.41 | V1: light | on | off | 1.58 | 25 | 0 | 2.0 | 0 | 23.9 | 0 | 0.00 |
| | V2: light | on | off | 1.58 | 25 | 0 | 2.0 | 1 | 23.9 | 0 | 0.00 |
| No.42 | V1: light | on | off | 1.71 | 20 | 0 | 1.9 | - | 15.7 | - | 0.00 |
| | V2: light | on | off | 1.71 | 20 | 0 | 1.9 | 0 | 15.7 | 0 | 0.00 |
| No.43 | V1: light | on | on | 1.58 | 65 | 0 | 74.4 | 0 | 98.0 | 3 | 0.09 |
| | V2: light | on | on | 1.58 | 40 | 0 | 10.6 | 3 | 67.4 | 1 | 0.01 |
| No.47 | V1: light | on | on | 1.58 | 35 | 0 | 5.5 | 1 | 51.8 | 0 | 0.01 |
| | V2: minivan | off | off | 1.71 | 35 | 0 | 26.8 | 1 | 76.1 | 2 | 0.93 |
| No.50 | V1: light | on | on | 1.71 | 65 | 0 | 84.5 | 4 | 98.2 | 3 | 0.23 |
| | V2: compact | on | on | 1.58 | 45 | - | 10.2 | 0 | 56.2 | - | 0.00 |
| No.51 | V1: compact | on | on | 1.58 | 30 | 1 | 1.8 | 1 | 16.7 | 0 | 0.00 |
| | V2: compact | on | on | 1.71 | 30 | 0 | 3.3 | 1 | 18.2 | 1 | 0.00 |
| No.52 | V1: compact | off | on | 1.71 | 45 | 0 | 42.6 | 1 | 86.5 | 3 | 1.85 |
| | V2: minivan | off | on | 1.71 | 50 | 0 | 66.1 | 1 | 95.3 | 0 | 3.88 |
| No.53 | V1: compact | on | on | 1.71 | 40 | 0 | 9.1 | 1 | 42.3 | 0 | 0.01 |
| | V2: minivan | on | on | 1.58 | 35 | 0 | 3.9 | 1 | 37.6 | 1 | 0.00 |
| No.54 | V1: compact | off | on | 1.71 | 45 | 1 | 47.1 | 1 | 87.2 | 1 | 1.55 |
| | V2: minivan | off | on | 1.71 | 40 | 1 | 29.7 | 1 | 84.2 | 1 | 1.93 |
| No.55 | V1: minivan | on | off | 1.71 | 35 | 0 | 8.4 | 1 | 40.4 | 0 | 0.01 |
| | V2: minivan | off | off | 1.71 | 35 | 1 | 24.1 | 0 | 75.2 | 0 | 1.07 |

(ii) Side impact

| Case ID | Vehicle type | Seat belt | Seat [mm] | Driver [m] | EBS [km/h] | Head AIS | Head $P_{AIS3+}$ | Thorax AIS | Thorax $P_{AIS3+}$ |
|---|---|---|---|---|---|---|---|---|---|
| 39868 | 2 | 1 | 255 | 1.57 | 26 | 0 | 95.6 | 5 | 16.0 |
| 31170 | 2 | 1 | 255 | 1.63 | 71 | 3 | 100.0 | 5 | 100.0 |
| 31159 | 3 | 1 | 255 | 1.65 | 84 | 5 | 100.0 | 3 | 100.0 |
| 32031 | 2 | 1 | 255 | 1.52 | 33 | 4 | 99.9 | 5 | 97.3 |
| 32297 | 2 | 1 | 255 | 1.57 | 19 | 0 | 30.6 | 4 | 0.2 |
| 49229 | 2 | 1 | 255 | 1.59 | 36 | 1 | 100.0 | 1 | 99.3 |
| 77797 | 2 | 1 | 255 | 1.57 | 34 | 4 | 99.9 | 3 | 97.7 |
| 91657 | 2 | 1 | 255 | 1.83 | 19 | 0 | 61.7 | 4 | 0.0 |
| 470047388 | 2 | 1 | 255 | 1.80 | 44 | 5 | 100.0 | 4 | 100.0 |
| 426041219 | 2 | 0 | 255 | 1.65 | 53 | 4 | 100.0 | 4 | 100.0 |
| 160113410 | 2 | 1 | 255 | 1.6 | 38 | 5 | 100.0 | 3 | 99.8 |
| 558007067 | 2 | 1 | 255 | 1.68 | 12 | 0 | 1.5 | 2 | 0.0 |
| 558018108 | 2 | 1 | 255 | 1.68 | 56 | 4 | 100.0 | 4 | 100.0 |
| 558021392 | 2 | 1 | 255 | 1.75 | 27 | 2 | 98.9 | 0 | 5.6 |
| 375026608 | 3 | 1 | 255 | 1.50 | 26 | 1 | 58.4 | 0 | 1.1 |
| 551060741 | 2 | 0 | 255 | 1.63 | 15 | 5 | 79.0 | 0 | 0.0 |
| 782006238 | 2 | 1 | 255 | 1.63 | 40 | 2 | 100.0 | 3 | 99.9 |
| 832075614 | 2 | 1 | 255 | 1.70 | 31 | 4 | 99.9 | 0 | 59.9 |
| 851113011 | 2 | 1 | 255 | 1.60 | 42 | 2 | 100.0 | 1 | 100.0 |
| 852114778 | 3 | 0 | 255 | 1.70 | 19 | 0 | 70.1 | 0 | 0.0 |

Two uninjury cases, vehicle 1 in case No.50 and No.43, which have highest collision velocity of 65 km/h, were over estimated.

Three out of four AIS 3+ thoracic injuries were correctly predicted. The algorithm was more likely to predict injuries severer than actuals, thus 13 cases were over estimated. The over estimated cases included minor injuries in vehicle 2 of case No.52 and No.54 in spite of non-seatbelted, and minor injury in vehicle 1 of case No.36 in spite of high collision velocity. Furthermore, the driver of the under estimated case, vehicle 2 of case No.40, was 58 years old elderly occupant.

$P_{AIS2+}$ for thigh injuries were less than 5%, and all of eight AIS 2+ injuries were under estimated. Especially, severe injuries in high velocity accidents including vehicle 1 of case No.43 and No.50, and both vehicles of case No.36 were miss predicted as minor injuries.

**Side Impact Crash** Severe injuries in the 20 cases of near-side impact crashes were predicted as shown in Table 5(ii). The agreement ratios for head and thoracic injuries were 60 and 70% respectively.

All of ten AIS 3+ head injuries were correctly predicted, while eight minor injuries were wrongly predicted as severe (over estimated). These minor injury cases were peculiar, since their collision velocities were not as high as in the severe injury cases.

Thoracic injuries of 14 cases were correctly predicted. In the three over-estimated cases, minor injuries occurred in spite of high collision velocities. On the other hand, in the three under-estimated cases, all of the occupants were over 59 years old.

## DISCUSSIONS

The agreement ratios of the injury prediction algorithms against real world accidents were in comparable to the URGENCY Algorithm, whose agreement ratio against 30 frontal crashes was reported to be 70% [2]. Furthermore, the algorithms could predict head and thigh injuries well, indicating that the development method of the algorithms using computer models can be an alternative to the present way using statistical analysis of real world accident database, though more accident cases were required for further evaluation.

Over estimations of minor head injuries in frontal crashes occurred in particular cases of high collision velocity and light vehicle. To overcome this problem, more accurate geometry and contact stiffness of cabin model is required in correspondence with vehicle type. In side impact crashes, over estimations also occurred, though the accident cases were not peculiar. Disregard of deformation and break of door window might cause this miss predictions. In the side impact tests, the door window leaned outward and broke, so the occupant head did not receive significant impact.

Thoracic injuries in frontal crashes were predicted severer than actuals. It could be caused by the condition that the seat-belt and airbag models did not adequately protect occupant models. Despite this fact, several under estimations occurred in cases of elderly occupants. Age and gender affect on injury tolerance, especially on thoracic injury [17][18]. To consider it in the simulation models is difficult because of the huge individual variations. A realistic approach was extracting the effects by statistical analysis of real world accident database, and then introducing it into the algorithm [19]. Furthermore, the occupant model did not consider chest deflection, which strongly relates to thoracic injury as reported by another [20]studies.

Thigh injuries in frontal crashes were predicted less severe than actuals. Disregard of interior panel intrusion might cause this result. In the accident analysis reports [14][15], deformation of interior panels was regarded as dominant cause of injuries. In high velocity frontal crash, the effect become more significant, and may cause under estimation in injury prediction.

## CONCLUSIONS

This study suggested a method to develop injury prediction algorithms by statistical analysis of results of hundreds numerical crash reconstructions using multi-body models of occupants and vehicle cabin.

The conclusions obtained from this study were as follows.

- Injury prediction algorithms for AIS 3+ or AIS 2+ injuries of head, thorax and thigh have comparable accuracy to the URGENCY Algorithm.
- Numerical crash simulation was a good alternative to develop reliable injury prediction algorithms for frontal and side impact crashes.
- For improving the accuracy of the algorithms, cabin deformation, age effects, and chest deflection are required to be considered, and the geometry and the properties of the cabin models, especially the restraint system are need to be validated more precisely.

## ACKNOWLEDGMENTS

The authors appreciated National Agency for Automotive Safety and Victim's Aid (NASVA) for providing the JNCAP data, and Takata Foundation for its support.
This study was a project under supervision of Exploratory Committee on Traffic Injury Prediction and Preventive Medical Care, which was established under Committee on Future Traffic Safety of the Japan Society of Automotive Engineers (JSAE).

## REFERENCES

[1] Tokyo Metropolitan Police Department. 2012. "General Status of Traffic Accidents in 2011."

[2] Augenstein, J. et al. 2001. "Development and Validation of the Urgency Algorithm to Predict Compelling Injuries." In Proceedings of the 17th ESV Conference, Paper No. 352.

[3] Miyazaki, Y. et al. 2008. "Influence of Individual Differences of Occupant Body or Head Shape on Brain Responses in Car Accidents Using Individual Digital Human Models." Transactions of the Japan Society of Mechanical Engineers, Series C, No.74, Vol.741, pp.1238-1245.

[4] Ma, D. et al. 1995. "Development of Human Articulating Joint Model Parameters for Crash Dynamics Simulations." SAE paper 952726.

[5] Miyazaki, Y. et al. 2011. "Development of Occupant Injury Prediction Method Based on Frontal Collision Accident Simulation using Multi-Body Model." Transactions of the Society of Automotive Engineers of Japan, Vol.42, No.1, pp.73-78.

[6] Ono, K. et al. 2007. "Biomechanical Response of Head/Neck/Torso and Cervical Vertebral Motion to Lateral Impact Loading on the Shoulders of Volunteers." In Proceedings of 20th ESV Conference, Paper No. 07-0294.

[7] Miyazaki, Y. et al. 2011. "Injury Prediction of Automobile Occupants in Side Impact using Multibody Simulation." Transactions of the Society of Automotive Engineers of Japan, Vol.42, No.2, pp.349-354.

[8] Johannsen, H. et al. 2007. "Review of the Development of the ISO Side Impact Test Procedure for Child Restraint Systems." In Proceedings of 20th ESV Conference, Paper No. 07-0241.

[9] Kent, RW. et al. 2000. "Structural Stiffness, Elastic Recovery, and Occupant Inertial Effects on Measured Door Response in a Laterally Struck Vehicle." International Journal of Crashworthiness, Vol. 5, pp. 235-248.

[10] National Highway Traffic Safety Administration (NHTSA). 1997. "Actions to Reduce the Adverse Effects of Air Bags FMVSS No. 208: II. Injury Risk Curves and Protection Reference Value." http://www.nhtsa.gov/cars/rules/rulings/80g/80g.html (accessed 2010-05-17).

[11] Eppinger, R. et al. 2000. "Development of Improved Injury Criteria for the Assessment of Advanced Automotive Restraint Systems – II." NHTSA.

[12] Kuppa, S. et al. 2001. "Lower Extremity Injuries and Associated Injury Criteria." In Proceedings of the 17th ESV Conference, Paper No. 457.

[13] Sohr, S. 2009. "Benefit of Adaptive Occupant Restraint Systems with Focus on the New US-NCAP Rating Requirements." In Proceeding of the 21st ESV Conference, Paper No. 09-0322.

[14] Institute for Traffic Accident Research and Data Analysis (ITARDA). 2007. "A Report on the Investigation Results of Vehicle Safety Measures based on Analytical Survey of Traffic Accidents in 2006. pp.27-152.

[15] Institute for Traffic Accident Research and Data Analysis (ITARDA). 2008. "A Report on the Investigation Results of Vehicle Safety Measures based on Analytical Survey of Traffic Accidents in 2007. pp.25-171.

[16] Crash Injury Research and Engineering Network (CIREN) Electronic Cases. http://nhtsanrdapps.nhtsa.dot.gov/bin/cirenfilter.dll (accessed 2010-07-29).

[17] Zhou, Q. et al. 1996. "Age Effects on Thoracic Injury Tolerance." In Proceeding of the 40th Stapp Car Crash Conference, Paper No. 962421.

[18] Kimpara, H. et al. 2003. "Biomechanical Properties of the Male and Female Chest Subjected to Frontal and Lateral Impacts." In Proceeding of the 2003 IRCOBI Conference, pp 235-247.

[19] Katagiri, M. et al. 2011. "Occupant Injury Prediction Based on Frontal Collision Accident Simulations Using a Human Model -Consideration of Age and Gender-." In Proceeding of 2011 JSAE Annual Congress, No.78-11, pp.15-18.

[20] Kroell, CK. et al. 1974. "Impact Tolerance and Response to the Human Throax II." In Proceeding of 18th Stapp Car Crash Conference, pp.383-457.

# PRELIMINARY EVALUATION OF NASS-CDS SIDE CRASH DELTA-V ESTIMATES USING EVENT DATA RECORDERS

**Nicholas S. Johnson**
**Hampton C. Gabler**
Virginia Polytechnic Institute and State University
United States of America
**Dinesh Sharma**
National Highway Traffic Safety Administration
United States of America
Paper Number 13-0240

## ABSTRACT

The severity of a planar crash is most commonly defined by the change in vehicle velocity, or delta-V (ΔV). In the National Automotive Sampling System – Crashworthiness Data System (NASS-CDS), ΔV is computed from post-crash vehicle damage using a CRASH3 – based computer program called WinSMASH. Prior studies have investigated the accuracy of NASS-CDS ΔV in real world frontal crashes. Those studies compared the WinSMASH ΔV estimates in NASS-CDS to the ΔV obtained from the crashed vehicles' Event Data Recorders (EDRs). In those studies, the EDRs only measured/recorded ΔV in the longitudinal direction. Accordingly, the accuracy of WinSMASH ΔV in side crashes has been assessed only through comparison with controlled crash tests, not real world crashes. Many newer vehicles are now equipped with EDRs that record both longitudinal and lateral ΔV. The objective of this study is to use these newer EDRs to compare WinSMASH ΔV estimations to EDR ΔVs for real-world side crashes in the NASS-CDS.

This preliminary study examines 22 side impact crashes from the NASS-CDS. All struck vehicles were cars and all striking vehicles were either cars or light trucks and vans (LTVs). EDR measurements of side impact ΔV were used to evaluate the accuracy of WinSMASH ΔV estimates for these real world side crashes. WinSMASH systematically overestimated ΔV for the examined crashes. Overestimation for crashes involving cars struck by cars appeared greater than for those involving cars struck by LTVs. Observed systematic ΔV error varied by the area of the vehicle which was impacted.

## INTRODUCTION

Planar crash severity is most commonly defined by delta-V (ΔV), which is the change in a vehicle's velocity vector during a crash. ΔV is the single best and most widely used correlate for occupant injury in automobile crashes (Gabauer and Gabler 2008). All ΔV estimates contained in the United States' (U.S.) National Automotive Sampling System – Crashworthiness Data System (NASS-CDS) are generated using a CRASH3-derived program called WinSMASH (Sharma et al. 2007; NHTSA 1981). The accuracy of WinSMASH ΔV estimates for real-world crashes have previously been examined by comparison with ΔV from Event Data Recorders (EDRs) of crashed vehicles (Hampton and Gabler 2010; Niehoff and Gabler 2006). Historically, most EDRs in the U.S. vehicle fleet have recorded only longitudinal ΔV as most U.S. vehicles have had only frontal air bags. Consequently, WinSMASH has been validated against real-world data for frontal crash reconstructions only. Prior validation for side-impact crashes has used only staged crash tests (Prasad 1987; Johnson 2011; Johnson, Hampton and Gabler 2009), which are not real world crashes. However, some EDRs from vehicles equipped with side air bags record biaxial (i.e. both longitudinal and lateral) ΔV. As side air bags have become more common in the U.S. fleet, it has become feasible to assess WinSMASH ΔV accuracy against real-world data for side crashes as has been done previously for frontal crashes.

## OBJECTIVE

This study will use biaxial ΔV data from newer EDRs to assess WinSMASH ΔV accuracy for real-world side crashes.

## METHODS

The NASS-CDS reconstructs crashed vehicle ΔV using WinSMASH whenever possible. Conveniently, it also obtains EDR data for these vehicles whenever possible with the consent of the vehicle owner. In this analysis, we selected single-event side impact crashes from the NASS-CDS for which a) WinSMASH ΔV had been coded and b) biaxial EDR data was available. For these crashes, we compared the

WinSMASH-estimated resultant ΔV with the EDR-recorded resultant ΔV to assess the accuracy of WinSMASH. Although crashes can involve multiple events, only single-event crashes were used because this eliminates any ambiguity as to which impact the EDR data corresponds to. Additionally, only EDRs from crashes where the air bags actually deployed were used. Air bag deployment prevents the crash record from being overwritten with data from subsequent events which may not be the event of interest.

We also used this biaxial EDR data to assess the accuracy of NASS-CDS estimates of Principal Direction of Force. Principal Direction of Force, or PDOF, is the orientation of the net crash impulse relative to the vehicle and is a key parameter in WinSMASH reconstructions. In the NASS-CDS, PDOF is visually estimated by crash investigators using various observations such as the vehicle deformation pattern and collision trajectories. Having both longitudinal and lateral ΔV from an EDR allows for computation of the actual PDOF in a crash, to which the NASS estimates can be compared.

**Extraction of Resultant ΔV, PDOF from EDRs**

Biaxial EDRs sense both longitudinal and lateral accelerations during a crash and process them to obtain longitudinal and lateral ΔV histories. Acceleration from each axis is measured and processed separately to obtain the ΔV history for that axis. In this analysis, we examined the maximum resultant EDR ΔV. To obtain this, resultant ΔV was first calculated at each time increment in the record using the longitudinal and lateral ΔV. The maximum of these resultant ΔVs was used as the resultant EDR ΔV for that crash. PDOF was then calculated as the arctangent of the longitudinal and lateral components of this ΔV.

Many older EDRs record only about 70 – 80 ms of ΔV data after the recording algorithm is triggered, which is shorter than most crash pulses. Because of this, older EDRs sometimes underestimate actual ΔV (Niehoff and Gabler 2006). However, newer biaxial EDRs typically record 200 – 300 ms of crash data, with some portion of that being pre-algorithm-trigger. Newer EDRs thus typically record the entire crash pulse. In this analysis, any records with resultant acceleration greater than 1 g between the last and second-to-last time steps were manually inspected for completeness, regardless of record duration. Most EDRs do not record acceleration, but only measure it to compute ΔV. Consequently, acceleration was calculated from the change in resultant ΔV between the final and penultimate data points.

**Comparison of WinSMASH ΔV and PDOF to Values Obtained from EDRs**

For each case examined, we compared 1) the WinSMASH-estimated resultant ΔV to the resultant EDR ΔV, and 2) the investigator's estimate of PDOF to the EDR-derived PDOF. We also examined WinSMASH ΔV and PDOF estimate accuracy with respect to a number of other parameters, such as vehicle bodystyle and area of the vehicle struck, to determine whether there was any correlation. WinSMASH was never intended to be a forensic reconstruction tool, but rather a standard benchmark that is accurate on average. The magnitude of the ΔV error in individual reconstructions is therefore of less importance than the *systematic* error over many cases. For ΔV, systematic error was computed as the slope of a linear regression of WinSMASH ΔV versus actual ΔV with the intercept fixed at zero. On a cross-plot of estimated ΔV versus actual ΔV, the amount by which the slope of such a regression deviates from unity gives an indication of the amount of systematic error in the estimated values (e.g. a slope of 1.050 would indicate a 5% overestimation).

Statistical testing was performed using SAS v9.2 (SAS; Cary, NC, United States). The NASS-CDS uses a stratified, clustered and weighted sample design allowing for nationally representative estimates to be made from the data. However, no attempt was made in this study to perform statistical testing using the NASS weights, as the sample size was insufficient. Therefore, this analysis is only representative of the population of crashes recorded in the NASS-CDS, and is not representative of all U.S. crashes nationally.

**Sample Summary**

**Table 1.**
**Data Set Composition**

| | |
|---|---|
| **Total Crashes:** | **22** |
| Struck Vehicle Make: | |
| *Ford* | 1 |
| *General Motors* | 21 |
| Struck Vehicle Bodystyle: | |
| *Cars* | 22 |
| Striking Vehicle Bodystyle: | |
| *Cars* | 8 |
| *LTVs* | 14 |

Table 1 gives a summary of the final dataset used in this analysis. The dataset consists of 22 single-impact crashes coded in the NASS-CDS (case years 2006 – 2010) for which both WinSMASH ΔV and biaxial EDR data (locked, air bag-deployment events) were available. Only crashes where cars were struck in the side by another vehicle were retained for this analysis. Struck-LTV crashes (2 cases: 2010-12-154 and 2010-49-65) and crashes involving fixed objects (1 case: 2006-50-46) were not available in sufficient numbers for a meaningful analysis of those crash configurations, so were excluded. Side impacts were identified by the General Area of Damage (GAD) coded in NASS. GAD is defined as part of the Collision Deformation Classification (CDC) code (SAE 1980); all cases in the sample have a GAD of "L" or "R" which stands for left or right side of the vehicle, respectively.

One case – NASS case 2007-80-045 – was excluded from the final sample for having an incomplete ΔV record. The EDR in this case came from a 1990 Honda Prelude and recorded only a 78 ms window of ΔV. Additionally, this EDR was unusual in that it provided a record of acceleration in addition to a record of ΔV. The recorded acceleration clearly indicated that the crash was not complete by the end of the recording. All other examined cases reported either 220 ms or 250 ms of ΔV data with some amount of that being pre-trigger ΔV, so pulse truncation is unlikely in the retained sample.

## RESULTS

### WinSMASH ΔV Accuracy

Figure 1 compares WinSMASH-estimated ΔV to EDR-measured ΔV for the dataset. WinSMASH appears to systematically over-predict ΔV in the examined side crashes by about 3.5%. Random error (RMS error about the regression line) is about 5.5 km/h. There was insufficient evidence to reject the assumption of normally distributed data; a paired t-test did not indicate that the ΔV over-prediction was significant (p=0.1360, PROC TTEST). This is due at least in part to the small sample size.

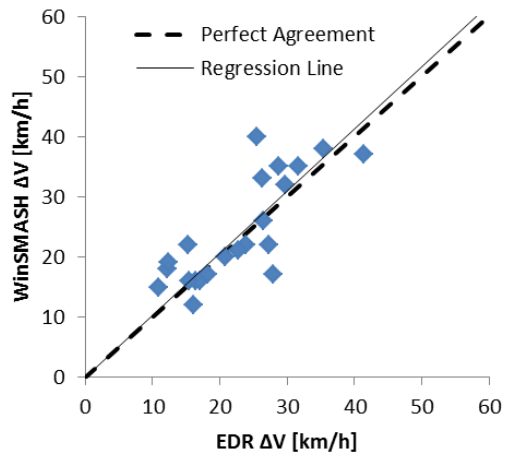


*Figure 1.* WinSMASH ΔV vs. EDR ΔV. Regression equation: y = 1.0347x. $RMS_{err}$ about regression line: 5.490 km/h.

### Effect of Striking Vehicle Body Type

Figure 2 and Figure 3 compare WinSMASH ΔV to EDR ΔV for cars struck by cars and cars struck by LTVs respectively. Cars are defined as NASS body type codes 1 – 11, 13 and 17 while LTVs are codes 14 – 16, 19 – 22, 30 – 33, 39 – 42 and 45. All vehicles in the sample fell into one of these two categories. WinSMASH ΔV for cars struck by other cars appears to be systematically higher than EDR ΔV by about 8.2%. For cars struck by LTVs, WinSMASH appears to have no systematic error. Observed random error was higher for striking LTVs than for striking cars (6.17 km/h vs. 4.09 km/h RMS error), but then there were more striking LTVs in the sample. The assumption of normally distributed data could not be rejected for either striking body type. An independent sample t-test did not find the difference in WinSMASH ΔV error between striking body types to be statistically significant (p=0.4434, equal sample variances, PROC TTEST).

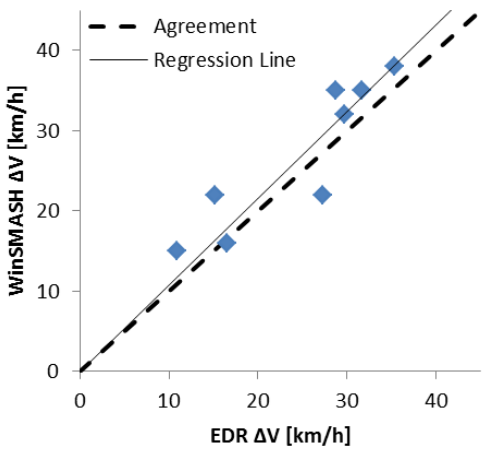


*Figure 2.* WinSMASH ΔV vs. EDR ΔV for cars struck by cars. Regression equation: y = 1.0824x. $RMS_{err}$: 4.090 km/h.

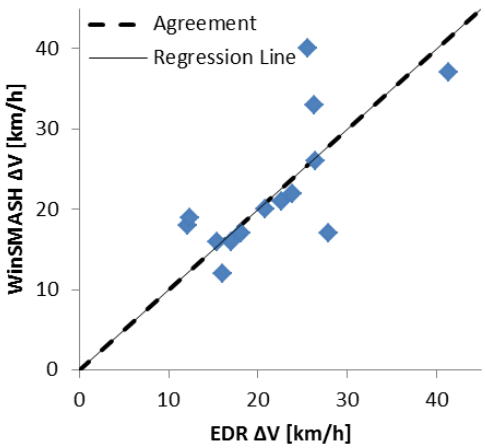


*Figure 3.* WinSMASH ΔV vs. EDR ΔV for cars struck by LTVs. Regression equation: y = 1.0006x. $RMS_{err}$: 6.170 km/h.

**Effect of Impacted Vehicle Region**

Figure 4 shows the Specific Horizontal Location (SHL) codes defined by the CDC standard (SAE 1980) and used by NASS-CDS to describe the particular horizontal area of the vehicle which was damaged in an impact. Figure 5 shows WinSMASH ΔV error broken down by SHL. WinSMASH appears to underestimate ΔV for crashes involving damage to F, while P and especially D appear to be overestimated. Note that the sample contained no B impacts. One-way ANOVA indicates that the mean errors for each SHL are not universally equal (p = 0.0079, PROC GLM).

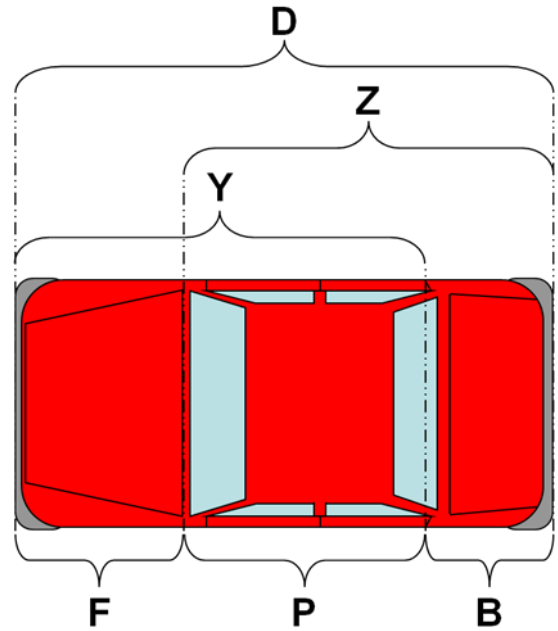


*Figure 4.* Specific Horizontal Location (SHL) codes defined by SAE standard J224 and used in NASS-CDS.

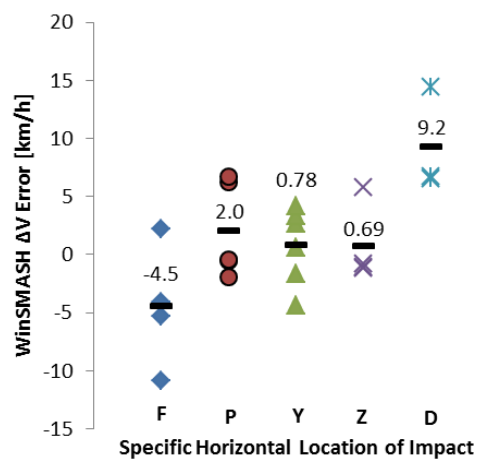


*Figure 5.* WinSMASH ΔV error vs. SHL of impact. Black bars indicate the mean ΔV error for each SHL value.

**Effects of WinSMASH Calculation Type**

WinSMASH can perform different types of reconstruction calculations depending upon what information is available for a case. The type of reconstruction performed for a case is coded by the DVBASIS variable in NASS-CDS. "Standard" and "Missing Vehicle" reconstructions (Sharma et al.

2007) are represented in the cases studied here. Figure 6 shows a small difference in ΔV error between Standard and Missing Vehicle reconstructions, but one-way ANOVA found it to be insignificant. Note that there were only 3 cases of the Missing Vehicle type.

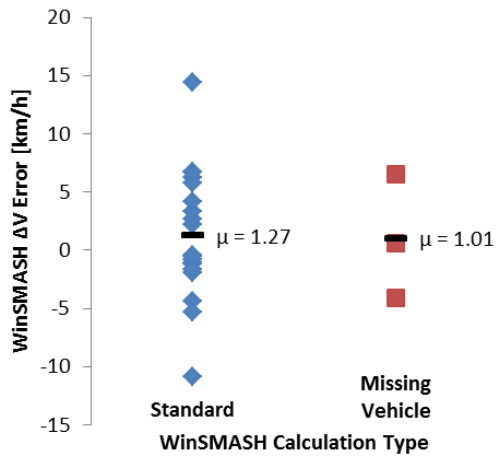


*Figure 6.* WinSMASH ΔV error vs. WinSMASH calculation type. Black bars indicate the mean ΔV error for each calculation type.

**Investigator PDOF Accuracy**

Figure 7 shows discrepancy in NASS investigator estimates of PDOF with respect to the PDOF computed from EDR data. Mean PDOF discrepancy was -4.5 °; this was not found to be significantly different from zero (p=0.1584, paired-sample t-test, normality not rejected for the sample). Also, note that NASS only codes PDOF to the nearest 10 °. Smith and Noga (1982) gave 95% confidence limits on the accuracy of field-recorded PDOF as ±20 °. Observed standard deviation in PDOF discrepancy here was 14.5 ° which equates to 95% confidence limits of ±28.3° assuming normally distributed error (1.96*standard deviation).

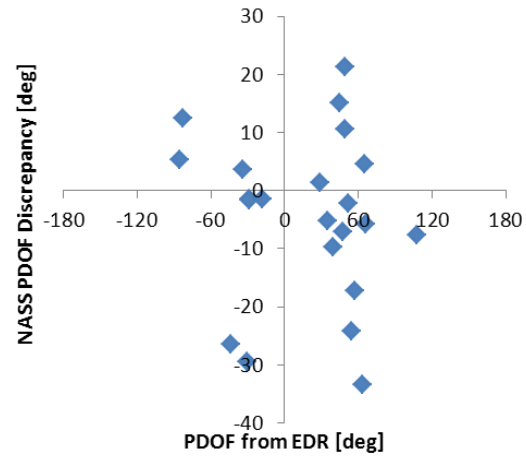


*Figure 7.* Discrepancy in NASS PDOF vs. EDR-derived PDOF. Mean NASS PDOF discrepancy: -4.515 °. Positive values are clockwise from the front of the vehicle when viewed from overhead, negative values are counterclockwise.

**Effect of PDOF Discrepancy on WinSMASH ΔV Accuracy**

Figure 8 shows a cross plot of WinSMASH ΔV error magnitude against PDOF discrepancy magnitude. There appears to be no correlation between PDOF discrepancy and WinSMASH ΔV error; the miniscule $R^2$ value for the regression ($R^2 < 0.0001$) indicates that it predicts virtually none of the observed variance in the data.

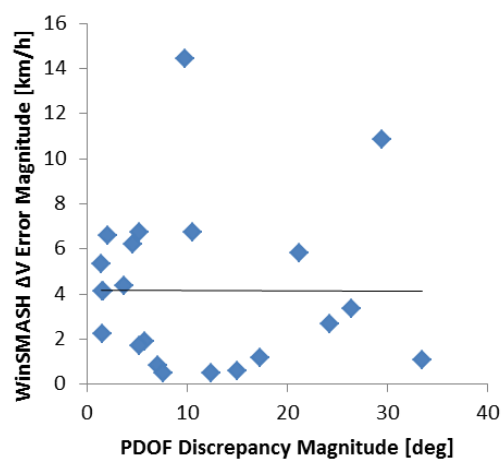


*Figure 8.* WinSMASH ΔV error magnitude vs. PDOF discrepancy magnitude. Regression equation: $y = -0.0021x + 4.1967$, $R^2 < 0.0001$.

## DISCUSSION

WinSMASH ΔV estimates do not include the effects of restitution, but EDR measurements of ΔV do. Hence, if WinSMASH were reconstructing collisions accurately it would systematically underestimate the ΔV given by EDRs, probably by about 10% on average (Ishikawa 1994, Johnson and Gabler 2011).

Figure 1, Figure 2 and Figure 3 all show that WinSMASH *over*estimates EDR ΔV by about 8% for cars struck by cars, and shows no overestimation (and no underestimation) for cars struck by LTVs. Johnson and Gabler (2011) examined WinSMASH ΔV accuracy for NHTSA side crash tests. In that analysis, test instrumentation made it possible to determine when restitution began and to obtain the vehicle's actual ΔV up to that point. That study found that for NHTSA side crash tests, WinSMASH overestimated pre-restitution ΔV – the precise ΔV that WinSMASH models – by about 19% for struck cars. Nineteen percent overestimation minus about 10% ΔV gain from restitution gives 9% overestimation compared to the total ΔV including restitution. This aligns with the 8% overestimation observed here for cars struck by cars. Unfortunately, EDRs do not record sufficient data to determine pre-restitution ΔV. Thus, a direct comparison with pre-restitution ΔV equivalent to the Johnson and Gabler (2011) study was not possible here.

WinSMASH uses "vehicle stiffness" parameters to estimate the energy dissipated in crashes from measurements of residual vehicle damage. Different stiffness parameters are used for damage to the front, side and rear of individual vehicles. All side crash stiffnesses used by WinSMASH are derived from damage in NHTSA side crash tests. These stiffnesses may not represent crashes with damage to areas different from the tests from which they are derived, as vehicle side structure is not homogenous. NHTSA side impact tests are Y (SHL) impacts verging on P, so the observed underestimation of ΔV for F crashes (Figure 4, Figure 5) may be due to the stiffer vehicle structures in this region absorbing more energy for a given amount of crush than do the softer structures of the P region (passenger compartment). The geometry of the striking vehicle itself also influences which areas of the impacted vehicle are engaged. LTVs tend to be taller and wider than cars, and may or may not have greater ground clearance. Given collisions of otherwise identical configuration, striking LTVs can engage different or additional structures compared to striking cars. This could account for the differences between Figure 2 and Figure 3.

WinSMASH calculation type (Figure 6) does not appear to make any significant difference in the systematic ΔV error. However, only three cases used a reconstruction type other than Standard. A larger sample is necessary to draw any conclusions about the possible effects of calculation type.

### PDOF and ΔV

In our sample, NASS PDOF estimates for side crashes (Figure 7) showed relatively little systematic discrepancy with EDR-derived values. Average observed discrepancy was -4.5 °, which could indicate that NASS investigator PDOFs tend to be slightly counterclockwise from the real value on average. However, it is far more likely that this is simply an artifact of the small sample size. Additionally, NASS only codes PDOF to the nearest 10 °; the observed magnitude of systematic discrepancy is thus within the measurement precision for PDOF. EDR-derived estimates of PDOF are also known to have a root mean square error of 4.4 ° and to differ from values obtained from crash test instrumentation by as much as 10 ° (Kusano, Kusano and Gabler 2012).

Based on the observed standard deviation in PDOF discrepancy, 95% confidence limits for side crash NASS PDOF are ±28.3 °. This is roughly similar to the 95% confidence limits of ±20 ° quoted by Smith and Noga (1982) for field measurements of PDOF. The way in which Smith and Noga arrived at their estimate is somewhat different than the approach used here, and recall again that NASS PDOF estimates are only precise to the nearest 10 °.

Figure 8 shows that there is no correlation between the magnitude of PDOF error and the magnitude of WinSMASH ΔV error. In the WinSMASH calculations, the relationship between PDOF error and ΔV error depends on other parameters describing the crash configuration, so this is perhaps unsurprising. This also indicates that the effects of PDOF error are being washed out by some other sources of error.

### Limitations

EDR measurements do not account for the effects of rotation. This could potentially skew their ΔV measurements, but any such skew would not be systematic and it would probably not be very large in comparison to the measured ΔVs. EDRs are not generally mounted far from the vehicle center of gravity, which would tend to reduce the effects of

rotation on ΔV measurements. Also, typical rotation rates in NHTSA side crash tests are a relatively slow 90 °/s (Johnson 2011). The crashes in this sample are much less severe than the typical NHTSA side crash test, and most of them have SHL values which suggest crash impulse moment arms that are not any larger than those of side crash tests. It therefore seems logical that rotation rates in these crashes would tend to be lower than the already low values observed in NHTSA side crash tests. Additionally, EDR-derived PDOF estimates, which are computed from biaxial ΔV measurements, have been observed to have a root mean square error of only 4.4 ° (Kusano, Kusano and Gabler 2012).

The findings of this study are not nationally representative, but pertain only to the analysis sample. The limited sample size precludes the use of statistical techniques necessary to perform significance tests with clustered, stratified and weighted NASS-CDS data. Also, small sample size is a limitation in its own right. The small sample size examined here is a result of the limited number of NASS CDS crashes for which EDR data is available, compounded by the additional requirements for biaxial EDR data and a single-event crash. The NASS CDS has only collected EDR data since 2000 and at first, NASS investigators could only read EDRs from Ford and General Motors. This is reflected in the near-total proportion of General Motors vehicles in the dataset. While the lack of makes other than General Motors could be seen as a limitation, it is unlikely to have a significant effect. WinSMASH vehicle stiffness parameters are derived from tests of individual vehicles, so any characteristics particular to a given manufacturer are already accounted for. In any case, as more vehicles equipped with side air bags are added to the NASS-CDS, the available sample size will increase fairly quickly. NASS investigators can now read EDRs used by many vehicle manufacturers, so the number of represented makes and models will likely increase as well.

## CONCLUSIONS

WinSMASH appears to overestimate struck vehicle ΔV for cars in real-world side crashes. This overestimation appears to be greater in cases where the striking vehicle was a car than in cases where it was an LTV. However, this observation only applies when cars are the struck vehicle. The analysis did not examine crashes where the struck vehicle was an LTV, nor did it examine fixed-object crashes of any type. It seems likely that the side impact stiffness parameters used by WinSMASH do not represent crashes which differ substantially from NHTSA side impact crash tests.

NASS field estimates of PDOF do not appear to exhibit any systematic discrepancy. The amount of random PDOF discrepancy observed here is consistent with the findings of prior studies. PDOF discrepancy magnitude showed no correlation with WinSMASH ΔV magnitude, which indicates that its effect is being washed out by other sources of discrepancy.

## REFERENCES


Gabauer DJ and Gabler HC (2008), “Comparison of Roadside Crash Injury Metrics using Event Data Recorders,” *Accident Analysis and Prevention*, vol. 40, issue 2, pp 548-558.

Hampton CE and Gabler HC (2010), “Evaluation of the Accuracy of NASS/CDS Delta-V Estimates from the Enhanced WinSMASH Algorithm,” Proceedings of the 54th Annual AAAM Conference.

Ishikawa H (1994), “Impact Center and restitution Coefficients for Accident Reconstruction,” SAE 940564, Society of Automotive Engineers.

Johnson N (2011), “Assessment of Crash Energy – Based Side Impact Reconstruction Accuracy,” Master of Science thesis, Virginia Polytechnic Institute and State University, pp. 32.

Johnson N, Hampton CE and Gabler HC (2009), “Evaluation of the Accuracy of Side Impact Crash Test Reconstructions,” *Biomedical Sciences Instrumentation 45*: pp. 250-255.

Johnson N and Gabler HC (2011), “Accuracy of a Damage-Based Reconstruction Method in NHTSA Side Crash Tests,” Traffic Injury Prevention, 13:1, pp.72-80.

Kusano KD, Kusano SM and Gabler HC (2012), "Automated Crash Notification Algorithms: Evaluation of In-Vehicle Principal Direction of Force (PDOF) Estimations." *Transportation Research Part C*, DOI 10.1016/j.trc.2012.09.005 (published online 28-November 2012).

NHTSA (1981), *CRASH3 (Calspan Reconstruction of Accident Speeds on the Highway) User’s Guide and Technical Manual*, Accident Investigation Division, N.C.S.A., National Highway Traffic Safety Administration, report no. HS-805 732.

Niehoff P and Gabler HC (2006), “The Accuracy of WinSMASH Delta-V Estimates: The Influence of Vehicle Type, Stiffness, and Impact Mode,” Proceedings of the 50th Annual AAAM Conference.

Prasad AK (1987), “CRASH3 Damage Model Reformulation”, Department of Transportation Report No. VRTC-87-0053, Vol. I & II

SAE, “Collision Deformation Classification,” SAE Surface Vehicle Standard J224. Society of Automotive Engineers, Warrendale, PA, U.S.A. 1980.

Sharma D, Stern S, Brophy J, Choi E (2007), “An overview of NHTSA’s crash reconstruction software WinSMASH,” Proceedings of the 20th International Technical Conference on Enhanced Safety of Vehicles, paper no. 07-0211.

# DEVELOPMENT OF METHODOLOGY FOR ESTIMATING SAFETY BENEFITS OF AUTOMATIC CRASH NOTIFICATION SYSTEMS

**Eunbi Jeong, Ph.D Student**
**Cheol Oh, Ph.D.**
Hanyang University at Ansan
Republic of Korea
**Jaewan Lee, Ph.D.**
Korea Transportation Safety Authority
Republic of Korea
Paper Number 13-0280

## ABSTRACT

The automatic crash notification system (ACNS) is a well-known technology with promising potential to reduce the crash response time (CRT) of emergency medical services. Reducing CRT will contribute to saving the lives of and alleviating the severity of injuries for crash victims. To fully operate the ACNS, it is important to quantify the safety benefits, which is fundamental for justifying public investment. This study proposed a methodology for quantifying the effectiveness of the ACNS and applied the methodology to the Korean freeway system. The proposed methodology consists of three steps. Fist, a statistical model was developed to predict injury severity using ordered logistic regression. Second, the amount of reduced CRT that would result from the ACNS was estimated. The effectiveness of the ACNS, which are defined as the number of reduced fatalities and severe injuries, were derived after considering the market penetration rate (MPR). When the proposed methodology is applied to 2010 freeway crash data, the result that fatalities are reduced by 11.8-18.1% when there is a 100% MPR. The outcomes of this study support decision making for public investments and for establishing relevant traffic safety policies.

## INTRODUCTION

"Platinum minutes", "golden hours", and "silver day" are well-known terms that emphasize the importance of rapid medical response to save crash victims' lives *(1-3)*. The results of existing studies reveal significant improvements in life savings when the medical response time is reduced *(4-9)*. In the recent literature, Sanchez-Mangas et al. *(10)* demonstrated that a 10 min reduction of the medical response time could result in a decrease in the probability of death by a third. In accordance with these findings, engineers and traffic safety researchers have made substantial efforts to accurately detect crashes and to rapidly notify crash information to emergency medical services (EMS). Advancements in information technologies, including sensors and communications, allow engineers and researchers to develop more effective technological countermeasures. The automatic crash notification system (ACNS) is a promising technology for reducing EMS response time after crashes. Reducing the response time will contribute to saving crash victims and alleviating the severity of their injuries.

Significant efforts have been made in many countries to employ the ACNS. For example, the National Highway traffic Administration (NHTSA) conducted field operational tests, which have been discussed for future applications *(11)*. The European Commission (EU) has mandated that all new vehicles in Europe be equipped with the eCall system, which is an emergency call that notifies EMS and reduces the medical response time in traffic crash situations *(12)*. In addition to public agencies, academic and private sectors continue to improve the ACNS for increased reliability. Akella et al. *(13)* evaluated the reliability of ACNS by analyzing the received signal strength indicator (RSSI). Delmelle et al. *(14)* analyzed the strength of the received signal to develop a spatial regression tool that evaluates the effectiveness of ACNS technology. Bose et al. *(15)* presented a computational methodology for predicting the post-crash injury severity and relaying injury data to emergency medical services. A commercialized system in the private sector demonstrated the effectiveness of reducing injury severity with the ACNS *(16)*.

One of the important research challenges is to accurately estimate the effectiveness of the ACNS with regard to traffic safety. Reliable assessments of the safety benefits would be useful for establishing and applying policies that will disseminate ACNS technology to reduce injury severity of crash victims. In addition, estimations of the safety benefits are valuable for improving the functionalities of the system and for developing new technologies. These needs comprise the motivation for this study.

The purpose of this study is to estimate the effectiveness of the ACNS by quantifying the reduction in injury severity. The main focus of our study is freeway traffic crashes, as freeway crashes are associated with high fatality rates and severe injuries. Freeways are more dangerous primarily because of higher vehicle speeds than on other road types. Another reason to focus on freeway crashes is that traffic surveillance and management systems on Korean freeways provide reliable crash-related information, such as the crash occurrence time, incident duration, emergency vehicle arrival time, and post-incident management information etc.

This study defines the ACNS-related reduction in the number of fatalities and injuries as the safety benefit. To quantify the safety benefit, a methodology that consists of three steps is proposed. First, a statistical model with ordered logistic regression is developed to predict discrete injury outcomes, such as fatality, severe injury, and minor injury. A variety of variables that contribute to injury severity are employed in the model, including crash response time (CRT), which is defined as the time interval between crash occurrence and the arrival of EMS at the crash location. Second, the reduced CRT that is associated with the ACNS is estimated. The safety benefits of the ACNS are then derived after considering the market penetration rates (MPR).

This paper is organized as follows. In Section 2, an overview of ACNS functionality is provided, and the opportunity to save lives is discussed. The methodology proposed in this study is described in Section 3, and the model development for the application of the proposed methodology and data analyses are discussed in Section 4. This paper concludes by discussing the research results and suggesting future research needs.

## OVERVIEW OF ACNS FUNCTUINALITY AND AN OPPORTUNITY TO SAVE CRASH VICTIMS

The ACNS is an effective tool that integrates vehicular and communication technologies to enhance the potential for saving crash victims. The ACNS has two primary functionalities: crash detection and crash notification to EMS providers. A key element for fully operating these functions is an in-vehicle device that can accurately detect crashes and reliably transmit crash information to EMS providers. In addition, for the ACNS to be effective, operations are required to dispatch EMS vehicles to crash scenes. Figure 1 provides a conceptual illustration of the ACNS.

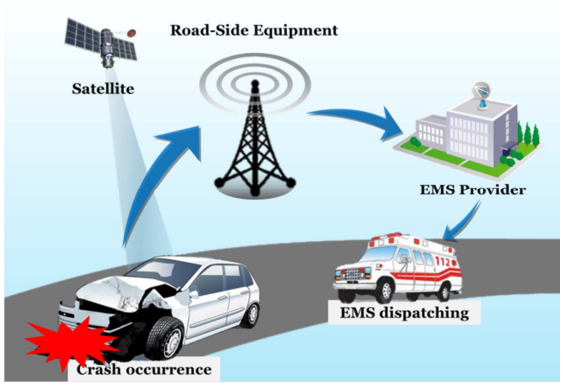


*Figure1*. ACNS framework

The ACNS saves crash victim lives by reducing CRT. Traffic management centers (TMCs) generally have specific crash management programs, including crash detection, crash verification, crash notification, and emergency dispatching. CRT consists of four time intervals between the crash detection time and the emergency dispatching time. Figure 2 compares CRTs 'with and without the ACNS'. When CRT is reduced with the ACNS, there will be a greater potential to save crash victim lives. Particularly, CNT can be reduced with the ACNS, which is shown in Figure 2. The reduction in CNT with the ACNS makes the safety benefit feasible.

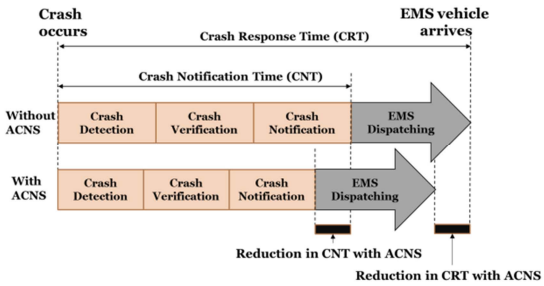


*Figure2*. Crash management process

Therefore, a key element for estimating the safety benefits is to obtain a reliable reduction in CNT ($\Delta$CNT). As was reported in the aforementioned literature, CRT is highly associated with injury severity, it is important to identify their relationship between CNT and CRT. Large reductions in CRT can lead to substantial safety benefits. Remaining problems include determining how to model the relationship between the probability of injury severity and CRT and estimating reduced CRT with the ACNS. Detailed descriptions of the proposed method are presented in the next section.

## METHODOLOGY

The methodology for quantifying the safety benefit involves estimating the number of crash victims

who will be saved or less injured with the ACNS. The proposed methodology consists of three steps. The first step is to identity the effects of various contributing factors on the injury severity of crash victims. A statistical modeling approach can be applied to derive a functional relationship between these factors and injury severity. Because the ACNS reduces CRT in the pre-hospital time after a crash occurs, CRT is an important independent variable in the model. An ordered logistic regression (OLR) is used for the modeling. Odds ratios for each independent variable can be used to estimate the percentage change in injury severity when a variable changes by one unit. In addition, the probabilities of injury severity can be calculated for with and without the ACNS. The second step is to estimate the average CRT 'with and without ACNS'. A functional form with components that impact CRT is constructed to estimate the average CRT. These components include the market penetration rate (MPR) and the reduction in CRT with the ACNS. A probability density function for CRT is derived and used for estimating a range of CRTs based on a given confidence interval. Next, the range of CRTs from Step 2 is applied to the injury severity prediction model in Step 1 to estimate the changes in the probabilities of injury severity in Step 3. Once we have the changes in injury severity, the total number of crash victims to who will be saved or less injured can be calculated. More detailed descriptions for each step are presented in the following subsections.

## [Step1] Identifying the Effect of CRT on Injury Severity

This study develops a statistical model that predicts injury severity of crash victims. The model is used to identify the effect of CRT on injury severity. Because crash injury severity is intrinsically ordered, the model must account for ordinal characteristics. For this reason, an ordered logistic regression technique is appropriate The ordered model can be specified as $y_i^* = \beta' x_i + \varepsilon_i$, where $y_i^*$ represents the injury severity of the crash victim and $x_i$ represents the independent variables that affect injury severity. These independent variables include vehicle characteristics, roadway geometric conditions, response activities to the crash, and environmental conditions. This study classifies injury severity into three levels: fatality, severe injury, and slight injury. Next, threshold values ($\mu$) are used to categorize the levels of severity as follows:

$$
\begin{aligned}
y_i(\text{severity}) &= 1,\ \text{'fatality'}, && \text{if } y^* \le \mu_1 \\
y_i(\text{severity}) &= 2,\ \text{'severe injury'}, && \text{if } y^* \le \mu_2 \\
y_i(\text{severity}) &= 3,\ \text{'slight injury'}, && \text{if } y^* \le \mu_3
\end{aligned}
$$

The maximum likelihood estimation method is used to calibrate the parameters:

$$
L(y|\beta;\ \mu_1, \mu_2, \mu_3) = \prod_{i=1}^{n} \prod_{j=1}^{3} \left[\gamma(\mu_j - \beta' x_i) - \gamma(\mu_{j-1} - \beta' x_i)\right]^{Z_{ij}},
$$

where

$\gamma_j$: cumulative probability,
$\gamma_j(x_i) = \gamma_j(\mu_j - \beta' x_i) = P(y_i \le j|x_i)$,
$\beta$: parameter to be calibrated, and
$Z_{ij} = 1$, if the observed category for the individual i is j, and 0 otherwise.

In addition, the probability that the injury severity y with the independent variable $x_k$ is less than j is estimated using Eq. (1). More detailed information on ordered logit models and the relevant derivations can be found in the literature *(17-18)*. The odds ratio for $x_k$, which is expressed as $e^{\beta_k}$, is used to quantify the changes in the probabilities of injury severity when $x_k$ changes by one unit. In this application, CRT becomes a key independent variable that affects the injury severity.

$$
\Pr(y \le j|x) = \frac{e^{\mu_j - \sum_{k=1}^{K} \beta_k x_k}}{1 + e^{\mu_j - \sum_{k=1}^{K} \beta_k x_k}} \qquad (1)
$$

## [Step2] Estimation of the Average Reduced Crash Response Time (CRT)

In this step, the average CRT is estimated with the assumption that the ACNS has been implemented with a given market penetration rate (MPR). Therefore, factors that affect the average CRT include the MPR and the reduction in CNT ($\Delta$CNT) with the ACNS. The average CRT with the ACNS and a given MPR is expressed in Eq. (2).

$$
\begin{aligned}
CRT_{ACINS} = &\left(CRT_{ACINS}^{No}\right)(1 - MPR_{ACINS}) + \\
&\left(CRT_{ACINS}^{No} - \Delta CNT\right)(MPR_{ACINS}) \qquad (2)
\end{aligned}
$$

where

$CRT_{ACNS}$: average reduced CRT (min) with the ACNS,
$CRT_{ACNS}^{No}$: observed CRT (min) from the existing freeway crash database without the ACNS,
$MPR_{ACNS}$: market penetration rate (%) of the ACNS, and
$\Delta$CNT: reduced CNT (min) with the ACNS (min)

The first term in Eq. (2) represents CRT for vehicles that are not equipped with an ACNS, and the second term represents CRT for ACNS-equipped vehicles. An important issue is to determine whether $CRT_{ACNS}^{No}$ and $\Delta$CNT in Eq. (2) are treated as parameters or constants in estimating

$CRT_{ACNS}$. In this study, $CRT_{ACNS}^{No}$ is regarded as a parameter that varies, as there are unknown factors that affect CRT in practice, including traffic conditions, the availability of EMS, and the crash severity. An approach for treating $CRT_{ACNS}^{No}$ as a parameter is to determine a statistically significant probability density function (PDF) with actual data from freeway crashes. Random sampling of $CRTs_{ACNS}^{No}$ from the derived PDF can then be repetitively conducted to generate a set of $CRTs_{ACNS}^{No}$, and the $CRTs_{ACNS}^{No}$ can be used to estimate $CRT_{ACNS}$. A set of MPRs is applied to estimate $CRT_{ACNS}$, because a 100% MPR is unlikely and would not be obtainable in a short time period. On the contrary, ΔCNT can be regarded as a constant, which depends on the technology; CNT varies less than CRT, as CRT depends on uncontrollable factors. In this application, we adopted the results from the National Highway Safety Administration (NHTSA) field operational test (FOT) *(19)*. The NHTSA reported that most CNTs for ACNS-equipped vehicles were less than 1 min. However, the average CNT for vehicles that are not equipped with the ACNS was 5.6min. In this study, 4.6 min was used for ΔCNT, which conservatively assumes that the average CNT for ACNS-equipped vehicles is 1 min.

## [Step3] Assessments of the Safety Benefits of the ACNS

The changes in the probabilities of crash injury severity with reduced CRTs are used to obtain the safety benefit. For example, as shown in Figure 3, the reduced changes in the probabilities for fatality and severe injury are regarded as safety benefits. Meanwhile, the probability of minor injury increases, as the function of the ACNS is to alleviate crash severity rather than to prevent crashes from occurring. That is, the total number of crashes does not change when the ACNS is applied. This study focuses on fatality and severe injury in estimating the safety benefits of the ACNS.

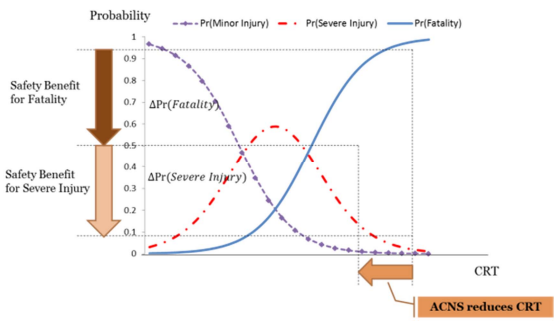


*Figure3*. Conceptual illustration of obtainable safety benefits by ACNS

An approach to quantifying the safety benefits of the ACNS is to determine the reductions in the number of fatalities and severe injuries. Because the ACNS can reduce CRT, the changes in the probabilities of injury severity can be computed with Eq. (1). Assuming that other independent variables ($X_i$) would not vary, the reduction in the percentage of fatality and severe injury can be expressed as Eq. (3) and Eq. (4). In addition, the reduced number of fatalities and severe injuries can be expressed as Eq. (5) and Eq. (6):

$$Eff_{Fatal} = Pr(Fatality|CRT_{ACNS}^{No}, X_i) - Pr(Fatality|CRT_{ACNS}, X_i) \quad (3)$$

$$Eff_{Severe} = Pr(Severity\ Injury|CRT_{ACNS}^{No}, X_i) - Pr(Severity\ Injury|CRT_{ACNS}, X_i) \quad (4)$$

$$\Delta NF = NF_{ACNS}^{No} \times Eff_{Fatal} \quad (5)$$

$$\Delta NS = NS_{ACNS}^{No} \times Eff_{Severe} \quad (6)$$

where

$Eff_{Fatal}$ : fatality reduction percentage with the ACNS,
$Eff_{Severe}$: severe injury reduction percentage with the ACNS,
$Pr(Fatality|CRT_{ACNS}^{No}, X_i)$ : probability of fatality without ACNS,
$Pr(Severe|CRT_{ACNS}^{No}, X_i)$ : probability of severe injury without the ACNS,
$Pr(Fatality|CRT_{ACNS}, X_i)$ : probability of fatality with the ACNS,
$Pr(Severe|CRT_{ACNS}, X_i)$ : probability of severe injury with the ACNS,
ΔNF: reduced number of fatalities with the ACNS,
ΔNS: reduced number of severe injuries with the ACNS,
$NF_{ACNS}^{No}$: number of fatalities without the ACNS,
$NS_{ACNS}^{No}$ : number of severe injuries without the ACNS.

## DATA

This study used freeway crash data from Korean freeways. As of 2010, the Korean freeway systems consist of 32 freeway lines with a total of 3,859km of freeway. In 2010, approximately 1,377,062,000 vehicles traveled freeways. The most recent three years of crash data, 2008-2010, were used in this study. During that time, 11,282 crashes occurred on Korean freeways, and there were 1,195 fatalities and 28,663 injuries. The Korea expressway corporation (KEC) is in charge of construction, maintenance, and traffic operations for Korean freeways. Crash management teams under the KEC collect crash-related data including crash severity, occurrence time, location, crash types and causes,

geometric conditions, traffic conditions, driver's characteristics, and weather conditions. The Korean freeway crash database is updated whenever a crash occurs. The database also has valuable information on crash response and clearance, which includes crash duration, clearance time, and arrival time of emergency medical service. In this study, we defined the time difference between crash occurrence time and arrival time of emergency medical service as CRT.

## AN APPLICATION OF PROPOSED METHODLOGY

A set of candidate factors that affect crash injury severity were extracted from the database. These factors include driver characteristics, geometric conditions, weather conditions, vehicle types, and crash response times. Table 1 presents the variables that were used in this study for developing a statistical model to predict crash injury severity. CRT was a continuous variable in minutes, but other variables were treated as nominal and discrete.

**Table1. Variable descriptions**

| Variable | | Descriptions |
|---|---|---|
| Dependent Variable | Injury severity | Fatality (2), Severe injury (1), Minor injury (0) |
| Independent Variable | Weather ($X_1$) | Clean/cloudy (0), Others (1) |
| | Daytime/nighttime ($X_2$) | Daytime (0), Nighttime(1) |
| | Horizontal alignment ($X_3$) | Tangent (0), Curve (1) |
| | Vertical alignment ($X_4$) | Level (0), Grade(1) |
| | Lighting ($X_5$) | Yes (0), No (1) |
| | Vehicle type ($X_6$) | Passenger car (0), Others (1) |
| | Driver gender ($X_7$) | Male (0), Female (1) |
| | CRT ($X_8$) | Continuous (min) |

The statistical software package program SPSS was used to predict injury severity. The results of the model development are summarized in Table 2. The value of Chi-square for the logistic regression model is 886.231. Among the eight candidate variables, but excluding weather ($X_1$), horizontal alignment ($X_3$) and gender ($X_7$), five variables were identified as statistically significant using Wald-statistic tests. The signs of the coefficients of the independent variables for daytime/nighttime ($X_2$), lighting ($X_5$), and CRT ($X_8$) are positive. On the contrary, horizontal alignment ($X_3$) and driver gender ($X_7$) had negative coefficients. These results imply that the injury severity increases when a crash occurs at nighttime and without lighting, with larger and longer CRTs, and when a male driver is involved. The probability model with the estimated coefficients is shown in Eq. (7-9).

**Table2. Regression modeling results**

| Para-meter | β | Wald statistic | Significance probability | Odds ratio $\exp(-\beta)$ |
|---|---|---|---|---|
| $\mu_1$ | 0.855 | 43.94 | 0.000 | - |
| $\mu_2$ | 1.308 | 99.05 | 0.000 | - |
| $X_2$ | 0.641 | 38.78 | 0.000 | 0.527 |
| $X_3$ | -0.395 | 13.69 | 0.000 | 1.484 |
| $X_5$ | 0.636 | 28.91 | 0.000 | 0.529 |
| $X_7$ | -0.463 | 7.14 | 0.008 | 1.589 |
| $X_8$ | 0.101 | 182.17 | 0.000 | 0.904 |

• MFI Chi-square: 886.231 (MFI sig.: 0.000)
• -2 log likelihood: 1209.974
• Nagellerke R-square: 0.212

$$Pr(Minor|X) = \frac{\exp(\mu_1 + \beta_2X_2 + \beta_3X_3 + \beta_5X_5 + \beta_7X_7 + \beta_8X_8)}{1 + \exp(\mu_1 + \beta_2X_2 + \beta_3X_3 + \beta_5X_5 + \beta_7X_7 + \beta_8X_8)} \quad (7)$$

$$Pr(Severe|X) = \frac{\exp(\mu_2 + \beta_2X_2 + \beta_3X_3 + \beta_5X_5 + \beta_7X_7 + \beta_8X_8)}{1 + \exp(\mu_2 + \beta_2X_2 + \beta_3X_3 + \beta_5X_5 + \beta_7X_7 + \beta_8X_8)} - \frac{\exp(\mu_1 + \beta_2X_2 + \beta_3X_3 + \beta_5X_5 + \beta_7X_7 + \beta_8X_8)}{1 + \exp(\mu_1 + \beta_2X_2 + \beta_3X_3 + \beta_5X_5 + \beta_7X_7 + \beta_8X_8)} \quad (8)$$

$$Pr(Fatality|X) = 1 - Pr(Minor|X) - Pr(Severe|X) \quad (9)$$

To estimate the $\mathrm{CRT_{ACNS}}$ (refer to Eq. (2)) that will be used in the injury prediction models in Eq. (7-9). 7,189 observed CRTs were analyzed from the crash database ($\mathrm{CRT^{No}_{ACNS}}$). The average and median of $\mathrm{CRTs^{No}_{ACNS}}$ are 11.00 and 10.00, respectively. The first task for estimating $\mathrm{CRT_{ACNS}}$ is to derive an appropriate PDF for $\mathrm{CRT^{No}_{ACNS}}$. A variety of probability density functions were fitted to the $\mathrm{CRT^{No}_{ACNS}}$ data. In this study, a normal density function ($N(\mu = 11, \sigma^2 = 7.39)$), which shows the smallest error value, was selected for the $\mathrm{CRT^{No}_{ACNS}}$ distribution function.

Next, normally distributed random $\mathrm{CRTs^{No}_{ACNS}}$ were extracted from the estimated normal PDF. A constant value of ΔCNT 4.6-min and the given MPRs ranging from 10 to 100% were applied to Eq. (2). A set of $\mathrm{CRTs_{ACNS}}$ was then established. In this case, an estimation of the CRT ($\widehat{\mathrm{CRT}}_{\mathrm{ACNS}}$) interval for a given MPR can be expressed as Eq. (10).

$$\overline{\mathrm{CRT}}_{\mathrm{ACINS}} - I \le \widehat{CRT}_{\mathrm{ACINS}} \le \overline{\mathrm{CRT}}_{\mathrm{ACINS}} + \mathrm{I} \quad (10)$$

where

$$\mathrm{I} = \frac{t_{\frac{\alpha}{2},8}\sigma_{\mathrm{CRT_{ACINS}}}}{\sqrt{n}}$$

$\overline{CRT}_{ACNS}$: average $CRT_{ACNS}$,
$\widehat{CRT}_{ACNS}$: interval estimation of $CRT_{ACNS}$,

$t_{\frac{\alpha}{2},\vartheta}$: t-statistic with degrees of freedom $\vartheta$ and significance probability α,
$\sigma_{CRT_{ACNS}}$ : standard deviation of $CRT_{ACNS}$, and
n: number of samples.

To estimate the safety benefits, the probabilities of injury severity are estimated with and without the ACNS. The CRTs that were derived from the above method are applied to Eq. (7-9) for minor injury, severe injury and fatality, respectively. The number of reduced fatalities and severe injuries can then be obtained using Eq. (5) and (6). As an application of the proposed methodology, the results of the estimated safety benefits of the ACNS, using 2010 crash data, are presented in Figure 4, 5. The total number of fatalities in 2010 is 389. Among them, approximately, 70 fatalities would be saved with a 100% MPR for the ACNS, which represents an 18.07% reduction in fatalities. Furthermore, up to 42 severely injured crash victims would be less injured with a 100% MPR, which represents a 1.49% reduction in severe injury. The relatively small reduction in severe injury can be explained by the fact that the injuries can either be severe injuries, fatalities, or minor injuries.

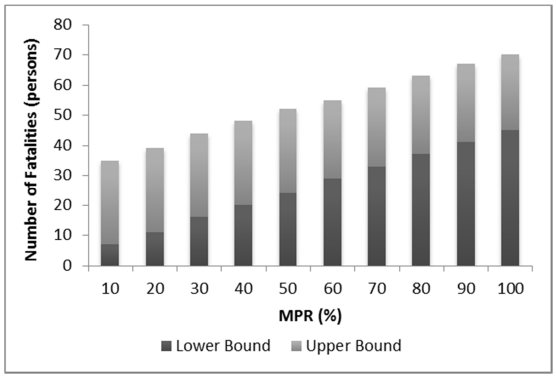


*Figure4*. Reduced number of fatalities with ACNS

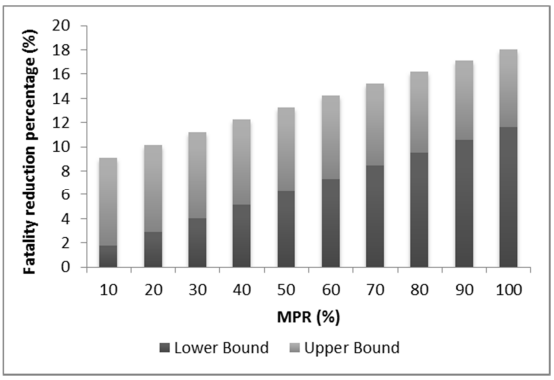


*Figure5*. Fatality reduction percentage with ACNS

## CONCLUSION

Substantial efforts have been made to enhance traffic safety on the road. These efforts can be comprehensively classified into two groups: preventing crashes and reducing injury severity. Preventing crashes is the preferred approach to enhance safety and to establish a crash-free transportation system. However, intricately related causal factors affect the occurrence of crashes. These complex causal relationships do not allow for the complete crash prevention. Therefore, reducing injury severity is an effective countermeasure after crashes occur.

A variety of technical countermeasures that can reduce injury severity have been widely developed in support of recent sensor and communication technologies. One promising countermeasure is the ACNS, which can reduce crash response time and provides additional opportunities to save the lives of crash victims. An important issue to fully utilize the ACNS is to quantify the safety benefits, which is fundamental for justifying the public investment. This study proposed a methodology for quantifying the safety benefits of the ACNS and applied the methodology to the Korean freeway systems.

The proposed methodology to estimate the safety benefits of ACNS consists of three steps. First, an injury severity prediction model based on OLR was developed. Various contributing factors, such as geometric conditions, weather conditions, and CRT, were used as independent variables in the model. Three levels of injury severity, including fatality, severe injury, and minor injury, can be predicted as probabilistic outcomes according to changes in the independent variables. The modeling result showed that following variables were statistically significant: daytime/nighttime, horizontal alignment, lighting, driver gender, and CRT. Second, $\mathrm{CRT_{ACNS}}$ was estimated using $\mathrm{CRT_{ACNS}^{No}}$, and ΔCNT was obtained with the ACNS at a given MPR. A nice feature was that a PDF for $\mathrm{CRT_{ACNS}^{No}}$ was derived with density function analyses, and used to generate a set of $\mathrm{CRTs_{ACNS}}$ to consider their variability. Afterward, various $\mathrm{CRT_{ACNS}}$ values were used as inputs to the injury prediction model to estimate the probabilities of injury severity. Then, the numbers of reduced fatalities and severe injuries were quantified. The reduction of CRT ranged from 4.85 min to 7.89 min in the case of a 100% MPR for the ACNS. This change would eliminate 70 fatalities and 42 severe injuries in the crash data from 2010.

A significant contribution of this research is to present a methodology for quantifying and analyzing the effectiveness of the ACNS in existing data. Nevertheless, further exploration is required to develop injury prediction models and to estimate $\mathrm{CRT_{ACNS}}$. Variables that represent traffic conditions,

such as speed or travel times, can be used as independent variables, as they impact CRT variability. Additionally, in addition to OLR, other modeling techniques would improve the statistical significance. Finally, crash data collected from signalized arterials and intersections should be analyzed.

The proposed methodology provides valuable insight into the development of methodology for evaluating other countermeasures that can reduce injury severity. In addition, the outcomes of this study support decision making for public investments and for establishing relevant traffic safety policies.

## ACKNOWLEDGEMENT

This research was supported by the Korea Ministry of Land, Transport and Maritime Affairs. It was also supported by the Korea Institute of Construction and Transportation Evaluation and Planning (Project No.: 11PTSI-C054118-03)

## REFERENCES

[1] Jacobs, L.M., A. Sinclair, A. Beiser, and R.B. D'Agostino. Prehospital Advanced Life Support: Benefits in Trauma. *Journal of Trauma 24, pp. 8–13,* 1984

[2] Lerner, E.B., and R.M. Moscati. The golden hour: scientific fact or medical urban legend? *Academic Emergency Medicine 8, pp. 758–760,* 2001.

[3] Blow, O., L. Magliore, J.A. Claridge, K. Butler, and J.S. Young. The golden hour and the silver day: detection and correction of occult hypoperfusion within 24 hours improves outcome from major trauma. *Journal of Trauma, Injury, Infection, and Critical Care 7, pp. 964–969,* 1999.

[4] Muelleman, R.L., and K. Mueller. Fatal motor vehicle crashes: variations of crash characteristics within rural regions of different population densities. *The Journal of Trauma: Injury, Infection and Critical Care 41, pp. 315–320,* 1996.

[5] Evanco, W.M. The potential impact of rural mayday systems on vehicular crash fatalities. *Accident Analysis and Prevention 31, pp. 455–462,* 1999.

[6] Clark, D.E., and B.M. Cushing. Predicted effect of automatic crash notification on traffic mortality. *Accident Analysis and Prevention 34, pp. 507–513,* 2002.

[7] Zwerling, C., C. Peek-Asa, P.S. Whitten, S.W. Choi, N.L Sprince, and M.P. Jones. Fatal motor vehicles crashes in rural and urban areas: decomposing rates into contributing factors. *Injury Prevention 11, pp. 24–28,* 2005.

[8] Li, M.D., J.L. Doong, K.K. Chang, T.H. Lu, and M.C. Jeng. Differences in urban and rural accident characteristics and medical service utilization for traffic fatalities in less-motorized societies. *Journal of Safety Research 39, pp. 623–630, 2008.*

[9] Gonzalez, R.P., G.R. Cummings, H.A. Phelan, M.S. Mulekar, and C.B. Rodning. Does increased emergency medical services pre-hospital time affect patient mortality in rural motor vehicle crashes? A statewide analysis. *The American Journal of Surgery 197, pp. 30–34,* 2009.

[10] Sanchez-Mangas, R., A. Garcia-Ferrer, A. Juan, and A.M. Arroyo. The probability of death in road traffic accidents. How important is a quick medical response? *Accident Analysis and Prevention 42, pp. 1048-1056,* 2010.

[11] National Highway Traffic Safety Administration. Automatic collision notice field test summary. *Ann. Emerg. Med. 38 (4), pp. 453-454,* 2001.

[12] European Commission. eCall-saving lives through in-vehicle communication technology. *Factsheet 49, Information Society and Media,* 2009.

[13] Akella, M.R., C. Bang, R. Beutner, E.M. Delmelle, R. Batta, A. Blatt, P.A. Rogerson, and G. Wilson. Evaluating the reliability of automated collision notification systems. *Accid. Anal. Prev. 35 (3), pp. 349-360,* 2003.

[14] Delmelle, E.M., P.A. Rogerson, M.R. Akella, R. Batta, R. Blatt, and G. Wilson. A spatial model of received signal strength indicator values for automated collision notification technology. *Transportation Research Part C 13, pp. 432-447,* 2005.

[15] Bose, D., J.R. Crandall, G. McGwin, J. Goldman, J. Foster, and P.R. Fine. Computational methodology to predict injury risk for motor vehicle crash victims: A framework for improving advanced automatic crash notification systems. *Transportation Research Part C 19, pp. 1048-1059,* 2011.

[16] Rauscher, S.R., G. Messner, and P. Baur. Enhanced automatic collision notification system-improved rescue care due to injury prediction-first filed experience. *The 21st International Technical Conference on the Enhanced Safety of Vehicles Conference (ESV) - International Congress Center Stuttgart, Germany,* 2009.

[17] Liao, T.F. Interpreting Probability Models; Logit, Probit, and Other Generalized Linear Models. *Quantitative Application in the Social Sciences 07-101, Sage Publication. California,* 1994.

[18] Maddala, G.S., *Limited-Dependent and Qualitative Variables in Econometrics.*

Cambridge University Press. New York, 1983.
[19] Kanianthra, J., A. Carter, and G. Preziotti. Enhancing post-crash vehicle safety through an automatic collision notification system. *The 17th International Technical Conference on the Enhanced Safety of Vehicles (ESV) - Amsterdam, Netherlands,* 2001.